

AD-777 218

HUMAN LIMITATIONS IN OPERATION OF  
AEROSPACE SYSTEMS: CIRCULATORY  
REGULATION DURING COMBINED FLIGHT  
STRESSES

Ernest P. McCutcheon, et al

Kentucky University

Prepared for:

Air Force Office of Scientific Research

31 August 1973

DISTRIBUTED BY:

**NTIS**

National Technical Information Service  
U. S. DEPARTMENT OF COMMERCE  
5285 Port Royal Road, Springfield Va. 22151

UNCLASSIFIED

SECURITY CLASSIFICATION OF THIS PAGE (When Data Entered)

REPORT DOCUMENTATION PAGE		READ INSTRUCTIONS BEFORE COMPLETING FORM
1. REPORT NUMBER <b>AEOSR - TR - 73 - 2321</b>	2. GOVT ACCESSION NO.	3. RECIPIENT'S CATALOG NUMBER
4. TITLE (and Subtitle) <b>HUMAN LIMITATIONS IN OPERATION OF AEROSPACE SYSTEMS: CIRCULATORY REGULATION DURING COMBINED FLIGHT STRESSES</b>		5. TYPE OF REPORT & PERIOD COVERED <b>Final</b>
7. AUTHOR(s) <b>Ernest P. McCutcheon, M.D. Charles F. Knapp, Ph.D.</b>		6. PERFORMING ORG. REPORT NUMBER
9. PERFORMING ORGANIZATION NAME AND ADDRESS <b>Department of Physiology and Biophysics The University of Kentucky Lexington, Kentucky 40506</b>		8. CONTRACT OR GRANT NUMBER(s) <b>F44620-69-C-0127</b>
11. CONTROLLING OFFICE NAME AND ADDRESS <b>Air Force Office of Scientific Research (NL) 1400 Wilson Boulevard Arlington, Virginia 22209</b>		10. PROGRAM ELEMENT, REPORT, TASK AREA & WORK UNIT NUMBERS <b>61102F 9777 681312</b>
14. MONITORING AGENCY NAME & ADDRESS (if different from Controlling Office)		12. REPORT DATE <b>31 August 1973</b>
		13. NUMBER OF PAGES <b>257</b>
		15. SECURITY CLASS. (of this report) <b>Unclassified</b>
16. DISTRIBUTION STATEMENT (of this Report)  <b>Approved for public release; distribution unlimited.</b>		15a. DECLASSIFICATION/DOWNGRADING SCHEDULE
17. DISTRIBUTION STATEMENT (of the abstract entered in Block 20, if different from Report)		
18. SUPPLEMENTARY NOTES		
19. KEY WORDS (Continue on reverse side if necessary and identify by block number)		
20. ABSTRACT (Continue on reverse side if necessary and identify by block number) The most significant accomplishments are: (1) Development of a Standard Experimental Preparation (SEP), composed of awake and anesthetized animals with acutely and chronically placed instrumentation providing a broad range of variables appropriate for analyses of the effects of single and multiple stressful stimuli, for evaluation of the physiological and biochemical responses to environmental stresses; (2) Implementation of the SEP for the study of awake, chronically instrumented animals exposed to vibration, the first series of investigations of this type to be reported; (3) Determination that a major factor underlying the		

DD FORM 1 JAN 73 1473

EDITION OF 1 NOV 65 IS OBSOLETE *ja*

UNCLASSIFIED

SECURITY CLASSIFICATION OF THIS PAGE (When Data Entered)

## 20. ABSTRACT (Continued)

cardiovascular effects of vibration in dogs is peak net transmitted force, maximum force transmission in the 3 to 6 Hz range for acceleration level of 1 G and above, use of frequency, displacement or acceleration alone does not give the consistent response pattern observed with peak net force as the parameter; (4) Development of a closed-loop, distributed parameter computer model which accounts for some of the wave characteristics of transient flow and for motion induced in the circulatory system by vibration; (5) Demonstration in the intact left ventricle first known evaluation of the relationship between the elastic modulus and the mean tangential stress of canine cardiac muscle.

# Human Limitations in Operation of Aerospace Systems: Circulatory Regulation During Combined Flight Stresses

FINAL REPORT  
1969-73

Air Force Office of Scientific Research  
Contract No. F44620-69-0127  
The University of Kentucky

Program Managers: Ernest P. McCutcheon, M.D.  
Charles F. Knapp, Ph.D.

The University of Kentucky  
Lexington, Kentucky 40506

To purchase: DTIC  
 NATIONAL TECHNICAL  
 INFORMATION SERVICE  
 U.S. Department of Commerce  
 Springfield, VA 22161

August 31, 1973

DDC  
RECEIVED  
APR 19 1974  
RECEIVED  
D

AIR FORCE COMMAND AND CONTROL RESEARCH (AFSC)  
 D. W. HARRIS  
 Technical Assistant Officer

Approved for public release;  
distribution unlimited

### Acknowledgements

This research was an interdisciplinary effort conducted by the members of the College of Engineering and the College of Medicine. The investigators are: Dr. E. P. McCutcheon, M.D., Dr. C. F. Knapp, Ph.D., Dr. R. G. Edwards, Ph.D., Dr. W. O. Griffen, M.D., and Dr. J. C. Collins, Ph.D.

The investigators wish to acknowledge the assistance of the technical staff of the Wenner-Gren Research Laboratory and the Department of Surgery, in particular A. Bhattacharya (Ph.D.), F. Wibel, M.S., R. Starnes, M.S., J. Evans, M.S., T. Lowery, B.S., E. Woods, B.S., T. Geoffroy, (M.S.), C. Woolfolk, R. Stanifer, Bob Boone, and S. Beaver, B.A.

The assistance of Ms. Marie Mason who typed this report is also acknowledged.

## Contents

I. PROGRAM SUMMARY 1969-73 . . . . .	1
A. Most Significant Accomplishments . . . . .	1
B. Publications Resulting from the Work Supported by this Contract . . . . .	3
C. Summary of Experimental Program . . . . .	7
II. PROGRESS REPORT 1972-73 . . . . .	13
A. Introduction . . . . .	13
B. Experimental Protocol . . . . .	27
1. Animal Preparation . . . . .	28
2. Experimental Procedures . . . . .	29
3. Data Acquisition and Analysis . . . . .	30
C. Results . . . . .	31
1. Experimental . . . . .	31
2. Computer Modeling . . . . .	36
D. Discussion . . . . .	38
E. Recommendations . . . . .	41
F. References . . . . .	43
III. APPENDICES	
A. Experimental Techniques	
B. Raytheon 704, Data Acquisition System	
C. Data Acquisition Specifications	
D. Mechanical Impedance Model: A Model to Predict the Mechanical Impedance of the Sitting Primate During Sinusoidal Vibration	
E. Computer Model of the Effects of Sinusoidal Vibration on the Cardiovascular System	

## I. PROGRAM SUMMARY 1969-73

### A. Most Significant Accomplishments

1. The establishment of a totally interdisciplinary effort in which the areas of physiology, psychology, and engineering interface to provide an optimal research capability. This interdisciplinary effort has also provided a major impact on the research and teaching capabilities of this University's Biomedical Engineering Program.
2. Development of a center of excellence as a resource for support of the DOD mission.
3. Establishment of effective communication links and collaborative efforts among other Air Force Contractors and Air Force Research Laboratories to provide continuing two way flow of information.
4. Organization and presentation of the first national symposium on Chronically Implanted Cardiovascular Instrumentation, and publication of the results by Academic Press.
5. Development of a Standard Experimental Preparation (SEP) for evaluation of the Physiological and Biomechanical responses to environmental stresses. The SEP includes awake and anesthetized animals with acutely and chronically placed instrumentation providing a broad range of variables appropriate for analysis of the effects of single and multiple stressful stimuli.
6. Implementation of the SEP for study of awake, chronically instrumented animals exposed to vibration stress, the first series of investigations of this type to be reported.
7. Combining the capabilities supported by this contract with additional support from the Vibration Branch, Wright-Patterson AFB, to measure multiple physiological variables in a monkey performing a tracking

task. Preliminary results were described in a Technical Report published by the Vibrations Branch and a second Technical Report is in press.

8. Determination of the facts that (1) a major factor underlying the cardiovascular effects of vibration in dogs is peak net transmitted force; (2) maximum force transmission in dogs and monkeys is in the 3 to 6 Hz range for acceleration levels of 1G and above; (3) use of frequency, displacement, or acceleration alone does not give the consistent response pattern observed with peak net force as the parameter; and (4) with repeated exposure, force transmission and heart rate extremes decrease, just as in human subjects.
9. Development of a closed-loop, distributed parameter computer model which accounts for some of the wave characteristics of transient flow and for the motion induced in the circulatory system by vibration.
10. Development of a novel approach for quantifying the coefficients of a two-mass, single-degree-of-freedom, bio-vibrational model and demonstration of its validity for predicting the mechanical impedance of the sitting primate during sinusoidal vibration.
11. Demonstration in the intact left ventricle that the elastic modulus ( $E$ ) is a linear function of the mean tangential stress ( $\sigma$ ) throughout isovolumetric systole, and the slope ( $K$ , modulus of stiffness) of the  $E$  vs.  $\sigma$  curve is 18.8, with one standard deviation of 0.9. This is the first known evaluation of the relationship between the elastic modulus and the mean tangential stress of canine cardiac muscle.
12. Demonstration of the relationship between a decrease in the amplitude of the somatosensory cortical evoked potential and the development of irreversible hemorrhagic shock.



B. Publications Resulting from the Work Supported by this Contract

1. Adams, R. N., McCutcheon, E. P., and Stanifer, R. R. Coherent schlieren and ultrasonics. Proc. 8th ICEMB, 10-2, 1969.
2. Shabetal, R. The dynamics of cardiac compression; A Flowmeter study of the differences between constrictive pericarditis and cardiac tamponade. J. Lab. & Clin. Med., Proc. of the Central Soc. for Clin. Res. 11: 1969.
3. Shabetal, R. and Bowles, S. The dynamics of cardiac compression: A flowmeter study of the differences between constrictive pericarditis and cardiac tamponade. 19th Ann. Scientific Sess., Amer. Coll. Card. Feb. 26-27, 1970, New Orleans, La.
4. Shabetal, R., Fowler, N. D., and Guntheroch, W. G. The hemodynamics of cardiac tamponade and constrictive pericarditis. Am. J. Card. 26:480, 1970.
5. Edwards, R. G., McCutcheon, E. P., Knapp, C. F., and Boone, R. Interaction of sinusoidal vibration and cardiovascular function in dogs. Physiologist 13(3):186, 1970.
6. McCutcheon, E. P., Frazier, D. T., and Boyarsky, L. L. Neuro-physiological changes associated with hypovolemia. Physiologist 13(3):258, 1970.
7. Edwards, R. G., Knapp, C. F., McCutcheon, E. P., Lange, K. O., and Griffen, W. O. Effect of vibration on blood flow and pressure in major arteries of dogs. Symposium on Biodynamic Models and their Application, Dayton, Ohio, Oct. 26-28, 1970.
8. Adams, R. N., McCutcheon, E. P., and Yoo, K. S. Acoustical frequency shifts due to bloodflow. IEEE Trans. Sonics and ultrasonics Su-18-44, 1971.

9. Adams, R. N., McCutcheon, E. P., and Yoo, K. S. Scattered ultrasound frequency shifts induced by pulsatile flow. J. Acoust. Soc. Amer., in press.
10. McCutcheon, E. P., Stanifer, R. R., and Boone, R. D. Characteristics of miniature solid-state pressure transducers. JAAMI 5:128, 1971.
11. Camill, P., Knapp, C. F., and Collins, J. Computer modeling of whole body sinusoidal accelerations on the cardiovascular system. Proc. 9th Ann. IEEE Region III, Convention, 25, 1971.
12. Higgins, A. M., Funk, J. E. and Lafferty, J. F. A rapid injection system for in vivo determination of dog ventricle stiffness. JAAMI 5:1971.
13. Morrow, D. H., and McCutcheon, E. P. Control and effect of drugs on the arterial circulation. Ann. Mtg., Amer. Soc. Anesthesiologists, N. Y., Oct., 17, 1970.
14. McCutcheon, E. P., Frazier, D. T., and Boyarsky, L. L. Changes in the somatosensory cortical evoked potential produced by hypovolemic shock. Proc. Soc. Exper. Biol. Med. 136:1063, 1971.
15. Higgins, A. M., Funk, J. E., McCutcheon, E. P., and Lafferty, J. F. In vivo determination of dog ventricle stiffness. Proc. 9th Ann. IEEE Region III, Convention, 25, 1971.
16. McCutcheon, E. P., Edwards, R. G., Knapp, C. F., and Griffen, W. O. Circulatory response to sinusoidal vibration and the effects of hypovolemia. Proc. Int. Union Physiol. Sci. 9:380, 1971.
17. Edwards, R. G., McCutcheon, E. P., and Knapp, C. F. Cardiovascular changes produced by brief whole-body vibration in animals. J. Appl. Physiol. 32:386, 1972.
18. Collins, J. C., Knapp, C. F., Starnes, R. G., and Bhargava, V. M. Electrical analog modeling of cardiovascular valves. Proc. 4th

Ann. Southeastern Symp. System Theory, 1972.

19. Lafferty, J. F., McCutcheon, E. P., Funk, J. E., and Higgins, A. M.  
In vivo determination of elastic modulus of canine cardiac muscle.  
ASME Winter meeting, BHF Div., New York, Nov. 26-30, 1972, published  
in J. Basic Eng., Dec., 1972.
20. McCutcheon, E. P. and Stone, H. L. Significance of chronic implan-  
tation of cardiovascular instrumentation. In McCutcheon, E. P.,  
Ed. Chronically Implanted Cardiovascular Instrumentation. Academic  
Press, 1973.
21. Collins, J. C., Knapp, C. F., Starnes, R. S., and Bhargava, V. M.  
Electrical analog modeling of cardiovascular valves. Proc. 4th  
Ann. Southeast. Symp. on System Theory, Lexington, Ky. Apr. 3-4,  
1972.
22. McCutcheon, E. P., Evans, J. M., and Stanifer, R. R. Direct blood  
pressure measurement: Gadgets vs. progress. Read at the 46th Cong.  
of the Int. Anesth. Res. Soc., Las Vegas, Mar., 1972, published in  
J. Anesth. Analg. Sept-Oct., 1972.
23. Edwards, R. G., and Knapp, C. F. Changes in whole body force trans-  
mission of dogs exposed repeatedly to vibration. Presented at Winter  
Annual Meeting. A.S.M.E., New York, Nov. 1972. A.S.M.E. paper No.  
72-WA/BHF-11, and published in Aero. Med. 44(8): 910-913, 1973.
24. McCutcheon, E. P., Evans, J. M., and Wibel, F. H. A fabric pouch  
for maintenance of multiple chronically implanted lead terminations.  
4th Ann. Meet. B.M.E. Soc., Los Angeles, Jan. 29-30, 1973.
25. McCutcheon, E. P., Evans, J. M., and Stanifer, R. R. Evaluation of  
miniature pressure gauges for direct blood pressure measurement. In  
McCutcheon, E. P., Ed. Chronically Implanted Cardiovascular Instru-  
mentation. Academic Press, 1973.

26. McCutcheon, E. P., Ed. Chronically Implanted Cardiovascular Instrumentation. 482 pp. New York: Academic Press, 1973.
27. Edwards, R. G. and Lafferty, J. F. A model to predict the mechanical impedance of the sitting primate during sinusoidal vibration. Am. Soc. Mech. Eng., paper No. 73-DET-78, 1973.
28. Lafferty, J. F., Edwards R. G., McCoy, D. F., McCutcheon, E. P., and Wekstein, D. R. A standard psychophysiological preparation for evaluating the effects of environmental vibration stress. Phase I: Development. U.S.A.F. Aero Med. Res. Lab. Tech. Report. AMRL-TR-72-112, March, 1973.
29. Knapp, C. F., Collins, J., and Starnes, R. G. Computer modeling of the effects of whole-body heart-synchronous accelerations on the circulation. Proc. Xth Int. Conf. Med. and Biol. Eng. Dresden, GDR, August, 1973.
30. Adams, R. N., and McCutcheon, E. P. Electronically steered ultrasonic beam using a single crystal. Proc. 26th ACEMB Conf. Minneapolis, Sept., 1973.
31. McCutcheon, E. P., Edwards, R. G., Evans, J. M., Lafferty, J. F., and McCoy, D. F. A standard psychophysiological preparation for evaluating the effects of environmental vibrational stress Phase II: Implementation. To be published as an AMRL tech. Report, 1973.
32. Camill, P., Collins, J. C., and Knapp, C. F. Computer modeling of changes in the cardiovascular system induced by whole-body sinusoidal accelerations. Submitted to Annals of Biomedical Engineering, Oct., 1973.

### C. Summary of Experimental Program

Of the various stresses imposed upon subjects performing critical tasks, time dependent accelerations (vibration) can produce some of the greatest discomfort and decrements in performance. The effects of this stress on the cardiovascular system are being investigated at this laboratory. Instrumented animals are used to evaluate the cardiovascular changes produced by whole body, sinusoidal vibration. Experiments are designed to evaluate the role of the five major mechanisms which current evidence indicates are the main factors producing these changes. The mechanisms important for vibrational stress of a given frequency, displacement, acceleration, transmitted force, axis, and duration are:

1. Reaction of the fluid and vessel system as determined by its mass, elastic, and damping characteristics.
2. Reaction of large body organ systems and the musculoskeletal system as determined by their mass, elastic and damping characteristics.
3. Reaction of the mechanoreceptors of the cardiovascular regulatory system as determined by the relationships to the fluid and vessel system, large body organ systems, and the musculoskeletal system and its mechanoreceptors.
4. Reaction of the endocrine, metabolic - hematological system as determined by the relationships to the musculoskeletal and large body organ systems.
5. Response mediation of the central nervous system and the psychophysiological system of conscious subjects acting through the above pathways to produce further alterations in metabolic and cardiovascular function.

Cardiovascular, hematological, and mechanical variables are used to evaluate the overall stress level and the role of the above mechanisms. Anesthetized and awake animals are used for both short and long term (30 sec. to 6 hr.) vibration stress exposures.

General Experimental Protocol: Responses of acutely and chronically instrumented dogs, primates and pigs have been studied. Special emphasis has been placed on the chronically implanted preparation which permits repeated awake and anesthetized tests on the same animal. Additional advantages include the closed chest protocol and more stable transducer characteristics, especially important for the vibration environment. Animals are restrained on the hydraulic table with the spine vertical, and vibrated along that axis. Short term tests consist of sequential exposures to sinusoidal vibration of 2-12 Hz and acceleration amplitudes ranging from 0.5 G to 3.0 G for 30 sec., 2 min., and 5 min. intervals. Long term exposures include durations varying from 30 min. to 6 hrs. at a selected vibration frequency and constant acceleration amplitude. The highest g-level for the awake animal is 1.5 g, and for the anesthetized animal is 3.0 g. The cardiovascular variables include heart rate, flow velocity from the aorta and peripheral arteries, arterial pressures from acceleration-insensitive intraaortic and intraventricular transducers,  $O_2$  consumption and body temp. and blood chemistries such as blood gases, cortisol, free fatty acids, and glucose, measured on samples withdrawn from indwelling atrial and arterial catheters. The design of the vibration exciters permits recording of force transmitted between subject and table, and also the vibration exciter velocity. From these variables and their phase relationship, complex mechanical velocity impedance can be determined. In addition, accelerometers implanted on large body organs provide information on the displacement of these organs relative to the animal torso and the input vibration. A Raytheon 704 data acquisition system is being programed for off-line and on-line analysis of the massive amount of cardiovascular and mechanical data. Additional aspects of the research program include analog and digital computer simulation of the effects of sinusoidal vibration on the hydraulic

and mechanical aspects of the cardiovascular system. The results from the computer study guide the planning of animal experiments and aid in the analysis of experimental data.

### Results

A. Short term exposure: In an effort to identify the parameters of vibration which may serve best as an index of stress to the cardiovascular system, special emphasis has been given to the role of the peak net force (PNF) transmitted between the animal and vibration exciter. A whole body resonance at 3-4 Hz was found for seven awake dogs tested at 1G acceleration amplitude. At this frequency (f), peak net force was about 1.7 times the body weight. For frequencies up to and including 6 Hz, the animal still transmitted a peak force greater than body weight (BW). Beyond 6 Hz this force continually decreased until at 30 Hz a peak force of only about 15% of body weight resulted. The effects of anesthesia as reflected in the force transmission data show, in general, that the anesthetized animal transmits approximately 30% more force at resonance and has a resonant frequency 1 to 2 Hz lower than the awake animal. At higher frequencies there have been no consistent force transmission differences between awake and anesthetized dogs. When the percent change in mean aortic flow (MAF) for the awake dogs was plotted versus PNF/BW, a linear relationship was found. Changes in MAF ranged from -30 to +150%. At this time, it appears PNF/BW describes best the changes in MAF, with only secondary correlations existing for frequency, acceleration and displacement. The mechanisms responsible for these changes in dogs (7 dogs, 10 experiments) can be provisionally catalogued as follows:

1. Changes in mean heart rate (MHR) and relatively small changes in stroke volume: Data from three tests showed a linear relationship between % change in MHR and peak net force, with stroke volume relatively unchanged.

2. Changes in stroke volume (SV) and relatively small changes in MHR:

Data from four tests showed a linear relationship between % change in stroke volume and peak net force, with % change in MHR relatively unchanged.

3. Equal changes in MHR and stroke volume: Data from three tests showed linear relationship between both % change in MHR, and % change in stroke volume and peak net force.

Furthermore, the type of changes in MAF could be correlated with pre-vibration values of MHR and SV. For example, if the previbration MHR was low, increases in MAF occurred principally by an increase in HR. (Category 1). If, however, previbration MHR was high, increases in MAF resulted from an increase in SV. (Category 2).

Similar observations were made for the data of the anesthetized dogs except that Category 3 was not as evident and that the previbration anesthesia profile also influenced the data. The slope of the line of MAF vs PNF/BW (best fit) for the data from 10 tests on 7 awake dogs and 7 anesthetized dogs was analyzed. For those experiments in which increases in MAF were produced principally by increases in SV, no significant differences were found between awake and anesthetized dogs run on the same vibration tests. When an increase in MHR was used to increase MAF, the slope of the line of MAF vs (PNF/BW) for the awake animals was 67% higher than that of the anesthetized animals data. Changes in MAF were found also to vary linearly with the log (MHR/vib. freq.).

In addition, transmissibility of the root of the aorta was found to be linearly related to PNF/BW, extremely dependent on vibration frequency, and to have a resonance at approximately 4 Hz, at which frequency the applied vibration amplitude (acceleration) was amplified approximately 2.4 times.



B. Long term exposure: For 90 min. exposures at a constant frequency and G level, no consistent changes in MAF were observed. The fluctuations which occurred over time were more numerous at 4 Hz (0.75G) than at 6 or 10 Hz. Of the limited tests performed, one out of 5 awake dogs changed MAF through significant changes in MHR and lesser changes in SV. Two out of five dogs changed MAF through significant changes in SV and lesser changes in MHR. No consistent changes in PNF/BW vs time were observed. Similarly, no definite trends were seen in tracking monkeys repeatedly exposed to multiple frequencies up to 3 hours duration.

C. Computer Model: A lumped parameter model was used to aid in determining the passive mechanical and hydraulic contribution to the total physiological response of the awake dogs to vibration. The effects of vibration are modeled by pressure source terms generated from values of the vibration g-level or resulting transmitted force. These pressure disturbances propagate and reflect, adding and subtracting with the pressure generated by the action of the heart, and as a result produce changes in flow as well. The value of PNF/BW vs f from the animal experiments was used to establish the values of the source terms for the different simulated vibration frequencies. Heart rate was varied in the model as observed in the animal experiment. The computer response of MAF vs PNF/BW was similar to those of the animal experiments with the actual % change values close to those found for the anesthetized dogs, in which SV remained relatively constant and HR changed, e.g. maximum % change in MAF was approximately 25%.

#### Discussion:

From a preliminary analysis of the data, it appears that of the changes in MAF (via changes in SV) of awake and anesthetized dogs subjected to vibration, approximately 60 to 70% is due to one or a combination of the mechanisms 3, 4 and 5 (i.e. reaction of mechanoreceptors of the cardiovascular regulatory system, the metabolic-hematological, and the psychophysiological system), with the

remaining 30 to 40% due to mechanisms 1 and 2 (i.e. reaction of the fluid vessel system, and the large body organ and musculoskeletal system). A comparison of the computer model studies with the anesthetized animal data in which changes in MAF were produced principally by changes in MHR, indicates that this anesthetized preparation, to the first approximation, responds as a passive "mechanical" system. Furthermore, the correlation of MAF with the ratio of heart frequency/table frequency suggests the influence of the phase relationship between the heart cycle and the vibration cycle (through the pathways of mechanism 1) in producing changes in MAF.

Analysis of these data indicates that in addition to the passive mechanical aspects, substantial changes are produced by other regulatory feedback mechanisms sensitive to vibrations. These vibration receptors may lead to sympathetic stimulation and/or possible heterometric regulation in the heart. The relative role of these various active mechanisms in producing changes in MAF is certainly not clear at this time. However, similar interactions between HR and SV in generating MAF as observed for these vibration studies have also been described for exercise. It will be of value to investigate this point further. Nevertheless, the use of awake animals for assessing the effects of vibrational stress on the cardiovascular system has been found most valuable. In addition, PNF/BW is an especially important parameter in assessing changes in MAF during vibrational stress. It is recommended that future studies should investigate the neural and mechanical mediation involved in the response of the cardiovascular system to vibration.

PROGRESS REPORT 1972-73

## II. PROGRESS REPORT 1972-73

### A. Introduction

Of the various stresses imposed upon subjects performing critical tasks, time dependent accelerations (vibration) can produce some of the greatest discomfort and decrements in performance. The effects of this stress on the cardiovascular system are being investigated and are the subject of this report. Instrumented animals are used to evaluate the cardiovascular changes produced by whole body, sinusoidal vibration. Experiments are designed to evaluate the role of the five major mechanisms which current evidence indicates are the main factors producing these changes. The mechanisms important for vibrational stress of a given frequency, displacement, acceleration, transmitted force, axis, and duration are:

1. Reaction of the fluid and vessel system as determined by its mass, elastic, and damping characteristics.
2. Reaction of large body organ systems and the musculoskeletal system as determined by their mass, elastic and damping characteristics.
3. Reaction of the mechanoreceptors of the cardiovascular regulatory system as determined by the relationships to the fluid and vessel system large body organ systems, and the musculoskeletal system and its mechanoreceptors.
4. Reaction of the hormonal, metabolic - hematological systems as determined by the relationships to the musculoskeletal and large body organ systems.
5. Response mediation of the central nervous system and the psychophysiological system of conscious subjects acting through the above pathways to produce further alterations in metabolic and cardiovascular function.

A proposed model of the interaction of these five mechanisms is illustrated in the block diagram of Figure 1. Cardiovascular, metabolic, hematological, and

mechanical variables are used to evaluate the overall stress level and the role of the above mechanisms. The following is a review of the available information on the relationship between the mechanical and physiological responses in animals and man exposed to vibrational stress.

Vibration Parameters: Any given vibration is characterized by its frequency, displacement, velocity, acceleration and waveform. While these parameters may define the vibration applied to a subject, they are not necessarily transmitted equally to all parts of the subject. For example the head might well vibrate with a displacement, velocity, acceleration, and waveform vastly different from that applied at the subject-vibration exciter interface. Thus, while certain parameters define the applied vibration, other parameters, dependent upon the properties of the vibrated subject, are necessary to characterize the response of the subject to the applied vibration. Such parameters include the transmitted force at the subject-vibration exciter interface, resonant frequencies (those frequencies corresponding to the maxima of total, integrated whole-body displacement with respect to the applied displacement), and the transmissibility of a particular body segment (transmissibility is defined simply as the ratio of the vibration amplitude of any given segment, e.g. the head, heart, shoulder, etc., to the applied vibration amplitude, measured at vibration exciter).

When attempting to determine the vibration response of any system the initial question arises as to what scheme of applied vibration parameters should be used? Consider the case of sinusoidal vibration where the displacement ( $x$ ) is  $x = x_0 \sin \omega t$ , the velocity ( $v$ ) is  $v = x_0 \omega \cos \omega t$  and the acceleration ( $a$ ) is  $a = -x_0 \omega^2 \sin \omega t$ . The peak acceleration amplitude relative to the gravitational constant  $g$  is often times written as  $a = \frac{x_0 \omega^2}{g}$  and referred to as "G level".

Some investigators favor applying various vibration frequencies each having the same displacement amplitude,  $x_0$ ; however, for this approach as frequency

increases the peak acceleration,  $a$ , increases with frequency squared. Therefore going from 1 to 10 Hz requires a peak acceleration 100 times greater at 10 Hz than at 1 Hz. Thus, this approach necessitates a very low acceleration amplitude at the lowest frequency in order to avoid lethal accelerations at the higher frequencies. A similar, but less extreme, condition results by applying different frequencies each with the same peak velocity,  $x_0 \omega$ . For this case as the frequency is increased the displacement amplitude must be reduced inversely with the frequency and the acceleration amplitude will increase linearly with frequency. The most common method employed by biovibratory investigators has been to apply various frequencies each having the same acceleration amplitude,  $\frac{x_0 \omega^2}{g}$ . For increasing frequencies, this approach requires decreasing the displacement amplitude by the inverse frequency squared. For any given peak acceleration the largest displacement amplitude is therefore required at the lowest frequency, and decreases rapidly with increasing frequency. From a mechanical viewpoint this constant peak acceleration approach has two important advantages; namely (1) mechanical measurements can be compared directly to the response of an "inert" mass of weight equal to that of the subject, since in this case the peak force transmitted between the vibration exciter and the imaginary inert mass is independent of frequency, and (2) from a practical view point, the displacement, velocity, and acceleration limits of the vibration exciter are not as easily exceeded using this approach as compared to applying various frequencies at either a constant displacement or velocity amplitude. Further information pertinent to this discussion is given by Lange and Edwards (1970).

A unique feature incorporated with the Wenner-Gren Research Laboratory's vibration exciters is a force measurement unit (force cell) which, during vibration, provides an analog output voltage proportional to the net force transmission between subject and restraint, i.e. the "live-load" force transmission

increases the peak acceleration,  $a$ , increases with frequency squared. Therefore going from 1 to 10 Hz requires a peak acceleration 100 times greater at 10 Hz than at 1 Hz. Thus, this approach necessitates a very low acceleration amplitude at the lowest frequency in order to avoid lethal accelerations at the higher frequencies. A similar, but less extreme, condition results by applying different frequencies each with the same peak velocity,  $x_0 \omega$ . For this case as the frequency is increased the displacement amplitude must be reduced inversely with the frequency and the acceleration amplitude will increase linearly with frequency. The most common method employed by biovibratory investigators has been to apply various frequencies each having the same acceleration amplitude,  $\frac{x_0 \omega^2}{g}$ . For increasing frequencies, this approach requires decreasing the displacement amplitude by the inverse frequency squared. For any given peak acceleration the largest displacement amplitude is therefore required at the lowest frequency, and decreases rapidly with increasing frequency. From a mechanical viewpoint this constant peak acceleration approach has two important advantages; namely (1) mechanical measurements can be compared directly to the response of an "inert" mass of weight equal to that of the subject, since in this case the peak force transmitted between the vibration exciter and the imaginary inert mass is independent of frequency, and (2) from a practical view point, the displacement, velocity, and acceleration limits of the vibration exciter are not as easily exceeded using this approach as compared to applying various frequencies at either a constant displacement or velocity amplitude. Further information pertinent to this discussion is given by Lange and Edwards (1970).

A unique feature incorporated with the Wenner-Gren Research Laboratory's vibration exciters is a force measurement unit (force cell) which, during vibration, provides an analog output voltage proportional to the net force transmission between subject and restraint, i.e. the "live-load" force transmission

occurring at the animal-seat interface, Sharp (1963). The force transmitted between animal and support (restraint) during vibration reflects the relative movement of internal body organ systems and parts. Correlations of large transmitted force values to corresponding changes in circulatory parameters can indicate that movement of internal systems caused the observed circulatory changes via vessel occlusion, mechanical stimulation of the heart and/or vessels, reciprocating internal pressures, mechanical stimulation of regulatory receptors, etc.

Literature Review: Numerous investigations have been concerned with establishing the mechanical response of man and animals to whole-body mechanical vibration. Coermann (1962) applied the theory of mechanical impedance of systems with one or more degrees of freedom to sitting and standing man vibrated at frequencies from 1 to 20 Hz. He was one of the first investigators to demonstrate that the force transmission response of man to whole-body vibration could be approximated by that of a simple mechanical system consisting of interconnected linear inertial, elastic, and damping components. Experimental data confirmed results predicted by his model, i.e., that man had a primary whole-body resonance in the 4 to 8 Hz frequency range. Thus, it was quantitatively established that vibration frequencies between 4 and 8 Hz induced the greatest internal body organ movement relative to that input to the body by the vibration exciter. White, et al. (1962) reported the effects of mechanically induced vibration upon the human abdomen by measuring the pressure at the rectal end of the colon sigmoideum. For the semi-supine posture a mean "peak-to-peak" vibration induced fluctuation of 57 mmHg at 4 and 4.5 Hz was recorded. The pressure resonances were correlated to resonances of body organs in the thoraco-abdominal region. Clark et al. (1963) determined the effects of forced vibration by measuring from semi-supine man the circumferential body strain of chest, abdomen, pelvis, and thigh. All subjects showed maximum body strain



near 7 Hz. Zechman et al. (1965) reported maxima of seated man's transpulmonary pressure during 5 Hz vibration for 0.5 G acceleration amplitude. Lange and Edwards (1970) vibrated human subjects in the supine attitude from 2 to 14 Hz and 0.2 to 0.5 G. A principal body resonance was reported between 5 and 7.5 Hz, where also the maximum body strain was recorded. Using skeletal muscle tonus as a parameter they found that muscle tightening increased the whole-body transmitted force by as much as 50% during vibration at the resonant frequency. Edwards and Knapp (1972) recorded the force transmitted during repeated vibration of awake dogs. Results indicated reductions as great as 36% in the transmitted force recorded from the initial to the 7th exposure of one animal during 4 Hz vibration at 0.7g. Evces and McElhaney (1971) studied the effects of drugs on the mechanical response of dogs to vibration and reported that drugs produced measurable changes.

The nonlinear behavior of biomechanical systems has been the subject of several investigations. Krause and Lange (1963) described such behavior during vibration at various acceleration amplitudes over the 2 to 15 Hz frequency range. Wittman and Phillips (1969) also presented data that indicated the recognition of nonlinearities as seen in the measured impedance response of human subjects seated erect in several impact and vibrational environments. Vykukal (1968) combined a sustained acceleration (via a centrifuge) with vibration to study man's nonlinear mechanical response, and Vogt et al. (1973) used a similar experimental technique to conclude that the human body stiffens with increasing sustained accelerations, and that the resonant frequency increases from 6 Hz under normal gravity to 8, 11, 13, and 15 Hz with 2 Gx, 3 Gx, 4 Gx, and 5 Gx, respectively.

Efforts have also been directed toward establishing tolerance criteria for man exposed to vibration. Magid and Coermann (1960) vibrated seated human subjects at various frequencies, each with increasing amplitude at 0.75 mm per second until the subject reported that he felt actual bodily harm would result (this

limit being beyond discomfort). Results indicated minimal short time tolerance between 4 and 8 Hz at accelerations between 1.5 and 2.0 G. Ziegenruecker and Magid (1959) in a similar investigation presented a "short time tolerance" curve to sinusoidal vibration by gathering subjective data from man under vibration at various frequencies and amplitudes, i.e., at various accelerations.

Von Gierke (1971) chaired a symposium on "Biodynamic Models and their Application" for establishment of environmental exposure limits, for interpretation of animal, dummy, and operational experiments, mechanical characterization of living tissue and isolated organs, models to describe man's response to impact, blast, and acoustic energy, and performance in biodynamic environments. Because of man's obvious limitations as a subject in biodynamic experiments, animal surrogates have been used in many studies. Bantle (1971) used three vibration conditions to determine which was the most damaging to 4 1/2 and 7 day mouse embryos. It was found that a 20 Hz (visceral resonant frequency) vibration was the most destructive, and the 4 1/4 day embryo was the most labile. He reported that vibration typically inhibited embryonic growth. Ashe et al. (1961) recorded body weight and temperature of rats subjected to whole body vibration and showed that observed and measured differences to changes in frequency and amplitude indicated that both factors played a role, but calculations indicated that the common denominator was not simply acceleration.

In animals subjected to very high levels of acceleration (0.6 to 50 g) and various frequencies, tissue damage and survival correlated with mechanical response (Pape, et al., 1963; Boorstin, et al., 1966). Clearly, there are significant body resonances, particularly in the range below 12 Hz. Organ system resonances account, in part, for the subjective discomforts experienced by humans (Pape, et al., 1963). The type of symptoms occurring in human subjects appear related to both displacement and acceleration (Linder, 1962). The symptoms appeared somewhat dependent upon the acceleration level reached in the studies of Temple, et al. (1964) also.

Several studies have dealt with analytical models which help to explain the mechanical response of subjects to vibration. Broderson and Von Gierke (1971) investigated the biomechanical parameters of the sitting rhesus monkey and their temporal changes during sinusoidal vibration at frequencies from 6 to 30 Hz. Results showed impedance magnitude and phase angle to decrease with time. The authors also derived a simple model for the impedance response of the sitting rhesus monkey. Payne and Band (1971) developed a "four-degree-of-freedom" lumped parameter model for seated man to study the problem of his response to vertical accelerations.

Broderson (1972) conducted a study investigating the biothermal response of rhesus monkeys to mechanical vibration. He concluded that core temperature increased particularly at resonance and varied with frequency. Prolonged 1.0g vibra-

tion at 30 Hz were shown to increase core temperature by about 1/2 C, and the primary mechanism was speculated to be frictional dissipation. Lafferty et al. (1973) and Edwards and Lafferty (1973) also conducted studies concerned with the response of the rhesus monkey to mechanical vibration. The mechanical impedance response, its variation with time during vibration at a given frequency and acceleration amplitude, and a mechanical model to predict the impedance response at different frequencies and accelerations up to 1.0 G are described by these investigators. The effect of vibration on a performance task, and related changes in physiological parameters were also discussed.

The effects of vibration on performance has been the subject of many investigations. Lange and Coermann (1963) measured the visual acuity of human subjects during whole-body vibration at various low frequencies. They reported that maximum decrements occurred at those frequencies where resonance of whole body and organ complexes had previously been determined, i.e., 4 - 8 Hz. O'Braint and Ohlbaum (1970) presented a method to describe the visual efficiency of vibrated man in terms of a Performance Index.

Studies of human tracking performance showed inconsistent effects when different frequencies and accelerations were the parameters (Frazer, et al.,

1961). In seated subjects performing a light-pattern psychomotor task using a control stick, Fraser, et al. (1961) found displacement to be the predominant factor in determining performance decrement. An increase in either displacement or frequency was significantly related to performance decrement, but a combination of any frequency with the lowest displacement did not produce a performance decrement. Increase in displacement at any frequency did produce a decrement which could be intensified by changes in frequency. The frequencies used were 2, 4, 7, and 12 Hz at displacements of 0.125, 0.25, 0.375, and 0.5 in. double amplitudes. Maximum peak acceleration was 3.67 g. Regression analysis showed mean error was most closely correlated to the product of the displacement and the square root of the frequency. Interestingly, the frictional resistance component of surface impedance is also proportional to the square root of frequency. A function of both displacement and impedance was suggested as the most satisfactory parameter (Fraser, et al., 1961).

In related studies, Catterson, et al. (1962) extended the analysis of the role of displacement and frequency in human tracking performance. Exposure duration was 20 min at 6, 8, 11, and 15 Hz and displacements of 0.13 and 0.26 in. double amplitude. A decrease in error occurred at all frequencies for 0.13 in. displacement, and an increase in error occurred at all frequencies for 0.26 in. displacement. As pointed out by Catterson, et al., acceleration is proportional to displacement times frequency squared, and functions determined by acceleration must reflect changes in frequency to a far greater extent than amplitude.

Grether et al. (1972) extended an earlier study in which they reported that a combination of heat, noise, and vibration stress had no greater, and for some measures slightly less, effect on physiological and performance functions than did the same levels of heat or vibration alone. The study searched for possible explanatory mechanisms for the apparently antagonistic stress interaction. It

was postulated that the heat stress might in some way have modified the biodynamic response of seated man so as to reduce the vibration transmitted to the subject's body. However, transmissibility data for the shoulder showed no evidence of any such effect. It was postulated that increased motivation and application of effort during the combined stress exposures might be the responsible mechanism. Sommer and Harris (1972) exposed 10 human subjects to vibration (5 Hz, 0.25 g) and noise (110 dB) while asking them to perform a mental arithmetric task. Results suggested that the phase of the circadian cycle could be a variable to be considered in studies on the effects of stress on human performance.

The effects of vibration on behavior has also been investigated. Wike and Wike (1972) reported results from seven experiments on low-frequency, whole-body vibration of rats as related to their escape conditioning. They concluded that vibration of sufficient amplitude is aversive for rats and that its brief termination is reinforcing. A direct relationship was evident between amplitude and the number of escape responses when frequency was held constant and amplitude was varied.

The area receiving the most attention is the effect of vibration on the cardiovascular system. Roberts and Dines (Oct., 1966) administered propranolol and atropine to anesthetized vibrated dogs and measured heart rate, cardiac output, total peripheral resistance, and  $(dp/dt)_{\max}$  of left ventricular pressure. They concluded that tachycardia during vibration resulted from a decrease in vagal efferent activity to the heart. In vibration tests using human subjects Roberts et al. (1969) concluded: "(1) clinically useful ECG's can be obtained from human subjects while they are being vibrated, even at relatively severe intensities, if our recommendations to accomplish this are followed, (2) short time vibration in the practical range used were only moderately stressing to healthy subjects, (3) vibration can elicit pre-

mature extrasystoles in man, (4) changes in configuration of ECG's observed during vibration were transient, terminating with termination of vibration, and (5) patterns of pulse rate changes during vibration are variable." Edwards (1970) and Edwards, McCutcheon and Knapp (1972) performed tests in which dogs were vibrated at 1-3G from 2 to 12 Hz, during which chronically implanted transducers enabled recording cardiovascular data, and showed the greatest changes occurred in the 3 to 9 Hz frequency range for any given acceleration amplitude. 3G vibration to 4 Hz produced (1) a maximum aortic peak flow rate of more than twice the maximum recorded from the resting animal, and (2) a minimum aortic peak flow rate of only 10% of the minimum observed in the resting animal. The results also indicated a correlation between relative motion of internal masses and large changes in the circulatory system during the vibration exposure.

Hooks, Nerem, and Benson (1969) performed a theoretical analysis of pulsatile flow in a rigid tube with longitudinal vibration by introducing as a boundary condition a sinusoidal wall velocity. Using a sinusoidal pressure gradient of constant amplitude they predicted flow rate increases of 400% or reductions to zero relative to the flow rate which occurred without vibration. Camil, Knapp, and Collins (1971) used the analog computer to model the response of the human cardiovascular system to 1-10 Hz sinusoidal vibration. Their study showed the most pronounced effects at 3-4 Hz for all acceleration amplitudes investigated. For an acceleration amplitude of 3G they reported the maximum difference in peak aortic pressure during one heart cycle tripled and the maximum peak aortic flow doubled, relative to the control values.

Arntzenius, Koops, and Hugenholtz (1969), Blok et al. (1969), Verdouw, Arntzenius, and Noordergraaf (1969), and Jackson (1971) reported a technique

employing Body Acceleration Synchronous with the Heartbeat (BASH) in which a particular type of whole-body vibration applied to both animals and man was reported to enhance cardiovascular performance. The use of vibration as a noninvasive cardiac assist device was thus reported.

Any effect primarily dependent on the degree of mechanical stimulation that increases with increasing amplitude of movement should increase with decreasing frequency if peak acceleration is held constant. If amplitude is held constant, the effect will increase with increasing peak acceleration and consequently increase with increasing frequency. This was found to be true for the responses of hyperventilation (Dixon, et al., 1961) and peripheral vasodilation (Liedtke and Schmid, 1969). Gaeuman, et al. (1962) cited the previous reports of Fraser, et al. (1961) and Catterson, et al. (1962) to substantiate their experimental design for the measurement of oxygen consumption. The subjects were exposed to a constant peak-to-peak displacement of 0.264 in. double amplitude, and frequencies of 2, 6, 8, 11, and 15 Hz. Since displacement amplitude was constant, acceleration should increase with frequency. The values given for peak acceleration at each frequency were 0.05, 0.45, 0.82, 1.55, and 2.88 g respectively. A clear frequency-displacement dependence of oxygen consumption was demonstrated, suggesting constant displacement was a useful parameter. Hoover and Ashe (1962) used displacements of 0.124 and 0.250 in. double amplitude at frequencies from 2 to 15 Hz. The peak acceleration range was 0.03 to 2.88 g. The magnitude of the resulting hyperventilation showed a mixed frequency-displacement dependence. Respiratory rate changes were predominant at a displacement of 0.124 in., while tidal volume changes were predominant at a displacement of 0.250 in. They concluded the respiratory response tended to be related primarily to table displacement.

An initial tachycardia, hypotension, increased cardiac output and decreased total peripheral resistance was the characteristic change in the anesthetized dogs studied by Dines, et al. (1965). The parameters were frequencies of 4, 7, and 11 Hz at a displacement of 0.5 in. double amplitude. They averaged the responses at all three frequencies, and did state the blood pressure dip was not evident at 11 Hz.

In contrast, a large body of data supports the primacy of a frequency-acceleration dependence of the above responses (Guignard, 1960; Goldman & von Gierke, 1960; Zechman, et al., 1965; Cavagna, 1970; Edwards, et al., 1972).

Acceleration dependence of cardiovascular changes has also been demonstrated in animals (Hood and Higgins, 1965; Liedtke and Schmid, 1969). More marked physiological effects were found at 1.2 g and 8 and 10 Hz than at 0.6 g and frequencies on either side of that range (Hood, et al., 1966). Clark, et al. (1967), in studies of anesthetized dogs, found significantly greater change in multiple systemic cardiovascular variables at 2 than at 1 g for frequencies of 10, 12, and 14 Hz. (Apparently 2 g runs were not made at 6 and 8 Hz).

The changes in oxygen consumption observed by Duffner, et al. (1962) were maximal at the lowest frequencies and greater at 0.35 than at 0.15 g acceleration.

Another type of physiological interaction of frequency and displacement is illustrated by the mechanoreceptor responses. Although the exact route by which muscle stimulation is connected to cardiovascular and respiratory responses is unclear, increases in systemic ventilation and blood pressure are produced by muscle stimulation such as rhythmic manual squeezing at 2 to 3 Hz, and the response is abolished by cutting the nerve (Guyton, et al., 1972, and McCloskey, et al., 1972). Of course the carotid sinus also has distinctive frequency-amplitude characteristics, but its



participation in the responses is likely to be minimal since its sensitivity is probably reduced (Bristow, et al., 1971).

Acceleration was a much more important factor than duration in cats exposed to severe vibration (10 to 15 g; Pape, et al., 1963). It would thus appear that dogmatic statements about the interaction of displacement, frequency, and acceleration are inappropriate, and each must be considered in evaluating the effects of vibration stimulus.

Previous studies of the integrated response of the cardiovascular system to vibration have also produced variable and often conflicting results. Components of cardiovascular function including heart rate, blood pressure, and cardiac output have been reported to decrease, increase, or remain unchanged during vibration. Hood and Higgins (1965) studied anesthetized, supine dogs restrained in a form-fitting metal frame and vibrated in the x-axis at selected frequency and acceleration levels. Cardiac output increased as a result of increased heart rate at the higher acceleration levels; i.e. stroke volume remained constant. At 6 Hz, mean arterial pressure increased slightly; at 10 Hz, it decreased. Total peripheral resistance was not significantly altered at 6 Hz but increased at 10 Hz. Overall, they were unable to identify any main effects of frequency or duration. Main effects of acceleration were present for most of the variables. There were interactions between acceleration and frequency for heart rate and mean arterial pressure.

In other studies, tachycardia, decreased arterial pressure, increased cardiac output, and decreased total peripheral resistance were indicated (Clark, et al., 1967; Dines, et al., 1965; Hoover, et al., 1961). Clark, et al., 1967 found mean arterial blood pressure decreased initially and then returned to control levels; stroke index remained constant. The effects were greater at higher G levels.

In the presence of pharmacological blockage of skeletal muscle contraction, dog forelimb resistance was decreased by vibration (Liedtke, and Schmid, 1969). The magnitude of the decrease was reduced with limb deervation but not eliminated.

There are no previous reports of the detailed cardiovascular changes produced by vibration of unanesthetized animals.

In the human subjects studied by Lamb and Tenney (Lamb, and Tenney, 1966), heart rate and blood pressure were unchanged. Hood, et al., 1966, described increases in mean arterial blood pressure, heart rate, and cardiac output in tightly restrained, semisupine humans exposed to 7 minutes of wholebody, x-axis vibration. In the tightly restrained, upright human subjects studied by Clark, et al., 1967, mean arterial blood pressure and heart rate increased slightly, and cardiac index approximately doubled.

The metabolic-hormonal effects of vibration have been similarly variable. Oxygen consumption has been found to increase, decrease, or remain unchanged in both anesthetized dogs and humans (Dixon, et al., 1961; Lamb and Tenney, 1966; Hoover and Ashe, 1962; Hutt, Horvath, and Spurr, 1958; Duffner, Hamilton and Schmitz, 1962; Gaeuman, Hoover and Ashe, 1962; Young, et al., 1963; Hood and Higgins, 1965; Hood, et al. 1966). Hood and Higgins, 1965, found decreased oxygen consumption at 6 and 10 Hz and 0.3 g acceleration amplitude; at 1.3 g it increased out of proportion to the increase in cardiac output. Levels of 17-hydrocortosone (17-OH-CS), epinephrine, and total catecholamines were elevated in supine dogs exposed to prolonged periods of whole body, Z-axis vibration. The effects decreased with increasing displacement and acceleration amplitude and were greater in awake than in anesthetized dogs (Black, 1965). Plasma and urine levels of 17-OH-CS decreased in humans exposed to three periods of three minutes of vibration at selected frequencies from 1 to 20 Hz and acceleration amplitudes of 0.75 to 3 G; even though decreased, values remained within normal limits (Homma, Kanda, and Watanabe, 1971).

Although the trend of these data bears a superficial resemblance to the changes occurring with exercise, the responses show great variation and differ in important ways from those usually produced with exercise. Analysis of the effects of vibration has been complicated by the limited combinations of frequency and amplitudes of displacement and acceleration used in previous studies. The purpose of this report is to clarify the previous observations on the cardiovascular effects of vibration by summarizing results from an extended series of tests over a wide range of sinusoidal vibration combinations applied to both awake and anesthetized dogs.

#### B. Experimental Protocol

Response of acutely and chronically instrumented dogs, primates and pigs have been studied. Special emphasis has been placed on the chronically implanted preparation which permits repeated awake and anesthetized tests on the same animal. Additional advantages of this preparation include the closed chest protocol and more stable transducer characteristics, especially important for the vibration environment.

Animals are restrained on the hydraulic table with the spine vertical, and vibrated along that axis. Short term tests consist of sequential exposures to sinusoidal vibration of 2-12 Hz and acceleration amplitudes ranging from 0.5 g to 3.0 g for 30 sec., 2 min., and 5 min. intervals. Long term exposures include durations varying from 30 min to 6 hrs. at a selected vibration frequency and constant acceleration amplitude. The highest g-level for the awake animal is 1.5 g, and for the anesthetized animal is 3.0 g. The cardiovascular variables include heart rate, flow velocity from the aorta and peripheral arteries, arterial pressures from acceleration-insensitive intraaortic and intraventricular transducers,  $O_2$  consumption and body temp. and blood chemistries such as blood gases, cortisol, free fatty acids, and glucose, measured on samples withdrawn from indwelling atrial and arterial catheters. The design of the vibration exciters

permits recording of force transmitted between subject and table, and also the vibration exciter velocity. From these variables and their phase relationship, complex mechanical velocity impedance can be determined. In addition, accelerometers implanted on large body organs provide information on the displacement of these organs relative to the animal torso and the input vibration. A Raytheon 704 data acquisition system is being programmed for off-line and on-line analysis of the massive amount of cardiovascular and mechanical data.

1. Animal Preparation: Two basic surgical procedures have been implemented. The most consistent results have been obtained with the intra-thoracic implantations involving the heart and large vessels. Instrumentation implanted may include aortic flow probe, aortic and left ventricular pressure transducers, right and left atrial and subclavian-aortic cannulae, pacemaker on right atrium, temperature probe within the chest, and an accelerometer (single axis) on the heart or proximal blood vessel. Abdominal and neck entries have been employed to a lesser extent for the measurement of peripheral cardiovascular parameters.

The choice of transducers to be implanted in both preparations is flexible although experience has shown that standardizing the surgical procedure and setting a limit on the number of devices implanted is necessary. As part of the program design, the chronic preparations have allowed a number of differing experimental protocols to be followed. Such experiments include vertical z-axis (and more recently, horizontal z-axis) vibration, hypovolemic shock, baroreceptor response, and animal performance tasks. A combined chronic-closed chest and acute-peripheral vessel preparation has also been used successfully.

A healthy animal and reliable implanted instrumentation make a successful animal preparation and will yield usable physiological data. Individual animals are tested for acceptance, and these guidelines, combined with previously published normals, provide control values for post-operative care. Along with

the hematological variables examined in the implanted animal, metabolic and hormonal determinations now include blood gases, cortisol, free fatty acids, and glucose.

Thorough evaluation, regular testing, and redesign of transducers and materials have become an integral part of our implantation schedule. In particular, pressure transducers and flow probes (as well as flowmeter instrumentation) have been subjected to these continuous tests. Experimental access to the implanted transducers and catheters stored in a fabric pouch of the chronic animal is quick and non-traumatic. Details of the animal preparation are presented in Appendix A.

2. Experimental Procedure: On the day of the experiment the dog is walked to the laboratory and placed in a nylon mesh sling. The monkeys are transported to the vibration room in an open-back restraint chair. While the leads are removed from the storage pouch, the vibration facilities are calibrated. If all the transducers and cannulae are functioning, the animal is then placed in the vibration chair and firmly restrained. Acute placement of a transducer, if necessary, is accomplished at this time using a local anesthetic (Xylocaine) and, if required, morphine I.M. (1-3 mg/kg).

Calibration of the pressure gauges is done with chronically placed cannulae and an extravascular pressure gauge, making sure that measurements do not include an additional hydrostatic pressure head. Some of the analog transducer signals are then sent to the computer for A/D conversion.

Following transducer calibration, the dog is placed in the restraint chair and the restraint chair is then attached to the hydraulic table. Pre-vibration control and post-vibration recovery periods normally last for 10 to 30 minutes. Depending on the vibration protocol, periodic blood sampling and instrument re-calibration and balancing may be done before, during, and after the experiment.

For an anesthetized preparation, the animal is given an intramuscular injection of morphine (3 mg/kg), a blood sample for blood gas controls is withdrawn, and after 30 minutes, the animal is anesthetized with chloralose-urethane given I.V. The level of anesthesia used is that required to suppress the voluntary ejection of a tracheotomy tube. The animal is then respiration with room air and blood gases are regularly monitored and controlled with the respiratory rate and/or volume.

Following the experiment, if the animal is to be used for further study, the lead connectors are sealed, cleaned, and returned to the pouch which is closed with interrupted sutures or steel clips. The pouch area is bandaged, a nylon jacket is placed on the animal (for monkeys, a leather jacket is also fitted), and the animal is returned to the animal care facility. Further details of the experimental procedure are presented in Appendix A.

3. Data Acquisition and Analysis: The Raytheon 704 system (Appendix B) is designed to fulfill two major requirements for the vibrational stress experiments. First, a real-time output of various physiological variables in terms of graphs on a storage oscilloscope and a printed record on a teletype is needed. This will provide feedback to the experiment controller so that the protocol may be varied according to the results being obtained. Secondly, the data reduction process must be speeded up and improved in accuracy. The 704 is fast enough to provide several real time outputs and at the same time store data on magnetic tape for later operator-controlled analysis.

The two program systems (Dye Curve and Mean Value) which have been implemented to date are described in detail in Appendix B.

The more ambitious part of the design system is now being developed. Outputs of pulsatile as well as average signals will be provided in real time. A real time CRT display of the physiological and mechanical variables will pro-

vide compression of the data and feedback to the experimenter. Preliminary specifications for this system are also presented in Appendix C.

## C. Results

### 1. Experimental

Physiological Responses: For unanesthetized dogs receiving short-term (30 sec) exposure to vertical, whole-body vibration, the major finding is the overall linear relationship between mean flow in the ascending aorta (MAF, equal to cardiac output less coronary flow) and the level of vibration stress as measured by the ratio of peak net transmitted force to body weight (PNF/BW) (Fig. 2). For 10 experiments on 6 dogs, the regression equation for the relationship between percent change in MAF and per cent change in PNF/BW was  $0.00 + 0.476 \text{ PNF/BW}$ , with a standard error of the estimate of  $\pm 26.71$  and a R(correlation coefficient) of 0.70.

At a PNF/BW level in the range of 1.5 to 2.0 times body weight, near the maximum values applied in these studies and in the region of resonance, the mean increase in MAF was 1.6 times the control value. For PNF/BW levels in the neighborhood of 0.8 times body weight, a few of the MAF values were unchanged or decreased from control levels. Extreme values for the change in cardiac output were +150 percent and -30 percent of the control value taken immediately preceding the exposure.

The relationship between MAF and PNF/BW was much more closely correlated in individual dogs (Figures 3 a and 4a). Also, mean aortic blood pressure was generally unaltered (Figure 3a) hence total peripheral resistance decreased (conductance increased). The relative contributions of heart rate and stroke volume to the increases in MAF exhibited three distinct classifications. In three of the 10 experiments (2 animals) MAF was increased by increased heart rate, with minimal or no change in stroke volume (Category 1, an example of one animal is shown in Figures 3a, b, and c). In 4 of the 10 experiments (3 animals)

MAF was altered primarily by changing stroke volume, with little or no change in heart rate (Category 2, an example of one animal is shown in Figures 4a, b, and c). Approximately equal contributions from changing heart rate and stroke volume were present in 3 of the 10 experiments (3 animals): in this category, both variables were linearly related to PNF/BW (Category 3, an example is shown in Figures 5a, b, and c).

Domination of heart rate as the principal mechanism for increasing MAF appeared to be a function of the heart rate level at the initiation of vibration exposure of Category 1 and 2 animals. In those animals with initial heart rates under 150 beats/min (BPM), altered heart rate was the major response (Category 1); for those animals with initial heart rates above 150 BPM, altered stroke volume was dominant (Category 2). Initial heart rates were not the significant factor for those animals changing both heart rate and stroke volume (Category 3). In this category initial heart rates ranged from 78 to 204 BPM.

The general pattern in the anesthetized dogs was similar, but grouped responses showed much more scatter (Figure 6). The regression equation for the relationship between percent change in MAF and percent change in PNF/BW was  $0.40 + 0.15 \text{ PNF/BW}$ , with a standard error of the estimate of  $\pm 7.8$  and a R of 0.27. Individual correlations between MAF and PNF/BW were again high.

In contrast to the three categories of MAF alteration in the awake animals, the anesthetized animals increased MAF through only two mechanisms, some exhibiting a modest increase in heart rate and others a more significant increase in stroke volume.

For the 3 of 6 animals altering MAF by a change in heart rate, the mean changes in the anesthetized animals were 95% lower than those in the unanesthetized animals (Fig. 7a, b and c). For the 4 of 6 anesthetized animals altering MAF primarily through changes in stroke volume, the differences were not statistically significant from those of the awake animals (Fig. 8a,b, and c). When examined individually, the slope of MAF vs PNF/BW varied directly with the initial stroke volume of the anesthetized dogs.



While the stress level as measured from peak net force is of major importance, it is not the exclusive determinant of the response, for the relationship between the percent change in MAF and the log of the ratio of mean heart rate to vibration frequency is also linear (Fig. 9).

Mechanical Responses: A portion of the research during the past year involved a coordinated effort between the AFOSR and the AMRL contracts. Work performed on the latter was primarily directed toward investigating the effects of vibration upon the tracking performance of Rhesus monkeys. Although the ultimate goals of the two contracts were different, each involved vibration testing of animals during which mechanical and physiological measurements were made. A part of the effort on each contract thus complemented the other. One such complementary phase involved the development of a two mass, single-degree-of-freedom analytical model to predict the mechanical impedance response of the sitting Rhesus monkey to 2 to 30 Hz vibration at acceleration amplitudes from 0.5 to 1.0g. Figure 10 illustrates the sequential development of the model, and figure 11 presents the final model with linear approximations for frequency dependent whole-body coefficients of elasticity and damping normalized by animal body weight. Figure 12 contains graphs of the elastic and damping coefficients versus frequency. The values were obtained for each test at each frequency by requiring the impedance of the model to match that of the primate. A part of the model is an empirical equation defining, as a function of vibration frequency and intensity, the ratio of non-reactive to reactive animal mass. After normalizing for body mass and averaging, functions for the elastic and damping coefficients were developed such that the impedance response of the model closely matched the experimental results throughout the 2 to 30 Hz range at 0.5 G (see Figure 13) and also at 1.0 G (see Figure 14). A detailed description of this study can be found in the appendix in the paper "A Model to Predict the Mechanical Impedance of the Sitting Primate

During Sinusoidal Vibration" by R. G. Edwards and J. F. Laffert (Appendix D). The amount of energy dissipated by viscous damping in a vibrated animal can be derived from the experimentally measured impedance data. Figure 15, for a sitting Rhesus monkey, contains graphs of dissipated energy versus time of vibration exposure for three different frequencies, i.e. 6, 12, and 20 Hz, each at 0.5 g acceleration amplitude. Although the data from the 12 and 20 Hz exposures did not indicate any significant temporal trends, the 6 Hz exposure did indicate a reduction in dissipated energy with increasing time of vibration exposure. During ten 1.5 g tests of two primates the acceleration at the top of the skull was recorded. This was accomplished by securely taping to the top of the animal's head a minute piezo-resistive accelerometer. The sensitive axis of the accelerometer was approximately along the axis of vibration. This measurement enabled the calculation of the ratio of head to vibration exciter acceleration, i.e. the head to vibration exciter transmissibility. The purpose here was to establish, as a function of frequency, how much of the input acceleration was actually transmitted to the subject's head. Figure 16 is a graph of average head to vibration exciter transmissibility versus frequency. At 3 Hz the 1.5 g applied to the subject resulted in an average peak acceleration at the head of approximately 1.6 times greater than the input value, i.e. of about 2.4 g. From 3 to 30 Hz the transmissibility decreased with increasing frequency. The acceleration of the head at frequencies less than 12 Hz was amplified relative to the input acceleration, i.e. the transmissibility was greater than 1.0, while from 12 to 30 Hz it was attenuated, i.e. it was less than 1.0. At 30 Hz only 20% of the input acceleration was transmitted to the head.

As an example of the impedance data of the dog tests consider the impedance modulus and phase angle versus vibration frequency graphs contained in Figure 17. Two curves appear on each graph; one for a 1 g test at frequencies from 2 to 20 Hz with the animal unanesthetized, and the other for a similar vibration protocol

but with the subject anesthetized with chloralose -urethane. Relative to the unanesthetized data, it is apparent from these graphs that anesthetizing the animal resulted in a 2 Hz decrease in the primary whole-body impedance resonant frequency, i.e. from 6 to 4 Hz, and, in general, a more "mass-like" response (compare to the inert mass, or "m" impedance response). At frequencies from 7 to 12 Hz the impedance phase angle for the drugged animal is approximately  $20^\circ$  greater than that for the unanesthetized condition. Since the phase angle for an inert mass is  $90^\circ$ , and those for a massless damper and massless spring are, respectively,  $0^\circ$  and  $-90^\circ$ , both the impedance modulus and phase angle data reflect a decreased muscle tonus, i.e. a decreased whole-body elastic coefficient, for the anesthetized (relative to the unanesthetized) dog. This kind of impedance data interpretation is particularly useful where applied in a model from which whole body coefficients of elasticity and damping can be extracted.

Similar to the aforementioned transmissibility measurement on the Rhesus monkey, it was desired to gain information on the transmissibility of certain internal organs and vessels for the vibrated dog, i.e. the amount of organ and/or vessel movement relative to that applied by the vibration exciter. A minute Konigsberg piezo-resistive accelerometer (Model A2) was securely sutured to an implanted aortic flow transducer on one animal for the purpose of gaining information as to the amount of input vibration that is transmitted to the aorta. The upper portion of Figure 18 is a graph of the ratio of acceleration at the aortic transducer location to that of the vibration exciter, i.e. to that of the input vibration, versus vibration frequency with 0.5, 1.0, and 1.5 g as parameters. The lower portion of Figure 18 is a corresponding graph of the phase relationship between the aortic transducer acceleration and that of the vibration exciter. The elastic nature of the thoracoabdominal system is clearly evident from these graphs. Although some differences do exist as a function of the input acceleration amplitude, a first approximation could well consider the response linear in

the 2 - 30 Hz range for acceleration amplitudes from 0.5 to 1.5 g. The magnitude curves clearly show a resonance at 4 Hz. A secondary resonance occurred at 9 Hz during the 0.5 and 1.0 g tests, but was not present in the 1.5 g test. During vibration at the 4 Hz primary resonant frequency a transmissibility of from 2.3 to 2.4 was recorded. For example, during 5 Hz vibration at 1.5 g an acceleration of approximately 3.6 g was recorded at the aorta. Beyond approximately 11 Hz the transmissibility drops below 1.0, i.e. there is less acceleration transmitted to the aorta than is applied to the animal. At 30 Hz only about 15% of the applied acceleration is measured at the aorta. The almost linear increase in phase angle with increasing frequency is indicative of an elastic-type response. The graphs of figure 18 illustrate the frequency dependence of the aortic transmissibility, i.e. of the amount of acceleration transmitted to the aorta as compared to that input by the vibration exciter. These data represent the transmissibility of the aorta with electromagnetic flow transducers and accelerometer attached. The added mass of these transducers result in transmissibility values different from those which would be measured from a "mass-less" accelerometer; however, these reported values are thought to be reasonably indicative. These graphs illustrate two very pertinent facts with respect to studies such as the current one; namely (1) the magnitude of any given applied whole body vibration transmitted to the aorta is extremely frequency dependent, and (2) there is a resonance at approximately 4 Hz, at which frequency the applied vibration amplitude is intensified approximately 2.4 times when measured at the aorta.

## 2. Computer Modeling

Cardiovascular modeling has progressed in two directions. The first of these is a closed-loop electrical analog model of the hydraulic and mechanical aspects of the CV system, which is an extension of an earlier open-loop model. These effects of vibration are simulated by pressure source terms generated from values of the vibration g-level or resulting transmitted force. These pressure distur-

bances propagate and reflect, adding and subtracting with the pressure generated by the action of the heart, and as a result produce changes in flow. The closed-loop model contains piecewise-linear representations of venous resistance and compliance which were included to accurately account for blood-volume shifts occurring during postural changes and application of time-varying whole-body acceleration. The possible enhancement of cardiac output by the application of whole body acceleration synchronously with the heart cycle was investigated by R. L. Starnes in an M.S. thesis study (see Appendix E). He found that simulated cardiac output could be enhanced by only a few percent when the acceleratory frequency was the same as the heart frequency (1.25 Hz). This study has recently been extended to acceleratory frequencies at whole multiples of the heart frequency. It has been found that an acceleratory forcing function of 3.75 Hz and 4 G peak amplitude enhances cardiac output by about 20 percent.

A preliminary study has begun in which experimental data of HR, SV and PNF are used as input parameters to the model. The value of PNF/BW vs frequency from the animal experiments is used to establish the values of the pressure source terms for the different simulated vibration frequencies. Heart rate was varied in the model as observed in the animal experiment. The computer response of MAF vs PNF/BW was similar to those of the animal experiments, with the actual percent change values close to those found for the group of anesthetized dogs changing MAF with minimal change in heart rate and little change in stroke volume, e.g. maximum percent change in MAF was approximately 25%.

The second direction of progress is the development of a digital model analogous to the analog model. Two primary reasons for moving in this direction are: (1) the digital model can be expanded if desired, to permit more detailed regional investigations. The analog model has been expanded to the point where present computer capacity is exhausted. (2) Nonlinear baroreceptor and other CNS control phenomena can be more easily modeled with the digital approach. The digital model has

successfully simulated cardiovascular performance in the prone position (no acceleratory stress) and is presently being adapted to account for postural changes and time-varying applied accelerations.

#### D. Discussion

For the range of vibration stress imposed on the dogs in this study in the vertical (z-axis) direction, the effect of vibration on mean aortic flow (MAF) was found to depend primarily on the net force absorbed by the whole body (peak net transmitted force, PNF). Other less important, but significant, factors are initial or control heart rate and stroke volume, vibration frequency, body weight, and duration of exposure. For brief exposures at PNF levels quadruple the body weight, MAF may be expected to reach levels nearly double those present immediately prior to the exposure. For PNF levels less than body weight, variation in response may include a few instances of unchanged or decreased MAF.

Detailed comparison of these findings with the results of previous investigations is difficult since frequency, displacement, and/or acceleration were the only vibration parameters available in earlier data. In the present study, testing of these three parameters generally resulted in much greater variability with poorly developed trends. Thus the major determinant of the response appears to be the net effect of the interaction of all three components as reflected in PNF.

The general tendency has been to equate the effects of vibration with those occurring in mild to moderate exercise. Our results support this comparison with regard to the extent of the change in MAF. For the vibration case, however, it is unlikely that the magnitude of the increase in MAF, and the interaction between heart rate and stroke volume, are metabolically dependent in the manner observed with exercise. For instance, heart rate and cardiac output with exercise in the dog are linearly related to oxygen consumption; this is probably not the case for vibration (Barger et al., 1956). Although the data are incomplete, the level of

vibration stress and oxygen consumption are probably related only to the extent that the imposed vibration leads to muscle contraction, especially for postural adjustments (Duffner, Hamilton, and Schmitz, 1962).

The extent of muscle contraction is somewhat difficult to estimate. The anesthetized animals of Hood and Higgins, 1965, responded to vibration with some increase in oxygen consumption which was reduced by curarization. However, in related studies in our laboratory of awake *Macaca mulatta* exposed to force levels similar to those used with the dogs, oxygen consumption changed with varying performance demands but was not dependent on PNF/BW. Results from selected measurements of arterial and venous pH,  $pO_2$ ,  $pCO_2$ ,  $O_2$  and  $CO_2$  content, and nonesterified fatty acids in the monkeys and in the dogs in the present study do not show any consistent dependence on PNF or other vibration parameters at the levels used.

Mediation of the response through cyclic muscle contraction induced by variation in the direction of the PNF is unlikely, since cardiac output did not follow sinusoidal exercise above 0.2 Hz (Ashkar, 1972): a rate much lower than in our studies.

Neural mediation appears to be a far more important determinant of vibration responses than direct metabolic effects. The effect on MAF was greatly attenuated in the group of anesthetized dogs with limited change in heart rate. The effect in the unanesthetized animals is analogous to a sustained state of alertness or alarm. In the group of dogs in which the level of anesthesia limited the increase in heart rate, the change in MAF was significantly different from that produced in unanesthetized dogs. Typically with exercise, the rapid onset and offset of the heart rate response is dependent on neural pathways (Rushmer, Donald and Shepherd); similar effects are present with vibration. Mediation through the carotid sinus is unlikely since the frequency content added to the phasic pressure waveform is relatively high (Edwards et al, 1972) and the increased heart rate in the unanesthetized animals suggests absence of

carotid sinus suppression.

The principal neural channel which could lead to the observed effects is afferent sensory information from peripheral mechanoreceptors. Small myelinated and unmyelinated fibers have been shown to be primary afferent pathways in cardiovascular and respiratory reflex responses (McCloskey, Matthews, and Mitchell, 1972). Vibration-sensitive receptors are included in the proprioceptors of these afferents. The primary afferents of muscle spindles are not significantly involved in these effects; high frequency (100 to 300 Hz) vibration of the triceps sura muscles of both hind limbs of decerebrate or anesthetized cats had no appreciable influence on systemic arterial blood pressure, heart rate, or respiratory rate or depth even though some reflex muscle contraction was produced (McCloskey, Matthews, and Mitchell, 1972).

The importance of neural pathways in whole-limb vibration is supported by the results of Liedtke and Schmid, 1969. Peripheral vasodilation in the intact limb was much greater than in the limb following denervation, and little alteration followed section of the carotid sinus and vagal nerves.

The initial value and slope dependence of the variables is most likely a secondary phenomenon in relation to the effects of vibration, but is of considerable interest. The dependence of the magnitude of a physiological response on the preceding level is to some degree inherent in the range and type of adjustments available. At high heart rates, further excitation cannot lead to a very large response in cardiac output through further increases in heart rate; therefore increases in stroke volume would be expected. The validity of the "law of initial values" (Wilder, 1957) (Lacey, 1967) for non-extreme levels has been difficult to substantiate, but for heart rate, strong presumptive evidence of its presence and mediation by central neural activity has been obtained in monkeys (Snapper, Kadden, and Schoenfeld, 1971). The fact that many of the unanesthetized dogs exhibited a combined heart rate and stroke volume response is



unexplained with respect to vibration, but is certainly an option available to the system. Dependence of MAF on the ratio of mean heart rate to vibration frequency suggests the presence of effects derived from the fluid-mechanical and time-dependent system properties. As previously discussed, in the absence of synchronization between vibration and cardiac cycles, this effect is relatively minor.

In summary, the peak net transmitted force has been shown to be a major variable determining the cardiovascular response of dogs exposed to brief, whole body, sinusoidal vibration applied in the spinal axis. The effect is markedly decreased when the heart rate response is limited by anesthesia.

Thus vibration appears to be a stress which can be graded to produce a quantifiable state of alertness resembling exercise, but separating the neural and metabolic components. Analysis of system properties based on this approach offers great promise for increasing our understanding of physiological regulation.

#### E. Recommendation.

1. Studies should be continued to evaluate further the role of the five mechanisms involved in producing changes in pressures and flows in the cardiovascular system exposed to vibration. Special emphasis should be placed on experiments which can separate and elucidate the role of the various mechanoreceptors - CNS pathways from the rest of the mechanism. This is especially important since these mechanisms are thought to produce about 70% of the changes observed in the awake animal.

2. More experiments in which  $O_2$  consumption is measured on animals under vibration should be conducted in order to confirm the analogy of vibration and exercise.

3. Experiments should be conducted in which the vibration frequency is extended below 2 Hz. This can be accomplished by using a variable radius centri-

fuge to produce slowly varying sinusoidal acceleration.

These experiments could provide some of the missing information which now exists between sustained acceleration (0 freq.) and vibration (above 1 Hz), i.e. the slowly varying time dependent acceleration range (0-1 Hz). These experiments would provide continuity in describing the response of the cardiovascular system from sustained acceleration to high frequency vibration.

4. The mechanical impedance model should be combined with the analog computer model of the hydraulic aspects of the cardiovascular system in order to define more realistically the vibration forcing function, PNF, in the computer studies.

5. The analog computer model should be expanded to include mechanoreceptor response and the digital model should be expanded to include more detailed sections of the arterial and venous system. These models are excellent guides in planning experiments and evaluating the resulting data.

## F. References

- Arntzenius, A. C., J. Koops, and P. B. Hagenhaltz. Cardiovascular responses in piglets to body acceleration given synchronously with the heartbeat (BASH). Circulation 39 & 40, Suppl. III: 38, 1969.
- Ashe, W. P., E. T. Carter, G. Hoover, L. B. Roberts, E. Johanson, F. Brown, and E. J. Largent, Jr. Some responses of rats to whole body mechanical vibration. Arch. Environ. Health, V2, pp. 369-377, 1961.
- Bantle, J. A. Effects of mechanical vibrations on the growth and development of mouse embryos. Aerospace Med., 42 (10): 1087-91, 1971.
- Blok, P., O. B. T. Tan, T. J. Vriesman, B. P. T. Veltman, R. G. Boiten, and A. C. Arntzenius. Design for cardiac assist device based on total body acceleration. Circulation 39 & 40, Suppl. III: 47, 1969.
- Broderson, A. B., and H. E. Von Gierke. Mechanical Impedance and its variation in the restrained primate during prolonged vibration. ASME paper No. 71-WA/BHF-8, 1971.
- Broderson, A. B., Biothermal response of the rhesus monkey to mechanical vibration. Reprint, Animal scientific meeting aerospace medical association, Bal Harbor, Fla., May 8-12, 1972.
- Camill, P., C. F. Knapp, and J. Collins. Computer modeling of whole-body sinusoidal accelerations on the cardiovascular system. Proc. Inst. Elec. Electron. Eng. 110-113, 1971.
- Clark, W. S., K. O. Lange, and R. R. Coermann. Deformation of the human body due to uni-directional forced sinusoidal vibration. Human Vibration Research, edited by S. Lippert, pp. 29-48, Oxford: Pergamon Press, 1963.
- Coermann, R. R. The mechanical impedance of the human body in sitting and standing position. Human Factors, V4, April, 1962.
- Edwards, R. G. Arterial blood flow and blood pressure in animals under mechanical vibration. Ph.D. Dissertation, University of Kentucky, Lexington, 1970.
- Edwards, R. G., E. P. McCutcheon, and C. F. Knapp. Cardiovascular changes produced by brief whole-body vibration of animals. J. Appl. Physiol. 32 (3): 386-90, 1972.
- Edwards, R. G., and C. F. Knapp. Changes in whole body force transmission of dogs exposed repeatedly to vibration. A.S.M.E. paper No. 72-WA/BHF-11, 1972.
- Evces, C. R., and J. H. McElhaney. Some effects of drugs on the low frequency whole body vibration response of dogs. Aerospace Med. 42 (4): 416-20, 1971.
- Fraser, T. M., G. N. Hoover, and W. F. Ashe. Tracking performance during low frequency vibration. Aerospace Med. 32 (9): 829-835, Sept., 1961.

- Grether, W. F., C. S. Harris, M. Ohlbaum, P. A. Sampson, and J. C. Guignard. Further study of combined heat, noise, and vibration stress. Aerospace Med. 43 (6): 641-45, 1972.
- Hood, W. B. Jr., and L. S. Higgins. Circulatory and respiratory effects of whole-body vibration in anesthetized dogs. J. Appl. Physiol., 20 (6): 1157-62, 1965.
- Hooks, L. E., R. M. Nerem, and T. J. Benson. A momentum integral solution for pulsatile flow in a rigid tube with and without longitudinal vibration. Engineering Science in Medicine Proceedings, Society of Engineering Science, Washington University, St. Louis, Nov., 1969.
- Jackson, D. H., Editor. Circulatory assist & ballistocardiographic studies. Proc. 15th Ann. Meet. Ballistocard. Res. Soc., Atlantic City, 1971.
- Krause, H. E., and K. O. Lange. Nonlinear behavior of biomechanical systems. ASME paper No. 63-WA-278, 1963.
- Lange, K. O., and R. R. Coermann. Visual acuity under vibration. Human Vibration Research, edited by S. Lippert, pp. 65-74, Oxford: Pergamon Press, 1963.
- Lange, K. O., and R. G. Edwards. Force input and thoraco-abdominal strain resulting from sinusoidal motion imposed in the human body. Aerospace Med. 41 (5): 538-43, 1970.
- Magid, E. B., and R. R. Coermann. Human whole body tolerance to sinusoidal vibration. Institute of Environmental Sciences Proceedings, pp. 135-54. 1960.
- O'Braint, C. R., and M. K. Ohlbaum. Visual acuity decrements associated with whole body  $\pm G_z$  vibration stress. Aerospace Med. 41 (1): 79-82, 1970.
- Payne, P. R., and E. G. V. Band. A four-degree-of-freedom lumped parameter model of the seated human body. Aerospace Medical Research Laboratory Technical Report No., AMRL-TR-70-35, Wright-Patterson AFB, O., 1971.
- Roberts, L. B., and J. H. Dines. Cardiovascular effects of vibration. NASA Grant NGR 36-008-041, Report No. 2, Ohio State University Research Foundation, Columbus, O., Oct., 1966.
- Roberts, L. B., and J. H. Dines. Physiological and pathological effects of mechanical vibration on animals and man. N.I.H. Grant No. OH-00006, Final Report, Ohio State University Research Foundation, Columbus, Ohio, Dec. 1966.
- Roberts, L. B., J. H. Dines, R. L. Hamlin, and E. J. Whitehead. Cardiovascular effects of vibration. NASA Grant NGR 36-008-041, Final Report - Part II, Report No. 6, Ohio State University Research Foundation, Columbus, Ohio, July, 1969.
- Sharp, T. D., A live load force table. Institute of Environmental Sciences Proceedings, 1963.

- Sommer, H. C., and C. Stanley Harris. Combined effects of noise and vibration on mental performance as a function of time of day. Aerospace Med., 43 (5): 479-82, 1972.
- Verdouw, P. D., A. C. Arntzenius, and A. Noordergraaf. Modification of left ventricular ejection in response to whole body acceleration. Circulation 39 & 40, Suppl. III: 208, 1969.
- Vogt, L. H., H. E. Krause, H. Hohlweck, and E. May. Mechanical impedance of supine humans under sustained acceleration. Aerospace Med. (2): 123-28, 1973.
- Von Gierke, H. E., Chairman. Symposium on biodynamic models and their applications. Aerospace Medical Research Laboratories Technical Report AMRL-TR-71-29, Wright-Patterson AFB, Ohio, 1971.
- Vykukal, H. C. Dynamic response of the human body to vibration when combined with various magnitudes of linear acceleration. J. Aerospace Med. Nov., 1968.
- White, G. H. Jr., K. O. Lange, and R. R. Coermann. The effects of simulated buffeting on the internal pressure of man. Human Factors, 4, Apr., 1962.
- Wike, E. L., and S. S. Wike. Escape conditioning and low frequency whole body vibration: The effects of frequency, amplitude, and controls for noise and activation. Psychon. Sci. 27 (3), 1972.
- Wittman, T. J., and N. S. Phillips. Human body nonlinearity and mechanical impedance analysis. J. Biomechanics, V2, pp. 281-88, 1969.
- Zechman, F. W., Jr., D. Peck, and E. Luce. Effect of vertical vibration on respiratory airflow and transpulmonary pressure. J. Appl. Physiol. 20 (5): 849-54, 1965.
- Ziegenruecker, G. H., and E. B. Magid. Short time tolerance to sinusoidal vibration. Aerospace Medical Research Laboratories Technical Report TR-391-AD, Wright-Patterson AFB, Ohio, 1959.

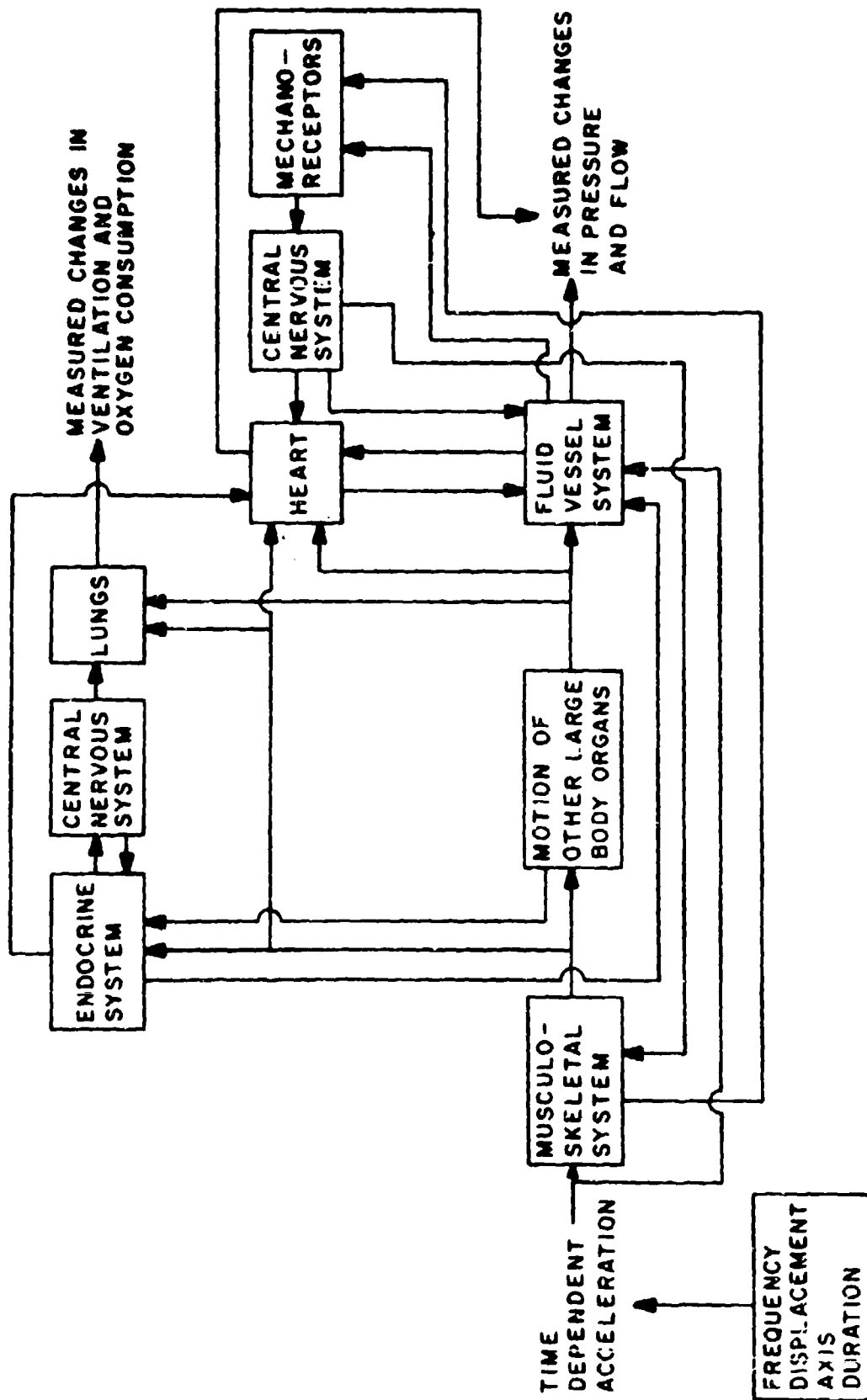


Fig. 1 Block diagram of the interaction of major physiological systems to produce changes in pressure and flow resulting from a vibration input into the whole system.

PERCENT CHANGE, MEAN AORTIC FLOW  
VERSUS PEAK FORCE/BODY WEIGHT  
10 DOGS VIBRATED AT 1.0G PEAK ACCELERATION.  
UNANESTHETIZED

- Dog #1630 (6/26/72)
- Dog #L199 (11/1/72)
- △ Dog #1419 (11/16/72)
- ▲ Dog #1607 (11/7/72)
- Dog #1600 (6/6/72)
- Dog #556 (1/26/73)
- ◇ Dog #5559 (3/29/72)
- Dog #1607 (10/25/72)
- Dog #1600 (6/13/72)
- × Dog #1600 (6/9/72)

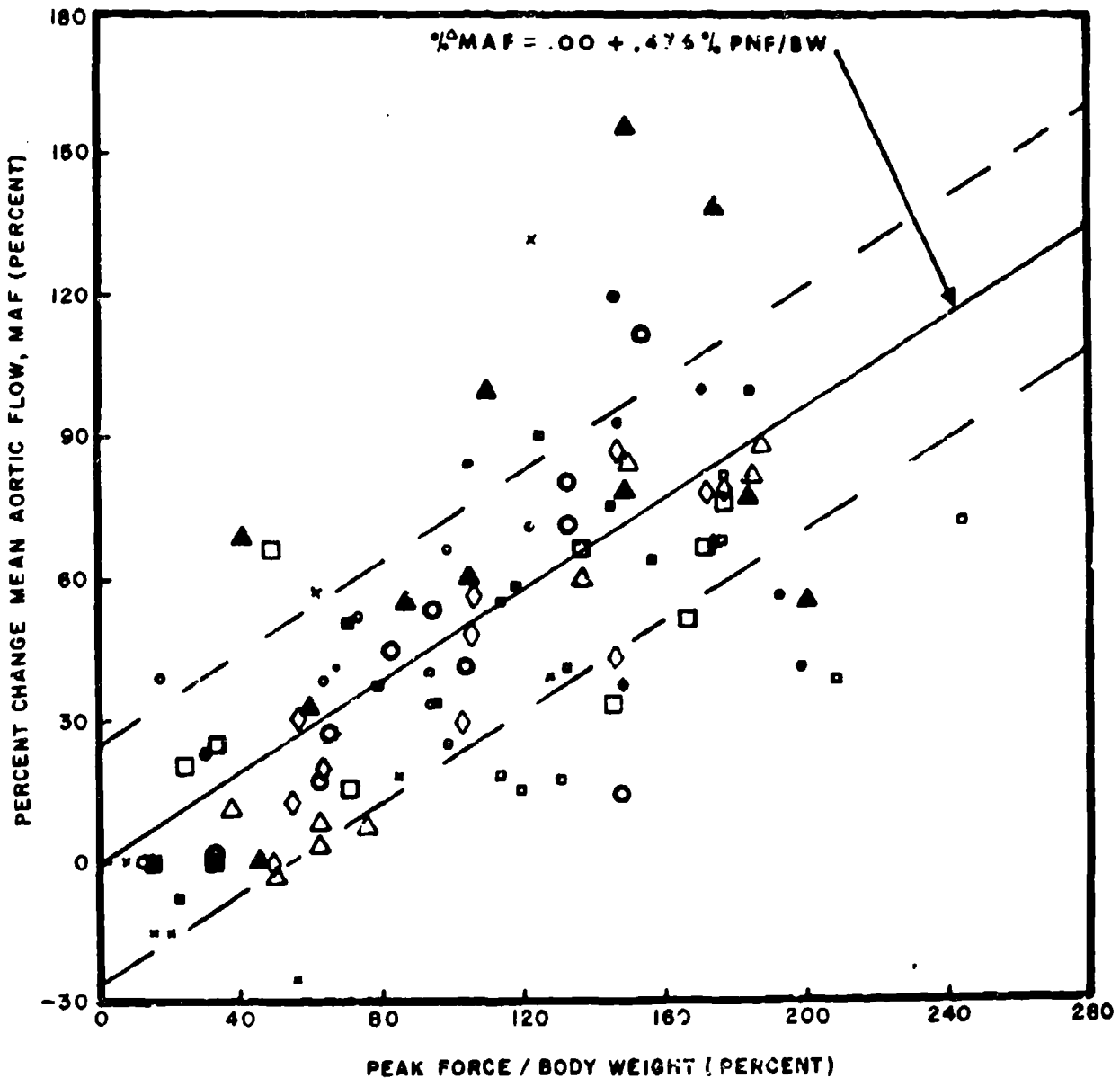


Fig. 2 Percentage change in mean aortic flow as a function of the ratio of peak net force to body weight in the awake animals.

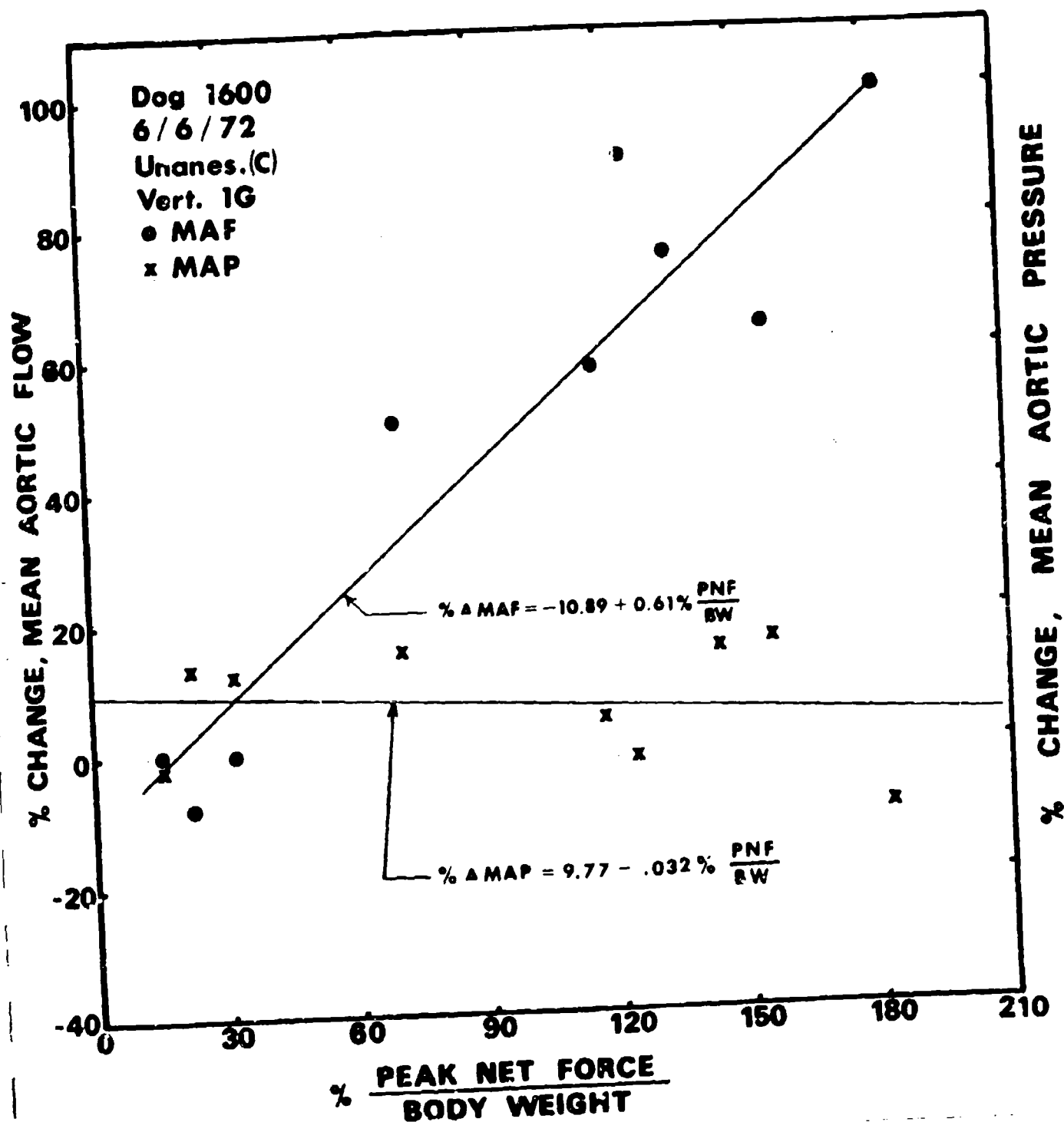


Fig. 3a Percentage change in mean aortic flow and mean aortic pressure as a function of the ratio of peak net force to body weight in an awake animal (1600) whose changes were mainly due to heart rate.



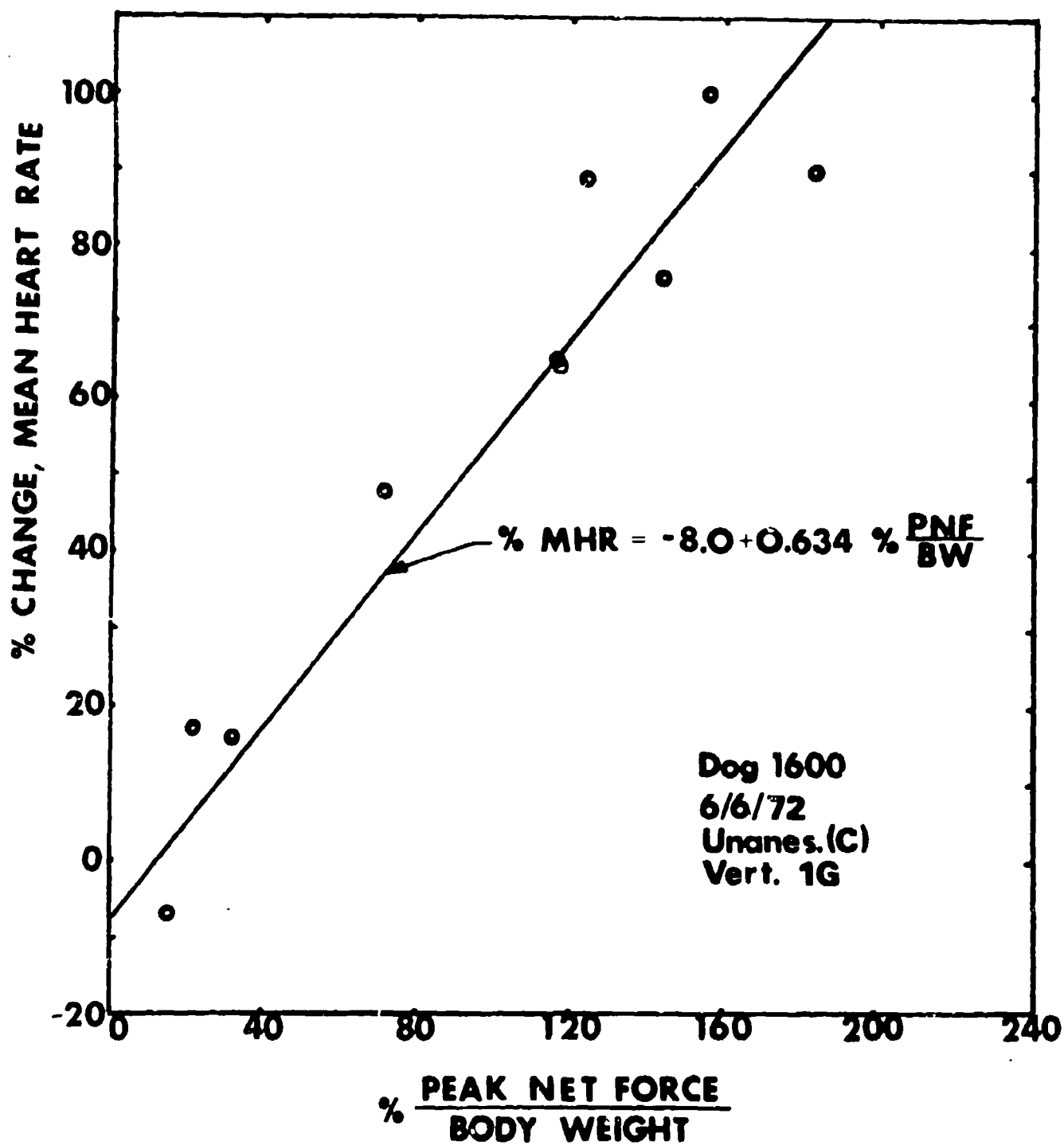


Fig. 3b Percentage change in mean heart rate as a function of the ratio of peak net force to body weight in animal 1600.

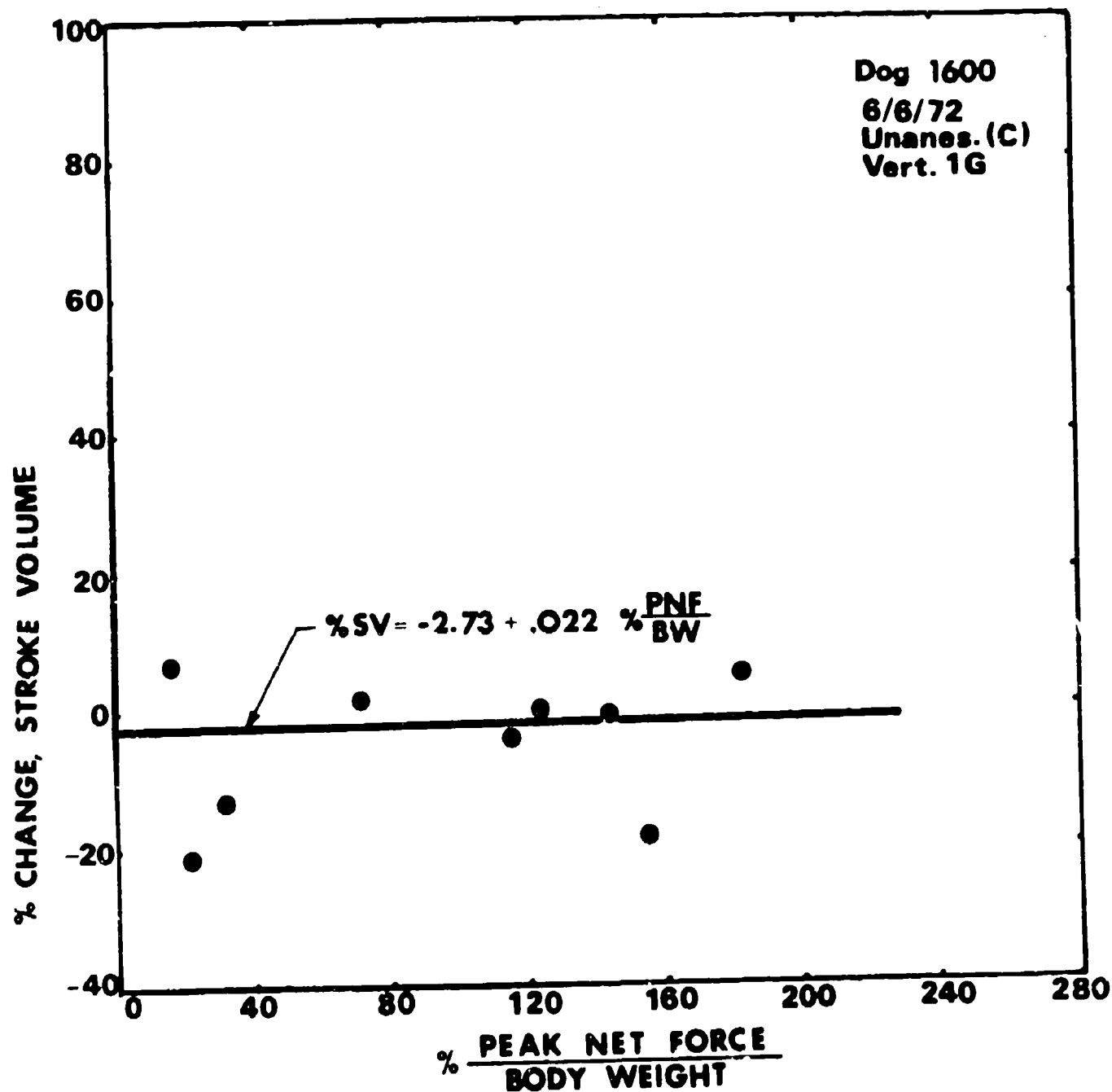


Fig. 3c Percentage change in stroke volume as a function of the ratio of peak net force to body weight in animal 1600.

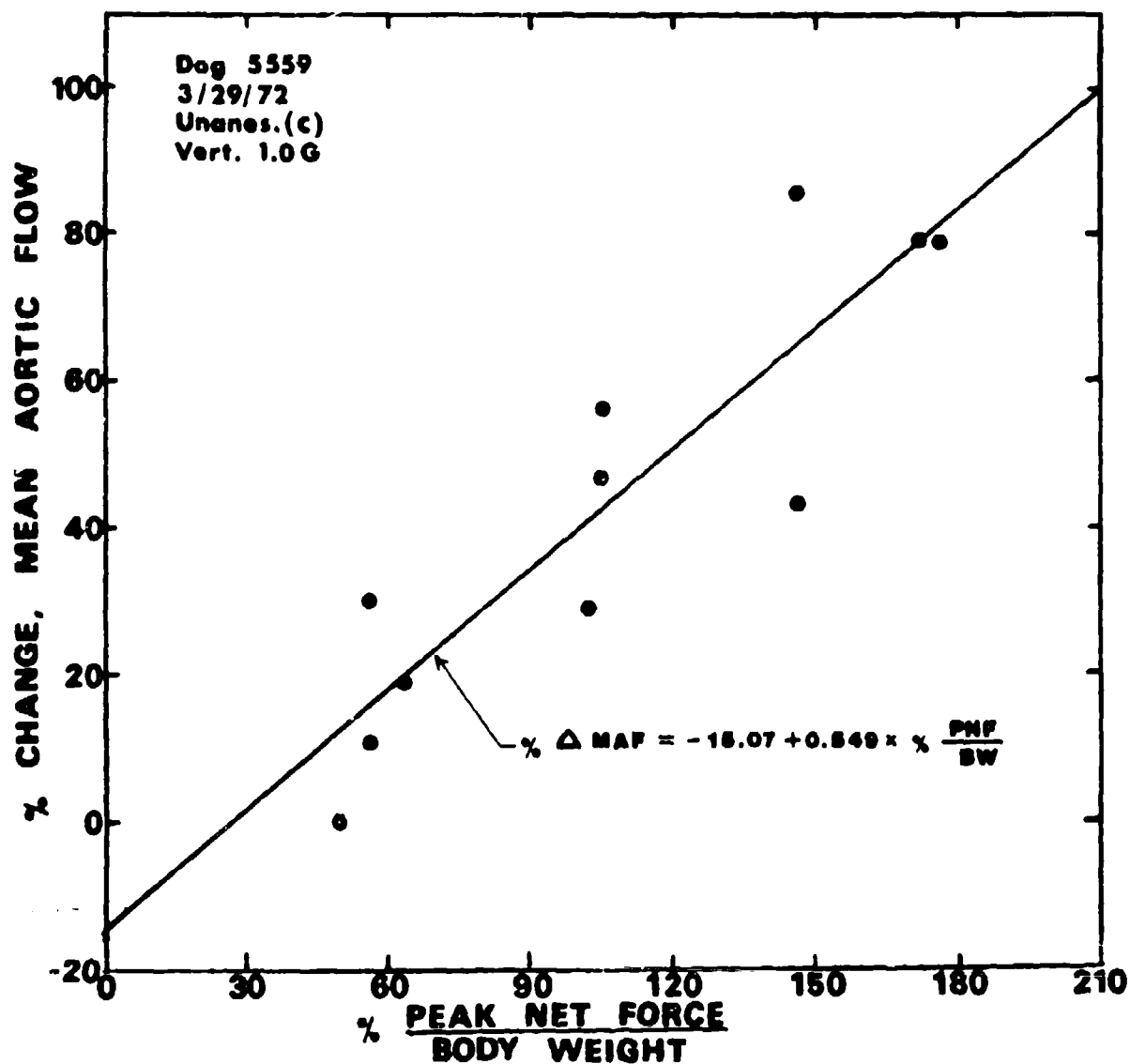


Fig. 4a Percentage change in mean aortic flow as a function of the ratio of peak net force to body weight in an awake animal (5559) whose changes were mainly due to stroke volume.

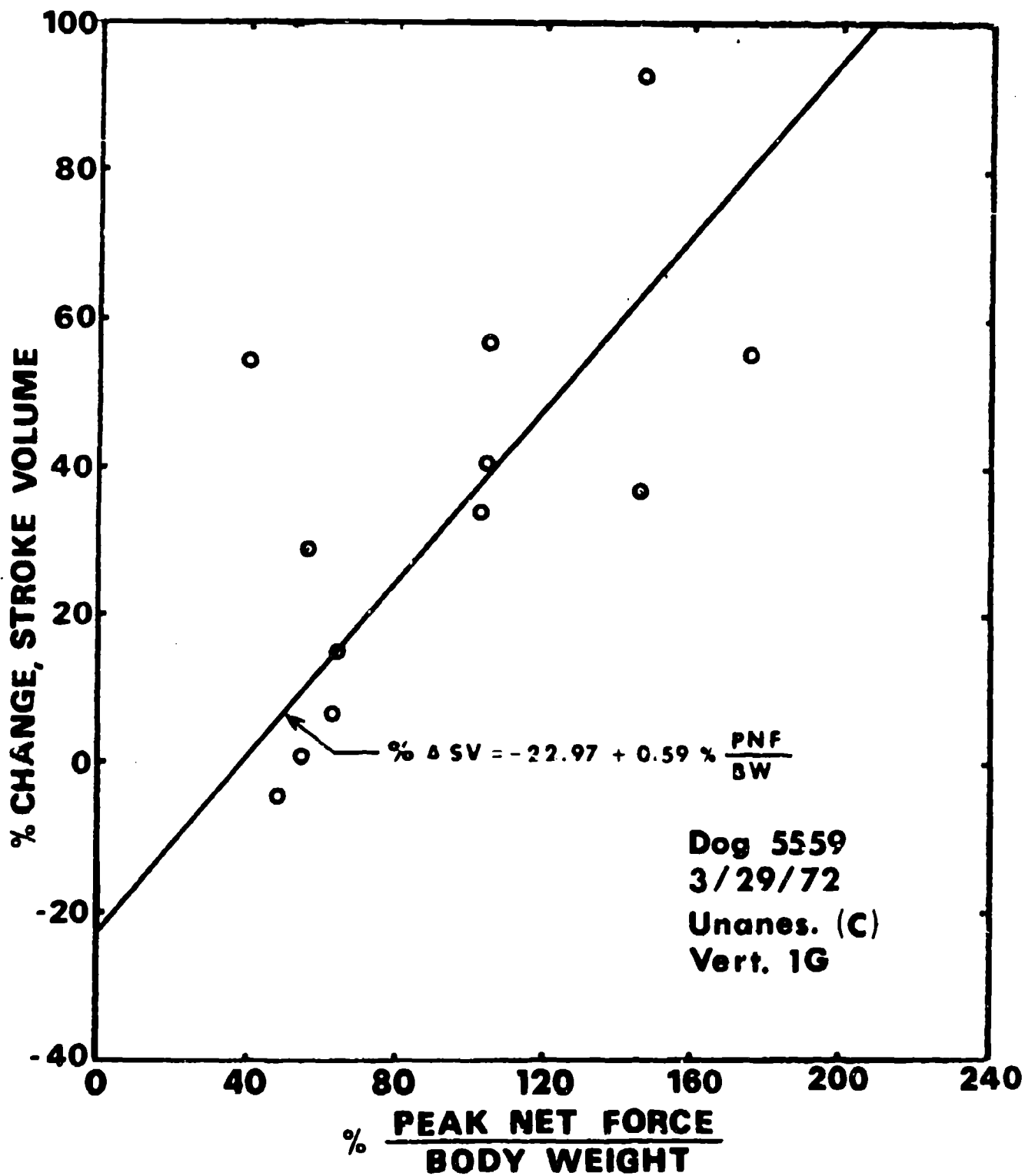


Fig. 4b Percentage change in stroke volume as a function of the ratio of peak net force to body weight in animal 5559.

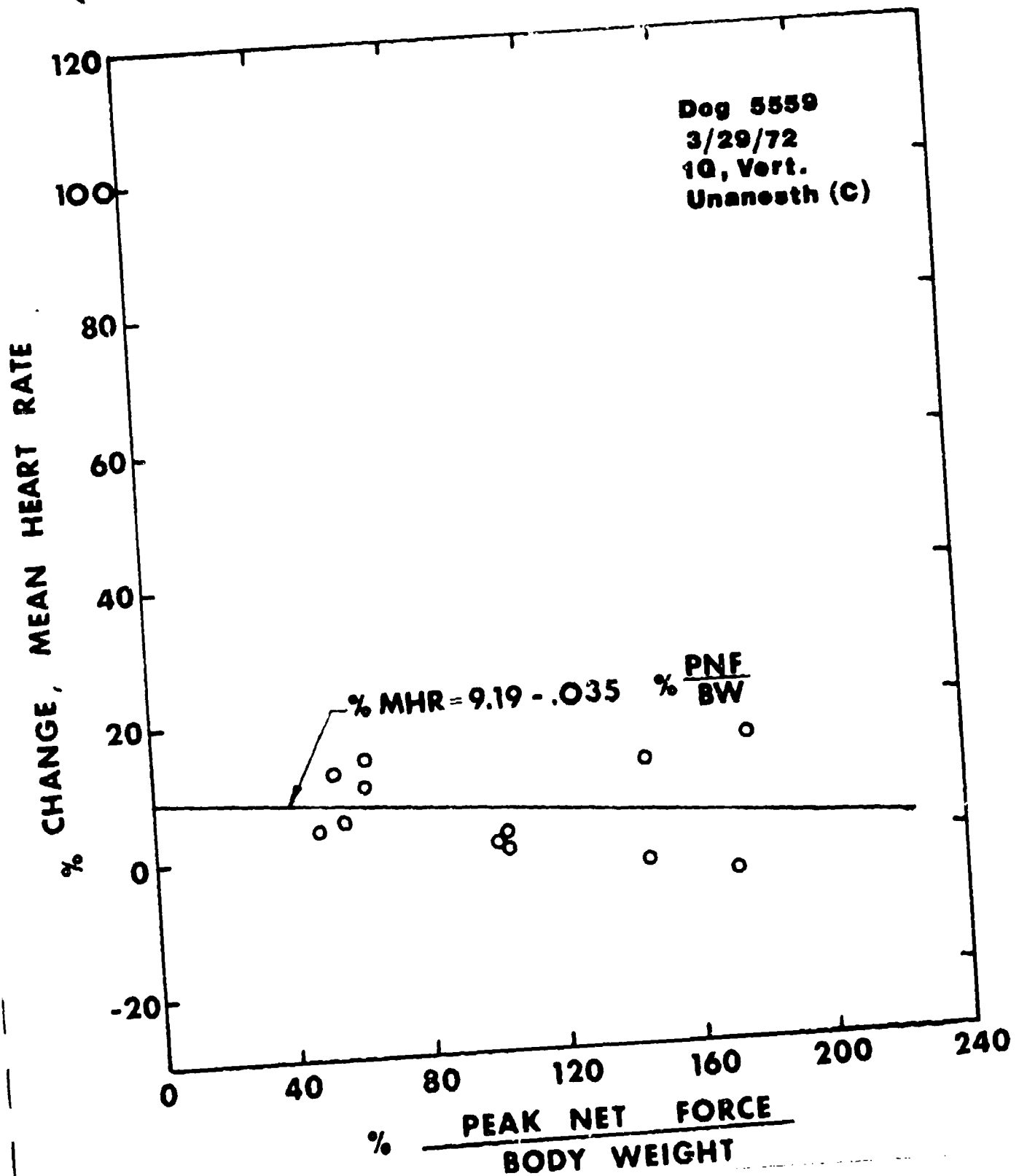


Fig. 4c Percentage change in mean heart rate as a function of the ratio of peak net force to body weight in animal 5559.

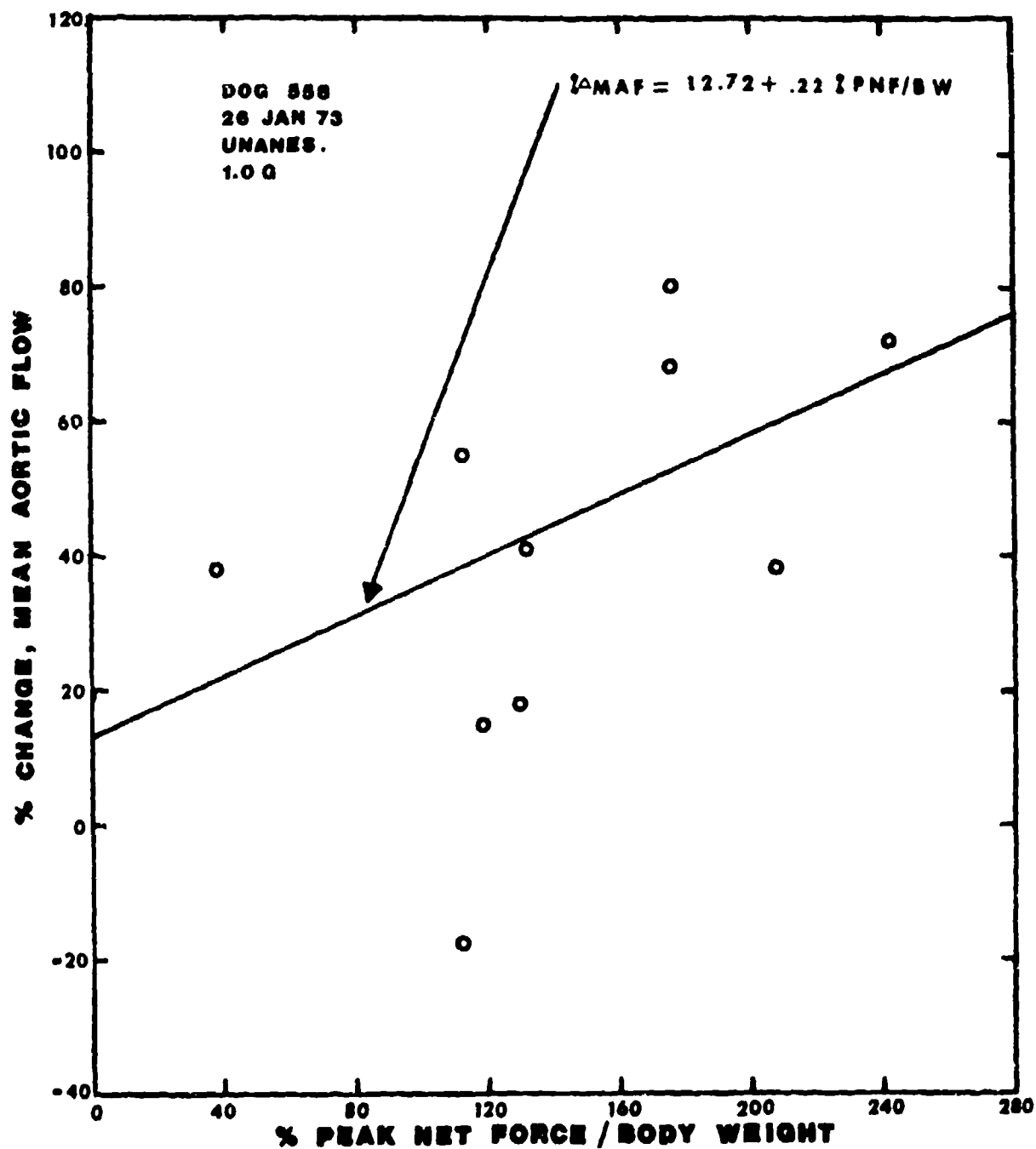


Fig. 5a Percentage change in mean aortic flow as a function of the ratio of peak net force to body weight in an awake animal (556) with fairly equal changes in mean heart rate and stroke volume.

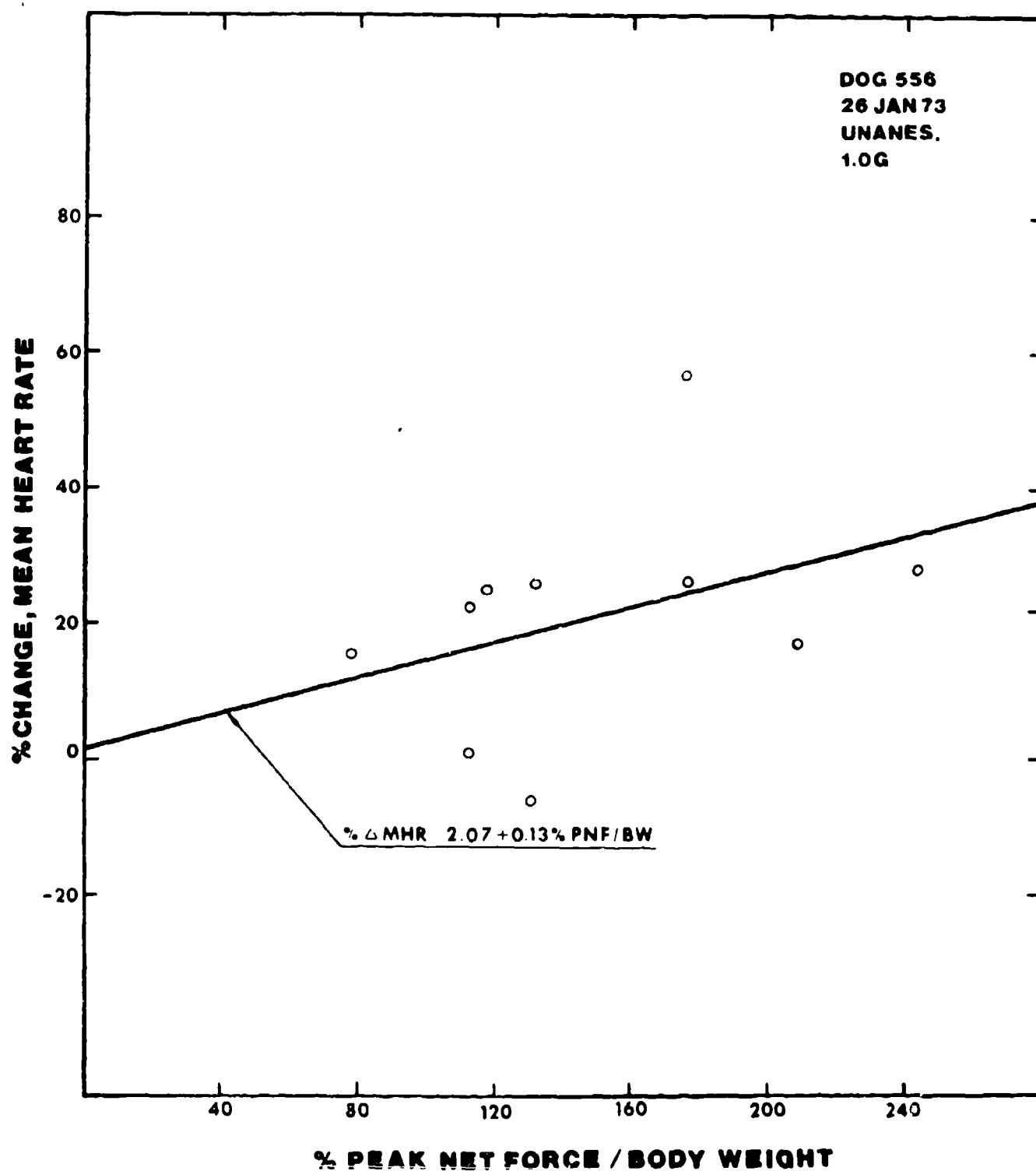


Fig. 5b Percentage change in mean heart rate as a function of the ratio of peak net force to body weight in animal 556.

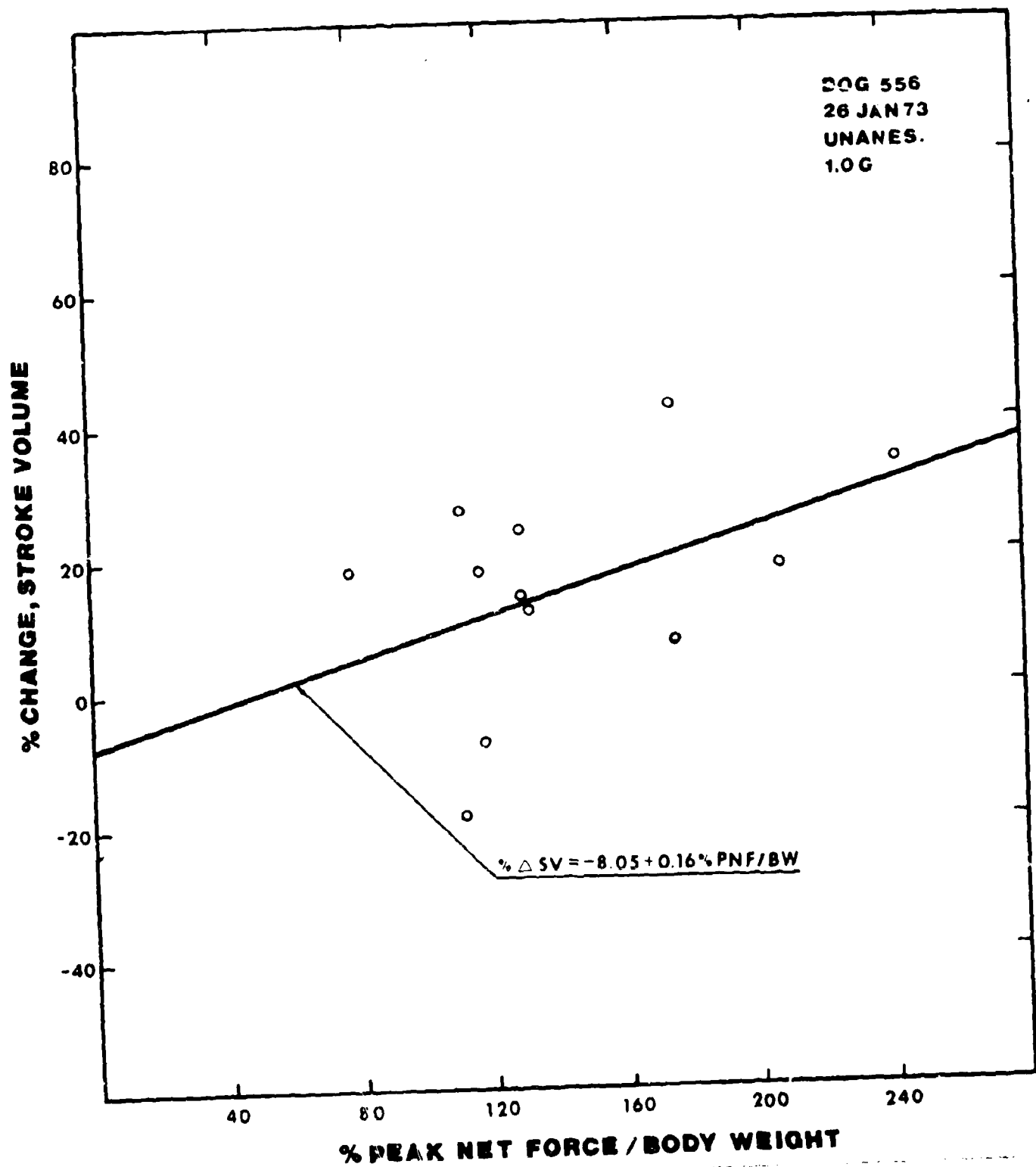


Fig. 5c Percentage change in stroke volume as a function of the ratio of peak net force to body weight in animal 556.



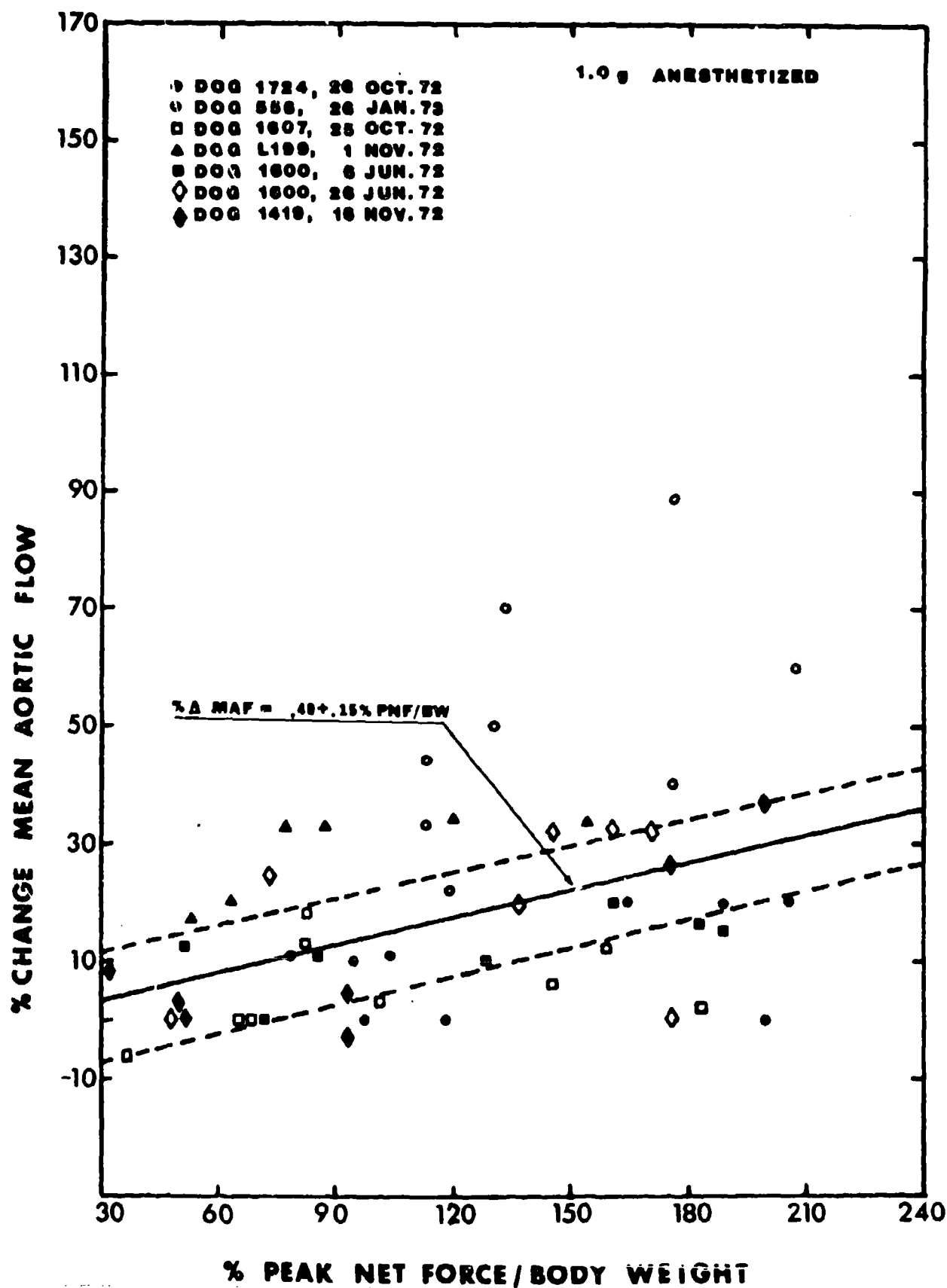


Fig. 6 Percentage change in mean aortic flow as a function of the ratio of peak net force to body weight in the anesthetized animals.

# CHANGES IN MAF MAINLY DUE TO CHANGES IN MHR

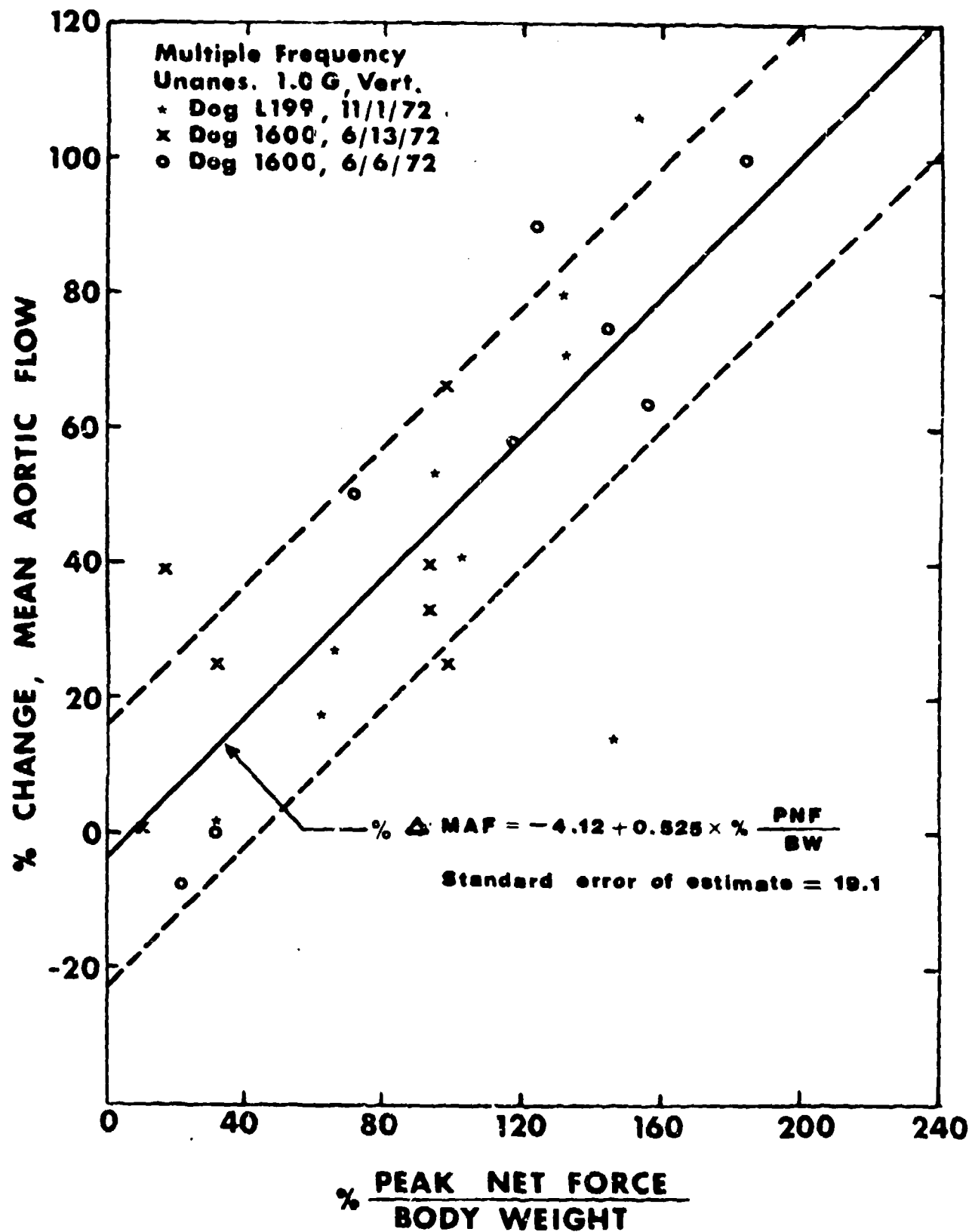


Fig. 7a Percentage change in mean aortic flow as a function of the ratio of peak net force to body weight for the group of awake animals whose changes were mainly due to heart rate.

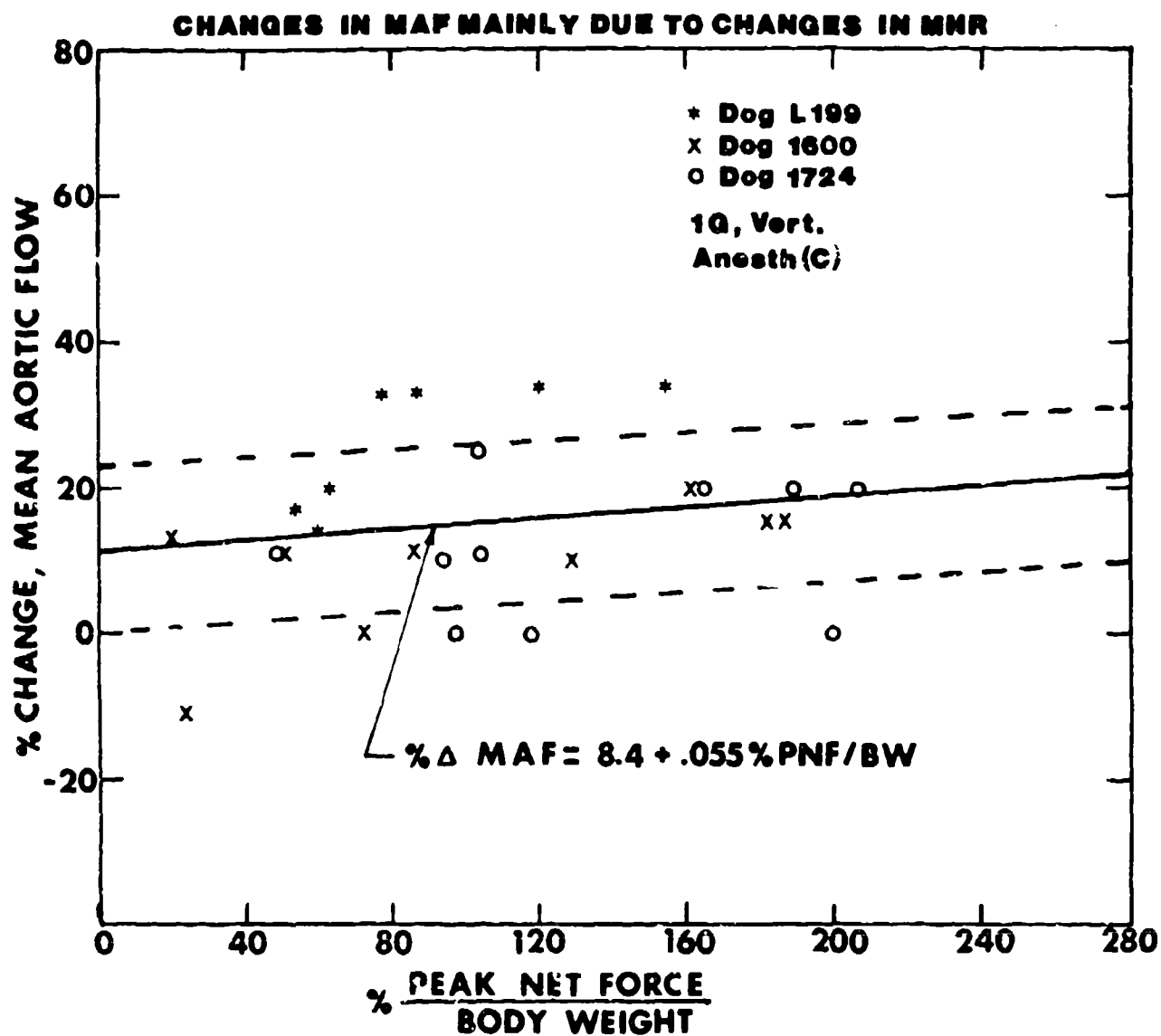


Fig. 7b Percentage change in mean aortic flow as a function of the ratio of peak net force to body weight for the group of anesthetized animals whose changes were mainly due to heart rate.

CHANGES IN MAF — MAINLY DUE  
TO CHANGES IN MHR

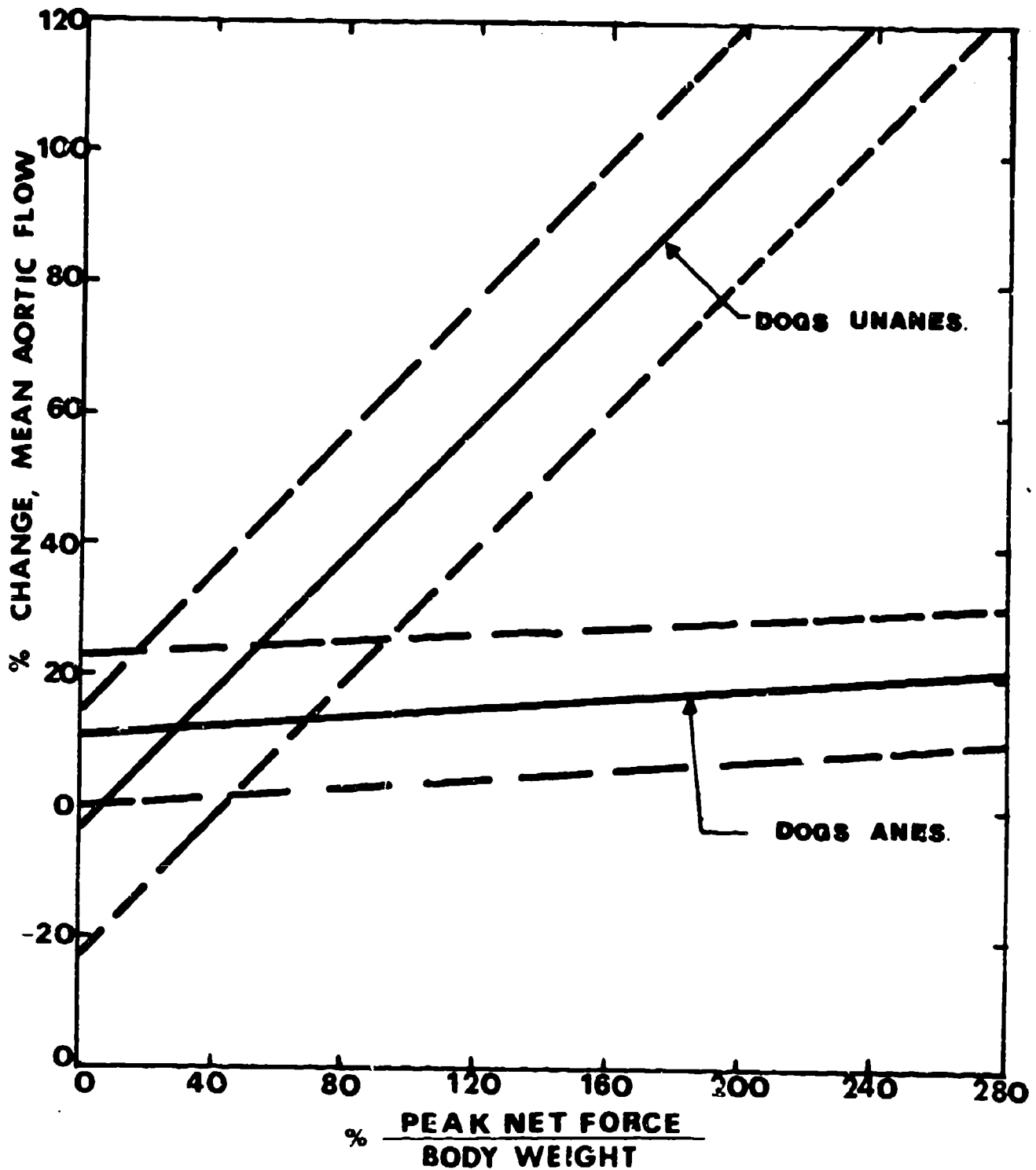


Fig. 7c Comparison of the percentage change in mean aortic flow as a function of the ratio of peak net force to body weight for the anesthetized vs. unanesthetized animals whose changes were due mainly to heart rate.

# CHANGES IN MAF MAINLY DUE TO CHANGES IN SV

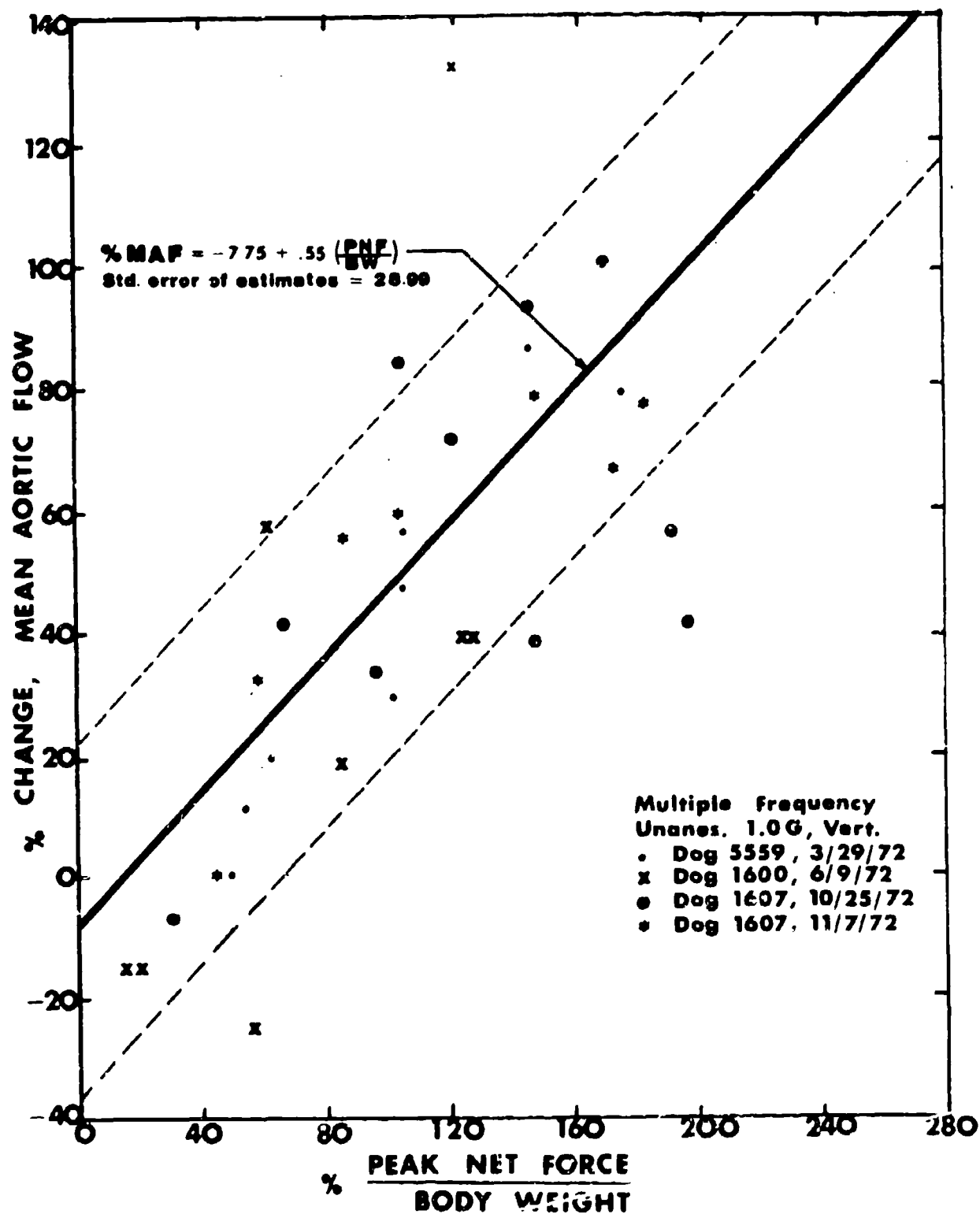


Fig. 8a Percentage change in mean aortic flow as a function of the ratio of peak net force to body weight for the group of awake animals whose changes were due mainly to stroke volume.

# CHANGES IN MAF MAINLY DUE TO CHANGES IN SV

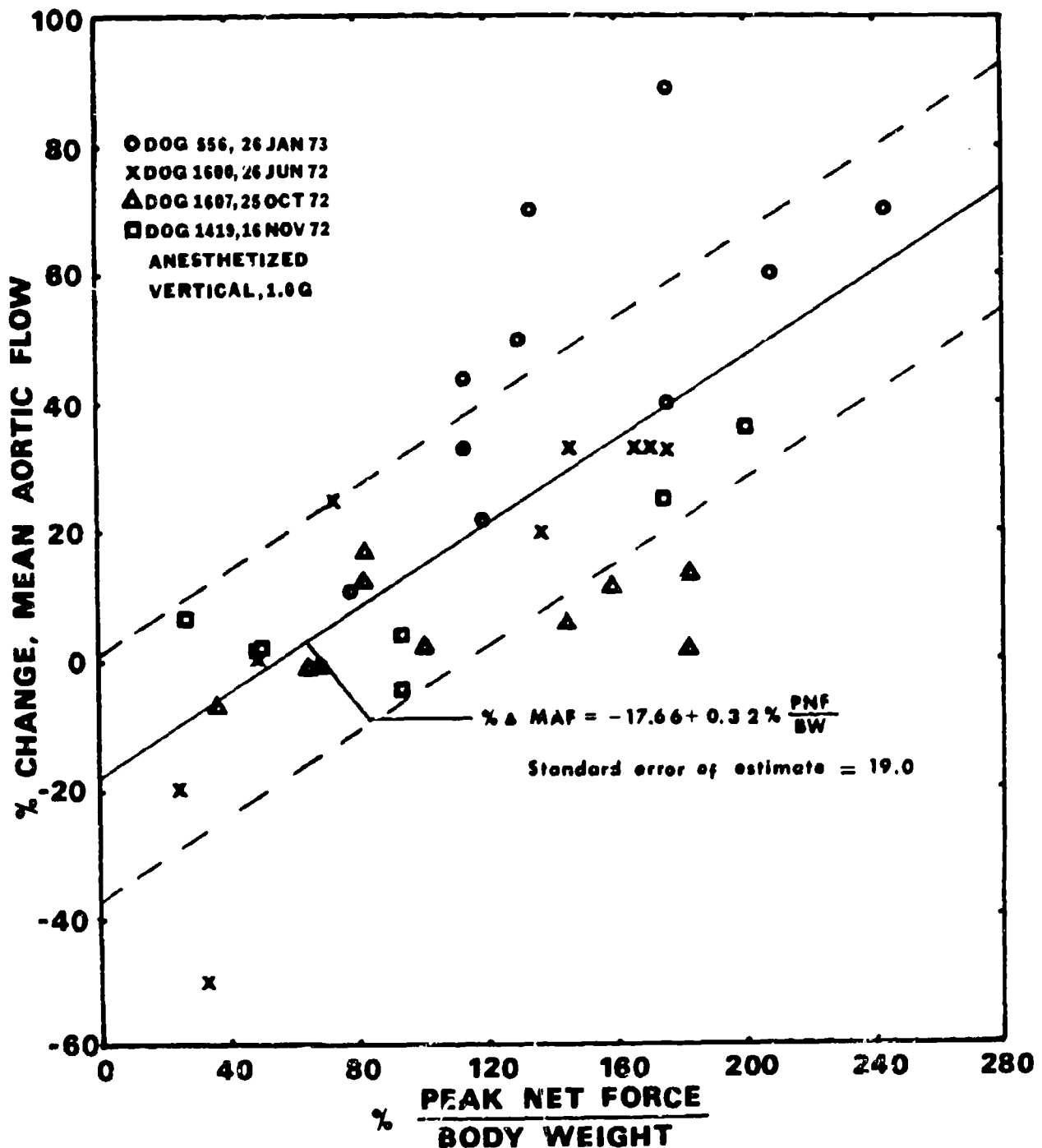


Fig. 8b Percentage change in mean aortic flow as a function of the ratio of peak net force to body weight in the group of anesthetized animals whose changes were due mainly to stroke volume.

# CHANGES IN MAF MAINLY DUE TO CHANGES IN SV

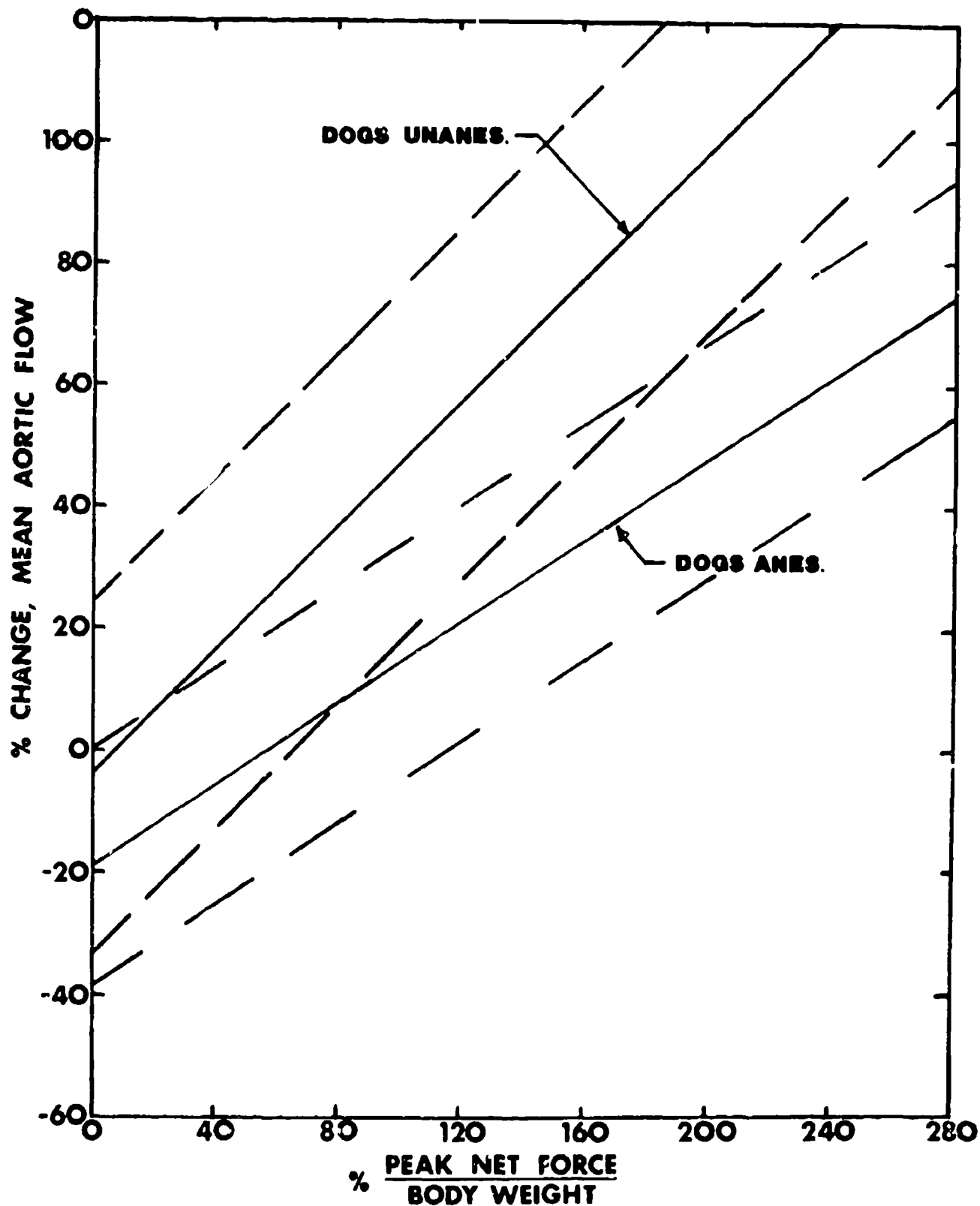


Fig. 8c Comparison of the percentage change in mean aortic flow as a function of the ratio of peak net force to body weight for the anesthetized vs. unanesthetized animals whose changes were due mainly to stroke volume.

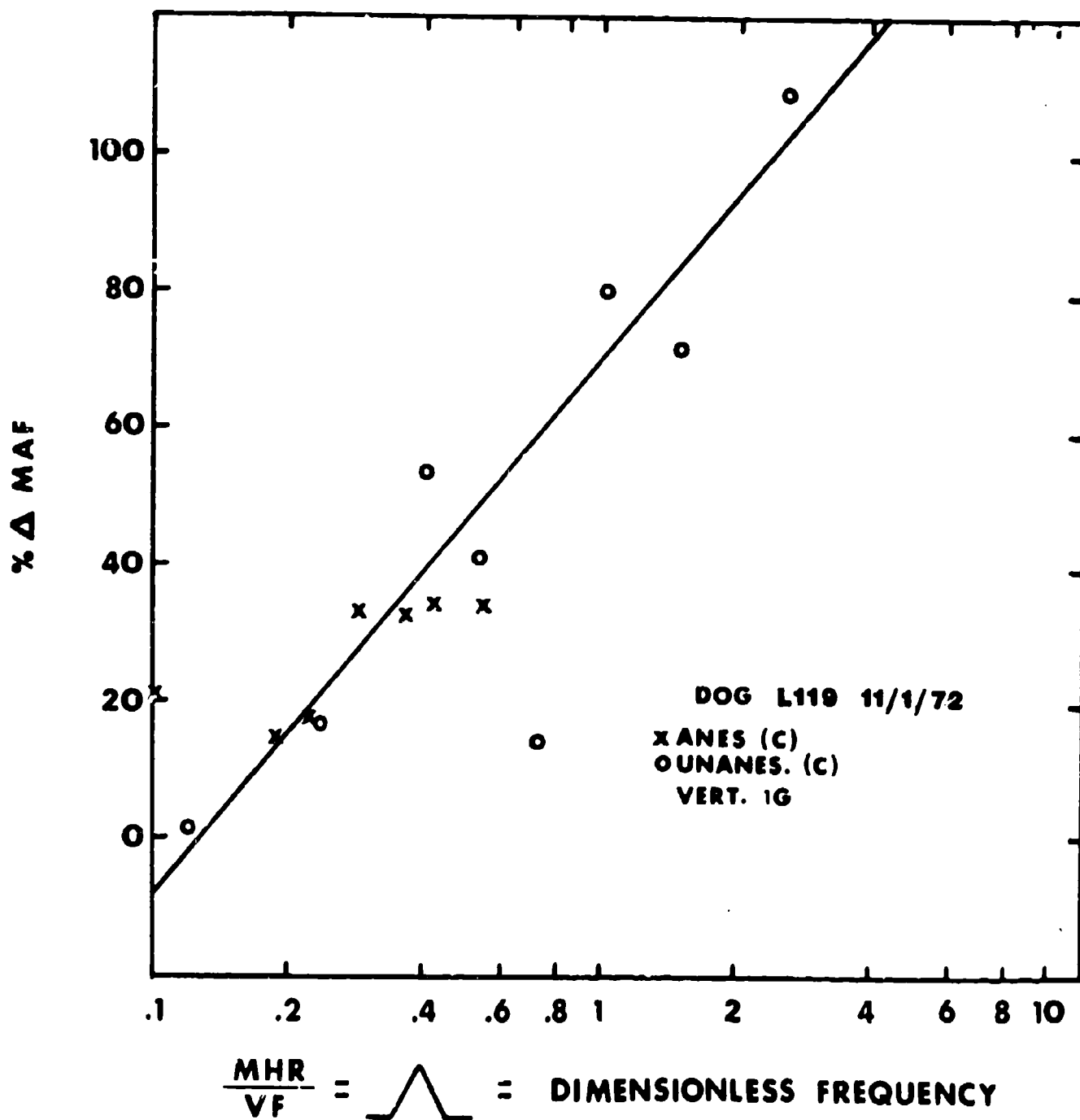


Fig. 9 Percentage change in mean aortic flow as a function of the log of the ratio of mean heart rate to vibration frequency for an animal studied both awake and anesthetized.



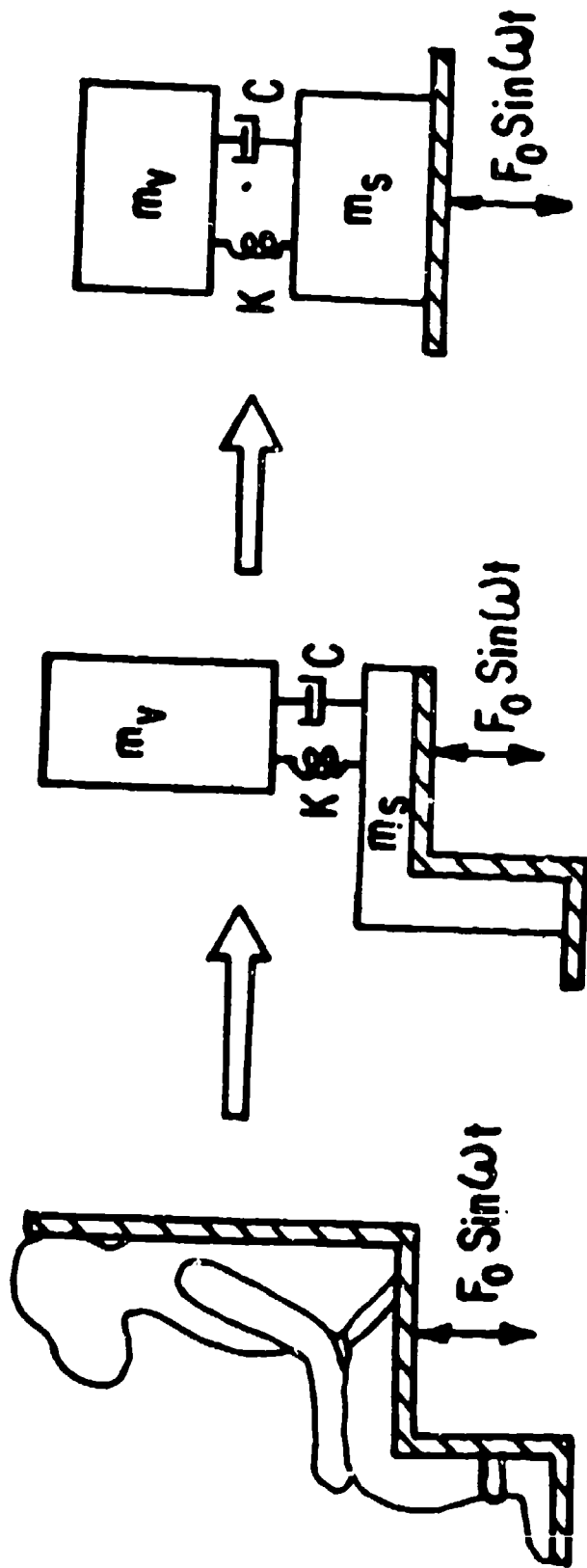
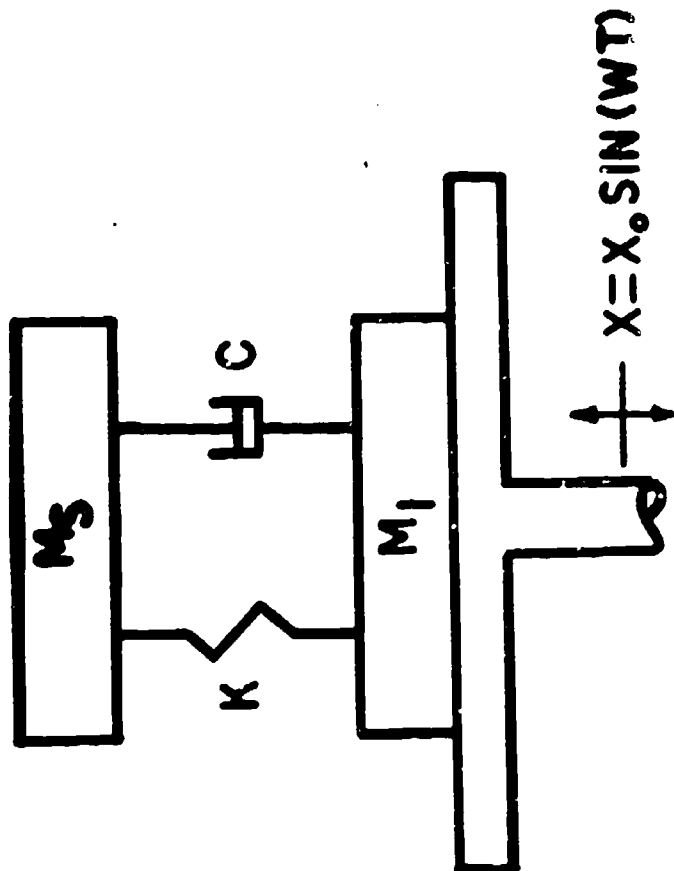


Fig. 10 Development of a single-degree-of-freedom model for impedance response of the restrained primate. From Broderson and von Gierke (1971).

$$M_1 / M_S = 2A / \sqrt{F}$$



$$K/W = 0.134 + 0.543F : 2 \leq F \leq 5 : C/W = -0.045 + 0.024F$$

$$2.54 + 0.062F : 5 \leq F \leq 10 : 0.096 - 0.004F$$

$$-1.15 + 0.431F : 10 \leq F \leq 30 : 0.0435 + 0.00125F$$

Fig. 11 A two-mass, single-degree-of-freedom model for impedance response of the sitting restrained primate.

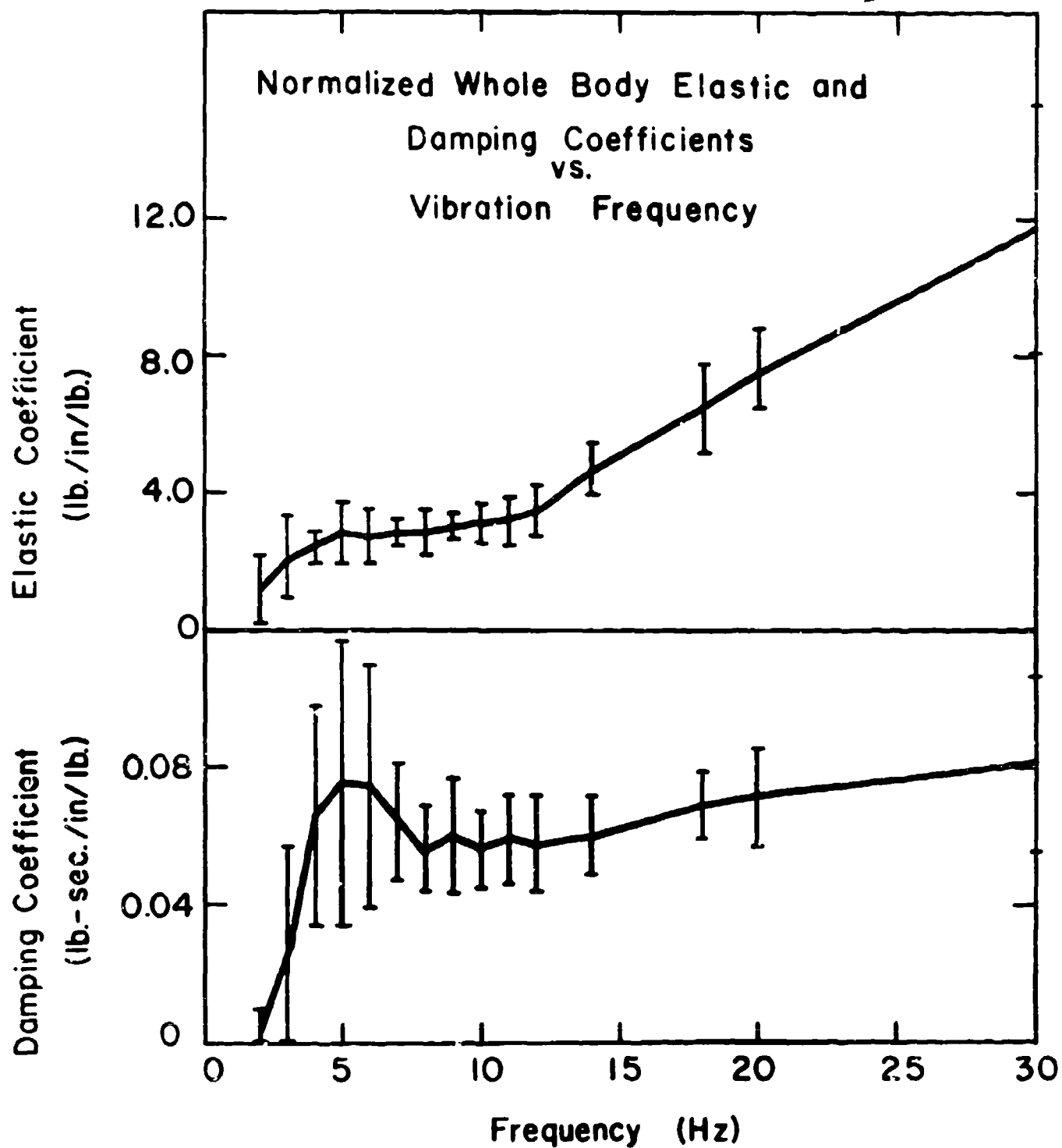


Fig. 12 Normalized whole body coefficients of elasticity and damping versus frequency for the sitting, restrained primate.

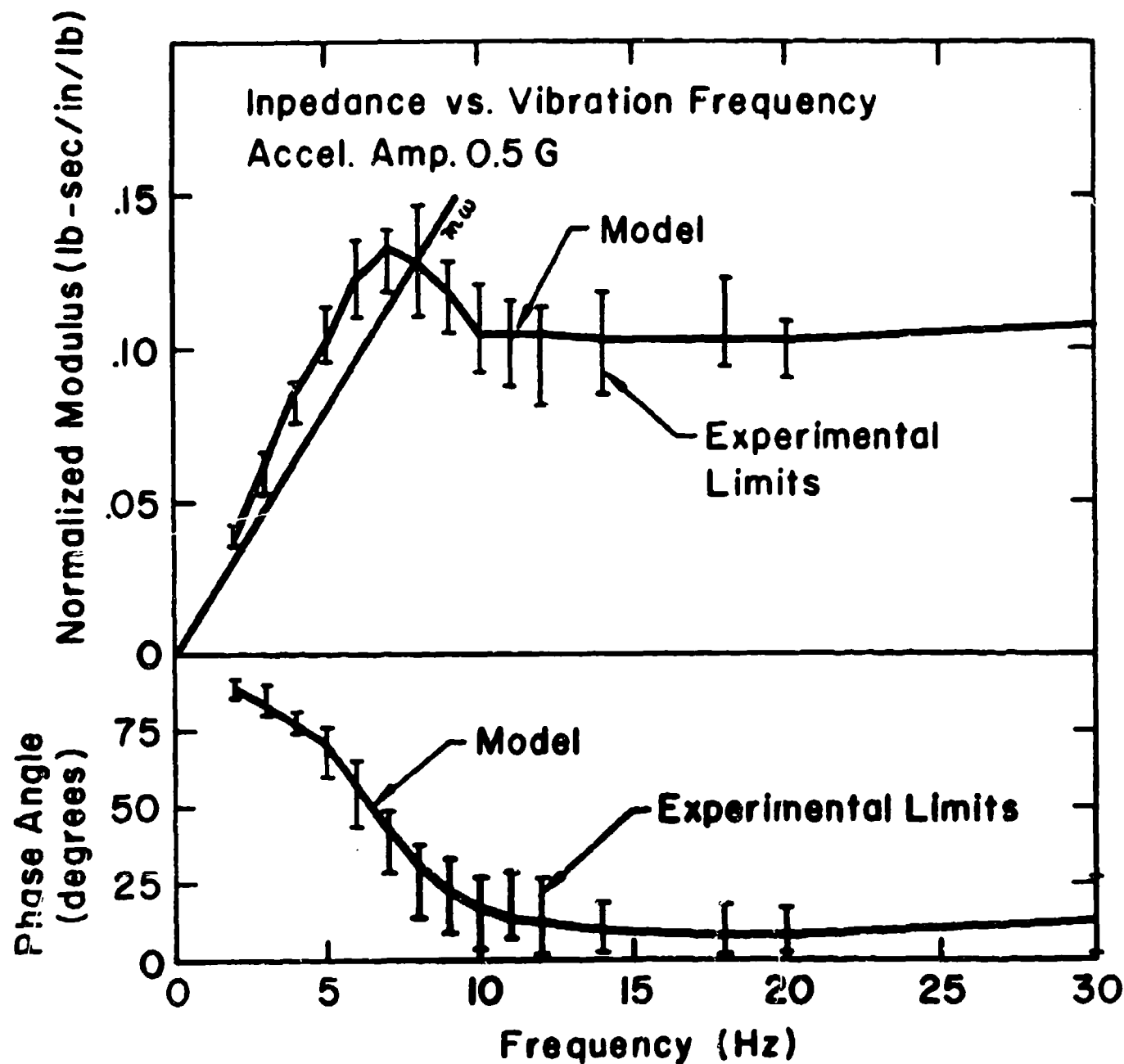


Fig. 13 Impedance phase angle and normalized modulus versus frequency for 0.5-g vibration of four primates compared to that predicted by the model of figure 11.

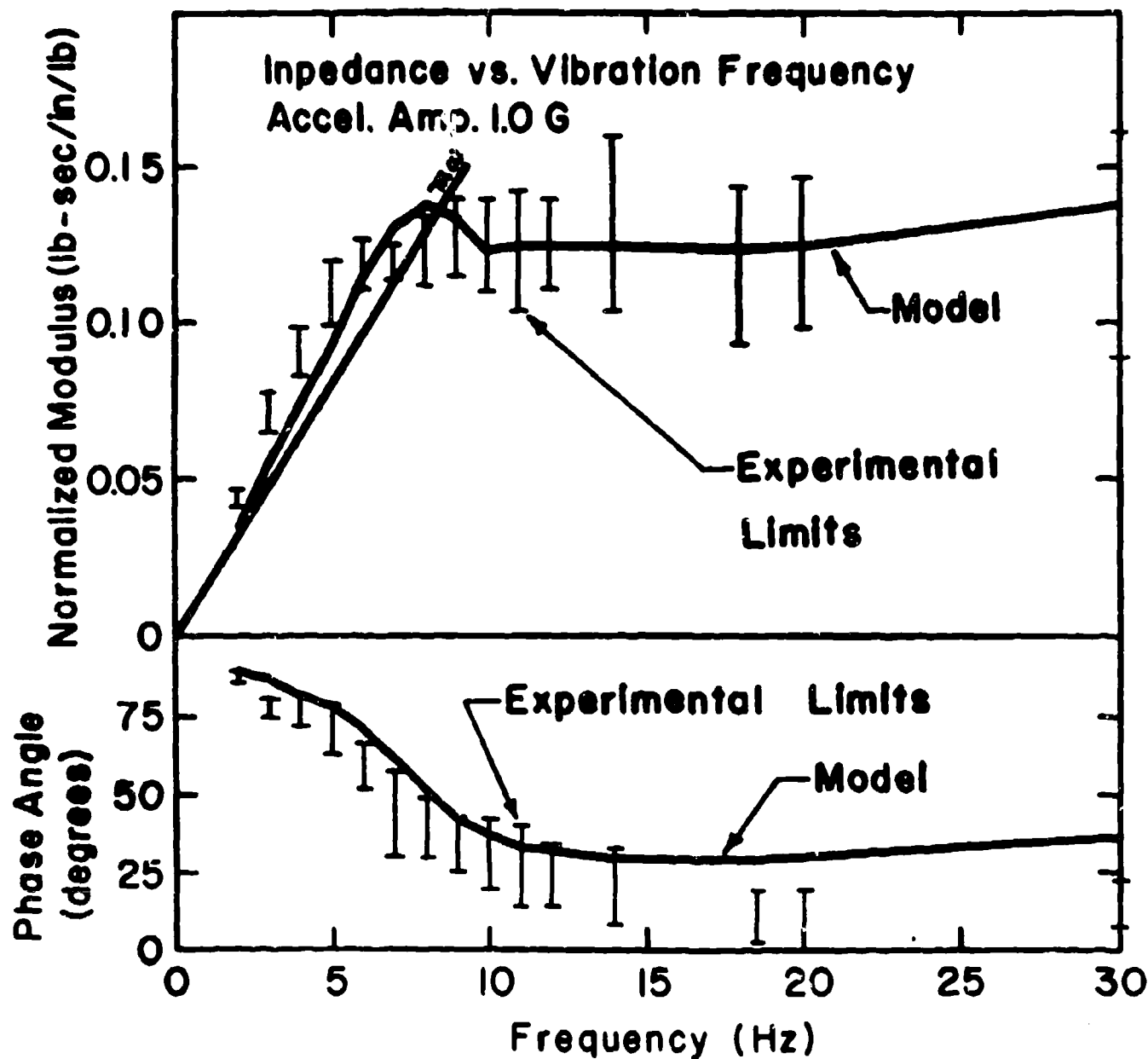


Fig. 14 Impedance phase angle and normalized modulus vs. frequency for 1.0 g vibration of four primates compared to that predicted by the model of Fig. 11.

DISSIPATED ENERGY VS TIME  
ANIMAL NO. 08G AT 0.5G

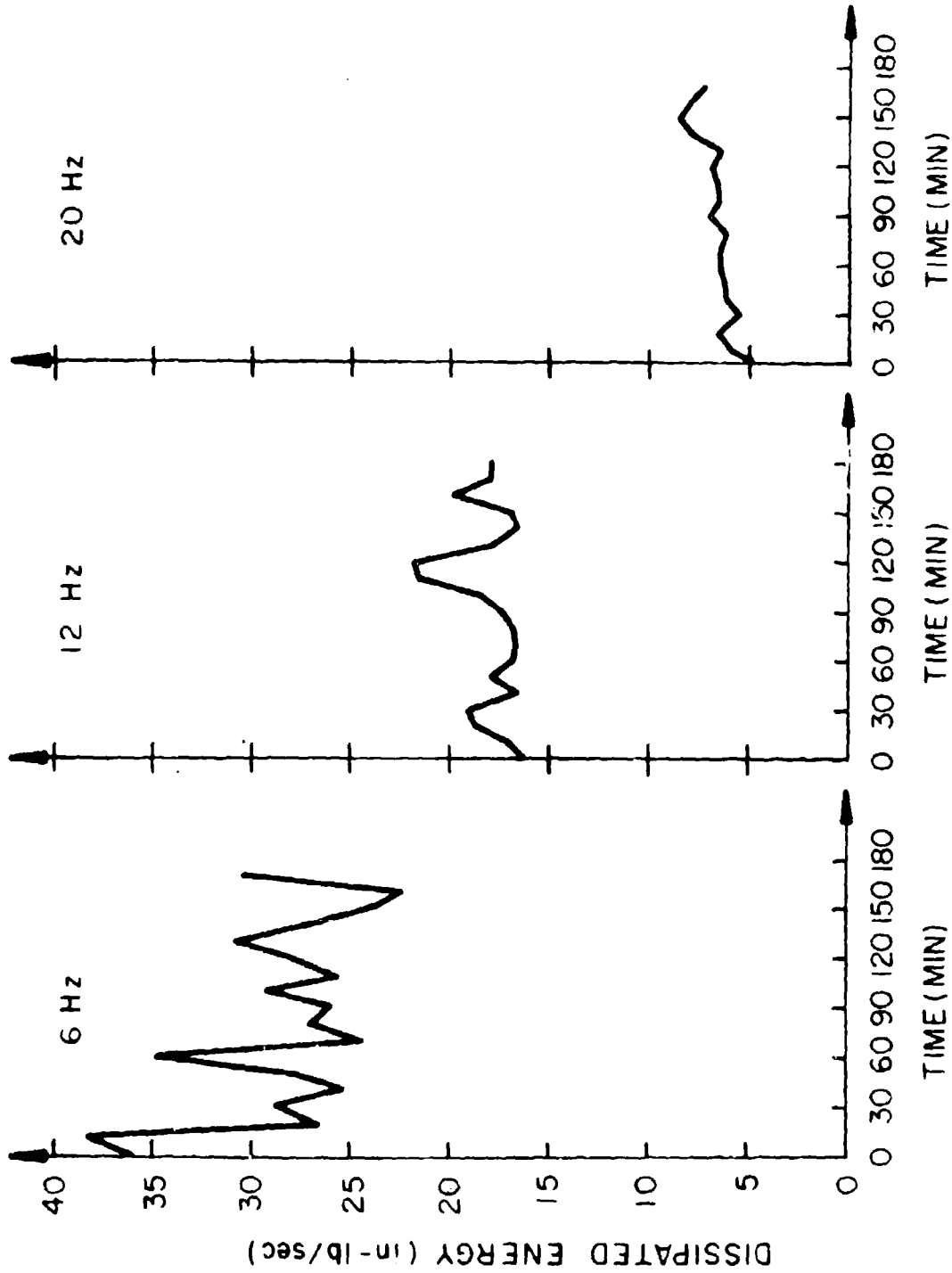


Fig. 15 Dissipated energy vs. time for one Rhesus monkey vibrated at 0.5 g and 6, 12, and 20 Hz.

RHESUS MONKEY HEAD TRANSMISSIBILITY  
VERSUS VIBRATION FREQUENCY  
MEAN OF TEN TESTS

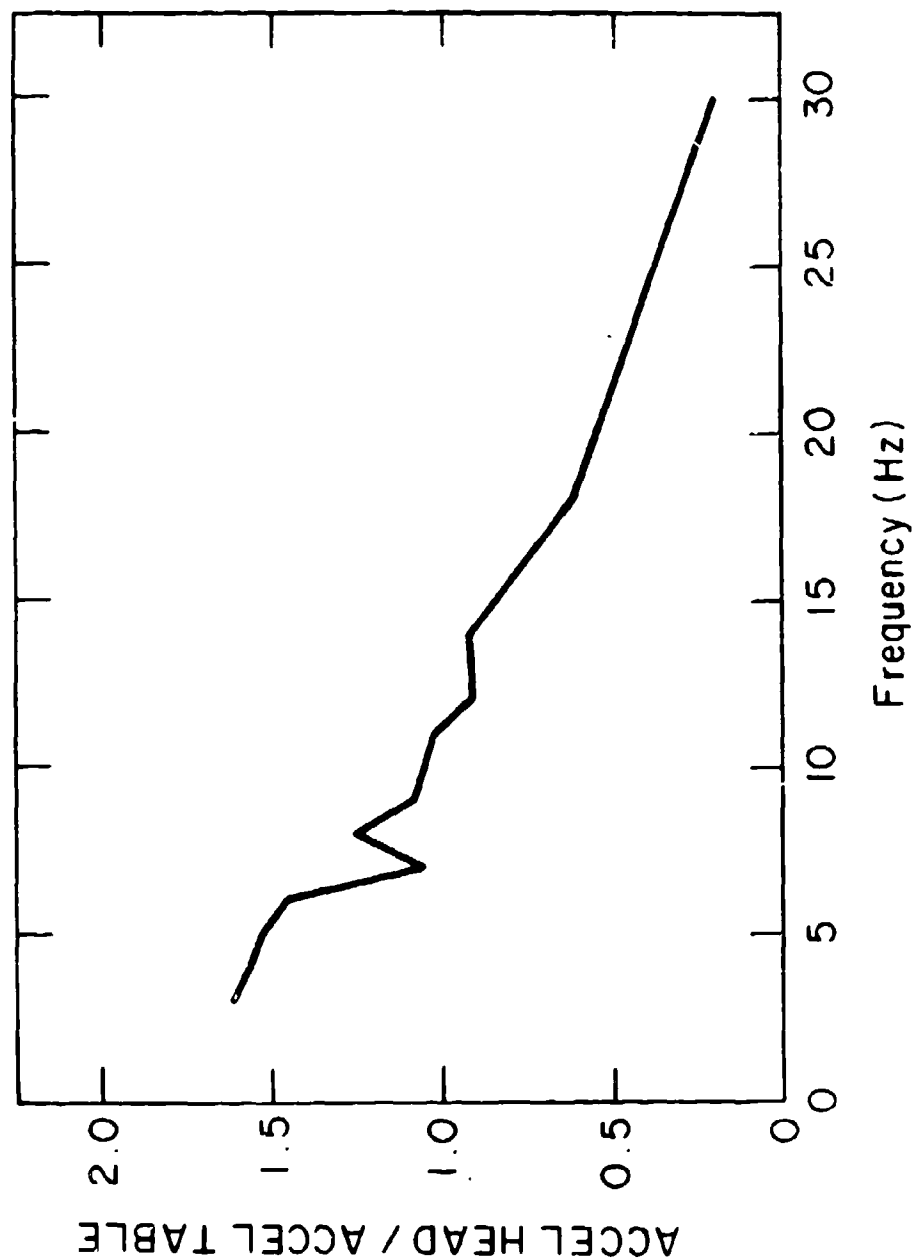


Fig. 16 Head transmissibility vs. vibration frequency for Rhesus monkey.

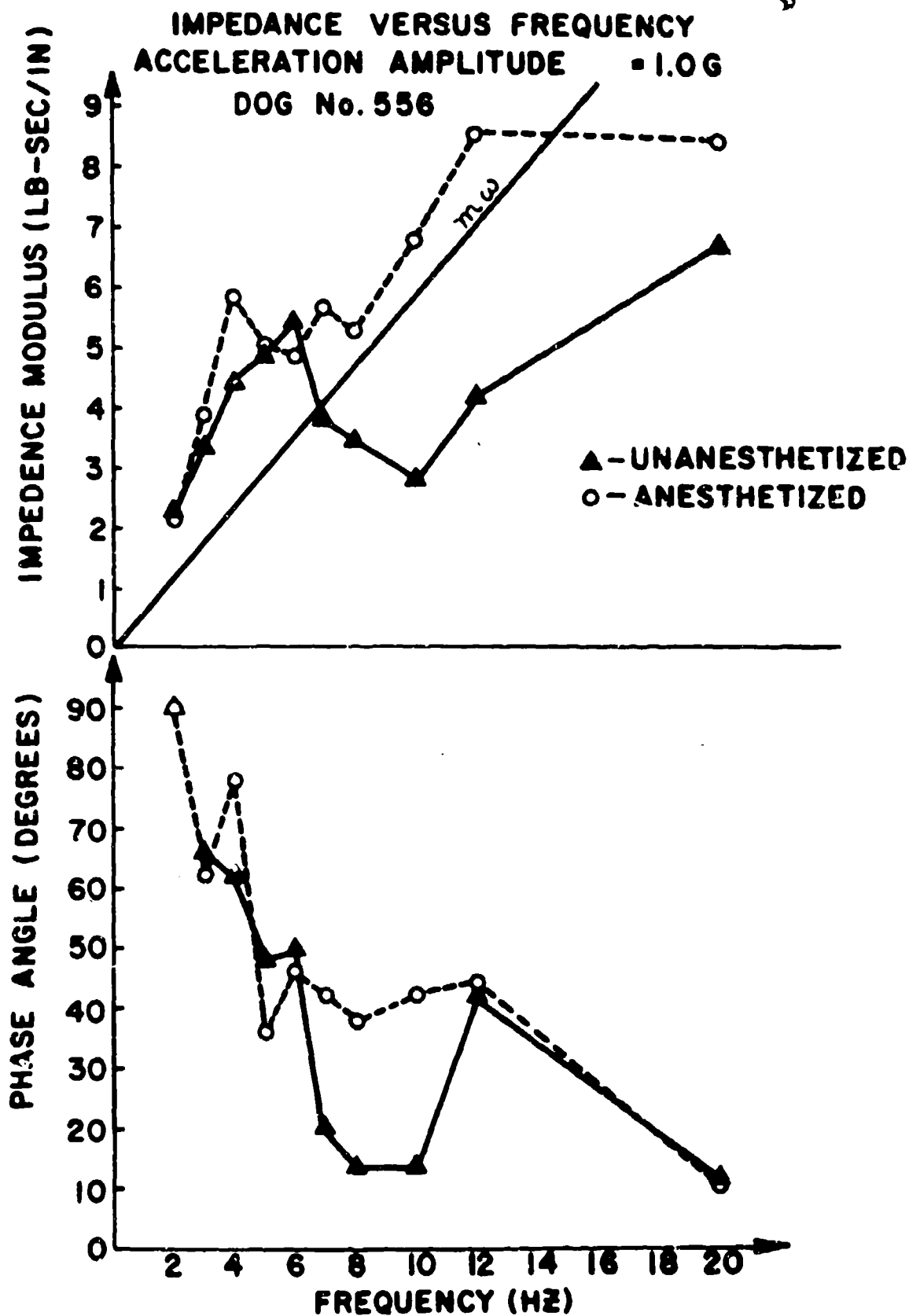


Fig. 17 Impedance modulus and phase angle versus vibration frequency for anesthetized and unanesthetized dog vibrated at 1.0 g.



TRANSMISSIBILITY (Aortic Flow Transducer Relative To Vibration Exciter)

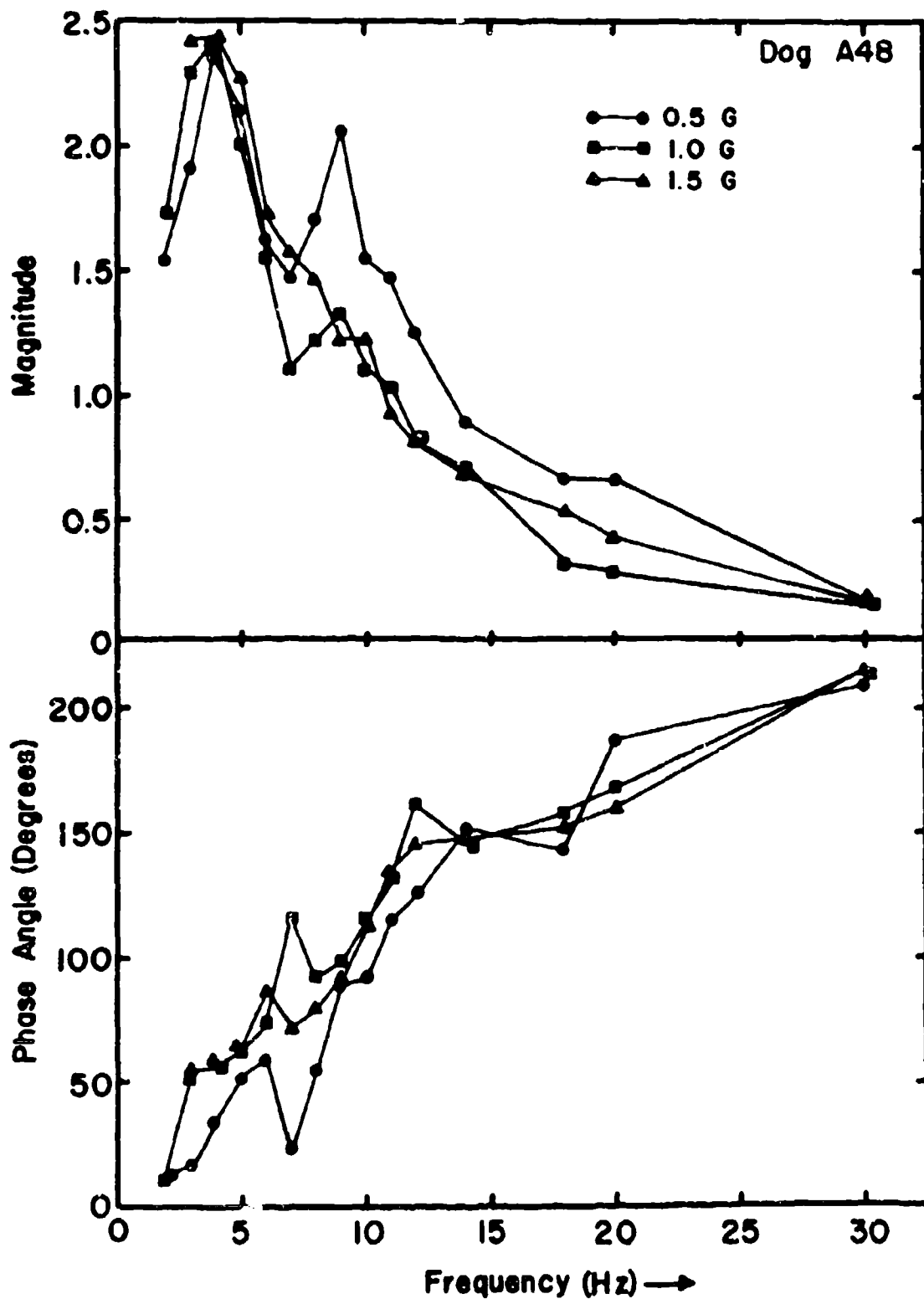


Fig. 18 Aortic transmissibility, magnitude, and phase angle, vs. vibration frequency for a dog vibrated at 0.5, 1.0, and 1.5 g.

### III. Appendices

## Appendix A

### Experimental Techniques

#### I. Animal Care

A. Pre-Operative Animal Care: Surgery for the chronically implanted instrumentation required for vibration studies has been performed in dogs and monkeys. Mongrel dogs (10-20 kg.) supplied through the University of Kentucky Medical Center have been generally satisfactory. An attempt to use purebred foxhounds for more uniformity was not successful - the mongrels were generally better behaved for awake studies and were much harder for thoracic surgery. Rhesus monkeys (*Macaca mulatta*), weighing 5-10 kg., have been generally healthy as supplied by the vivarium at Wright Patterson AFB. As an alternate to the Rhesus, pigtail monkeys (*M. Nemistrina*) of a similar size purchased from Primate Imports (Long Island, N.Y.) have undergone surgical experimentation although none have been exposed to vibration.

Successful chronic implantation procedures and techniques and surgical procedures used in the chronically instrumented animal must begin with a healthy animal. Success is directly proportional to the standards set. Because some of our investigations include unanesthetized preparations in an environment which tends to be stressful to the animal, behavior patterns, such as nervousness, must be discerned before choosing a surgical subject.

The physiological guidelines for determination of normality include physical examination, qualitative estimation from behavior patterns, and results of hematological, bacterial culture, and x-ray examinations. Therapy for canine intestinal parasites is repeated until stools are negative. For the dogs a hematocrit value of 45 and white cell count of 10,000 or below is expected. The hematocrit for monkeys should be 40 to 42 with a white count of less than 15,000. In addition to these determinations, values for many

commonly used variables in dogs appear in Table A-1. Multiple similar variables for monkeys are listed in the report by McCutcheon, et al. (to be published).

B. Surgery-General Procedure: Inclusion of each of the following criteria involving the surgical procedure has been found necessary to produce a successful chronic animal preparation:

1. sterile preparation
2. surgically convenient and properly prepared implants
3. minimal trauma and resultant minimal fibrosis within surgical area
4. isolation of implants from external environment

The above criteria complement each other - details of each and specific aspects of surgery are found in the sections below. Following immediately is a general overview of the surgery performed on animals which have met pre-implantation standards.

Surgery is performed with complete sterile precautions using the facilities in the Experimental Surgery Laboratory of the University of Kentucky Medical Center. The principles of laboratory animal care as outlined by the National Society for Medical Research were rigorously observed. The monkey is premedicated with sernylan and atropine, induced with thiopental, intubated, and anesthetized with halothane. For the dog, the procedure is identical with the exception that sernylan and atropine are not given. The approach to the chest is through the left fourth intercostal space with the various transducers placed as required. Each lead is passed through different spots using intercostal spaces other than the one for entry. The rib cage is closed in the usual manner and the leads are tunneled under muscle layers to emerge between muscle and skin in the center of the back, between the scapulae. The

skin is undermined and freed up from the original incision to the point where the leads emerge. The leads are gathered together and placed in a fabric velour bag of our own design (McCutcheon, et al., 1973a) and left under the unbroken skin. The muscle layers and skin of the original incision are closed in the usual manner. A chest tube connected to a water bottle suction is left in for twenty-four to thirty-six hours.

The abdominal approach is through a mid-line incision in the linea alba. Females are much more suitable for the abdominal procedure. The probe leads are placed on the back in a manner similar to that used for the thoracic implantation.

The fabric velour pouch used to store the transducer connectors under the skin is sewed from nylon velour fabric (fig. A-1). More recently, a dacron velour material has been tested. The pouch is initially gas sterilized, and after its implantation the site is left undisturbed to allow connective tissue growth into the fabric.

Approximately 8 to 12 days after surgery, the level of recovery is adequate to open the pouch ("windowing" process) and obtain access to the leads. Under tranquilization and local anesthesia, an appropriate length of skin over the pouch is incised. The pouch is opened with scissors and the leads removed and tested (fig. A-2). The edges of the skin are retracted and sewn to the outer layer of the pouch. The inner fabric layer is closed with suture or steel clips (fig. A-3).

After the bag has been opened, the area is kept covered with a dressing and a nylon mesh jacket. The jacket has prevented access by the dogs to any exposed connectors or to the bag itself. Additional caution is exercised with the monkey - a custom-fitted jacket of porous girdle material is the first covering, and a second jacket of leather is fitted over this. Both jackets are closed by sewing them together at the back.

C. Surgery - Instrument Implantation Schedule: The standard intrathoracic instrumentation in the dog includes the following:

1. Flow probe on ascending aorta
2. Pressure gauge in apex of left ventricle
3. Pressure gauge in thoracic aorta just distal to arch
4. Pacemaker ECG leads on right atrium
5. Cannulae in right atrium, left atrium, and through subclavian artery into aorta.

Other implanted devices which have been substituted for some of the above include an intrathoracic temperature probe (thermistor bead) and single axis accelerometer.

The standard intrathoracic instrumentation in the monkey includes the following:

1. Flow probe on ascending aorta
2. Pressure gauge in:
  - a. Descending thoracic aorta with subclavian arterial cannulae or
  - b. Apex of left ventricle
3. Cannulae in right atrium and left atrium (unless subclavian cannula present)
4. Thermistor temperature probe

A few carotid implants have succeeded but recording from this vessel is not yet a standard procedure. In order to acquire more experience with implantation techniques in the Rhesus and Pigtail monkeys, several animals were implanted with right and left atrial cannulae and intrathoracic temperature probe.

Instrument placement in the abdomen (dogs only) includes the following:

1. Flow probe and occluder on renal artery
2. Flow probe and occluder on mesenteric artery
3. Flow probe and occluder on iliac artery .

D. Post-Operative Animal Care: Aside from the procedures involved with "windowing" the implanted pouch, routine post-operative management includes antibiotic coverage, blood hematology and chemistry tests, dressing changes, exercise and training (if necessary), x-rays, and maintenance of transducer lead integrity and catheter patency. The fact that these animals have undergone major surgery and need most if not all of the preceding diagnostic tests and care cannot be overemphasized.

The post-operative antibiotic schedule is coordinated through veterinarians at Wright-Patterson AFB and the University. Cultures of suspect areas are taken and upon receiving sensitivity results, corrective medication is administered. Simultaneous blood hematological (i.e. hematocrit, white blood cell count, differential leukocyte count, platelet estimation) and chemical diagnostics (total protein, glucose, electrolytes) aid determination of the animal's condition and also resultant trends following antibiotic dosages. Since many antibiotics adversely affect renal function, urine chemistries (glucose, protein, bilirubin) and sediment analysis are monitored and trends noted.

In the dog, the original chest incision site has occasionally failed to heal completely, and over an extended implantation time the tissue actually begins to break down. The source of the infection has been both external and internal, the latter arising from one of the lead tracts exiting from the windowing pouch. Adequate care, including fluid drainage if necessary, and bacterial cultures have been successful courses of action. Of the cultures taken, most have shown *Staphylococcus aureus* (coagulase positive and negative) while others have grown *Staphylococcus epidermis*. Other than topical ointments or powders, post-surgical treatment is accomplished routinely using Combiotic (sometimes in combination with Ioridine) for 7 to 14 days. Later cultures having

the above mentioned growths have usually been sensitive to and treated with Erythromycin or Keflin.

Intensive antibiotic treatment in the monkey has been the only route to curb a frequently occurring infection usually beginning in the outer tissue surrounding the fabric pouch. Common species found have been primarily *Pseudomonas aeruginosa* with others being *Proteus mirabilis*, *Enterobacter aerogenes*, and *Escherichia coli*. As with the dogs, Combiotic is also given after surgery followed by treatment with other antibiotics if necessary. This latter course has included Gentsamycin and sometimes Carbenicillin, Chloramphenical, Loridine, Ampicillin, and Keflin.

The animal is weighed periodically and quality and quantity of intake and output are observed. If nutrition seems inadequate, special efforts are made to tempt him with favorite foods, and hand-feeding is performed if necessary. Blood status is monitored as indicated, and injections of iron and vitamins are given.

The usual use of x-rays over the period of implantation provides a valuable diagnostic tool not only in determining the health course of the animal but also the status of the implanted transducers. Lung inflammation and other abnormalities within the chest region can be detected. Often if a transducer does fail, an x-ray will bring out a broken wire connection or kink in a cannula and corrective measures, if possible, are taken. A representative family of x-rays taken from a dog and monkey are shown respectively in figures A-4 and A-5. In these post-operative pictures the absence of congestion and abnormalities with concurrent blood analysis and observations are used to determine the qualification of each subject for experimental investigation.

One further aspect of post-operative care which is very important to our particular protocol is that the animal receive some exercise and a form of adap-



tive training. Both dogs and monkeys are normally caged, and the routine of daily or nearly daily walks or tasks is necessary to examine fitness for vibration, speed recovery, and adapt the animal to the personnel involved with the experiment. Experience has shown that prior awareness of (not necessarily adaptation to) the vertical restraint chair (especially dogs) tends to calm the animal and result in a more meaningful experiment. Adaptation to over-the-head helmets for respiratory studies has also been beneficial. Further improvements in post-operative behavioral care are being worked upon and the preceding examples only illustrate this complex, yet often overlooked, area of animal care.

Since the chronically instrumented animal is usually sacrificed under investigator control, an autopsy can be performed. Much vital information is available from these examinations which have been routine upon the death of a chronic animal. Tissue specimens are sent to a pathology laboratory and the results of the microscopic examinations have guided us during program development, particularly in three areas: 1) tissue ingrowth patterns of the nylon (and dacron) velour materials; 2) specific diagnosis of any pathology, if present, in the major organs of the animal (i.e. heart wall) muscle, kidney, aortic vessel wall); 3) improvements in surgical technique or implanted transducer design. Specific references to such results are found in succeeding sections of this report.

## II. Chronically Implanted Instrumentation

The selection of instrumentation and/or materials for implantation is one of the more difficult aspects of developing a chronic animal preparation. Experience is a large asset and careful evaluation of any device prior to and during chronic implantation is of the utmost importance. The failure of one component in such a preparation can be costly in terms of money, manpower, and time. Therefore, in our laboratory we have devoted a great deal of effort to these concerns. The following sections describe the implanted instrumentation used in our laboratory, and the procedures we follow. Included with each description are design considerations, specific surgical techniques, and results of evaluation tests. The techniques are covered in considerable detail since they are extremely important for overall program success.

### A. Blood Flow

1. Implantation: Blood flow measurement is one of the most valuable components of the techniques used for evaluation of the circulatory effects of vibration. For our standard chronic animal preparation, electromagnetic cuff-type flow probes are placed around the base of the ascending aorta. At this location, a satisfactory physiological zero flow baseline is present - vessel occlusion is unnecessary, in contrast to the situation for peripheral vessels. Unfortunately, however, the wall of the blood vessel under the probe at this site is subjected to large stresses due to the rhythmical wall pulsations and limited anatomical space for probe placement. The effects of vibration (see results section concerning accelerometer placement on the flow probe) compound this trauma to the vessel.

To strengthen the flow probe-aortic tissue interface, and to minimize the occurrence of vessel rupture, some of the probes have been narrowed to decrease the probe-vessel contact area and allow the probe cuff to surround a shorter

section of aorta. A common curtain material (Sears "Entree Tailored Panel, 100% polyester Sheer Marquissette") around the vessel under the probe seems to minimize deterioration of the aortic wall. Dacron mesh or silastic used in a similar manner was not as successful. Even with these methods coupled to careful surgical implantation, rupture of the aorta, generally between the heart and probe, accounts for 60% of the deaths in our chronically-prepared animals (note: improving the procedures for implantation of the aortic pressure gauge has nearly doubled this percentage).

A representative pathology report describing the effects on an intact aortic wall under the probe after 56 days (cause of death in Dog 1600 was rupture of thoracic aorta at pressure gauge site; flow probe: In vivo metric SL-1B, #2108, 20 mm I.D. probe, curtain material) was as follows:

Sections of the aorta from the region of the curtain reveals the material on the outer surface of the aorta and each of the individual threads is surrounded by fibrous tissue. The aorta progressively becomes normal toward the intimal side. The outer half of the aorta in this area reveals separation of the elastic fibrils with fibrosis between them. In the most outer portion there is some fragmentation of elastica. The curtain appears to be firmly embedded with this adventitial tissue.

The changes are more extensive when the cause of death is aortic rupture proximal to the flow probe. The pathology report typical for this latter situation (Dog 822, Zepeda #923, 18 mm I.D., Dacron mesh, duration of implantation 20 days) was as follows:

Section of the aortic wall under the flow probe near the site of rupture reveals a portion of the aorta with a zone of fibrosis in the outer two-thirds of the aorta, merging with fibrosis within the adventitia and the meshwork. At one point at the very edge the wall appears completely necrotic. This probably represents the point of rupture.

Alterations in the aortic wall in monkeys are similar to those of dogs. The intact vessel wall under the flow probe (Pigtail monkey PT4: Zepeda AA-#1142, 9 mm I.D., curtain material, duration 51 days) was the subject of the following report:

Section of the aorta shows an intact intima and an intact media. There is evidence of the foreign material of the curtain in the adventitia associated with fibrosis and some degeneration in the very outer portions of the media. There is also associated intimal fibrosis.

The above results support the conclusion that a reinforcing material under the probe probably provides a useful additional interface between the vessel wall and probe.

2. Flowmeter and Flowprobe Evaluation: For a flow probe located on the ascending aorta, a satisfactory physiological zero flow baseline reference is present. This baseline can drift, however, depending upon the flow probe and/or the flowmeter to which the probe is connected. A number of specific causes have been detailed (Gordon, 1971; Cappelen, 1968; Hagnestad, 1961, Dobson, et al., 1966; Spencer and Denison, 1959; Fryer and Sandler, 1971) in the literature.

Electromagnetic flowmeters undergo continuing evaluation in our laboratory. Those currently in use are clearly not optimum instruments (Biotronex laboratory, Maryland, Model 610 Pulsed Logic Flowmeter, and Zepeda Instruments, Seattle, Washington Model SWF-2 Square Wave Flowmeter). For instance, the Biotronex device has no "zero" capability. The Zepeda flowmeter, with careful bench calibration, is reported to provide a "magnet zero" within 5% of the true blood zero. Preliminary bench tests indicate that for moderate flows ( $1 \text{ L/min} < \text{flow} < 5 \text{ L/min}$ ), the magnet zero is no more than 5% from actual zero baseline flow. However, no internal calibration for checking flowmeter and recorder amplifier gain is available on the Zepeda instrument. More long-term drift studies need to be done to permit adequate comparisons of different probes over a period of time or the same probe over different time intervals. Evaluation of flow meters measuring smaller peripheral flows with chronically implanted probes requires vascular occlusive devices more satisfactory than any developed to date in our laboratory. Further acute animal studies are now underway to add more information and direct our efforts to solve this problem (see also section B).

Three different manufacturers' probes have been implanted in our chronic animals. In the dogs, we have used flow probes made by Zepeda Instruments, Biotronex Laboratory, and In Vivo Metric; in monkeys, we have implanted Zepeda and Biotronex transducers. When connected to the EL 610 flowmeter, all the larger probes exhibited essentially the same output characteristics in all chronic animals. The IVM probes tended to be the least stable during bench calibrations and implantation, probably as a result of their narrower width and smaller electrode area. The Zepeda probe, now the standard in our laboratory, is quite stable although its greater width contributes to some of the trauma seen within the wall of the ascending aorta. Both the Biotronex and IVM probes used have been more susceptible to internal or connector failures while implanted and during recycling checks between implants.

The outer diameters of the ascending aorta of the monkeys implanted to date ranged from 7 to 12 mm. In this range the flow probe most used has been the axial lead, symmetrical core Zepeda probe. A minor drawback of this probe, the narrow slot key opening, which makes surgical manipulation slightly more difficult, is more than offset by its stable performance and durable construction.

A still smaller range of probe sizes has been briefly studied during abdominal implantation. Three to five millimeter lumen diameter probes from the three manufacturers listed above have been used. An evaluation of the performance of these probes will be available following more experimentation and bench calibration now in progress.

The technique of flow probe connector placement within a subcutaneous fabric pouch places additional restraints on the probes selected. Requiring a larger pouch volume and window slit area, the bulky button or bullet connector, standard with many flow probes, is unsuitable for our particular chronic preparation. The Zepeda connectors have a base of shrink-tight tubing and male pins sealed with shrink-tight during storage. These have proven satisfactory in terms

of storage space and reliability. It has yet to be determined whether a connector system of two small diameter (2.25 mm), silastic covered leads is more compatible with our particular chronic animal preparation than the single larger (O.D. 2.5 mm) silastic insulated lead common with the button connector found on large probe sizes.

3. Bench Calibration: All incoming flow probes are tested and bench calibrated before use. Probes in use are tested for electrical continuity between implants and are periodically calibrated using saline and/or blood. The purpose of the bench calibration is to evaluate the linearity of the probe with age (especially for low flows), and to provide a flow calibration number (CAL) which can be compared with in vivo dye curves. A listing of some of these results is found in Table A-2 which also illustrates some of the variables employed for bench calibration.

For larger probes (18 to 22 mm I.D.) cellophane dialysis tubing has been used as a substitute for the blood vessel wall. Soaked for approximately thirty minutes prior to testing in normal saline, the tubing is connected into a gravity flow system where the pressure at the probe level is held constant at 125 mmHg. Besides being convenient, the dialysis tubing forms a stable seat for the cuff-type probes tested. Multiple probe testing can be accomplished with this system providing care is taken to minimize possible electrical interference between nearby probes.

Typical bench calibrations using normal saline and blood of varying hematocrits (derived from packed red cells mixed with normal saline) are plotted for two Zepeda flow probes in Figures A-6 and A-7. Representative straight lines fitted to the points (least squares method) indicate that in both plots (except for one case), the probes had greater sensitivity with saline. Higher hematocrits tended to result in lower sensitivity. For other probes, the direction of sensitivity when using dialysis tubing has been consistently the

same. The overlap of points indicates other factors that may influence the curve slope such as daily variations in methodology (Fryer and Sandler, 1971; Cuthbertson and Gilfillon, 1971; Cappelen, 1968). No definitive pattern has been seen in relation to the duration of implantation and/or age.

For the smaller monkey probes, a variety of materials have been used to anchor the probe for calibration trials. Dialysis tubing has only been available for the 6mm size. Blood vessels (abdominal aorta of small pigs) and latex tubing have been used for the other sizes. The probe is inserted within this latter material and the leads are brought out through a sealed joint.

For the calibration plot of a Zepeda (7mm I.D.) symmetrical probe appearing in Fig. A-8, the probe was placed inside the tubing. No specific trend in sensitivity is evident in the plot. Similar probes calibrated from a position within the flow stream have yielded results also indicating saline produced a greater relative output. Bench tests using saline and excised pig aortas resulted in increased sensitivity, compared to the system employing direct blood electrode contact.

Flow probes having a lumen diameter less than 6mm and intended for peripheral vessel use have usually been calibrated on an intact vessel by bleed-out volume/time determinations. When done either acutely or chronically, this procedure provides an adequate calibration factor in lieu of dye curve determinations which become more complex for peripheral vessels. Bench calibrations on small probes have been accomplished using dialysis tubing or latex tubing (probe in flow), but such techniques are used only for linearity evaluations and CAL signal comparisons.

4. Dye Curve Technique: A standard procedure for calibrating chronically implanted electromagnetic flow probes by the dye-dilution technique has been developed in the laboratory. Chronically implanted catheters in the right atrium, left atrium, and subclavian artery make possible several combinations of dye injection and blood withdrawal. Normally, a bolus of indocyanine-green dye (approx-

mately 2.5 mg for dogs and 1.0 mg for monkeys) is injected through the dye-filled right atrial line without flushing. The blood-dye mixture is withdrawn from the left atrium at 10 ml/min. Both right and left atrial injections combined with aortic pickup have given reasonable results, although in several cases the latter situation appeared to give suspiciously high outputs, perhaps due to inadequate mixing. The concentration of this mixture is measured with a Waters XP-300A Densitometer equipped with an XC-302 cuvette and recorded on a Honeywell Visicorder (Fig. B-3). The output of the electromagnetic flow probe is recorded in both phasic (to establish flow zero) and mean modes simultaneously with the output of the densitometer. The height of the mean flow trace above the phasic zero is measured during the passage of dye through the cuvette and this trace is analyzed to give cardiac output.

The analysis of the dye curve is by the Stewart-Hamilton method (semi-log replot and extrapolation under the assumption of an exponential decay). An on-line computer analysis of the curves is operational (see Appendix B) and allows immediate interpretation.

5. Comparison of Flow Probe Calibration Results: When the bench calibrations are compared with dye curve results for a specific probe on a particular animal, a wide range of differences from the reference CAL signals is evident. The dye curves have generally read approximately 30% higher than the bench CAL signal assigned the Zepeda probes. This is approximately the result expected from theory. However, as evident in Table A-2 this percentage figure is not consistent; in fact, some probes having stable bench numbers have had a wide range of dye curve calibrations assigned to them.

The varied dye curve versus CAL results are particularly noticeable for the Zepeda probe SN922. There seems to be little correlation between the derived CAL and hematocrit, cardiac output, or cardiac output normalized to body weight. A curious and unsolved dilemma concerns Dog #1607 for which two dye



determinations were done. This particular dog eventually died from an aortic rupture at the flow probe site, indicating that aortic wall thickness may have been decreasing during implantation. Similarly, Dog L185 died from aortic rupture just two days after the dye curves, and the dye curve CAL was low.

Variations in probe electrode contact and wall thickness during implantation may account for the range of differences illustrated in Table A-2. In the previous literature, there are many conflicting findings and uncertainties regarding calibration techniques and dependent variables. For this reason, coupled with our findings, we rely on the dye curve results to yield a CAL signal value since the dye dilution measurement is sufficiently reproducible and is recorded under in vivo conditions.

#### B. Vascular Occluder

When an accurate electronic blood flow zero is not available, mechanical occlusion of a vessel to obtain a zero flow baseline is essential. Currently we use the occluder design outlined by Khouri and Gregg (1967). A dipping process yields small latex cuffs of varying sizes dependent upon the stainless steel mold used. In vitro and in vivo (dog) testing with two sizes is underway. A smaller size (3 mm diam) is planned for coronary artery implants, and a larger size (5 mm diam) for peripheral vessels such as the femoral artery.

After removal from the mold, the C-shaped latex body is cured for ten minutes in a steam autoclave (15 psi). An umbilical tape backing and "Tygon" tubing (I.D. = .030", O.D. = .072", Norton Plastic and Synthetics Div., Akron, Ohio) are attached to the latex with DAB cement (R.M. Hollingshead Corp., Camden, N. J.). Stainless steel wire loops are glued with DAB to each end of the occluder so that the ends can be drawn together when implanted around the vessel.

These occluders, when tested following the animal's post-operative recovery period of approximately two weeks, have provided only a few successful occlusive cycles before malfunction, usually the result of a blow-out. Preliminary results

indicate the addition of one or two more coats of latex to the original three layers considerably improves its durability without sacrificing its performance.

#### C. Blood Pressure

Recordings from the implanted pressure gauges have been reliable and stable. Our signal processing system consists of Honeywell strain gauge modules (Accudata 105) and associated DC amplifier units (Accudata 120 DC Amplifier). Variable bridge excitation voltage and amplifier gain are available to the operator and are used during our transducer evaluation tests.

Standard acceptance evaluation tests are run on all pressure gauges that are used in our laboratory as previously described (McCutcheon, et al., 1972a; McCutcheon, et al., 1973b). The transducers are examined for sensitivity, frequency response, and temperature drift - schematics of the test and experimental apparatus are shown in Figure A-9. Between the transducer's removal and subsequent implantation, the sensitivity is checked. Further testing (e.g. temperature drift) is done periodically to insure the transducer is operating properly.

To illustrate the results of the above mentioned test, a chronological series of tests and recycling checks done on an implantable pressure gauge is listed in Table A-3. The transducer chosen is a Konigsberg P-21 (SN 15) although many of our other gauges could also have been similarly represented. Including a total of 12 chronic implantations ranging from 11 to 56 days, Table A-3 represents the transducer's history from its evaluation test during June, 1971 to the most recent examination in September, 1973.

The column labelled "sensitivity" needs further explanation, for in our laboratory we set the excitation voltage to match a constant output voltage for a given input pressure. To accomplish some standardization with previous literature, the output voltages were normalized to the excitation voltage. Percent changes in sensitivity reflects the difference from implantation to subsequent

recycling during which the sensitivity is recalibrated. The change in sensitivity varied from -1.9% to +0.8% with no consistent pattern seen as the transducer aged, and the percent change in sensitivity remained small.

Evaluation tests on the P-21 #15 showed little change from 1971 to 1973. The linearity test (including hysteresis) was accomplished by subjecting each gauge to 25mmHg pressure increments from 0 to 300 mmHg followed by 25 mmHg decrements to zero pressure at 37°C. Temperature stability tests include zero-pressure drift measurements over a 32°C to 42°C range in a water bath, water (37°C) to ambient air to water (37°C) transients, and a long-term three to four hour stability test in a 37°C water bath. Further test specifications and methods may be found in previous articles (McCutcheon, et al., 1972a. McCutcheon, et al., 1973b).

Currently in use as implantable pressure transducers are Konigsberg (Pasadena, California) and Bio-Tec (Pasadena, California) models. In dogs for aortic and left ventricular placement, 5.0mm (P-19) and 7.0mm (P-21) Konigsberg gauges as well as 6.5mm (BT-250T) Bio-Tec transducers have been used. Smaller 4.0mm (P-13) and 4.5mm (P-12) Konigsberg transducers have been implanted in the monkey's aorta and left ventricle. The above gauges have been satisfactory in terms of performance and durability. Occasional transducers have failed our acceptance evaluation tests and were returned to the manufacturer.

After the pressure gauge has been tested, a silicone rubber (General Electric RTV-112 Adhesive) "washer" is molded behind the sensing element. A typical preparation is shown in Figure A-10. The gauge head is then briefly treated with TDMAC and heparin anticoagulants (see Cannulae section for details) before gas sterilization.

A significant improvement in aortic wall integrity at the pressure gauge site has occurred since placing a silicone rubber "washer" between the sensing element and vessel wall. Since the initiation of this method, 16 dogs have been implanted with an aortic gauge and no deaths have resulted from wall rupture at

this site. Previously, damage at the aortic gauge site accounted for approximately 25% of the deaths. Apparently, the motions resulting from the heart's contractions (and probably the experimental vibration) caused the sharp edges of the pressure gauge sensing head to break down the surrounding tissue. Pressure transducers in the left ventricle are also fitted with a silicone washer. At the aortic implantation site, silastic sponge material (Dow Corning #812) is also fitted around the vessel for additional support.

Clot formation over the treated portion of the transducer within the vascular system has generally not been a problem. Proper placement within a vessel or chamber is very important. Autopsy results have shown that when the gauge is inserted too deeply into the vessel (aorta), there have been occasional, yet well developed clot formations anchored to the gauge's wire connector. The depth of penetration of the pressure transducer in the left ventricle appears also to be a critical feature, especially in the monkey. Clot formation in this location has been minimal, although when the gauge is pulled closely to the wall at the apex, a combination of tissue growth and/or thrombus formation has occurred. With this latter placement, or when placed too deeply into the ventricle, the resulting ventricular pressure trace has exhibited an abnormal waveform, probably as a result of pressure transients arising from lateral compression of the transducer. None of our dogs have shown such phenomena. The relatively small size of the monkey's left ventricular chamber coupled with possible changes in contractile patterns associated with the increased cardiac output of stress may also account for the occasional presence of these sharp artifacts.

Both the Konigsberg and Bio-Tec transducer connectors have been generally reliable and durable. When not opened for a period of two weeks during implantation, both connectors have exhibited some fluid leakages when sealed as recommended. A commercial cleaner (Freon TF Degreaser, Miller - Stephenson) has worked well for cleaning these female pin connectors. Being relatively small (approximately

0.25" diam., 1.5" long) the connectors are well suited for the fabric pouch used in the chronic animals.

Extravascular transducers have been used for calibration of implanted gauges or pressure measurements during an experiment. These transducers undergo much the same evaluation tests as do the implantable gauges. In vivo calibration of the implanted aortic gauge is accomplished by using a gauge (Ailtech MS-10B, City of Industry, Calif.) connected to the aortic cannula. The ventricular gauge is calibrated by measurement of left atrial pressure through the cannula to that chamber. A manometer-tipped catheter (PC-350, Millar Instrument Co., Houston, Texas) has been used to measure pressures when vessel cutdowns are necessary or appropriate. In contrast to the system employing a fluid filled line, the catheter-tip gauge exhibits minimal vibration artifact.

#### D. Pacemaker Probe

Since some of the more recent investigations require control of heart rate, a pacing probe has also been implanted routinely. Earlier attempts to place a pacing catheter acutely (femoral and external jugular vein entry) prior to the experiment were not always successful, especially when the animal was subjected to vibration. Capture of the cardiac pacemaker was intermittent, probably due to failure of the pacemaker electrode to seat itself firmly in the right ventricle during vibration. To pace the animal we have been using a Grass Stimulator (Model S4G) connected to the pacemaker lead via an isolation unit (Grass Model SIU-4B). The bipolar pacing lead has also allowed relatively artifact free monitoring of an ECG signal during non-pacing experiments. No pacemakers have been implanted in monkeys.

During implantation the pacemaker wire is sutured to the surface of the right atrial wall. A commercial semi-floating pacing probe (Elecath #561, 4 Fr., 100cm) has been implanted in the majority of dogs, and because this pacemaker is intended to be disposable, and is in fact quite fragile, a new pacemaker must be used for

each dog. Recently, we have also used silicone rubber insulated wires (#29-51 x 46 Stranded Copper Conductor, Caltron Industries, Berkeley, Cal.) terminated on the atrial end by a soldered ring and on the pouch end by a small male connector fitting. This latter approach again employs two conductors (bipolar pacing) and we further coat the wires with medical grade Silastic (#861, Dow Corning). Further studies need to be accomplished to determine if lead corrosion over a nominal implantation time of 30 days adversely affects the pacing pulse. To date, qualitative results have been satisfactory.

#### E. Cannulae

Placement of cannula directly into the right and left atria of both monkeys and dogs has become a routine feature of the animal surgery. To calibrate an implanted pressure gauge located just below the arch in the descending aorta, an additional cannula is inserted into the left subclavian artery which is then tied off. With these cannulae, mixed venous and arterial blood samples can be taken. When an extravascular pressure transducer is connected to the left atrial line, a pressure equivalent to left ventricular end diastolic pressure may be obtained.

The reliability of the cannulae for blood sampling and pressure calibration has varied depending upon the animal, the care taken in placement, and cannula design and construction. The tubing used in all our cannulae is "Tygon" plastic tubing (Norton Plastic and Synthetics Div., Akron, Ohio) having an I.D. of .038" and O.D. equal to .072". Joints between the tubing and fitted materials (e.g. polyethylene y-yoke) are made with DAB cement (R.M. Hollingshead Corp., Camden, N. J.). Resistance to kinking has been excellent and it has held up quite well for implantation times of four months. The anti-coagulant treatment (see below) tends to reduce the tubing's plasticity, but not enough to cause kinking or splitting after implantation. Tissue growth over the cannula tips in the atria has caused occasional problems by acting as a one-way valve. Different shapes for the inlet portion of the cannula are still being investigated. The portions of the

cannulae which would be placed in the atrial chambers are illustrated in Figure A-11. Both designs are being used presently, the straight tip in the left atrium and y-yoke in the right atrium. Getting a consistently reliable right atrial sample has posed a still unsolved dilemma as autopsies have regularly demonstrated rampant tissue growth over any cannula tip in the right atrium while the left atrial tip has remained free. The y-yoke tip (s) present a large surface area for sampling - in fact, their use has been prohibited with some of the smaller Rhesus monkeys - but the same type of one-way valves have formed. At present, our solution to maintaining right atrial sampling has been to check catheter patency as soon as possible after surgery, and to flush daily. The cannulae inserted through the subclavian artery (Fig. A-11) into the aorta do not seem to have the problem of tissue blockage and have been very reliable for sampling and pressure measurements.

Another method for obtaining mixed venous blood using the cannula in Fig. A-11 has been in the testing stage to date. Entry through a branch of the vena cava, such as the azygous vein, into the atrium, and then possibly across the tricuspid valve into the right ventricle has shown some preliminary success. Apparently less tissue can accumulate on a "floating" type of cannula as opposed to the tubing rigidly attached to the atrial wall.

#### Anticoagulant

A coating of "TDMAC" (Tridodecylmethylanmonium Chloride - Polysciences, Inc.) and heparin prior to implantation has been successful in preventing clot formation on the implanted tubing. A two-step process is currently used (Grobe, 1972), and the tubing is allowed to dry thoroughly between and after treatments. Because the TDMAC solution tends to remove plastomers from the "Tygon" tubing (Leininger, 1972), the cannula tip is briefly dipped into and flushed with the TDMAC solution. After drying, the tubing is soaked in and flushed with the heparin solution for approximately 10-15 seconds, then allowed to dry before gas sterilization.

#### F. Accelerometers

To enhance the study of vibration-induced acceleration, individual organ accelerations may be examined with an implanted commercial accelerometer (Konigsberg single axis accelerometer, Models A1 and A2). Data have been obtained from the ascending aorta (rigidly attached to the flow probe) and from the descending thoracic aorta below the arch. To facilitate surgical placement and allow axis identification, a silastic base was molded to the accelerometer at a cost of adding some mass to the accelerometer. Further development of surgical technique and/or smaller silastic anchoring hinges is progressing to reduce that particular drawback. Other organ acceleration sites are planned, but these should present no implantation problems.

The implanted accelerometer received in our laboratory is subjected to evaluation and calibration tests (some of which are similar to those involving implantable pressure transducers described previously). Static tests include temperature drift,  $\pm 1G$  sensitivity ratings, and cross-axis responses. Dynamic sensitivity, frequency response, and cross-axis response are tested using the vibration system facilities and precalibrated accelerometers in the Wenner-Gren Laboratory. The Konigsberg accelerometers have generally been satisfactory (although one accelerometer developed an erratic sensitivity due to an internal malfunction shortly after receipt). An in-vivo  $\pm 1G$  calibration for an experiment is accomplished by rotating the animal in the desired axis.

#### G. Temperature

To record an accurate internal temperature, a precalibrated thermistor bead (Yellow Springs, Inc.) has been implanted in the thoracic cavity and sutured to the muscle layers. Earlier troubles with fluid leakage into the connector wire and wire breakage have been nearly eliminated by encasing the lead in flexible silastic tubing, sealing the bead end with silastic adhesive, and closing the connector end with suture tie and shrink-tight tubing. In cases where an intra-



thoracic probe was not implanted, rectal temperature has been measured via an acutely placed probe (Yellow Springs, Inc.). This recording has not been as reliable as information from the implanted sensor since we have had some problem maintaining a standard anatomical (and temperature) reference point during the z-axis vibration. Either a Honeywell Temperature Module or Yellow Springs Scanning Telethermometer serves as the first interface between the probe and paper chart recorder and/or computer.

#### H. Implant Support Materials

Included in this section are the qualitative evaluations of materials associated with the devices implanted in the animals. The investigation revolves primarily around the use of nylon and dacron velour fabrics. Determination of the success of the implant material has depended upon the results of tissue examinations and gross observations made during the chronic animal's implantation period.

In the majority of implanted animals, the skin tissue - velour fabric pouch margin has formed a tight seal upon both gross and microscopic examinations as summarized in Table A-4. Sections generally show skin with an unremarkable epidermis and upper dermis. Further microscopic findings indicate the pouch fibers are embedded in fibrous tissue arising from the subcutaneous layers.

Excepting instances where many pouch openings can be expected (i.e., most of our monkeys have required almost daily attention to maintain right atrial cannula patency), the double layer nylon velour pouch has become the standard pouch implanted. The dacron pouch serves as an alternative as it is a stronger material over long implant times than nylon. Different tissue ingrowth patterns have not been noted between these two velour fabrics, but our experience with dacron has been limited.

Because of the nylon velour's capacity to form a firm fabric-tissue interface, this material's use has been extended to other areas of the surgical pre-

paration. Autopsy examination of the velour covered leads has revealed that an effective tissue seal has formed along what would have been the lead track. The extent of the foreign body (tubing, DAB cement, velour) reaction has not been sufficiently defined at present. Without the velour, various degrees of fistulae have formed along the lead sites regardless of the composition of the implant devices' leads we currently employ: silastic coated wires, polyvinyl-chloride insulation, "Tygon" tubing, and various other plastics.

The addition of a velour layer to the leads does, however, create more lead volume and more tissue must be disturbed when routing leads from the chest to the pouch. If bacteria invade the implanted velour, the treatment of the infection is a much more severe problem than if the material were not there, for the fabric site containing the bacteria is nearly inaccessible. Whether the addition of velour to the leads is beneficial to the overall chronic animal preparation has not yet been determined.

### III. NON-INVASIVE MEASUREMENTS

#### A. ECG & Temperature

Depending upon the particular experimental protocol, skin electrodes (Beckman) are also available for external measurement of ECG. Skin temperature probes (Yellow Springs, Inc.) are applied for measurements of surface temperature.

#### B. Oxygen Consumption

Oxygen consumption has been measured on both unanesthetized and anesthetized animals. A flow-through system (Fig. A-12) is employed for awake dogs and monkeys; that is room air drawn past the animal's head will show a decrease in oxygen content dependent on the amount of  $O_2$  consumed by the animal. In an anesthetized preparation, oxygen consumption is determined from the known respiratory volume and rate and by sensing the partial pressure of oxygen in the output port of the respirator.

Further helmet-mask development for the dog (Fig. A-13) is occurring with emphasis, as was done for the monkeys, on obtaining a uniform room air flow rate past the exhalation site.

Not all dogs have accepted the plexiglass helmet upon initial trials and it has been necessary to acquaint the dogs with the helmet. The helmet in its preliminary design is secured to the vibration restraint chair with tape and padding. Helmet design requires allowance for space for the dog to pant as they do during a vibration protocol. Our brief experience with a latex mask, which did not have enough dead space to allow panting, showed that a dog's internal body temperature rose noticeably in a short time period.

The monkey helmet (Fig. A-14) is formed from lightweight, transparent plastic and is secured to the vibration restraint chair by a large hose-clamp. With the present design for monkeys, we use two different size helmets depending on the size of the monkey. The bottom plate of the helmet has holes allowing a controlled room air inflow and a rubber seal which fits loosely around the monkey's neck.

Room air flow rates are controlled by an electric blower and monitored continuously by a Fleisch pneumotachograph (Instrumentation Associates, Inc.) connected to a differential pressure gauge (Statham). This combination, after calibration, results in a hard-copy recorder printout. For the monkeys, an air flow rate of 10 L/min is generally used. For dogs, this is increased to 15 or 20 L/min. Flow rates below these values tend to compromise the quality of the mixing of exhaled and room air plus altering the normal partial pressures of inhaled gases. The sensitivity of the measurement decreases with increasing flow rate.

The mixed ratio of exhaled air and room air is then sampled continuously with a vacuum pump at approximately 400 ml/min. To eliminate varying temperature-humidity effects in the open system, before entering the oxygen sensor cell (Applied Electrochemistry Inc.), this sampled mixture is pulled through a drying tube. A readout voltage proportional to percent oxygen content is then available for the recorder and computer (where  $O_2$  consumption over a selected period of time is calculated).

Calibration of the air-flow system is accomplished with the use of a bubble-flowmeter (precalibrated) and vacuum line. The  $O_2$  sensor has been periodically checked with tank oxygen concentrations: a high end of 98%  $O_2$  and low end of 11%  $O_2$  are used. Daily standardization is accomplished by reading "dry" room air.

The response time of the AEI thermal cell sensor is in milliseconds, but the overall response times of the flow-through system are much larger. Depending upon the dead space volume in front of the sampling line, the delay is generally 2 to 5 seconds. The drying tube adds another 6 seconds to the response time and therefore the final breathing pattern seen is quite damped. To determine a respiration rate more accurately using this method, the air in the system can be heated to the internal body temperature and drawn through the sensor while saturated with water vapor. At present, this latter method is being developed.

#### IV. Summary of Chemistry-Hematology Measurements

Depending upon the animal's condition and the experimental protocol, the following tests as summarized are conducted on a routine basis:

1. pH,  $pO_2$ ,  $pCO_2$  (Radiometer determination - Radiometer A/S, Copenhagen, Denmark).
2.  $O_2$  and  $CO_2$  content (Van Slyke technique or nomogram calculations from radiometer and hemoglobin measurements).
3. Free Fatty Acids (modified technique from Novak, 1965, in Lafferty, et al., 1973).
4. Cortisol (competitive protein binding assay of Murphy, 1967 and Beamer, et al., 1972).
5. Glucose (glucose oxidize - peroxidase method-GOD-Perid, Boehringer Mannheim Corp., N. Y., N. Y.).
6. Hemaglobin (cyanmethemoglobin method - Globintest, Pfizer Diagnostics Div., N. Y., N. Y.) and Hematocrit (capillary tube).
7. White Blood Count (hemacytometer) and Differential WBC count (slide using Quik Stain, Chemstat, Inc., Inglewood, Calif.).
8. Other hematology tests such as sedimentation rate, red cell fragility, and reticulocyte count are performed when indicated.



Fig. A-1 Isolated nylon velour pouch with inner surface exposed to show construction details of double layer and overall shape.



Fig. A-2 Close-up of nylon velour pouch implanted for 21 days in a dog (1607). The lead connectors and cannulae had just been removed from storage before experimentation. This pouch has been opened for two prior experimental sessions each on separate days.



Fig. A-3 Implanted nylon pouch after closure with steel clips following experimentation noted in Fig. A-2.





DOG 1600	5/8/72 Pre-Op.	DOG 1600	5/25/72 Post-Op. 11 day	DOG 1600	6/14/72 Post-Op. 21 day
WBC = 12,800/mm <sup>3</sup>	WBC = 22,700/mm <sup>3</sup>	WBC = 15,500/mm <sup>3</sup>			
HCT = 36%	HCT = 31%	HCT = 34%			
TEMP. (RECTAL) = 37.8°C	TEMP. (RECTAL) = 38.3°C	TEMP. (RECTAL) = 38.3°C			
WEIGHT = 19.1 Kg.	WEIGHT = 18.6 Kg.	WEIGHT = 18.0 Kg.			

Fig. A-4 Serial X-rays with corresponding hematological data for Dog 1600 summarizing animal's general health and serving as a guide for antibiotic treatment if necessary.



<p>MONKEY 42</p> <p>1/5/73 Pre-Op.</p> <p>WBC = 10,000/mm<sup>3</sup> HCT = 39% WEIGHT = 5.7 Kg.</p>	<p>MONKEY 42</p> <p>5/21/73 Post-Op. 11 day</p> <p>WBC = 16,250/mm<sup>3</sup> HCT = 34% WEIGHT = 6.4 Kg.</p>	<p>MONKEY 42</p> <p>5/31/73 Post-Op. 21 day</p> <p>WBC = 14,300/mm<sup>3</sup> HCT = 36.5% WEIGHT = 6.0 Kg.</p>
--	---	---

Fig. A-5 Successive hematology values, x-rays, and pertinent data for Monkey 42 indicating progressive recovery from thoracic surgery.

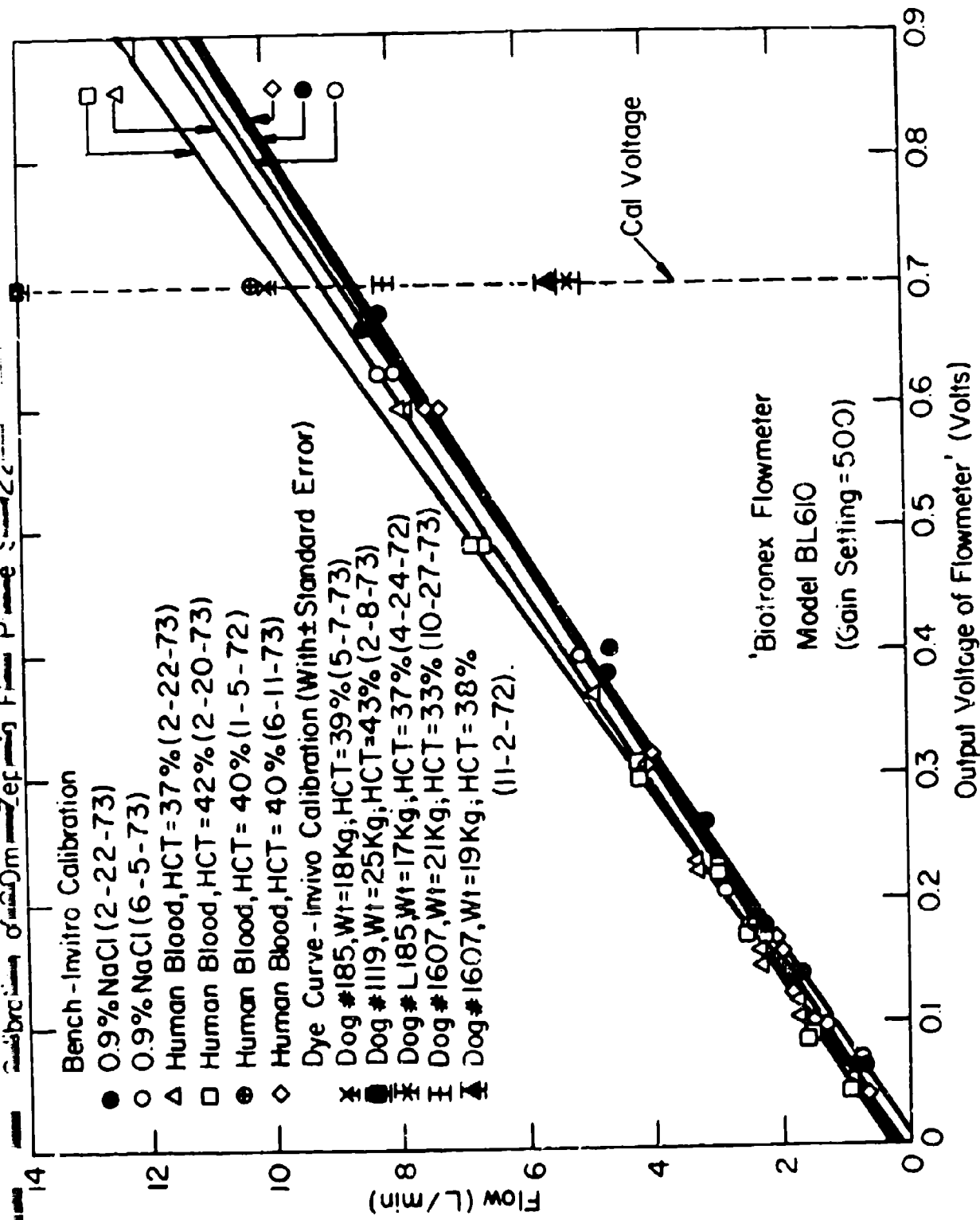


Fig. A-6 Plot of flow points for various media during bench calibration (on dialysis tubing) and dye curve results for one flow probe.

# Calibration of 18mm Zepeda Flow Probe SN923

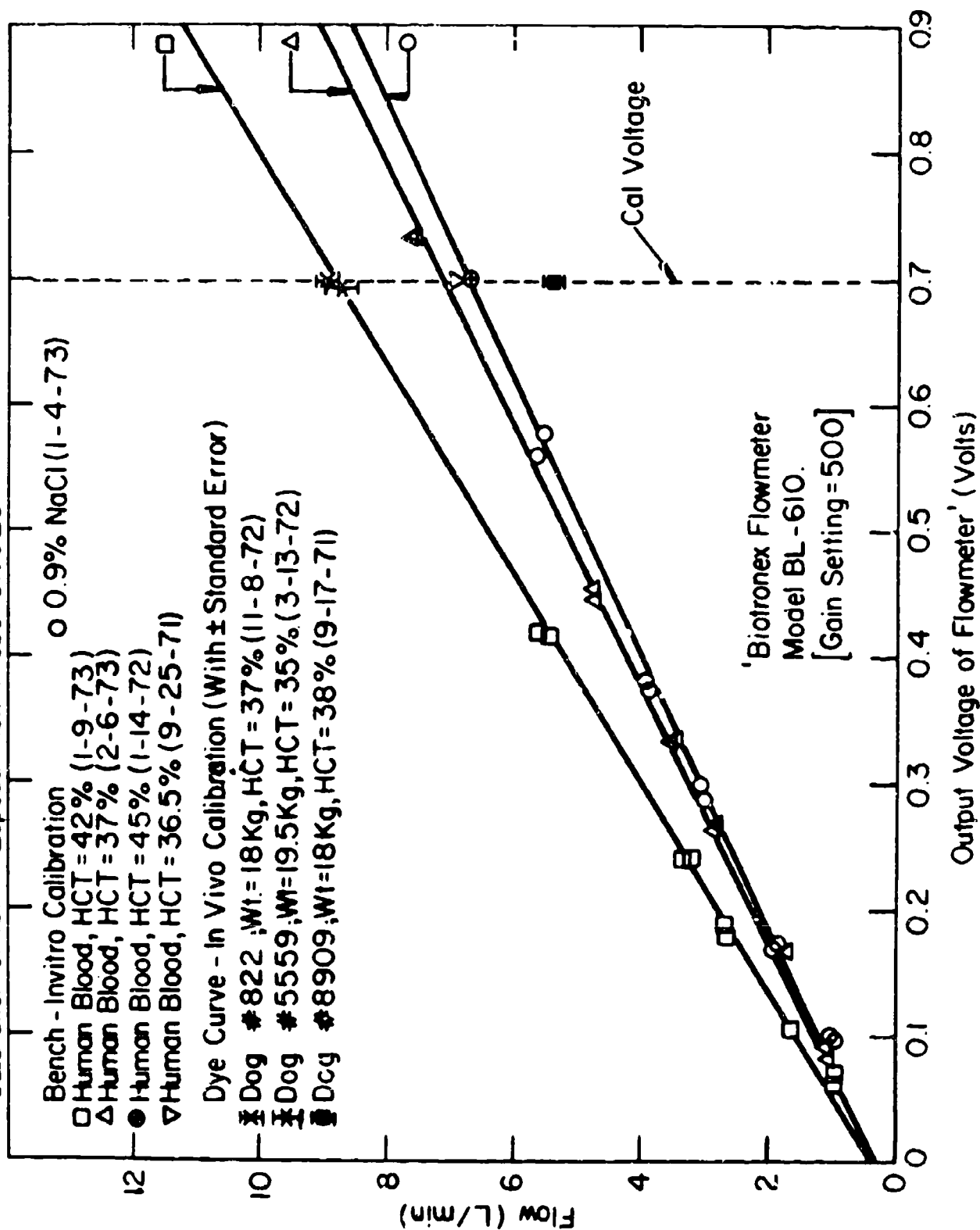


Fig. A-7 Least squares fitted calibration curves for 18 mm. Zepeda probe SN 923.

# Calibration of 7 mm Zepeda Flow Probe SN1039

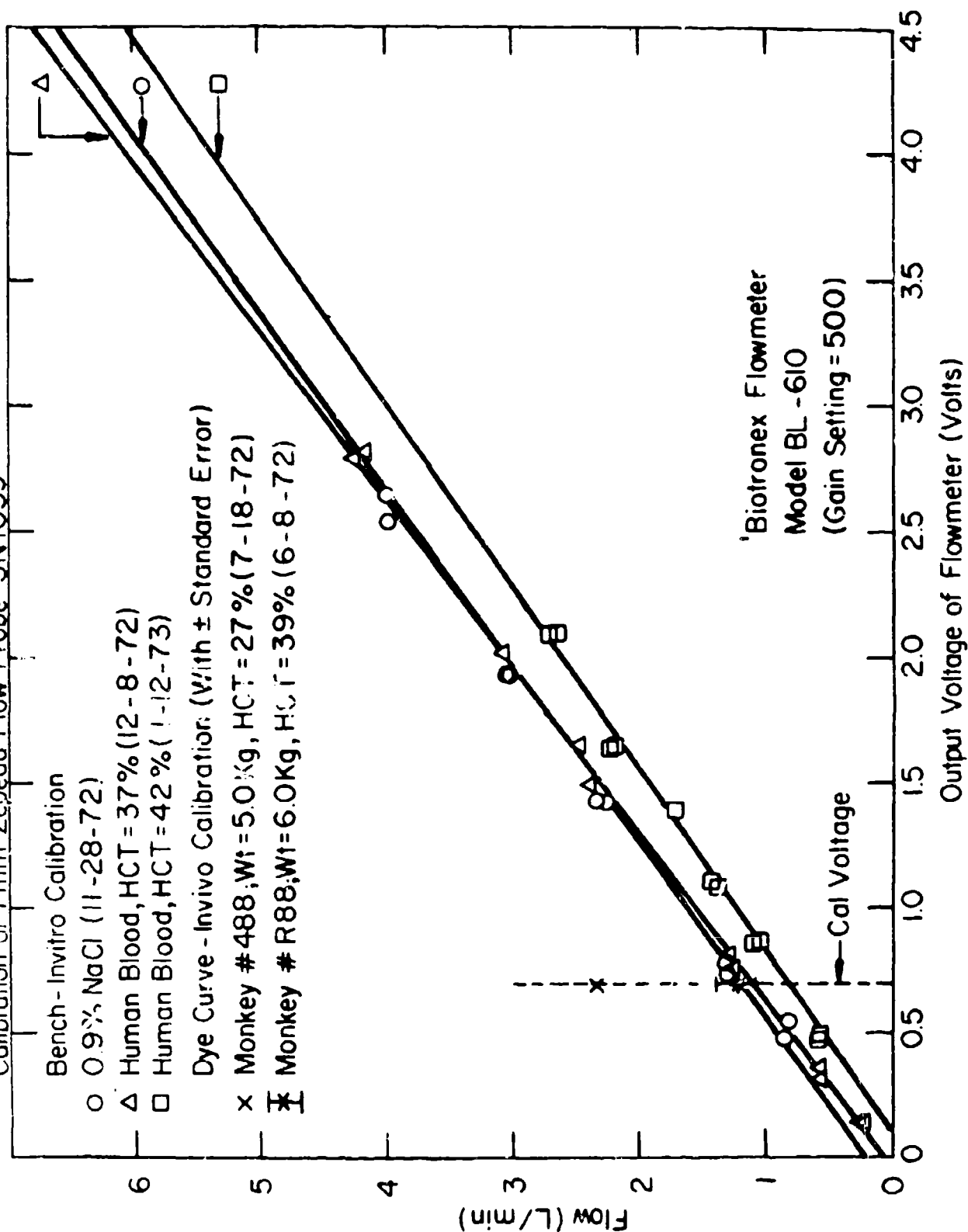
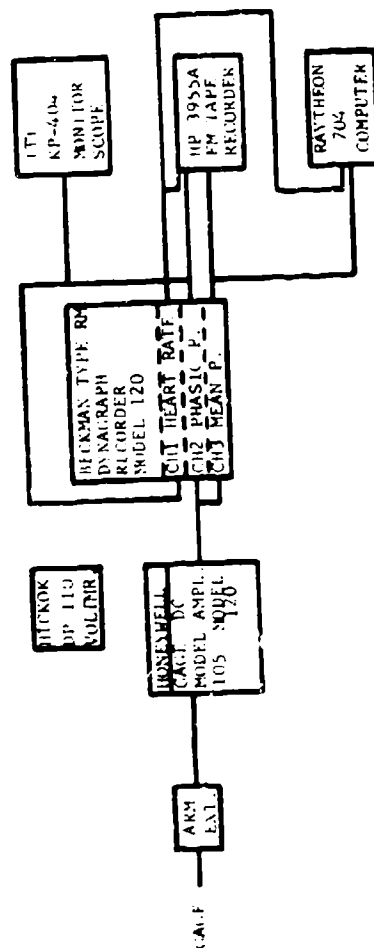


Fig. A-8 Bench calibration (direct electrode contact with fluid) and dye curve points for a 7 mm. Zepeda flow probe SN 1039.

# Typical Pressure Gauge Instrumentation For An Experiment



## Pressure Gauge Instrumentation For Testing

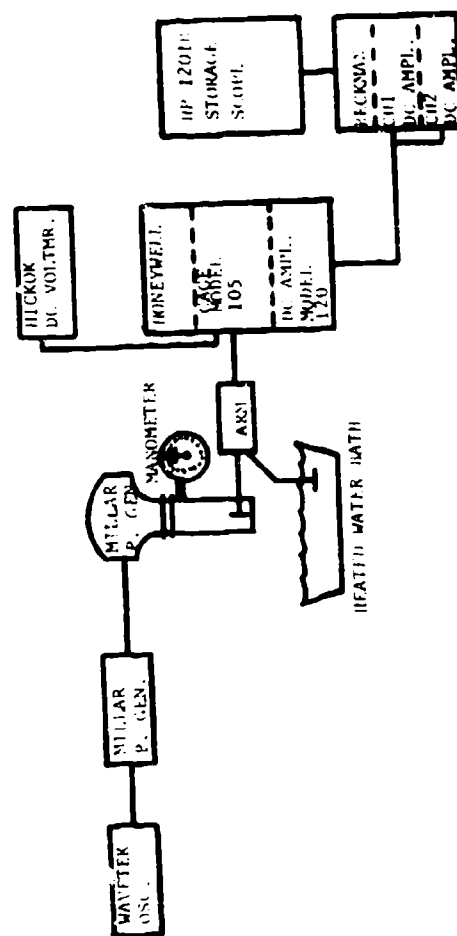


Fig. A-9 Block diagrams of pressure transducer testing and evaluation equipment and the normal configuration for an experimental session.



Fig. A-10 Silicone rubber washers are used as an interface between the vessel wall and the gauge head of Bio-Tec and Konigsberg pressure transducers to be implanted.

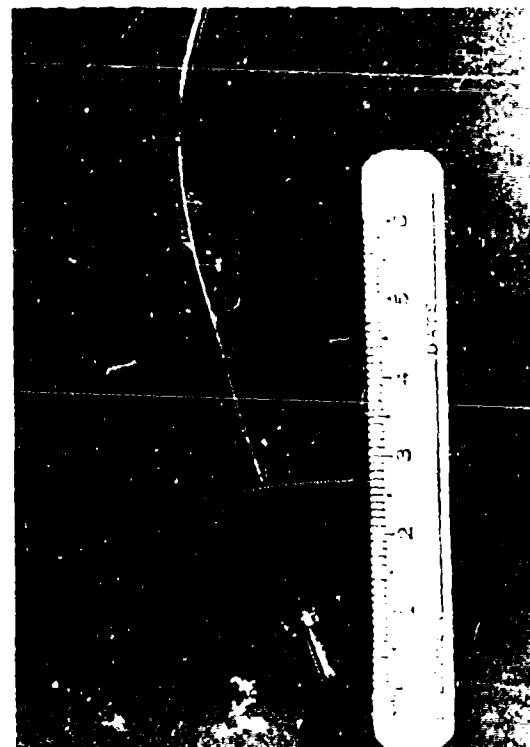
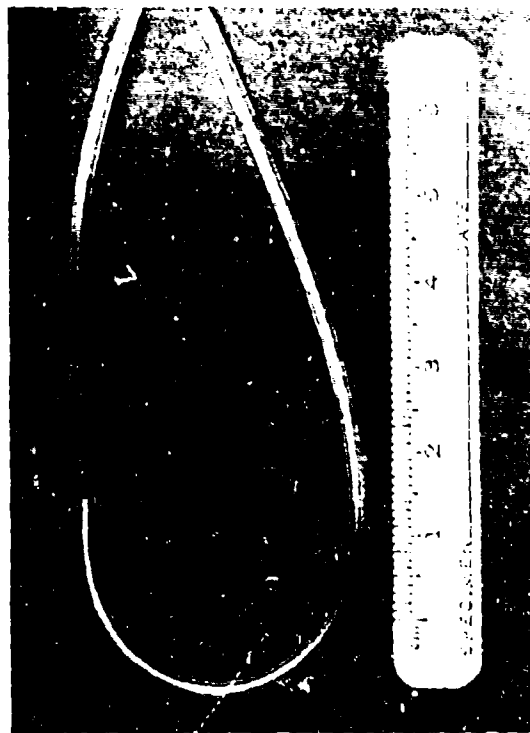
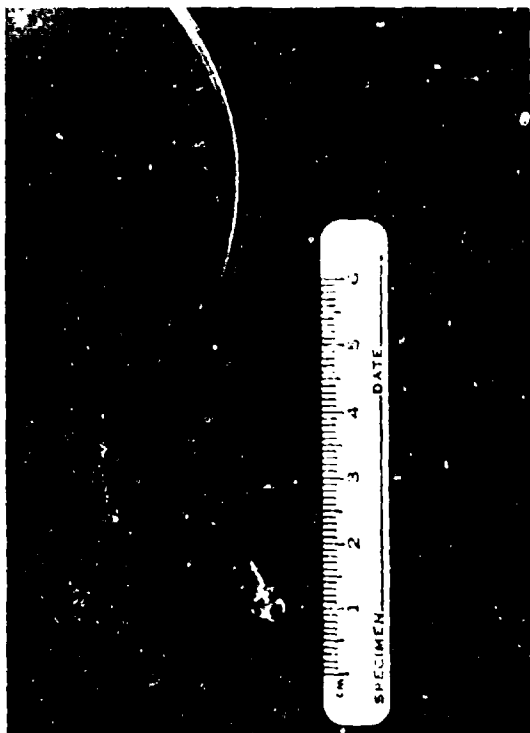
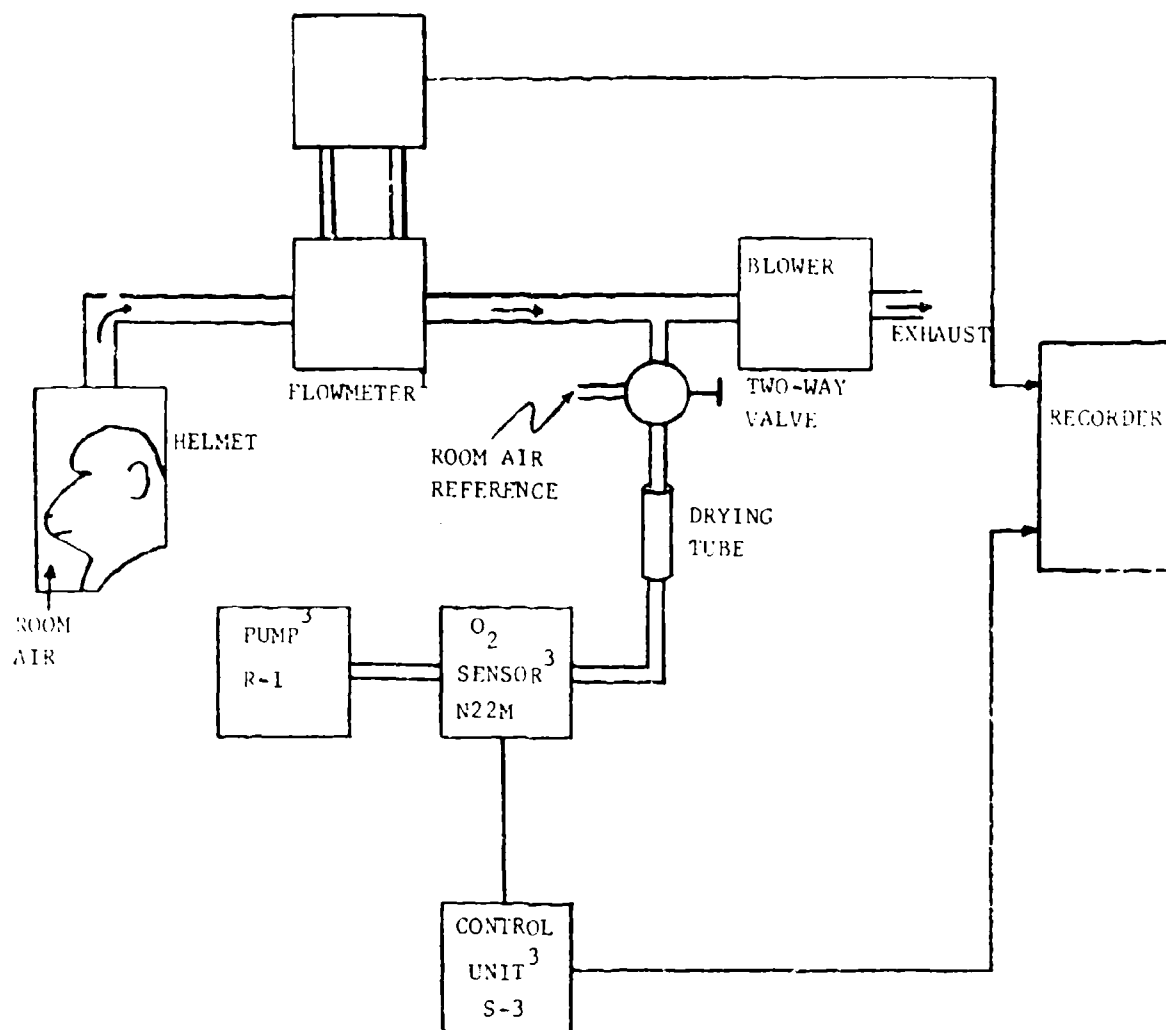
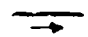




Fig. A-11 Various cannula tips used in our implantation schedule are shown (starting from upper left-hand corner going clockwise): subclavian artery, entry tip, v-yoke opening for right atrial placement, straight tubing and disc for atria, and extended straight tubing for azygous vein entry.



# DIFFERENTIAL PRESSURE TRANSDUCER<sup>2</sup>



-  Main Gas Flow
-  Gas Sampling Line
-  Electrical Connection

1. Fleisch Pneumotachograph-Instrumentation Assoc., Inc. (6V, 0.75 inch inlet diam.)
2. Statham #10303
3. O<sub>2</sub> Analyzer System-Applied Electrochemistry, Inc.

Fig. A-12 Block diagram of open system to measure oxygen consumption of a conscious, vibrating animal.



Fig. A-13 Conscious dog in vertical vibration restraint chair showing preliminary design of helmet to measure  $O_2$  consumption using system illustrated in A-12.

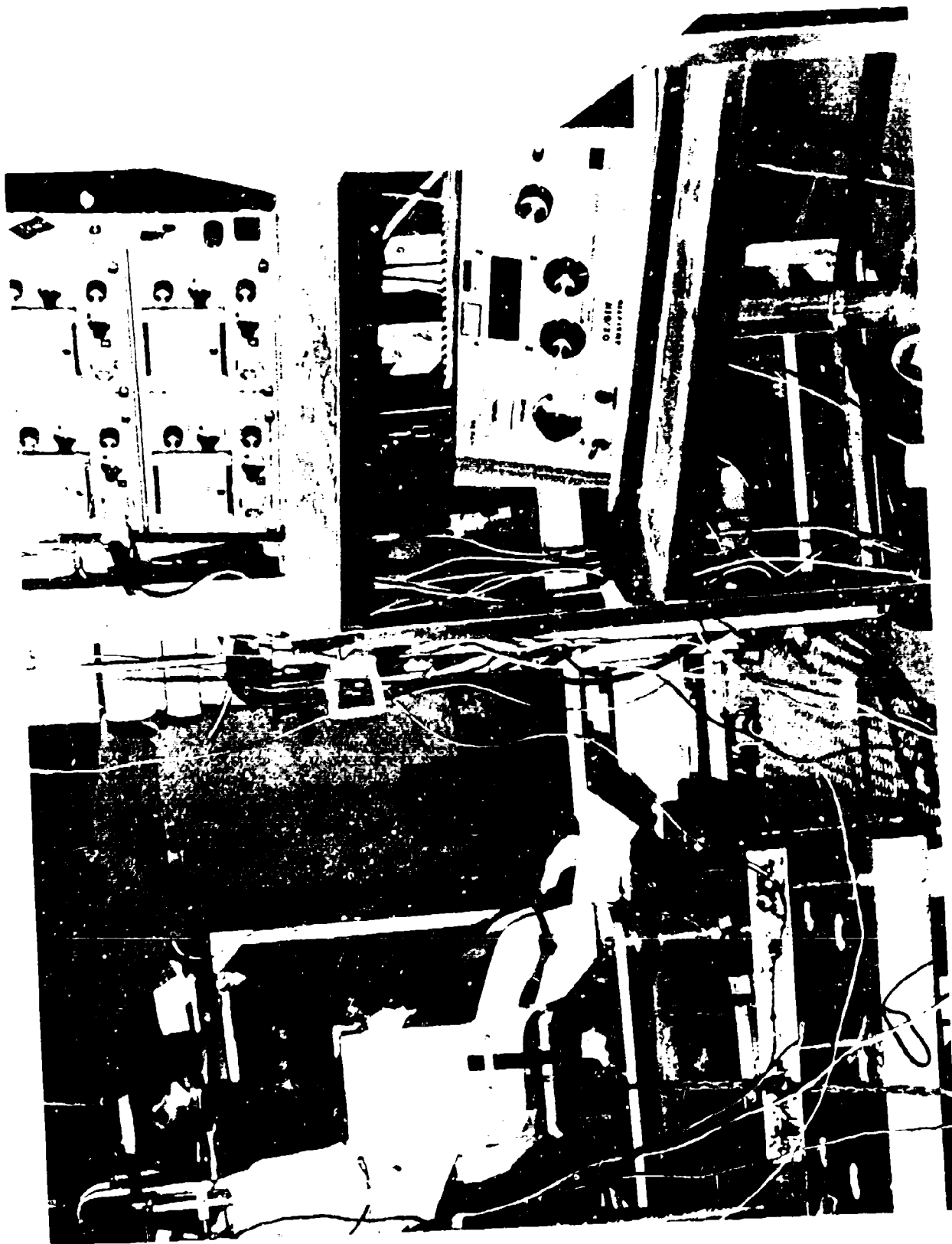


Fig. A-14 Experimental set-up featuring conscious monkey in vertical vibration restraint chair. A transparent plastic helmet is fixed to the chair and air is drawn through the helmet. Note blood flow and oxygen analyzer devices.

TABLE A-1a

TYPICAL CARDIOVASCULAR AND HEMATOLOGIC VARIABLES FOR BOTH  
AWAKE AND ANESTHETIZED DOGS TAKEN FROM THE PRESENT STUDY  
AND A SURVEY OF RECENT LITERATURE

TYPICAL CARDIOVASCULAR VARIABLES FOR \*DOGS

SOURCE	n	VT	HEART RATE	SYSTEMIC ARTERIAL PRESSURE						CENTRAL VENOUS PRESSURE		CARDIAC OUTPUT		CC per BODY WEIGHT		STROKE VOLUME		TOTAL PERIPHERAL RESIST.		TPE per BODY WEIGHT		LVEDV		EDV	
				SYSTOLIC			DIASTOLIC			MEAN		ml/min		l/min		ml		mmHg/l/min		ml/min/kg		ml		ml	
				mmHg			mmHg			mmHg		ml/min		l/min		ml		mmHg/l/min		ml/min/kg		ml		ml	
				H	SD	H	SD	H	SD	H	SD	H	SD	H	SD	H	SD	H	SD	H	SD	H	SD	H	SD
Present Study	7-12	19	104	33	150	33	108	27	112	27		2.04	1.00	68	44.0	20.4	16.3	67.7	4.4	3.26	1.36				
Anesthetized awake	10-37	19	119	46	143	34	108	34	111	30		2.48	1.11	136	76.0	19.8	7.8	40.8	18.9	2.83	4.32				
Abel & Weidmann (1948)	5	17	116	10																					
Abel & Weidmann (1948)	6	17	107	11																					
Abel & Weidmann (1948)	5	17	112	10																					
Adams et al (1973)	10	24	96	7																					
Anderson & Brady (1973)	28	11	78		158		88		96																
Anderson & Brady (1973)	44	11	90		158		72		96																
Conrady & Rapraet (1972)	10	18	158	14																					
Felix & Bess (1973)	9		130	20								2.48	.56												
French & French (1970)	21	12							116					160											
Parvizi et al (1973a)	5	23	142						163	5														7.0	0.1
Parvizi et al (1973b)	19	18	136						157																
Parvizi et al (1973)	1		214		142		110		123			3.60				16.7								7.7	73.5
Reit et al (1968)	9	18	83									2.10		114		25.6									72
Reit & Blagden (1965)	27	17	71	78					108	73	3.8	7.4													
Sumida et al (1970)	13	20	103	10	159	74	105	74	123	71	1.2	1.5													
Lake et al (1973)	5	17	86	3	125	7	77	4	93	5		3.02	0.44	99	70.0										
Lehla et al (1973)	18		135																						
Increased heart rate	18		191																						
Strom et al (1967)	21	13	101	4					114	6				130	6.0										

\* All values are from awake animals unless otherwise noted.

\* Anesthetized with chloralose

\* Anesthetized with urethane, alpha-chloralose, pentobarbital

\* Anesthetized with chloralose urethane

\* Standard error of mean

TYPICAL HEMATOLOGIC VARIABLES FOR \*DOGS

SOURCE	n	VT	HCT	HGB	TOTAL WBC COUNT	DIFFERENTIAL								ERYTH LPTS SPAN	BLOOD VOLUME	TOTAL PROTEIN			
						PMNL		LYMPH		EOS		OTHER							
						%		%		%		%							
						H	SD	H	SD	H	SD	H	SD						
		H <th>SD</th> <th>H</th> <th>SD</th> <th>H</th> <th>SD</th> <th>H</th> <th>SD</th> <th>H</th> <th>SD</th> <th>N</th> <th>H</th> <th>SD</th> <th>H</th> <th>SD</th>	SD	H	SD	H	SD	H	SD	H	SD	N	H	SD	H	SD			
Present Study	1-15	18.0	39.7	5.3	14.0	10.1	8.9	64.0	5.4	8.5	5.2	1.7	1.5	5.1	3.0				
Albright (1952)	18																		
Baker	10													115	86.9		5.8		
Bale et al	10														91.0				
Billings	106		42.0											107	81.9				
Brown & Tadie	14														83.6				
Cruz and Oliveira (1953)																			
Deutch & Goodwin (1943)																			
Fisch et al	50		47.6											110	92.7				
Gibson et al (1938)														110					
Harmon et al																			
Isaksson & Nilner (1964)	11	11														5.0			
Control	11	11														5.5			
Exercise (End 30 min.)	11	11														5.0			
Recovery (End 60 min.)	11	11																	
Harmon	40		38.6		13.0	11.2		74.0		20.0		2.0		4.0					
Morris	31				15.1	11.5		71.9		22.0		5.4		0.8					
Phillips	27				14.4	10.7		74.9		19.3		4.1		1.8					
Reit	8														92.0				
Scarborough	500				18.0	11.6		69.0		20.1		5.0		7.0					
Schalm	78				11.5	2.8		64.1		24.9		2.8		6.5					
Strom & Russell (1973)	150	20.0	45.6	5.9	15.4	15.4	5.9	69.1	11.2	15.4	10.8	2.9	3.8	2.5	2.0	120	86.0	6.8	0.8
Strom et al (1955)	11		44.0													94.1		5.9	3.0
Wicks																90.0			
Stewart et al	81		43.6		14.6	13.3		71.8		20.1		4.4		3.7					
Franklin																			

\* From Probst &amp; C'ann (1963)

\* From Albright &amp; Dittmer (1961)

\* From Schalm (1963)

TABLE A-1b

TYPICAL BLOOD GAS AND RESPIRATORY VALUES FOR BOTH AWAKE  
AND ANESTHETIZED DOGS TAKEN FROM THE PRESENT STUDY AND  
A SURVEY OF RECENT LITERATURE

TYPICAL BLOOD GAS &amp; RESPIRATORY VALUES FOR \*DOGS

SOURCE	N	Wt	pH		PO <sub>2</sub>		PCO <sub>2</sub>		O <sub>2</sub> CONTENT		CO <sub>2</sub> CONTENT	
		kg			mmHg		mmHg		Vol %		Vol %	
		M	M	SD	M	SD	M	SD	M	SD	M	SD
<b>PRESENT STUDY</b>												
Anesth. (Art.)	3 to 9	20.3	7.36	.06	83.1	13.6	43.1	4.9	15.8	3.1	43.8	4.5
Awake (Art.)	3 to 11	20.1	7.43	.06	81.6	8.7	36.2	5.2	16.3	1.8	40.3	4.8
Anes. (Ven.)	3 to 9	20.3	7.27	.07	41.6	3.8	34.3	4.3	10.7	2.8	48.0	5.9
Awake (Ven.)	3 to 11	20.1	7.37	.05	42.8	2.1	40.5	3.4	9.7	1.2	46.9	1.2
Courtney & Marotta (1972)	10	17.5	7.32	.02								
• Carrell & Milhorn (1971)	54	13.9			75.0	1.0						
• Furnival et al (1973a)	5	25.0	7.34		197.0		38.5					
• Furnival et al (1973b)	19	19.0	7.35		213.7		37.4					
Park et al (1964)	20		7.42	.01					21.5	0.7	37.7	1.0
Park et al (1970)	6		7.39	.01	98.2	3.7	39.4	1.8				
Perman et al (1972) 3eo	6	13.1	7.41	.01	81.0	3.1	36.0	1.7				
Reeves and Brown (1958)	17		7.39	*0.1			37.2	*1.6				
Toncoroni et al (1960)	6		7.32	.08			43.3	7.6			50.0	7.3
• Shaffer et al (1971) 6an		17.0	7.39		87.2		38.1					

SOURCE	N	Wt	RESPIRATORY RATE		MINUTE VOLUME		O <sub>2</sub> CONSUMPTION		CO <sub>2</sub> OUT		INTERNAL TEGP.		A-V O <sub>2</sub> DIFFERENCE	
		kg	hr/min		L/min		ml O <sub>2</sub> /min		ml CO <sub>2</sub> /min		°C		%	
		M	M	SD	M	SD	M	SD	M	SD	M	SD	M	SD
<b>PRESENT STUDY</b>	2-75						105	1.0					5.1	1.9
• Baillie et al (1971)	1												4.7	
Exercise	3						200						15.3	
• Berger et al (1956)	3						850						6.4	
Exercise	3												11.2	
Courtney & Marotta (1972)	10	17.5	25.0	12.0										
• Gelvao (1947)	59	13.9					76	5.2						
• Gelvao (1947)	31	12.4					71	6.3						
Gold et al (1963) Control	4	11.0					90							
Exercise (25 min)	4	11.0					500							
Recovery	4	11.0					90							
• Hovlin & Smith (1967)		21.0	15.5	12.4	2.92	2.60					38.3	.6		
Neibrun (1952)											38.7	.6		
Hood & Higgins (1965)	27	17.0	14.0	*2.0										
• Maxwell (1959)	245						103						4.5	
Issekutz & Miller (1962)														
Control		11.0					120							
Exercise (40 min)		11.0					600							
• Martin & Fuhrman (1955)	14	20.8					124	39.2			39.0			
Martin & Fuhrman	5	16.3					99	24.8			39.0			
Paul & Issekutz (1967)														
Control (Untrained)		15.0					120		3.0					
Exercise (15-40 min)		15.0					900		23.0					
Recovery (end 15 min)		15.0					150							
Control (Trained)							90							
Exercise (15 min - 4 hr)							430							
Perman et al (1972)	6	13.1	14.0		3.04	.38					38.5			
Precht et al (1959)											38.9			
Spector (1956)			18.0		5.20									

\* All values are arterial samples from  
awake animals unless otherwise noted.  
• Anesthetized with chloralose urethane.

\* Anesthetized with sodium pentobarbital.  
• Standard error of mean  
• From Altman & Dittmer. Respiration & Circulation (1971)

TABLE A-1c

TYPICAL METABOLIC AND HORMONAL VALUES FOR BOTH AWAKE  
AND ANESTHETIZED DOGS TAKEN FROM THE PRESENT STUDY  
AND A SURVEY OF RECENT LITERATURE

TYPICAL METABOLIC AND HORMONAL VALUES FOR \*DOGS

SOURCE	n	WT		FPI.		BUN/PT.		TOTAL 17-ONES		CORTICO- STERONE		CORTISOL		ALDO- STERONE		BOST		SGPT	
		kg		μg/L		μg/L		μg/L		μg/L		μg/L		μg/L					
		M	SD	M	SD	M	SD	M	SD	M	SD	M	SD	M	SD	M	SD	M	SD
Arbore et al (1956)																			
Venous	24			.030	.01	.17	.03												
Anesthetized (Venous)	18			.140	.17	.23	.16												
Oliva et al (1955)	23																		
Anesthetized (Control)	23											7.0	1.5						
END 3Ha, (1g) Vibration	23											16.4	3.8						
END 6Ha, (1g) Vibration	23											17.0	4.0						
Bojars & Daga (1961)	4	20												28.3	8.5				
Bojars & Daga (1961)	2													13.0					
Braden et al (1970)	215																		
Venous (Female)	84															40.4		20.4	
Venous (Male)	112																	25.2	
Cornelius et al (1959)	24															22.7	5.4		
Cornelius et al (1959)	12																	21.8	6.2
Cornelius et al (1959)	25															19.6	7.5		
Cornelius et al (1959)	12																	21.0	10.7
Cramer et al (1969)																			
Fasted, Venous (Male)	5																		
Fasted, Venous (Female)	5																		
Silman & Brissner (1956)	49	18						5.0	0.41										
Fenn et al (1967)																			
Frogman (Ym)	3											5.3							
Frogman (Art)	3											8.6							
Fetal (Wired)												4.4							
Harvey (1969)	7																		
Harwood & Mason (1954)																			
Venous	17	26						2.8											
Bee & Harvey (1961)	11																		
Bee & Jahara (1967)	16																		
Kalpers et al (1958)																			
Venous (6 dogs)	47	25						1.7	0.14										
Malhotra (1960)																			
Mangan & Mason (1958)																			
Anesthetized (Arterial)	8			.038	.05	.34	.35												
Snow (1971) Venous	5																		
Van der Vliet (1961)	5																		
Volk & Price (1956) Anest. (Art)	3			.181		.03				1.0	9	5.6	2.5						

SOURCE	n	WT		FPA		GLUCOSE (PLASMA)		LACTATE	
		kg		Mm/L		Mg/L		Mg/L	
		M	SD	M	SD	M	SD	M	SD
Present Study									
Anesthetized	6	20	0.8	.27					
Awake	12	20	0.8	.20	88				
Armstrong et al (1961)	5	21	1.0	11	111	7.5			
*Gold et al (1963)									
Control	11		0.8					10.0	
Exercise (end 25 min)	11		0.3					50.0	
Recovery (end 30 min)	11		0.5					15.0	
Isokubota et al (1964)									
Control (fit dog)	2							6.0	
Exercise (end 40 min.)	2							30.0	
Control (unfit dog)	1							5.0	
Exercise (end 40 min.)	1							70.0	
Control (normal dog)					125			40.0	
Exercise (end 50 min.)					125			40.0	
Isokubota & Miller (1962)									
Control	11	11	0.5		85			20.0	
Exercise	11	11	0.2		86			40.0	
Recovery	11	11	0.4		82			15.0	
Miller et al (1971)	9	13	0.5						
*Paul & Isokubota (1967)									
Control (untrained)	13		0.5		90			9.0	
Exercise (end 40 min.)	13		0.5		90			40.0	
Recovery (end 1 hr.)	13		0.2		90			15.0	
Optical (trained)	13		0.3		103			11.0	
Exercise (end 4 hr.)	13		2.5		72			5.0	
Geerd & Pennell (1973)	150	20			63	8.4	14.7	4.5	

\* All values are from awake animals  
unless otherwise noted

\* Standard error of mean

\* Sampled via chronic catheters

TABLE A-2

BENCH CALIBRATIONS USING VARIOUS FLOW MEDIA AND DYE  
CURVE CALIBRATION RESULTS ARE COMPARED

Probe Mfg. Ser. No. Size (I.D.)	BENCH CALIBRATION			DYE CURVE CALIBRATION								% DIFFERENCE <sub>3</sub> = $\frac{\text{Dye-Bench}}{\text{Dye}} \times 100$
	CAL <sub>1</sub> -X L/MIN	THCT	DATE	CAL <sub>1</sub> -Y L/MIN	±L/MIN	Animal	N <sub>2</sub>	THCT	C.O. L/MIN	C.O. L/MIN WT. KG	DATE	
Zepeda SN 924 (22 mm)	10.7 8.8 8.8 6.5 5.7	Sal. 37% 42% Sal. 42%	6/5/73 2/22/73 2/20/73 2/22/73 1/17/73	14.30 12.85 7.24	1.66 0.25 1.46	DOG 18 DOG 202 PIC 575	3 2 2	37% 37% 44%	3.59 3.11 6.52	0.200 0.173 0.466	4/30/73 4/19/73 11/30/71	+38% +31% +21%
	$\bar{X} = 8.1$			$\bar{Y} = 11.5$								$\frac{\bar{Y}-\bar{X}}{\bar{Y}} \times 100 = +30\%$
Zepeda SN 922 (20 mm)	10.2 9.6 9.1 8.7 8.7 8.6	40% 42% 37% Sal. Sal. 40%	1/5/72 2/20/73 2/22/73 6/5/73 2/22/73 6/11/73	10.00 14.00 5.26 5.46 8.10	0.33 1.40 0.18 1.19 0.40	DOG 185 DOG 1119 DOG L185 DOG 1A07 DOG 1607	3 3 3 5 3	39% 43% 37% 38% 38%	2.35 2.60 3.83 3.50 3.31	0.131 0.106 0.226 0.183 0.158	5/7/73 2/8/73 4/24/72 11/2/72 10/27/72	+16% +31% -73% -66% -12%
	$\bar{X} = 9.2$			$\bar{Y} = 8.6$								$\frac{\bar{Y}-\bar{X}}{\bar{Y}} \times 100 = -70\%$
Zepeda SN 921 (20 mm)	9.8 8.1 7.7	42% 42% Sal.	11/1/72 1/17/72 6/8/73	11.60	0.70	DOG 774	4	42%	3.25	0.251	5/10/73	+16%
	$\bar{X} = 8.5$											
Zepeda SN 767 (20 mm)	8.7 8.6 8.3 8.1	37% Sal. 42% Sal.	2/6/73 7/13/71 1/17/72 7/5/73	12.60	0.55	DOG L199	3	44%	4.43	0.296	10/30/72	+34%
	$\bar{X} = 8.4$											
In Vivo- Metric SL-18 2109 (20 mm)	29.2 26.2 21.0 20.4	42% 42% Sal. 37%	1/10/73 10/31/72 1/8/73 12/13/72	12.24	0.79	DOG 1615	4	47%	5.97	0.230	7/7/72	-138%
	$\bar{X} = 26.2$											
Zepeda SN 931 (18 mm)	8.6 8.2 6.8	42% Sal. 45%	1/10/73 1/3/73 1/18/72	10.45	1.20	DOG 1973	4	39%	2.99	0.187	7/31/71	+18%
	$\bar{X} = 7.9$											
Zepeda SN 923 (18 mm)	8.8 7.1 6.8 6.7 6.7	42% 37% 36.5% Sal. 45%	1/9/73 2/6/73 9/25/71 1/4/73 1/14/72	8.90 8.75 5.41	0.50 1.58 0.37	DOG 822 DOG 5559 DOG 38909	4 4 2	37% 35% 38%	2.63 4.57 3.50	0.146 0.235 0.194	11/8/72 3/13/72 9/17/71	+20% +22% -31%
	$\bar{X} = 7.2$			$\bar{Y} = 7.7$								$\frac{\bar{Y}-\bar{X}}{\bar{Y}} \times 100 = +7\%$
Zepeda SN 793 (18 mm)	9.3 9.3 5.5	47% 37% Sal.	2/20/73 2/22/73 2/22/73	10.80	1.50	DOG 556	7	48%	3.68	0.230	1/24/73	+14%
	$\bar{X} = 8.0$											
Zepeda SN 1039 (7 mm)	1.1 1.2 1.1	37% Sal. 42%	12/8/72 11/28/72 1/12/73	2.35 1.26	0.16 0.15	PKY 418 PKY 483	3 5	27% 39%	1.27 1.28	0.254 0.213	7/18/72 6/8/72	+53% +15%
	$\bar{X} = 1.1$			$\bar{Y} = 1.8$								$\frac{\bar{Y}-\bar{X}}{\bar{Y}} \times 100 = +39\%$
Biotronex BL-5070- B21 (7 mm)	3.0 7.7 1.8	Sal. 35% 49%	6/8/73 6/21/72 4/8/70	7.32	0.27	PKY 500	6	35%	1.45	0.208	6/21/72	-5%
	$\bar{X} = 4.2$											

Notes: (1) CAL = Biotronix Flowmeter BL610 voltage signal for which an equivalent flow is determined.

(2) N = Number of dye curves used for flow signal calibration.

(3) % Difference is calculated using equivalent parameters (THCT, DATE) for both bench and dye curve CAL figures.

TABLE A-3

CHRONOLOGICAL HISTORY OF A KONIGSBERG P21 (SN15) IMPLANTABLE PRESSURE TRANSDUCER CURRENTLY USED IN THE LABORATORY. VERY SMALL CHANGES IN SENSITIVITY ARE EVIDENT AND THE LATER TESTS DONE ON THE GAUGE SUGGEST THERE IS MORE TEMPERATURE STABILITY WITH LONGER GAUGE LIFE.

DOG NUMBER	IMPLANT TO REMOVAL DATE	DURATION OF IMPLANT (DAYS)	TRANSDUCER SITE	SENSITIVITY $\frac{\mu V}{V}$ cmHg	% CHANGE SENSITIVITY
8274	8/7/71 - 8/19/71	13	Aorta	101.1	-
10171	10/1/71 - 10/7/71	7	Aorta	100.7	-0.4
101871	10/18/71 - 11/8/71	22	Lt. Vent.	100.7	-
112371	11/23/71 - 12/10/71	18	Aorta	98.8	-1.9
5791	2/28/72 - 3/10/72	11	Lt. Vent.	98.8	0
5897	3/17/72 - 3/22/72	6	Lt. Vent.	98.8	0
L185	4/7/72 - 4/27/72	21	Aorta	99.3	+0.5
1600	5/24/72 7/19/72	56	Aorta	99.3	0
1416	11/1/72 - 11/19/72	19	Lt. Vent.	99.3	0
1119	1/24/73 2/11/73	19	Lt. Vent.	101.1	+0.8
18	4/3/73 - 5/20/73	48	Lt. Vent.	99.8	-1.3
495	8/1/73 - 9/14/73	45	Lt. Vent.	100.6	+0.8



TABLE A-4

SUMMARY TABLE OF SUBCUTANEOUS NYLON AND DACRON VELOUR POUCHES IMPLANTED TO STORE TRANSDUCER LEADS. THE TYPE OF POUCH INDICATES WHETHER A SINGLE OR DOUBLE LAYER OF VELOUR WAS USED ON THE "WINDOWED" SIDE. NOTE THAT THE POUCH FUNCTIONED FOR A VARIABLE IMPLANTATION SCHEDULE

NUMBER	TYPE OF POUCH		AVERAGE SURVIVAL TIME (DAYS)	CONNECTORS STORED		EXPERIMENTAL SESSIONS (AVERAGE/ANIMAL)	TIME OF POUCH WINDOWING AFTER SURGERY		DEGREE OF TISSUE-POUCH INGROWTH	
	SINGLE	DOUBLE		NUMBER	ANIMALS		DAYS	NUMBER	FULL	PARTIAL
26 DOGS	7	19	28	1	2	3	6-7	2	23	3
				6-7	17		8-10	12		
				8	7		11-14	12		
9 MONKEYS	5	4**	50*	3-4	3	4	6	2	5	4
				5-6	7		8	2		
							10-12	5		

\*INSTRUMENTATION REMOVED FROM ONE ANIMAL AFTER 24 DAYS WITH SATISFACTORY RECOVERY; TWO ANIMALS ARE MORE THAN 83 AND 126 DAYS POST-OP (AS OF 8-1-73).

\*\*THREE OF THESE POUCHES WERE DACRON VELOUR

## References

- Abel FL and Waldhausen JA. Effects of anesthesia and artificial ventilation on caval flow and cardiac output. *J. Appl. Physiol.* 25(5):479-484, 1968.
- Adams JD, Erickson HH, and Stone HL. Myocardial metabolism during exposure to carbon monoxide in the conscious dog. *J. Appl. Physiol.* 34(2):238-242, 1973.
- Albritton EC, Ed. *Standard Values in Blood*. Philadelphia: W. B. Saunders, 1952, pp. 117-119.
- Altman PL, and Dittmer DS, Eds. *Blood and Other Body Fluids*. Washington, D. C.: Committee on Biological Handbooks, Federation of American Societies for Experimental Biology, 1961.
- Altman PL and Dittmer DS, Eds. *Metabolism*. Bethesda: Committee on Biological Handbooks, Federation of American Societies for Experimental Biology, 1968.
- Altman PL and Dittmer DS, Eds. *Respiration and Circulation*. Bethesda: Federation of American Societies for Experimental Biology, 1971.
- Anderson DE and Brady JV. Preavoidance blood pressure elevation accompanied by heart rate increases in the dog. *Science* 172:595-597, 1971.
- Armstrong DT, Steele R, Altszuler N, Dunn A, Bishop JS, and De Bobo RC. Regulation of plasma free fatty acid turnover. *Am. J. Physiol.* 201(9), 1961.
- Aronow, Howard, and Wolff. Plasma epinephrine and norepinephrine content in mammals. *J. Pharm. Exp. Ther.* 116:1, 1956.
- Baillie MD, *et al.* *J. Appl. Physiol.* 16:107, 1961.
- Baker CH and Remington JW. Role of the spleen in determining total body hematocrit. *Am. J. Physiol.* 198:906, 1960.
- Bale WF, Yuile CR, DeLaVergne L, Miller LL, and Whipple GH. Hemoglobin labeled by radioactive lysine. *Erythrocyte Life Cycle*. *J. Exp. Med.* 90:315, 1949.
- Barger AC, *et al.* *Amer. J. Physiol.* 184:613, 1956.
- Basu A, Passmore R, and Strong JA. The effect of exercise on the level of non-esterified fatty acids in the blood. *Quart. J. Exptl. Physiol.* 45:312, 1960.
- Beamer, *et al.* Protein binding of cortisol in the Rhesus monkey (*Macaca mulatta*). *Endocrinology* 90:325, 1972.

- Beck R, et al. Calibration characteristics of the pulsed-field electromagnetic flowmeter. Med. Elect. April-June, 87-91, 1965.
- Billings HH and Brown EB. Effect of splenectomy on changes in plasma and blood flow volume produced by inhalation of 30% and 40% CO<sub>2</sub> in dogs. Am. J. Physiol. 180:363, 1955.
- Blivaiss BB, Litta-Modignani R, Galansino G, and Foa PP. Endocrine and metabolic response of dogs to whole body vibration. Aero. Med. 36:1138-1144, 1965.
- Bojesen E and Degn H. A double isotope derivative method for the determination of aldosterone in peripheral plasma. Acta Physiol. 37:541, 1961.
- Bojesen E and Degn H. Influence of changes of blood volume on the concentration of aldosterone in peripheral plasma of intact unanesthetized dogs. Nature 190:352, 1961.
- Bond RF, Manning ES, and Gonzalez RR. Methods for chronically implanting coronary artery blood flow probes, arterial occluders and coronary sinus catheters. In McCutcheon EP, Ed. Chronically Implanted Cardiovascular Instrumentation. 482 pp. New York: Academic Press, 1973, pp. 781-788.
- Brown IW Jr. and Eadie GS. An analytical study of the in vivo survival of limited populations of animal red blood cells tagged with radioiron. J. Gen. Physiol. 36:327, 1953.
- Brunden, Clark, and Sutter. A general method of determining normal ranges applied to blood values for dogs. Amer. J. Clin. Pathol. 53:332, 1970.
- Cappelen C Jr, Ed. New Findings in Blood Flowmetry. Norway: Universitetsforlaget, 1968.
- Carlson LA, Ekelund LG, and Orö L. Studies on blood lipids during exercise. IV. Arterial concentration of plasma free fatty acids and glycerol during and after prolonged exercise in normal men. J. Lab. Clin. Med. 61:724, 1965.
- Carrell DE and Milhorn HT Jr. Dynamic respiration and circulatory responses to hypoxia in the anesthetized dog. J. Appl. Physiol. 30(3):305-312, 1971.
- Cobb LA and Johnson WP. Hemodynamic relationships of anaerobic metabolism and plasma free fatty acids during prolonged, strenuous exercise in trained and untrained subjects. J. Clin. Invest. 42:800, 1963.
- Cornelius, Bishop, Switzer, and Rhode. Serum and tissue transaminase activities in domestic animals. Cornell Vet. 49:116, 1959.

- Court JM, Dunlop ME and Leonard RF. High-frequency oscillation of blood free fatty acid levels in man. *J. Appl. Physiol.* 31:345, 1971.
- Courtney GA and Marotta SF. Adrenocortical steroids during acute exposure to stresses: I. Disappearance of infused cortisol. *Aero. Med.* 43:46-51, 1972.
- Cramer, Turbyfill, and Dewes. Serum chemistry values for the beagle. *Amer. J. Vet. Research* 30:1183, 1969.
- Cuthbertson EM and Gilfillon RS. Evaluation and calibration of square-wave electromagnetic flow probes for chronic implantation. *Med. Res. Eng.* 10:20, 1971.
- Debley VG. Miniature hydraulic occluder for zero flow determination. *J. Appl. Physiol.* 31(1):138-139, 1971.
- Dobson A, Sellers AF, and McLeod FD. Performance of a cuff-type blood flow-meter in vivo. *J. Appl. Physiol.* 21(5):1642-1648, 1966.
- Eagan CJ, Durrer JL, and Millard WM. Arctic Aeromed. Lab., TDR 63-40:1, 1963.
- Eik-nes and Brizzee. Adrenocortical activity and metabolism of 17-hydroxycorticosteroids in the thyroidectomized dog. *Am. J. of Physiol.* 184:371, 1956.
- Erickson HE, Bishop VS, Kardon MB, and Horwitz LD. Left ventricular internal diameter and cardiac function during exercise. *J. Appl. Physiol.* 30(4):473-478, 1971.
- Finch CA, Wolff JA, Rath CE, and Flaharty RG. Iron Metabolism. Erythrocyte iron turnover. *J. Lab. and Clin. Med.* 34:1480, 1949.
- Folts JD and Rowe GG. Silicone rubber encapsulated flow probes for chronic implantation on the ascending aorta. In McCutcheon EP, Ed. *Chronically Implanted Cardiovascular Instrumentation*. 482 pp. New York: Academic Press, 1973, pp. 35-42.
- Fonzo, Doglio, Lauro, and De Martinis. Distribution of free and protein-bound plasma cortisol in pregnant dogs and their respective fetuses. *Folio Endocrinol.* 20:129, 1967.
- Friedberg SJ, Harlan WR, Trout DL, and Estes EJ. The effect of exercise on the concentration and turnover of plasma nonesterified fatty acids. *J. Clin. Invest.* 39:215, 1960.
- Fronek K and Fronek A. Combined effect of exercise and digestion on hemodynamics in conscious dogs. *Amer. J. Physiol.* 218(2):555-559, 1970.
- Fryer TB and Sandler H. Miniature battery-operated electromagnetic flowmeter. *J. Appl. Physiol.* 31(4):622-628, 1971.

- Furnival CM, Linden RJ and, Snow HM. Chronotropic and inotropic effects on the dog heart of stimulating the efferent cardiac sympathetic nerves. J. Physiol. 230:137-153, 1973(a).
- Furnival CM, Linden RJ, and Snow HM. The inotropic effect on the heart of stimulating the vagus in the dog, duck and toad. J. Physiol. 230:155-170, 1973(b).
- Galvao PE. Am. J. Physiol. 148:478, 1947.
- Gold M, Miller HI, Issekutz B Jr, and Spitzer JJ. Effect of exercise and lactic acid infusion on individual free fatty acids of plasma. Am J. Physiol. 205:902, 1963.
- Gold M, Miller HI, and Spitzer JJ. Removal and mobilization of individual free fatty acids in diabetic dogs. Am. J. Physiol. 202:1002, 1962.
- Gordon AS. Practical Aspects of Blood Flow Measurements. Statham Instruments Inc., Oxnard, California, 1971.
- Grode GA. Personal Communication. Battelle - Columbus Laboratories, Columbus, Ohio, 1972.
- Hamilton RW Jr. Continuous sampling of arterial blood of unanesthetized animals. J. Appl. Physiol. 20(3):555-557, 1965.
- Hamlin RL and Smith CR. Amer. J. Vet. Res. 28:175, 1967.
- Harrison BA, Barwell EL, and Finch CA. Erythrocyte life span in small animals. Fed. Proc. 10:357, 1951.
- Harvey DG. Some observations on the estimation of serum glutamic pyruvate transaminase (SGPT) in the dog. J. Small Animal Pract. 10:13, 1969.
- Harwood and Mason. Effects of intravenous infusion of autonomic agents on peripheral blood 17 - hydroxycorticosteroid levels in the dog. Am. J. Physiol. 186:445, 1956.
- Hawthorne EW, Walker ML, Hinds JE, Kraft-Hunter F, Gordon AG. A user-interactive data acquisition and reduction system for the study of cardiac dynamics. In McCutcheon EP, Ed. Chronically Implanted Cardiovascular Instrumentation. 482 pp. New York: Academic Press, 1973, pp. 455-478.
- Heatley NG and Weeks JR. Fashioning polyethylene tubing for use in physiological experiments. J. Appl. Physiol. 19(3):542-545, 1964.
- Heilbrun LV. Outline of General Physiology. Philadelphia: W. B. Saunders, 1952.

- Heitz DC, Shaffer RA, and Brody MJ. A device for chronic exteriorization of indwelling vascular catheters. *J. Appl. Physiol.* 26(5):664-666, 1969.
- Henry WL, Ploeg C, Kountz SL, and Harrison DC. An improved hydraulic vascular occluder for chronic electromagnetic blood flow measurements. *J. Appl. Physiol.* 25(6):790-792, 1968.
- Herd JA and Barger AC. Simplified technique for chronic catheterization of blood vessels. *J. Appl. Physiol.* 19(4):791-792, 1964.
- Hoe CM and Harvey DG. An investigation into liver function tests in dogs: Part-1, serum transaminases. *J. Small Animal Pract.* 2:22, 1961.
- Hoe CM and Jabara AC. The use of serum enzymes as diagnostic aids in the dog. *J. Comp. Path.* 77:245, 1967.
- Hognestad H. Square wave electromagnetic flowmeter with improved baseline stability. *Med. Res. Eng.* 5:3, 28-33, 1966.
- Hoh Z, Carlton N, Lucien HW, and Schally AV. Long-term plastic tubing implantation into the external jugular vein for injection or infusion in the dog. *Surgery* 66(4):768-770, 1969.
- Hohenleitner FJ and Spitzer JJ. Changes in plasma free fatty acid concentrations on passage through the dog kidney. *Am. J. Physiol.* 200:1095, 1961.
- Hohenleitner FJ and Spitzer JJ. The effect of glucagon on free fatty acid metabolism. *Am. J. Med. Sci.* 245:251, 1963.
- Holt JP, Rhode EA, and Kines H. Ventricular volumes and body weight in mammals. *Am. J. Physiol.* 215(3):704-715, 1968.
- Hood WB Jr and Higgins LS. Circulatory and respiratory effects of whole-body vibration in anesthetized dogs. *J. Appl. Physiol.* 20(6):1157-1162, 1965.
- Howell CD, et al. *Amer. J. Physiol.* 196:193, 1959.
- Issekutz B Jr. Effect of exercise on the metabolism of plasma free fatty acids. In Rodahl and Issekutz, Eds. *Fat as a Tissue*. New York: McGraw Hill, 1964.
- Issekutz B Jr, Bortz WM, Miller HI, et al. Plasma FFA response to exercise in obese humans. *Metabolism* 16:492-502, 1967.
- Issekutz B Jr, Bortz WM, Miller HI, et al. Turnover rate of plasma FFA in humans and in dogs. *Metabolism* 16:1001-9, 1967.
- Issekutz B Jr, Issekutz AC, and Nash D. Mobilization of energy sources in exercising dogs. *J. Appl. Physiol.* 29:691, 1970.

- Issekutz B Jr and Miller HI. Plasma free fatty acids during exercise and the effect of lactic acid. *Proc. Soc. Exptl. Biol. Med.* 110:237, 1962.
- Issekutz B Jr, Miller HI, Paul P and Rodahl K. Source of fat oxidation in exercising dogs. *Am. J. Physiol.* 207:583, 1964.
- Issekutz B Jr, Miller HI, Paul P, and Rodahl K. Effect of lactic acid on free fatty acids and glucose oxidation in dogs. *Am. J. Physiol.* 209:1137, 1965.
- Issekutz B Jr, Miller HI, and Rodahl K. Lipid and carbohydrate metabolism during exercise. *Fed. Proc.* 25:1415, 1966.
- Issekutz B Jr and Paul P. Intramuscular energy sources in exercising and pancreatectomized dogs. *Am. J. Physiol.* 215:197-204, 1968.
- Issekutz B Jr, Paul P, and Miller HI. Metabolism in normal and pancreatectomized dogs during steady-state exercise. *Am. J. Physiol.* 213:857-62, 1967.
- Issekutz B Jr, Paul P, Miller HI, *et al.* Oxidation of plasma FFA in lean and obese humans. *Metabolism* 17:62-73, 1968.
- Jacobson ED and Swan KG. Hydraulic occluder for chronic electromagnetic blood flow determinations. *J. Appl. Physiol.* 21(4):1400-1402, 1966.
- Kantronitz P and Kingsley B. A survey of the clinical measurement of cardiac output. *Med. Res. Eng.* 10:12-19, 1971.
- Khoury EM and Gregg DE. An inflatable cuff zero determination in blood flow studies. *J. Appl. Physiol.* 23(3):395-397, 1967.
- Kliman and Peterson. Double isotope derivative assay of aldosterone in biological extracts. *JBC* 235:1639, 1960.
- Klein RR, Troyer WG, Bach KW, Hood TC, and Bogdonoff MD. Experimental stress and fat mobilization in lean and obese subjects. *Metabolism* 14:17, 1965.
- Kuipers, Ely, and Kelley. Metabolism of steroids: the removal of exogenous 17 - hydroxycorticosteroids from the peripheral circulation in dogs. *Endocrinology* 62:64, 1958.
- Kumeda M, Schmidt RM, Sagawa K, and Tan KS. Carotid sinus reflex in response to hemorrhage. *Am. J. Physiol.* 219(5):1373-1379, 1970.
- Lefebvre PL, Luyckx AS, and Federspil G. Muscular exercise and pancreatic function in rats. *Isr. J. Med. Sci.* 8:390, 1972.
- Leininger, RI. Personal Communication, Battelle - Columbus Laboratories, Columbus, Ohio, May 12, 1972.

- Leskin SJ, Wildenthal K, Mullins CB and Mitchell JH. Left ventricular dimensions determined by biplane cinefluorography of chronically implanted radiopaque markers: critique of the method. In McCutcheon EP, Ed. Chronically Implanted Cardiovascular Instrumentation. 482 pp. New York: Academic Press, 1973, pp. 123-132.
- McCutcheon EP, Ed. Chronically Implanted Cardiovascular Instrumentation. 482 pp. New York: Academic Press, 1973.
- McElroy WT Jr and Spitzer JJ. Hypoxia as a stimulus for free fatty acid mobilization in dogs. J. Appl. Physiol. 16:760, 1961.
- McQuarrie DG. A simple method for introduction of cardiac cannulae in a conscious dog. J. Appl. Physiol. 21(3):1136-1138, 1966.
- Malherbe. J. S. Afr. Vet. Med. Assoc. 31:159, 1960.
- Mangan GF and Mason JW. The fluorometric measurement of plasma epinephrine and norepinephrine concentrations in man, monkey, and dog. J. Lab. Clin. Med. 51:484, 1958.
- Marple DN, Aberle ED, Forrest JC, Blake WH, and Judge MD. Effects of humidity and temperature on porcine plasma adrenal corticoids, ACTH, and growth hormone levels. J. Animal Sci. 34:809, 1972.
- Martin AW and Fuhrman F. Lummated tissue metabolism in mouse and dog. Physiol. Zool. 28:18-34, 1955.
- Mayerson HS. The blood cytology of dogs. Anat. Rec. 47:259, 1930.
- Miller HI. Plasma free fatty acid appearance in plasma triglycerides. Metabolism 16:1096, 1967.
- Miller HI, Bortz WM, and Durham BC. The rate of appearance of FFA in plasma triglyceride of normal and obese subjects. Metabolism 17:515, 1968.
- Miller HI, Gold M, and Spitzer JJ. Removal and mobilization of individual free fatty acids in dogs. Am. J. Physiol. 202:370, 1962.
- Miller HI, Issekutz B Jr, and Rodahl K. Effect of exercise on the metabolism of fatty acids in the dog. Am. J. Physiol. 205:167, 1963.
- Miller HI, Yum KY, and Durham BC. Myocardial free fatty acid in unanesthetized dogs at rest and during exercise. Am. J. Physiol. 220:589, 1971.
- Mills J and Simmons D. An arterial catheter for chronic implantation in dogs. J. Appl. Physiol. 23(2):285-286, 1967.
- Morris ML, Stelton NB, Allison JB, and Green DF. Blood cytology of the normal dog. J. Lab. Clin. Med. 25:353, 1940.



- Mulligan RM. Quantitative studies on the bone marrow of the dog. *Anat. Rec.* 79:101, 1941.
- Murphy BEP. Some studies of the protein-binding and their application to the routine micro and ultramicro measurement of various steroids in body fluids by competitive protein-binding radioassay. *J. Clin. Endocrin. and Metab.* 27:973, 1967.
- Nelson Paul J. Silastic skin button for chronic exteriorization of tubing in dogs. *J. Appl. Physiol.* 27(5):763-764, 1969.
- Novak M. Colorimetric micromethod for the determination of free fatty acids. *J. Lipid Res.* 6:431-433, 1965.
- Park JF, Clarke WJ, and Bair WJ. Chronic effects of inhaled plutonium in dogs. *Health Physics* 10:1211, 1964.
- Park JF, Clarke WJ, and Bair WJ. Respiratory Systems. In Anderson, Ed. *The Beagle as an Experimental Dog*. Ames: Iowa State Press, 1970, p. 292.
- Paul P and Issekutz B Jr. Role of extramuscular energy sources in the metabolism of the exercising dog. *J. Appl. Physiol.* 22:615-22, 1967.
- Paul P, Issekutz B Jr, and Miller HI. Interrelationship of free fatty acids and glucose metabolism in the dog. *Am. J. Physiol.* 211:1313, 1966.
- Penman RW, Luke KG, and Jarboe TM. Respiratory effects of hypochloremic alkalosis and potassium depletion in the dog. *J. Appl. Physiol.* 33(2):17C-174, 1972.
- Platts RGS, Wilson P, and Shaw KM. Design for a chronic right ventricular catheter for dogs. *Lab. Animal Sci.* 22(6):900-903, 1972.
- Plentl A. Preparation of plastic T-catheters and devices for the collection of body fluids. *J. Appl. Physiol.* 21(2):338-342, 1967.
- Portman AW, Behrman RE, and Soltys P. Transfer of free fatty acids across the primate placenta. *Am. J. Physiol.* 216:143, 1969.
- Prosser CL and Brown FA Jr. *Comparative Animal Physiology*. 2nd Ed. 688 pp. Philadelphia: W. B. Saunders, 1965.
- Precht H, Christopherson J, and Hensel H. *Temperatur und Leben*. 514 pp. Berlin: Springer-Verlag, 1955.
- Reeve EB, Gregersen MI, Allen TH, and Sear H. Distribution of cells in the normal and splenectomized dog and its influence on blood volume estimates with P<sup>32</sup> and T-1824. *Am. J. Physiol.* 175:195, 1953.

- Reeves JL and Brown EB Jr. Respiratory compensation to metabolic alkalosis in dogs: influence of high oxygen concentration. *J. Appl. Physiol.* 13: 179, 1958.
- Rodman HM and Bleicher SJ. Plasma cortisol during normal glucose tolerance. *Metabolism* 22(5):745-747, 1973.
- Ron-oroni AJ, Pocidalo JJ, Lissac J, and Amiel. Response resperatoires du chien a l'alcalose metabolique aigue. *Acta Physiol Latinam.* 10:241, 1960.
- Rynberk A, der Kin dern, and Thyssen. Investigations on the adrenocorticol function of normal dogs. *J. Endocrin.* 41:395, 1968.
- Scarborough RA. The blood picture of normal laboratory animals. *Yale J. Biol. and Med.* 3:359, 1931-32.
- Schalm OW. *Veterinary Hematology.* 664 pp. Philadelphia: Sea & Febiger, 1965.
- Secord DC and Russell JC. A clinical laboratory study of conditional mongrel dogs and laborador retrievers. *Lab. An. Sci.* 23(4):567-571, 1973.
- Shaffer AB, Solorio M, and Weinstein H. Pulmonary artery-left heart circulatory transfer function in hemorrhagic hypotension. *J. Appl. Physiol.* 31: 801-807, 1971.
- Sham BG, et al. A constrictive and occlusive cuff for medium and large blood vessels. *J. Appl. Physiol.* 28(4):510-512, 1970.
- Shug AL and Shrago E. A proposed mechanism for fatty acid effects on energy metabolism of the heart. *J. Lab. Clin. Med.* 81:214, 1973.
- Smith HP, Arnold HR, and Whipple GH. Blood volume studies. VII. *Am. J. Physiol.* 56:336, 1921.
- Snow DH. The effects of dichlorvos on several blood enzymes levels in the Greyhound. *Aust. Vet. J.* 47:468, 1971.
- Spector WS, Ed. *Handbook of Biological Data.* Philadelphia and London: W. B. Saunders, 1956.
- Spencer P. and Benison AB Jr. The square-wave electromagnetic flowmeter. Based on a paper presented at Blood Flowmeters Symposium, Omaha, Nebraska, June, 1959.
- Spitzer J. Metabolism of free fatty acids in skeletal muscle and myocardium. In Rodahl and Issekutz, Eds. *Fat as a Tissue.* New York: McGraw-Hill, 1964.

- Spitzer JJ and Gold M. Effect of catecholamines on the individual free fatty acids of plasma. Proc. Soc. Exptl. Biol. Med. 110:645, 1962.
- Spitzer JJ and Gold M. Free fatty acid metabolism by skeletal muscle. Am. J. Physiol. 206:159, 1964.
- Spitzer JJ, Gold M, and Branson BJ. Oxidation of free fatty acids by dog liver. Proc. Soc. Exptl. Biol. Med. 118:149, 1965.
- Spitzer JJ and McElroy WT Jr. Epinephrine-insulin antagonism on free fatty acid release. Am. J. Physiol. 201:815, 1961.
- Spitzer JJ, Nakamura H, Gold M, Altschuler H, and Liebersohn M. Correlation between release of individual free fatty acids and fatty acid composition of adipose tissue. Proc. Soc. Exptl. Biol. Med. 122:1276, 1966.
- Stone HL, Bishop VL, and Dong E Jr. Ventricular function: cardiac-denervated and cardiac-sympathectomized conscious dogs. Circ. Res. XX:587-593, 1967.
- Stewart WB, Stewart JM, Izzo MJ, and Young LE. Age as affecting the osmotic and mechanical fragility of dog erythrocytes tagged with radioactive iron. J. Exp. Med. 91:147, 1950.
- Suzuki, Kotaro, and Plentl. Chronic implantation of instruments in the neck of the primate fetus for physiologic studies and production of hydramnios. Am. J. Obst. & Gynec. 103(2):272-281, 1969.
- Taylor AW, Shoemann DS, Lovlin R, and Lee S. Plasma free fatty acid metabolism with graded exercise. J. Sports Med. Phys. Fitness 11:234, 1971.
- Timm GW et al. Intermittent occlusion system. IEEE Trans Bio. Med. Eng. October, 1970.
- Tosev J, Daley L, and Hilton A. A method for recording intrapleural pressure in conscious, semirestrained mammals. J. Appl. Physiol. 27(6):902-903, 1969.
- Turney Z and Blumenfeld W. Heated Fleisch pneumotachometer: a calibration procedure. J. Appl. Physiol. 34(1):117-121, 1973.
- Valk AT and Price HL. The chemical estimation of epinephrine and norepinephrine in human and canine plasma. J. Clin. Invest. 35:837, 1956.
- Van der Vies J. Individual determinations of cortisol and corticosterone in a single small sample of peripheral blood. Acta Endocrinologica 38: 399-406, 1961.
- Van Leon EJ and Clark BB. Hematology of the peripheral blood and bone marrow of the dog. J. Lab. and Clin. Med. 28:1575, 1943.

Wahlquist ML, Kaijser L, Lassers BW, Low H, and Carlson LA. The role of fatty acid and of hormones in the determination of myocardial carbohydrate metabolism in healthy fasting men. Europ. J. Clin. Invest. 3:57, 1973.

Weil R, Ho PP, and Altszuler N. Effect of free fatty acids on metabolism of pyruvic and lactic acids. Am. J. Physiol. 208:887, 1965.

van der Vies J. Individual determination of cortisol and corticosterone in a single small sample of peripheral blood. Acta Endocrin. 38:399, 1961.

APPENDIX B

B.i

## RAYTHEON 704 DATA ACQUISITION SYSTEM

### A. 704 Description

The Raytheon 704 Computer System is a general purpose digital computer system primarily intended as the central element for data acquisition and control applications. Some important hardware characteristics are 16 - bit word length, 1.0 microsecond cycle time, automatic priority interrupt, direct input/output to control processor, direct memory access and a full line of peripheral options. Only assembly language is supported. The configuration of the U.K. system is shown in Figure B-1.

The direct memory access feature allows peripherals to communicate directly with core memory independently and simultaneously with any program which may be executing. Slower speed peripherals communicate with the CPU via the DIO bus. The 16 priority interrupts may be connected to Raytheon peripherals or user devices such as the 'start' and 'stop' buttons or a trigger from the ECG of the animal under study. Several peripherals such as a time code generator controller, experiment status switches, and a digital link to a remote computer will be connected to the DIO bus and the priority interrupts.

### B. Mean Value Program

The programs of this system are designed to give a real-time print-out of the average values of up to five analog input channels and to store these average on digital magnetic tape. The voltages on these channels represent slowly changing parameters such as body temperature, mean blood flow, etc. A sampling rate of 256 readings per 10 seconds (25.6 Hz) was selected with a minimum print-out interval of 10 sec. Sampling at a rate of 1 Hz would have been sufficient but we wanted to examine the speed of the computer. The print-out interval may be set at any integral multiple of 10 sec. but the data are stored on magnetic tape every

10 sec. The printed values always represent the average taken over the period since the previous print-out; a typical print-out appears in Fig. B-2.

The programs in this system were designed to be very interactive and almost completely dependent upon interrupts for execution. All programs are in core at all times and a lower priority program is interruptable without damage, by one of higher priority. The 704 has sixteen interrupt levels which may be connected to external devices such as the 'start' and 'stop' buttons or peripherals such as a timer or the analog to digital converter. When an interrupt occurs, the computer begins execution at the specific location assigned to that level, provided no higher priority level is in service.

Once the programs are loaded, INITIALZ executes automatically and performs various initialization chores, enables the 'start' button, starts the clock, and exits to the wait loop (WAIT). In this wait loop the sense switches are checked and the type buffer is examined to see if any printout is requested. When no other program is in execution, the computer runs in this loop continuously.

Calibration is performed by reading the voltage corresponding to at least two (maximum four) points in the range of each input channel. Since the inputs must be linear (the equation  $y = Mx + B$  is used) the values M and B are calculated using a least squares fit over the points which were read and then stored in the calibration tables. The print-out will be in the appropriate physiological units.

When the 'start' button is pressed, a program (START) starts the A/D converter and then returns to WAIT. When the A/D converter is through with the requested number of channels (20 microseconds per chan.) it provides an interrupt which brings CALC into execution.

CALC is the program which performs the arithmetic on the data. The voltages just read are added to their summing buffers. If it is time to print-out or to write on magnetic tape, these sums are divided to get the average and multiplied by the calibration factor to give output units of beats per minute, mmHg, etc. Then they are stored in the 'type' or 'magnetic tape' buffers. CALC also starts a programmable timer whose period is equal to the desired sampling period minus the program execution and A/D conversion times. When this timer times out an interrupt causes PIT to start the A/D converter again.

This cycle is repeated (approximately every 40 milliseconds when the sample rate is 25.6 Hz) until the 'stop' button is pressed. The computer then loops in WAIT until the 'start' button is pressed again.

#### C. Dye Curve Program

Measurement of cardiac output by the dye dilution technique is one way to calibrate chronically implanted electromagnetic flow probes (Rothe, 1973). The classical Stewart-Hamilton analysis requires a plot of the downslope of the dye curve on semilog paper with subjective assessment of the exponential decay constant. According to this theory, the shape of the downslope should be an exponential decay until recirculation occurs. Therefore, fitting an exponential to the downslope before recirculation and extrapolating to the baseline should give an accurate indication of dye disappearance with time. The area under the first part of the curve is added to the area under the extrapolated exponential with the sum being inversely proportional to cardiac output.

Application of this same method with a digital computer is a relatively straightforward matter. The signals from the densitometer (Waters Model XP300 with Cuvette Model XC-302) after passing through analog signal conditioners illustrated in Fig. B-3 are sampled by the A/D converter at 10 Hz (Stenson, Crouse,



Harrison, 1972). The computer must have at least one calibration where a quantity of blood with a known dye concentration is passed through the densitometer cuvette while the voltage is recorded. For the monkeys and dogs under study, concentrations of 2.5, 5.0, and 7.5 mg dye/liter blood are normally used. The calibration signals are monitored on an oscilloscope by an operator who presses 'start' and 'stop' (interrupt level) buttons to allow the computer to read only the flat portion of the curve. Each calibration signal is read for a period of 5 to 15 seconds. Due to some drift arising from the densitometer system, operator control is necessary. Following the calibration levels, a second pure blood zero is read which allows the operator to determine the magnitude of the shift, if any, in the blood zero baseline and gives a more meaningful calibration factor when averages are computed.

The dye curve is read, as above, under operator control at a rate of 10 Hz and recorded point by point in an array (300 point maximum). When the 'stop' button is pressed, the computer locates the peak point of the curve, and then by a process of iteration the blood zero baseline prior to the injection of dye is calculated. This value is subtracted from each point in the curve to eliminate the offset.

The area under the dye curve is then calculated. Starting after the peak at a magnitude of 0.9 peak voltage, the curve is examined in 3 second overlapping segments (30 points each). Each segment is fitted to a true exponential by the least squares method and variance and exponential decay constant ( $\tau$ ) are calculated and recorded. After each segment has been examined, the constant  $\tau$  which had the smallest variance is selected and an exponential decay curve is extrapolated from that point down to the baseline (zero). The area under the first part of the curve

is calculated using Simpson's Rule and added to the exponential area. The cardiac output is then calculated with the following equations:

$$CAL = \frac{\text{mg dye/liter blood}}{\text{volts}}$$

$$C.O. = \frac{\text{amount of dye injected}}{\text{area under curve} \times CAL}$$

$$C.O. = \frac{\text{mg}}{\text{volts} \times \text{minutes} \times \frac{\text{mg/liter}}{\text{volts}}} = \text{liter/minute}$$

The cardiac output is printed out along with several intermediate results - see sample output in Fig. B-4. The operator may now choose to read another dye curve using the same calibration, read another calibration, or exit to the system monitor.

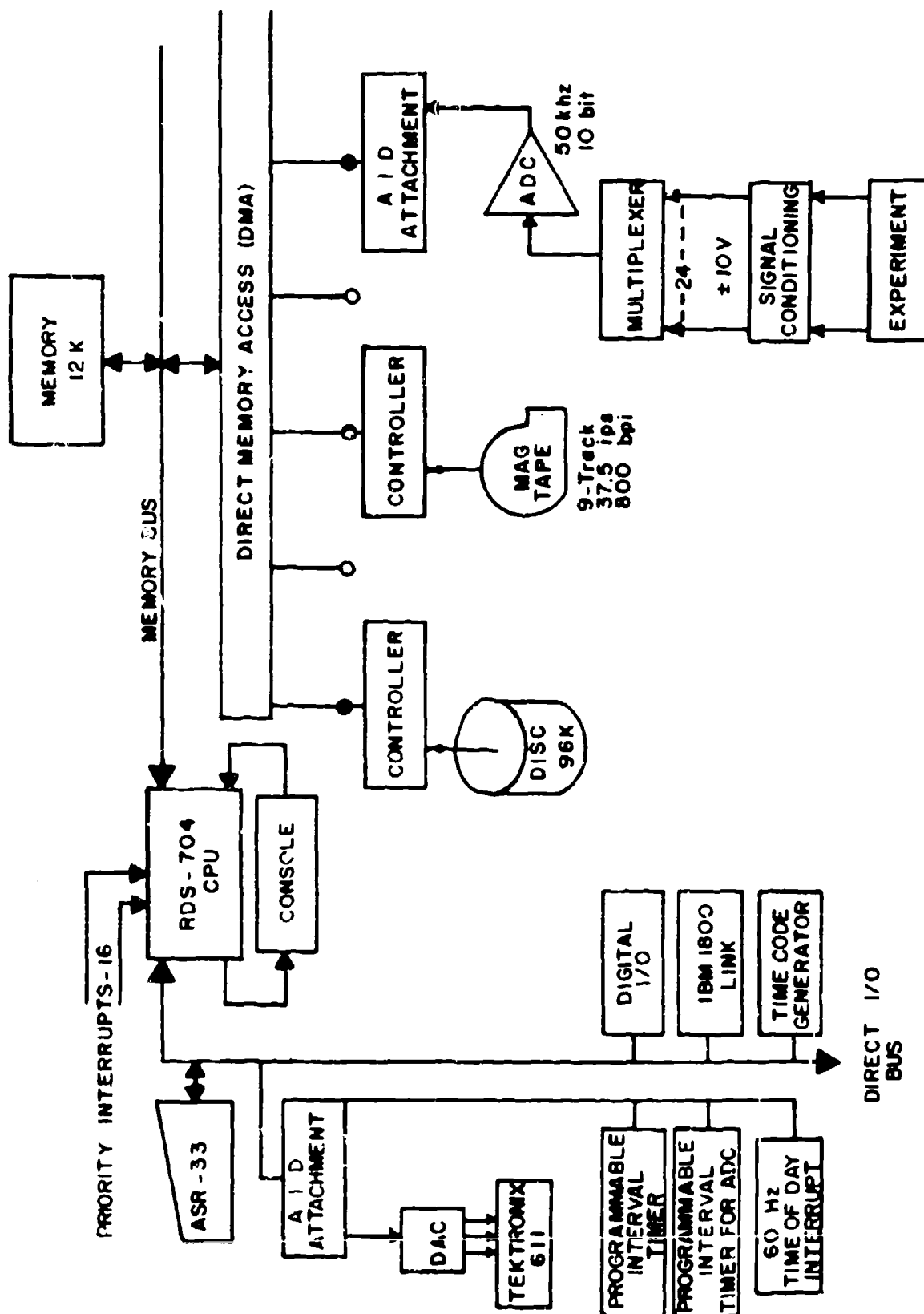


Fig. B-1 Block diagram of Raytheon 704 system currently in use showing peripheral communication with the CPU.

VV73M42#12

5/29/73

TIME	HR	LVP	AF	O2	TEMP	
11:40:36	217.38	50.30	0.92	59.04	40.33	CONTROL
11:41:36	218.58	50.82	0.90	61.36	40.31	
11:42:36	216.22	50.57	0.90	60.43	40.31	
11:43:36	220.53	52.60	0.97	61.73	40.30	
11:44:50						TABLE UP VIB, 16, 12HZ
11:45:50	213.77	41.04	1.10	36.01	40.29	
11:46:50	239.94	47.91	1.20	32.98	40.29	
11:47:50	250.06	50.08	1.20	34.07	40.27	
11:48:50	252.58	50.79	1.22	33.62	40.27	

Fig. B-2 Printout of MEAN VALUE program showing five mean variables: heart rate (BPM), left ventricular pressure (mmHg), aortic flow (L/min), oxygen consumption (ml/min), internal thoracic temperature ( $^{\circ}$ C). The data represents control and vibration variables for a Rhesus monkey.

VV73M42#12

5/29/73

TIME	HR	LVP	AF	O2	TEMP	CONTROL
11:40:36	217.38	50.30	0.92	59.04	40.33	CONTROL
11:41:36	218.58	50.82	0.90	61.36	40.31	
11:42:36	216.22	50.57	0.90	60.43	40.31	
11:43:36	220.53	52.60	0.97	61.73	40.30	
11:44:50	213.77	41.04	1.10	36.01	40.29	TABLE UP VIB, 1G, 12HZ
11:45:50	239.94	47.91	1.20	32.98	40.29	
11:46:50	250.06	50.08	1.20	34.07	40.27	
11:47:50	252.58	50.79	1.22	33.62	40.27	

Fig. B-2 Printout of MEAN VALUE program showing five mean variables: heart rate (BPM), left ventricular pressure (mmHg), aortic flow (L/min), oxygen consumption (ml/min), internal thoracic temperature ( $^{\circ}$ C). The data represents control and vibration variables for a Rhesus monkey.

# Dye Curve Instrumentation

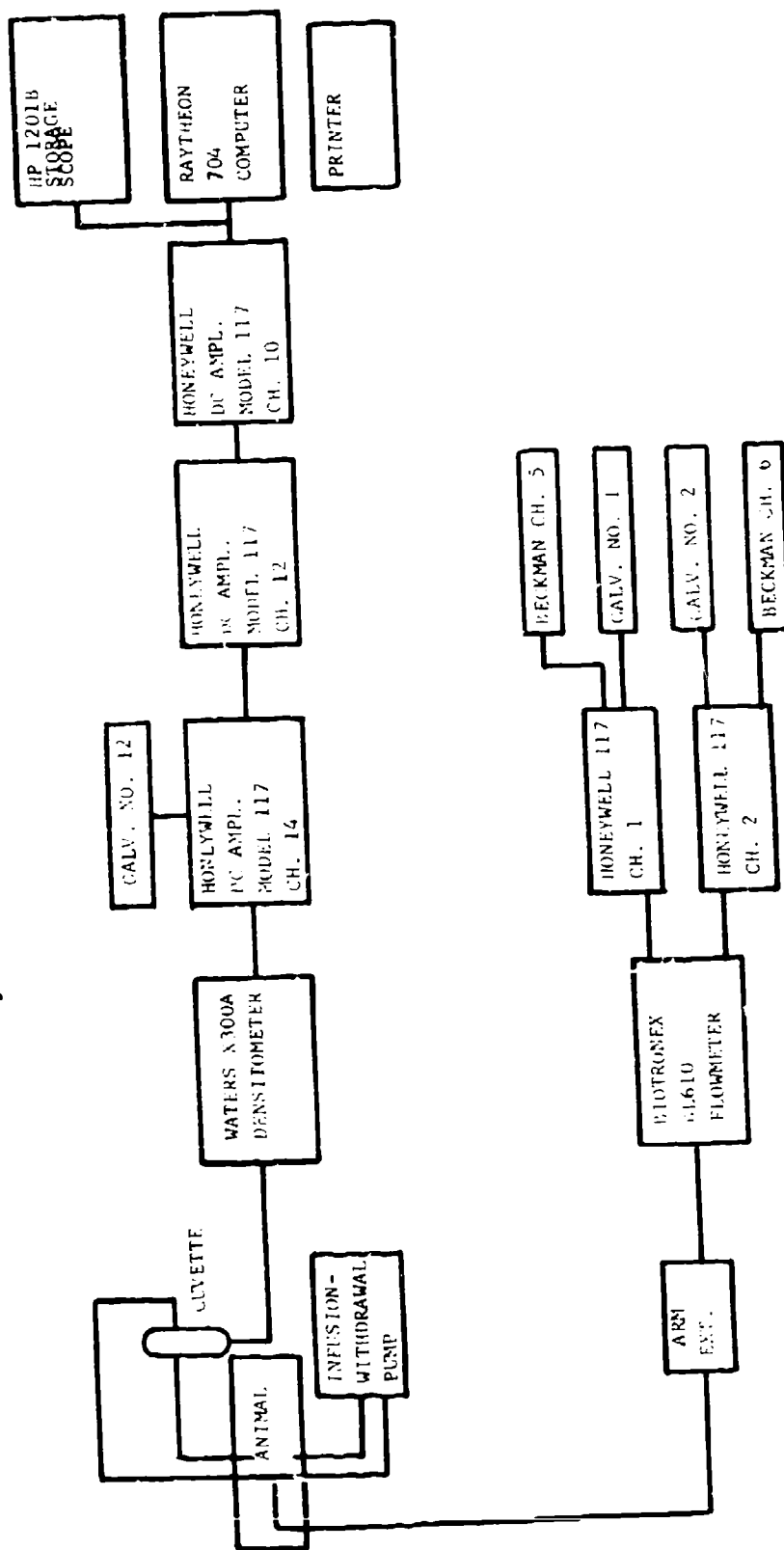


Fig. B-3 Block schematic of instrumentation involved in processing of dye curves on both dogs and monkeys.

CV# ID #      DATE  
 XX\*\*XXXX\*\*XX/XX/XX  
 01 1607 11 02 72  
 SPAN= 185    FREQ= 10    CAL= 1.8851  
 BASE= .2163    PEAK= 4.1085 AT I= 96  
     TAU      VARIANCE    I TO I  
 -.0268      .0034    106    136  
 -.0282      .0024    111    141  
 -.0284      .0022    116    146  
 -.0281      .0026    121    151  
 -.0273      .0026    126    156  
 -.0271      .0025    131    161  
 -.0267      .0026    136    166  
 -.0252      .0041    141    171  
 -.0219      .0065    146    176  
 -.0167      .0088    151    181  
 SIM A= 14.182 V\*SEC    I= 60 TO 116  
 EXP A= 10.325 V\*SEC    V= 2.934  
 CARDIAC OUTPUT = 3.25 LITERS/MINUTE

CV# ID #      DATE  
 2 1607 11 2 72  
 SPAN= 160    FREQ= 10    CAL= 1.8851  
 BASE= .3166    PEAK= 4.9671 AT I= 86  
     TAU      VARIANCE    I TO I  
 -.0339      .0033    95    125  
 -.0354      .0019    100    130  
 -.0355      .0018    105    135  
 -.0345      .0029    110    140  
 -.0325      .0042    115    145  
 -.0296      .0052    120    150  
 -.0252      .0069    125    155  
 -.0191      .0096    130    160  
 SIM A= 15.214 V\*SEC    I= 41 TO 105  
 EXP A= 9.517 V\*SEC    V= 3.382  
 CARDIAC OUTPUT = 3.22 LITERS/MINUTE

Fig. B-4    Representative printout of on-line dye curve program illustrating output of two dye curves done on Dog 1607. Intermediate values other than cardiac output reflect computer calculations of baseline, peak, and slope of curve along with Simpson and exponential areas. B-9

Preliminary Specifications

DIGITAL DATA ACQUISITION AND ANALYSIS

for

THE PHYSIOLOGICAL RESPONSE TO VIBRATION STRESS AND EASE

by

M. Vannier, C. Knapp, E. McCutcheon, F. Wibel, and T. Lowery

WENNER-GREN RESEARCH LABORATORY  
University of Kentucky  
Lexington, Kentucky

May, 1973



## TABLE OF CONTENTS

1. Preface . . . . .	3
2. Introduction . . . . .	4
2.1 Measurement of Cardiovascular Stress . . . . .	4
2.2 Measurement Interval . . . . .	6
3. Data Acquisition Characteristics . . . . .	8
3.1 Vibration Facility . . . . .	8
3.2 Signal Conditioning . . . . .	9
3.3 Analog-to-Digital Conversion . . . . .	11
4. Data Analysis Requirements . . . . .	12
4.1 Within-beat Signal Processing . . . . .	12
4.2 Time Averages of Slowly Varying Signals . . . . .	12
4.3 Time Relationship of Analog Signals . . . . .	15
4.4 Phasic Variables . . . . .	15
4.5 Other Parameters of Interest . . . . .	18
4.6 Calibration . . . . .	18
5. Data Storage Requirements . . . . .	19
5.1 Magnetic Tape Storage . . . . .	19
5.2 Intermediate Disk Storage . . . . .	20
6. Data and Results Presentation . . . . .	21
6.1 Teletype Formats . . . . .	21
6.2 CRT Graphic Output . . . . .	21
7. Operation of System . . . . .	25

## PREFACE

1.1 The purpose of this document is to present an overview of the data acquisition and analysis requirements for the Vibration Facility at the Wenner-Gren Laboratory. The equipment available is a combination of analog signal conditioners and digital data processors including a dedicated Raytheon 704 digital computer (Appendix B), supplemented by a remote data processing system.

1.2 The data processing protocol presented here is designed to fulfill the requirements of measurement of the physiological responses to vibration (AFOSR Contract No. F44620-69-C-0127), and to Externally Applied Synchronous Energy for Cardiac Support (EASE, NIH Contract No. NO1-H6-3-2928.).

1.3 These specifications are intended to provide the base for initiating the design and implementation of processing programs which will serve to satisfy the data storage, on-line (real-time), and off-line processing requirements and will use existing equipment at the Wenner-Gren Research Laboratory Vibration Facility.

1.4 This document does not imply any commitment on the part of the investigators to implement any or all of the specifications outlined.

## INTRODUCTION

### 2.1 Evaluation of Physiological Stress

Determination of the effects of stress imposed on an organism may be accomplished by measuring a number of physiological variables. Heart rate, blood pressures and flows, respiration rate, oxygen consumption, and body temperature are examples of appropriate physiological measurements. Evaluating relative changes in these variables caused by a given stress requires correlation with characteristics of the imposed function. For the particular stress of vibration with which the current studies are concerned, such parameters are table displacement, and internal organ acceleration.

2.1.1 Dogs and monkeys chronically implanted with flow and pressure transducers are used routinely as experimental subjects in vibration stress studies at the Wenner-Gren Research Laboratory. The animal is strapped to a table and accelerated (Section 3.1) in either the vertical (vibration-stress case) or horizontal (vibration-stress and EASE) direction. The table is actuated externally, and moves in a sinusoidal pattern at various frequencies and levels of acceleration. Calibration of all physiological transducers is accomplished immediately prior to a run. After a control period of stable values, the experimental series of appropriate design is conducted. A recovery period follows. In all case, both hard copy records on chart-paper and a multi-channel analog tape recording are produced continuously during the experimental period. Digital data processing based on the Raytheon 704 Computer is used to supplement the analog data acquisition facilities with real-time (on-line) reports, and to produce an edited and condensed record of experimental variables on digital magnetic tape for permanent storage and off-line analysis. All acquisition equipment records a digital time code in HH:MM:SS format for later comparison and synchronization of data. The typical experimental arrangement is shown in Fig. 2.1.

2.1.2 The Digital Data Acquisition System (DAS), described elsewhere in this report, requires a remote operator control panel with lights, switches and a tele-

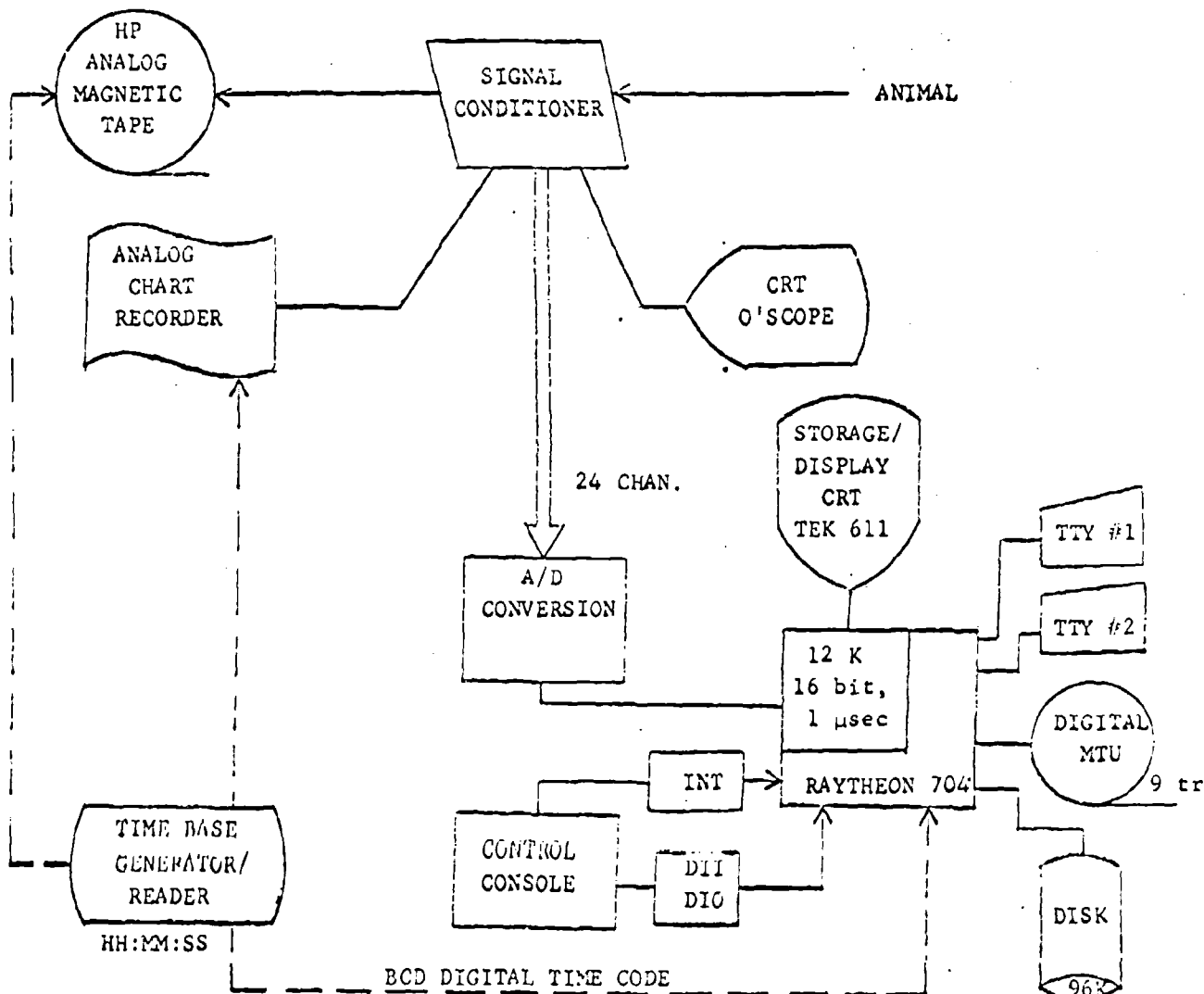


Figure 2.1 Functional Diagram of Experimental Configuration for Vibration Test Facility.

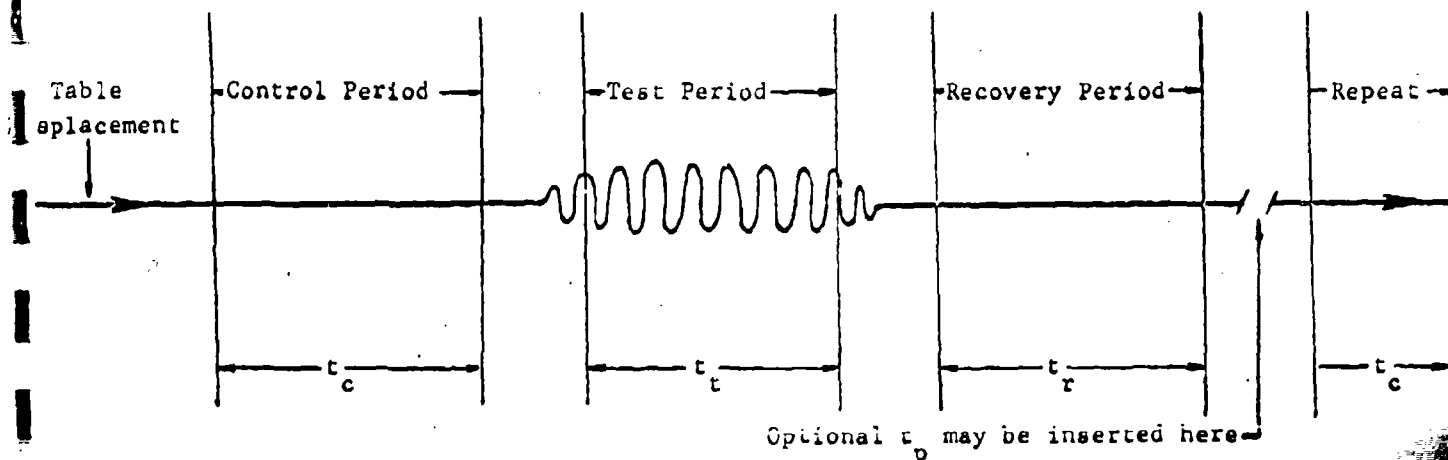


Figure 2.2. Measurement Periods Required by Basic Experimental Protocol

type to control the DAS, as well as a bank of appropriate indicator lights which inform the operator of the DAS measurement conditions. A data coordinator is also present during an experiment to inspect measurements as they are acquired.

## 2.2 Definition of Measurement Interval

The experimental protocol is based on a four-component measurement interval which may be repeated a maximum of 50 times and will not exceed 6 hours. The procedure is outlined in Fig. 2.2. and shows the three components:

- A. Control period, of duration  $t_c$  seconds. - Defined as the period of no time-varying acceleration preceding a test period.
- B. Test period, of duration  $t_t$  seconds. - Defined as a period where the animal is submitted to steady whole-body acceleration.
- C. Recovery period, of duration  $t_r$  seconds. - Begins upon termination of the test period and ends with an operator command; no time-varying acceleration during this period.
- D. Pause period, of duration  $t_p$  seconds. Data are not recorded on digital magnetic tape during this period, but listing on the teletype continues.

2.2.1 Duration of Test: The total measurement period within a given experiment for a certain frequency and waveform will be defined as  $t_{total} = t_c + t_t + t_r + t_p$  seconds. The maximum total duration of a single test interval ( $t_{total}$ ) will not exceed 390 minutes in any circumstance; the minimum duration of a single test interval will not be less than 150 seconds.

2.2.2 The range of the control ( $t_c$ ), test ( $t_t$ ), recovery ( $t_r$ ) and pause ( $t_p$ ) periods is specified as follows:

<u>IDENTIFICATION</u>	<u>MINIMUM DURATION</u>	<u>MAXIMUM DURATION</u>	
	(seconds)	(seconds)	(minutes)
$t_c$	60	900	15
$t_t$	30	21,600	360
$t_r$	60	900	15
$t_p$	10	21,600	360

The digital data acquisition facility will halt measurements during the off-line period (as defined in the System Operation Section, paragraph 7.1).

2.2.3 Because the measurement interval and its components may vary over a wide range, a procedure for period identification is necessary. The procedure must be flexible and applicable at the time data are acquired. The onset of the Recovery Period ( $t_r$ ) will be identified by data acquisition system (DAS) detection of the shake-table oscillator output. The other periods will be identified by signals from the operator control panel teletype (Section 7.0).

## DATA ACQUISITION CHARACTERISTICS

### 3.1 Vibration

Both Horizontal and Vertical Shake Tables are in use at the Wenner-Gren Laboratory. During any test using animals with chronically implanted flow, pressure, and other transducers, several parameters are measured by the Raytheon 704 Data Acquisition Processing System (DAS). The horizontal shake table is designed for use with the Externally Applied Synchronous Energy (EASE) experiments. The vertical table is reserved for use in measurement of animal response to whole-body vibration, especially with regard to physiological stress measurements.

3.1.1 The tables themselves are actuated hydraulically on cue from external control equipment. The displacement of the table is determined by a voltage function generator. The signals supplied to the table are specified to be pure sine waves with frequencies between 2 and 30 Hz. The frequency of the sine wave will be entered by the operator and is sampled by the DAS, with the direction and zero-crossings of the shake table oscillatory output noted for use in calculating phasic relationships. A period of lost data not exceeding 2.5 seconds at the start of a test period is available for frequency analysis.

3.1.2 A digital time code is acquired by the DAS and is placed on the digital magnetic tape for subsequent identification of test periods. The time code is recorded in BCD format as HH:MM:SS. Hardcopy records of the time-of-day and various average parameters are emitted periodically.

3.1.3 Calibration of all flow and pressure transducers is accomplished immediately prior to and following the experimental procedure. Periodic rechecks may be requested during the experiment. These calibration results are input to the DAS both prior to and during an experiment. The DAS calculates calibration factors from the input data and uses the factors for calculations of the physiological variables.

### 3.2 Signal Processing

3.2.1 All physiological signals are conditioned by various analog circuits before presentation to the DAS. Insofar as possible, random noise, drifting baselines, interference from external electrical equipment and intermodulation distortion are maintained at the lowest possible values. However, flawless data acquisition is not possible, and a certain amount of error detection by the DAS is required. Channels which present illegal data, such as zero, constant or out-of-range values should be omitted from calculations, after emitting an error code and channel identification to the operator.

3.2.2 The physiological and vibration parameters of interest measured by the DAS may be classified as follows:

#### I. Physiological

##### A. Cardiovascular

1. Pressure, Left Ventricular
2. Pressure, Aortic
3. Pressure, Arterial
4. Flow, Aortic
5. Flow, Coronary
6. Heart Rate

##### B. Other

1. Respiration Rate
2. Oxygen Consumption
3. Body Temperature

#### II. Vibration

##### A. Acceleration

1. Table
2. Body Organs



B. Other

1. Table Displacement

2. Net Force

III. Time Relationships (between groups I and II).

3.2.3 Based on their data acquisition requirements, the parameters of interest can be grouped into three categories; (1) within-beat processing, (2) 10-second averages, and (3) time-related variables. Along with these groups, a 24-bit time code (HR:MIN:SEC) in BCD format, and periodic experimental comments in ASCII are entered on the digital tape.

3.2.4 The following analog signals are sampled during the experimental procedure (not all signals are sampled continuously during the measurement interval):

VARIABLE	CODE	SAMPLING RATE (msec)	NO. OF SAMPLES per sec.
Left Ventricular Press.	LVP	2	500
Aortic Pressure	AP	5	200
Arterial Pressure	ARP	5	200
Aortic Flow	AF	2	500
O <sub>2</sub> Consumption	O2	100	10
Acceleration (Internal Organs)	ACCI	5	200
Net Force	NF	5	200
Displacement of Table	TD	5	200
Mean Coronary Flow	CFM	500	2
Mean Heart Rate	HRM	500	2
Mean Aortic Pressure	APM	500	2
Mean Arterial Pressure	ARPM	500	2
Body Temperature	T	1000	1
Table Acceleration	ACC <sub>T</sub>	5	200
<u>for possible later addition:</u>			
Venous Pressure	VP	5	200
Venous Flow	VF	5	200
Left Ventricular Dimension	LVD	5	200
Respiration Rate	RR	10	100
Peripheral Arterial Flow	PF	5	200

3-axis acceleration (Internal Organ ACCI<sub>1</sub>, ACCI<sub>2</sub>, ACCI<sub>3</sub>)

### 3.3 Analog-to-Digital Conversion

The Raytheon 704 DAS incorporates a 24-Channel "Milliverter" (Model MADC 10-06) analog-to-digital converter. This device contains a 24 single-ended input multiplexer with sample-and-hold amplifier. Full-range input analog signals are converted to 9 bits plus sign at a 50 kHz rate. Conversion time is 9.8  $\mu$ sec, aperture time is 100 nsec, and approximate through-put rate (single-channel) is 50 kHz (max).

3.3.1 In order to maximize the precision in all measurements, the range of signals measured by the Analog-to-Digital converter (ADC) in the Raytheon 704 System is extended to full 9 bit significance. In other words, the voltage range of these signals is extended to  $\pm 10.0$  volts. A full significance reading by the ADC is expected to include 1 part in 512 accuracy, plus the sign of the input signal. This is equivalent to 1.95 mv in 10 v. For a blood pressure calibration of 100 mmHg/10 V, 1 mmHg = 100 mv, and resolution would be on the order of  $\pm 0.2$  mmHg. For a flow calibration of 10 L/min/10 V, resolution would approximate  $\pm 20$  ml/min.

3.3.2 During Pause periods, any A/D channel may be selected for output on a D/A channel to a monitor CRT for direct visual comparison in order to verify satisfactory A/D operation.

## DATA ANALYSIS REQUIREMENTS

### 4.1 Within-Beat Signal Processing

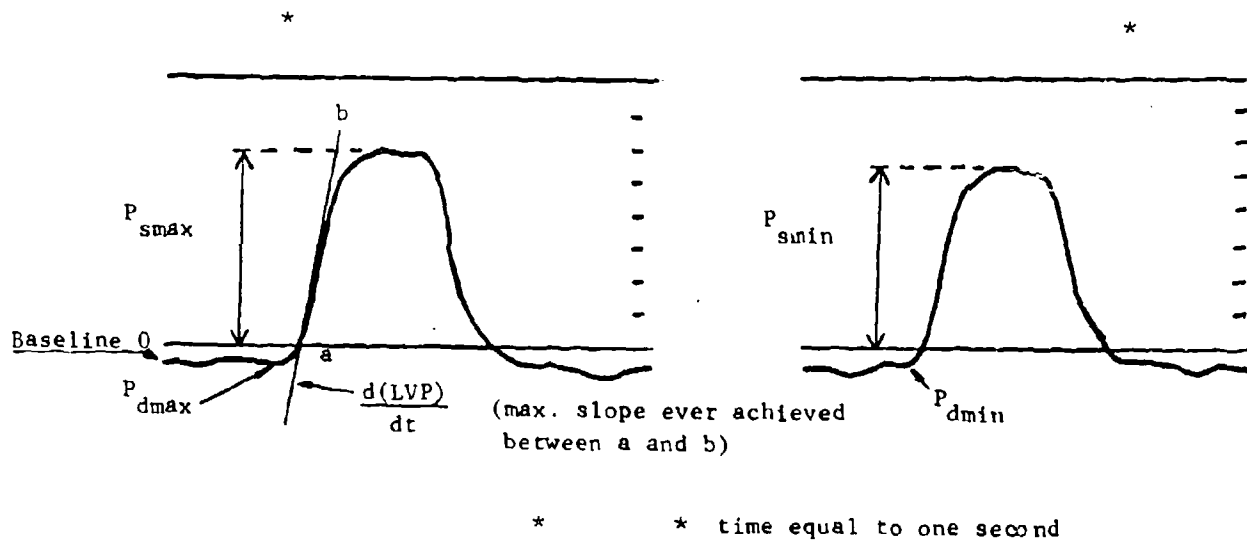
A beat-by-beat analysis of several parameters is required. These parameters are illustrated in Figs. 4.1.1, 4.1.2, 4.1.3 and include:

<u>VARIABLE</u>	<u>CODE</u>
Left Ventricular Pressure	LVP
Aortic Pressure	AP
Arterial Pressure	ARP
Aortic Flow	AF

Upon receiving an external trigger signal, the within-beat interval will be identified and the DAS will begin searching for valid data. The maximum sampling rate shown in section 3.2.4 will continue until completion of the beat is identified by the DAS, at which time sampling will cease until the next trigger is received. The data will then be condensed into ten second intervals. For those variables designated as maximum and minimum values, single points (maximum and minimum) for that ten second interval are to be identified and stored on tape. For each within-beat parameter (i.e., peak aortic flow ( $Q_g$ ), peak  $\frac{d(LVP)}{dt}$ , peak  $\frac{d(AF)}{dt}$ , etc.) which is not averaged before input to the DAS, values for all beats within the ten-second interval are averaged and this mean value is stored on magnetic tape.

### 4.2 Processing of Averaged or Slowly-Changing Values

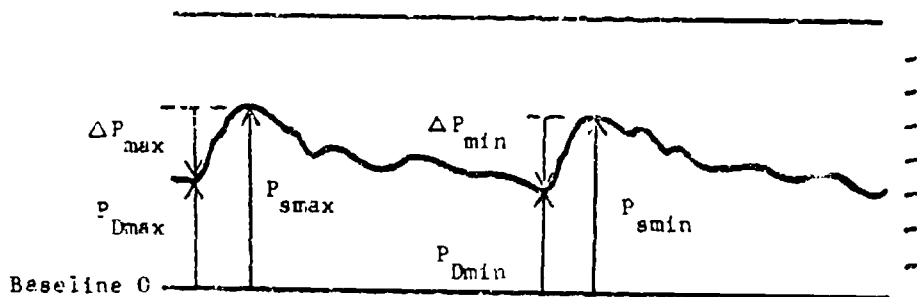
Preprocessed averages of several parameters are acquired. The variables are to be sampled as indicated and averaged over intervals of some multiple of 10 sec. An option is to be available for reporting these 10 sec. averages either individually or as averaged 10 second blocks in integer multiples up to 30. But always data recorded on digital magnetic tape will be in 10 sec. blocks.



Parameters measured:

$P_{smax}$	$P_{dmax}$	$\frac{d(LVP)}{dt}$	max
$P_{smin}$	$P_{dmin}$	$\frac{d(LVP)}{dt}$	min
$P_{smean}$	$P_{dmean}$	$\frac{d(LVP)}{dt}$	mean

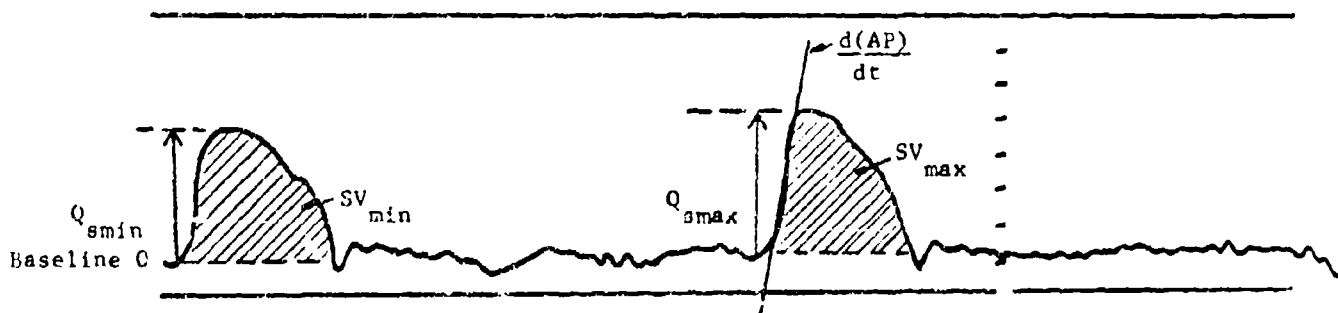
Figure 4.1.1 Left Ventricular Pressure



Parameters measured:

$P_{dmax}$ ,  $P_{dmin}$   
 $P_{smax}$ ,  $P_{smin}$   
 $\Delta P_{max}$ ,  $\Delta P_{min}$

Figure 4.1.2 Aortic Pressure (AP) and Arterial Pressure (ArP).



Parameters measured:

$Q_{smax}$   $\frac{d(AF)}{dt}$  |  $SV_{max}$   
 $Q_{smin}$   $\frac{d(AF)}{dt}$  |  $SV_{min}$   
 $Q_{smean}$   $\frac{d(AF)}{dt}$  |  $SV_{mean}$

Figure 4.1.3 Aortic Flow (AF)

The averaged parameters include:

<u>VARIABLE</u>	<u>CODE</u>
Mean Heart Rate	HPM
Temperature	T
Oxygen Consumption	O2
Mean Aortic Pressure	APM
Mean Coronary Flow	CFM
Mean Arterial Pressure	ARPM

#### 4.3 Time Relationship of Analog Signals

An analysis of the time relationship between the physiological variables (AP, LVP, AF) and the shake table variables (displacement, organ acceleration, table acceleration, transmitted force) will be required. The term  $\phi_T$  will be used to define the relationship of the vibration table to the cardiac cycle. Specifically,  $\phi_T$  is defined as the time from the null position of the table to some event of interest. An example is illustrated in Fig. 4.3.1. For example,  $\phi_{TAF}$  defines the elapsed time from the passage of the table through zero to the initiation of aortic flow for the next heart beat.

#### 4.4 Phasic Variables

Parameters of the vibration table and acceleration of internal body organs resulting from the vibration input are required. These parameters include:

<u>VARIABLE</u>	<u>CODE</u>
Table Acceleration	$G_t$
Organ Acceleration	$G_I$
Net Force	$F_N$
Table Displacement	W

Examples of these parameters are shown in Figs. 4.4.1, 4.4.2, 4.4.3, and 4.4.4.

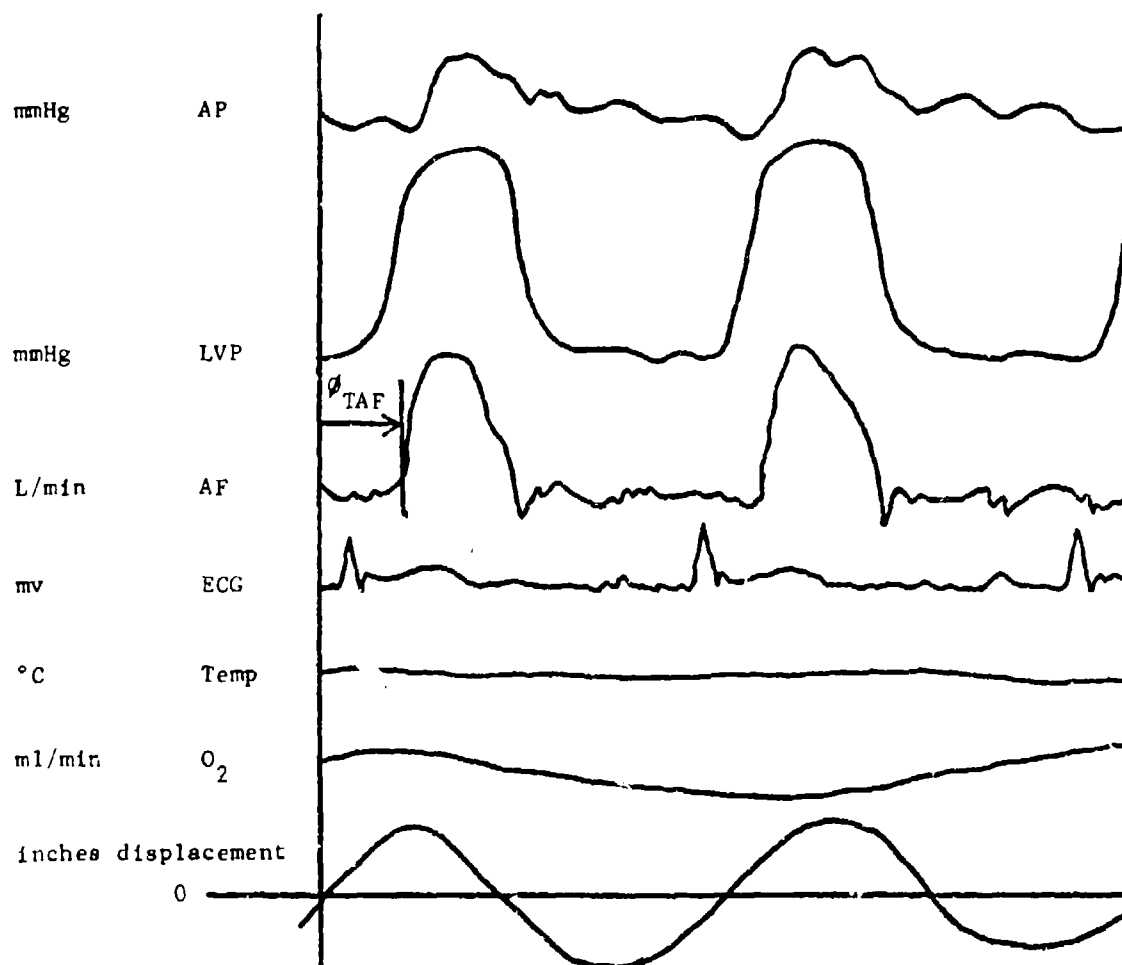


Figure - Time Relationships of Physiological and Acceleration Variables.

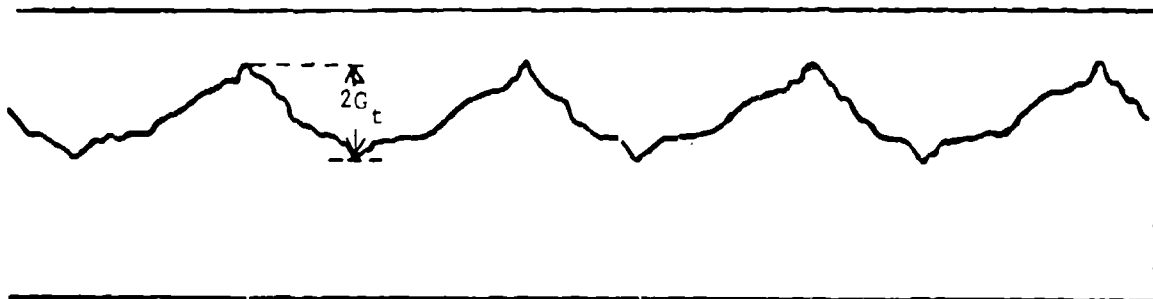


Figure 4.4.1 Table Acceleration ( $G_t$ )

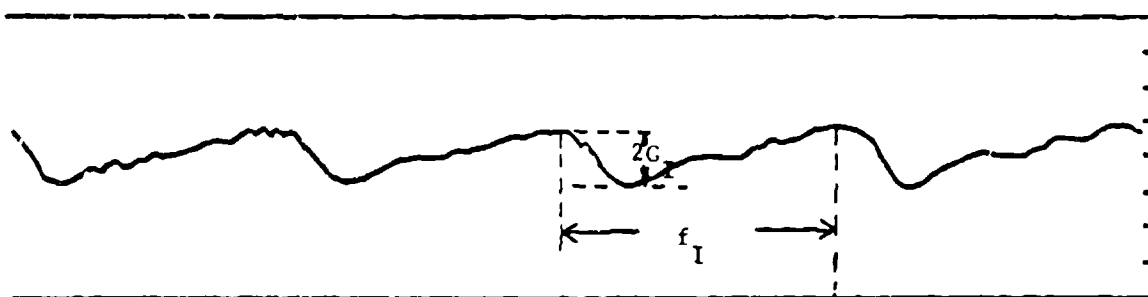


Figure 4.4.2 Organ Acceleration ( $G_I$ )

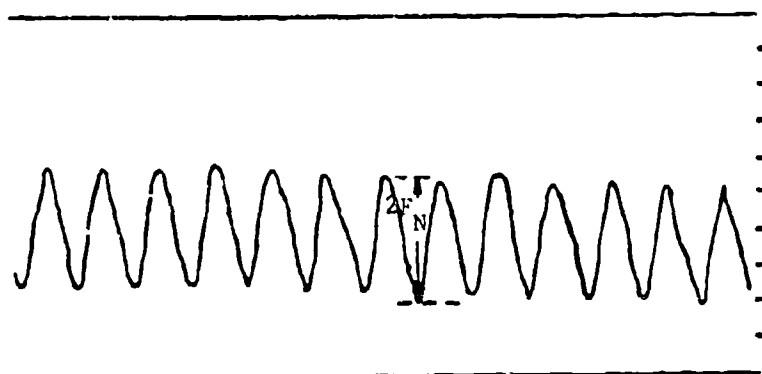


Figure 4.4.3 Net Force ( $F_N$ )

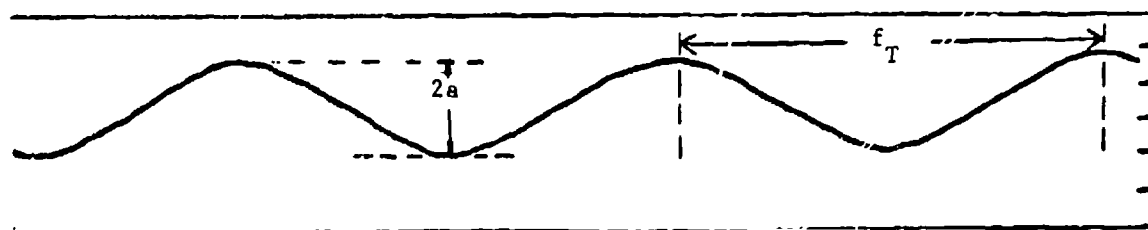


Figure 4.4.4 Table Displacement ( $w$ )



#### 4.5 Other Parameters of Interest

As time permits, the following variables should be measured by the DAS, and recorded on digital magnetic tape. Digital processing of these data is of low priority and should be accomplished only if no interference with the aforementioned measurements can occur.

<u>VARIABLES</u>	<u>CODE</u>
Venous Pressure	VP
Venous Flow	VF
Left Ventricular Dimension	LVD
Respiration Rate	RR
Peripheral Arterial Flow	PF

#### 4.6 Calibration

A calibration table will be constructed by reading standard signals from each channel under operator control at the beginning of the experiment. All channels will be linear, so two values will be required for each channel, i.e.  $y = mx + b$ ;  $m$  and  $b$  will be calculated by the calibration program and stored in a table. It should be possible to re-calculate the calibration for a channel during the experiment (during a pause or 'stop' period) and change the calibration table.

## DATA STORAGE REQUIREMENTS

### 5.1 Magnetic Tape Storage

Data acquired during an experimental procedure are stored on both analog tape and digital tape. All raw data are stored in unmodified form on analog tape along with an IRIG-standard time-code superimposed on a 1 kHz carrier. This time code may be converted into HH:MM:SS format by the time code reader, permitting the off-line retrieval of raw data at a later time.

5.1.1 Data stored on digital magnetic tape will have undergone sampling and considerable data compression. An identification record incorporating the following is required at the beginning and end of every test tape on each animal:

1. Animal number
2. Date: MM/DD/YY
3. Comments

The header for each data block will include:

1. Time of Day; HH:MM:SS
2. Vibration Frequency, (Hz)
3. G-Level
4. Period: Control, test, or recovery.

Results from no more than one experimental animal are to be stored on a single digital magnetic tape. Data retrieval at a later time may be accomplished by entering the start and end time in HH:MM:SS whereupon the entire contents of the tape between the two times are dumped on the teletype.

5.1.2 As required by the specific data presentation demands explained in Section 6.0 of this report, CRT display of the physiological data may be accomplished off-line, i.e. during pause and stop periods.

5.1.3 All digital magnetic tape files for a specific experiment are to be kept on separate tapes, one animal per tape. Storage is accomplished in IBM-compatible, 9 track 800 bpi format with NO header or trailer labels. The end

of a data run is delimited by 3 file marks on the tape. Odd parity and binary format for numbers are required. Integer values for physiological data are used wherever practical.

## 5.2 Intermediate Disk Storage

Buffer area on the fixed-head disk is required for on-line analysis and data presentation. This area should be of sufficient size to allow graphic presentation of all the variables listed in Section 6. These displays may be requested by the system operator during pause or stop periods, for a "display update" or at the end of the run for a "summary display". The formats for these display patterns are explained in section 6 of this report.

## DATA AND RESULTS PRESENTATION

### 6.1 Teletype Formats

In the data acquisition protocol described here, two teletypes (KSR33) are required, i.e., teletype #1 for a chronolog of averaged physiological data, and teletype #2 for entering operator comment statements regarding the progress of the experiment. Teletype #1 output is required for an on-line record of integer multiples of 10 second average values of the physiological parameters. This record is used to assess the present state of the experiment and to review data from the beginning of the experiment. The format for printing these data is presented in Fig. 6.1.1. Teletype #2 is used to type and preview comments before they are entered on the magnetic tape and printed output of teletype #1.

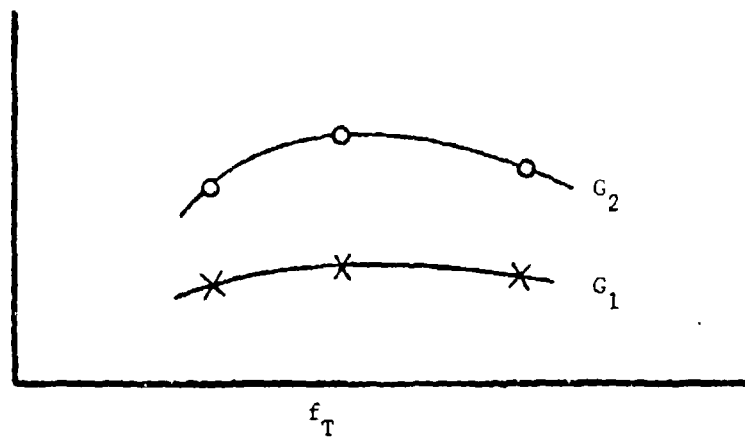
### 6.2 CRT Graphic Display Output

A Tektronix 611 storage and display oscilloscope is available for use by the DAS. The CRT display may be requested in three possible formats. Parameters of interest may be plotted against (1) table frequency, (2) test interval, or (3) time relationship,  $\emptyset_T$ . An example of each with the parameters of interest is shown in Fig. 6.2.1. At any one time up to four dependent variables may be plotted against the same independent variable. A typical display is illustrated in Fig. 6.2.2. An "update" display is defined as a graphic plot which can be viewed as the data points are added at the completion of each test period. A "summary display" is defined as a plot with all data points for the experiment shown, and is available only in off-line mode at the end of a complete experiment.

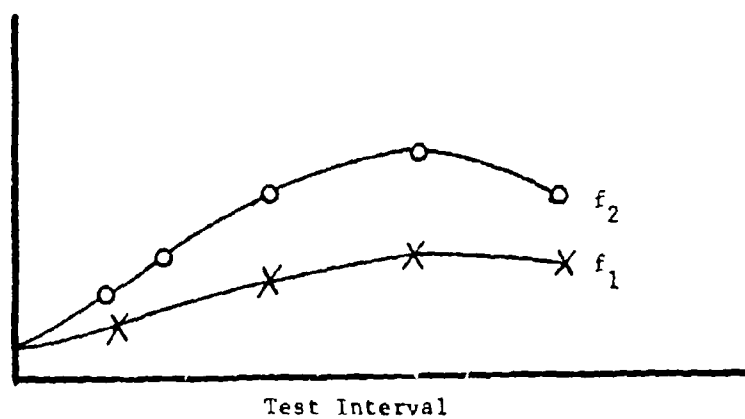
TIME	HR	APM	AFM	O <sub>2</sub>	T	dLVP	P	f	G	Comments
11:23:35	102.	102.	0.86	-0.03	37.	3000.	C	0	0	02 CAL
11:23:45	79.	102.	0.75	-0.03	37.	2900.				
11:23:55	66.	101.	0.51	-0.03	37.	2950.				
11:24:05	69.	102.	0.67	-0.03	37.	3100.				
11:24:15	72.	100.	0.58	-0.03	37.	3250.				
11:24:25	72.	102.	1.00	-0.03	37.	2980.				
11:24:35	68.	100.	1.10	-0.04	37.	3000.				

FIGURE 6.1.1.1 - TIME, HR, APM, AFM, O<sub>2</sub>, Temp, d/dt (LVP) PERIOD, f, G, Comment (Limit to X characters)

%  $\Delta$  LVP<sub>max</sub>



AP<sub>mean</sub>



SV

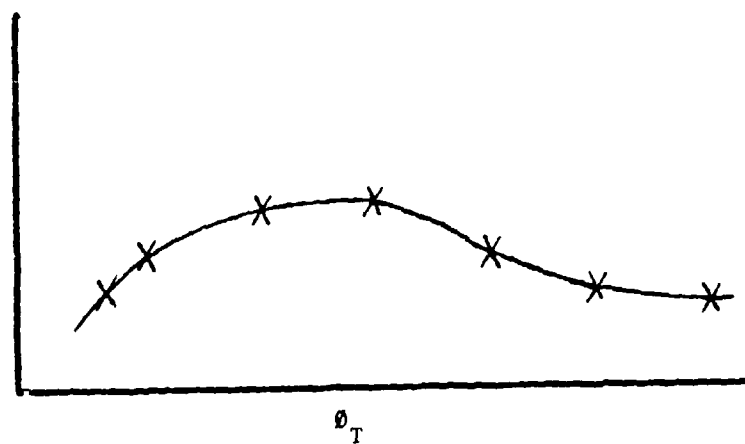
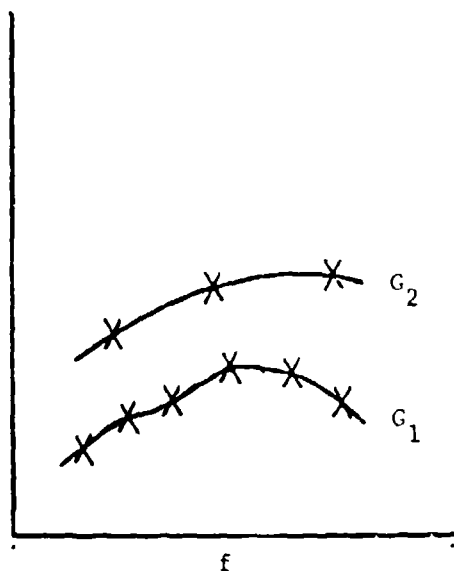
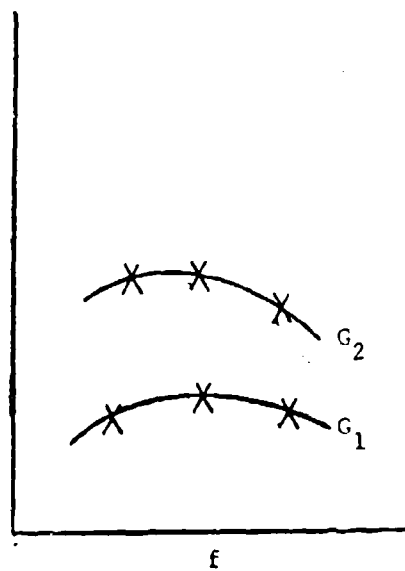


Figure 6.2.1 Graphic Display Examples.

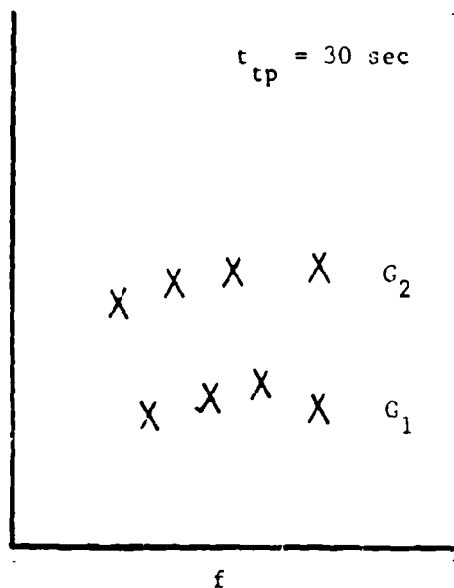
$\% \Delta AP_{\max}$



$\% \Delta SV$



$\% \Delta \frac{d(LVP)}{dt}$



$\% \Delta AF_{\max}$

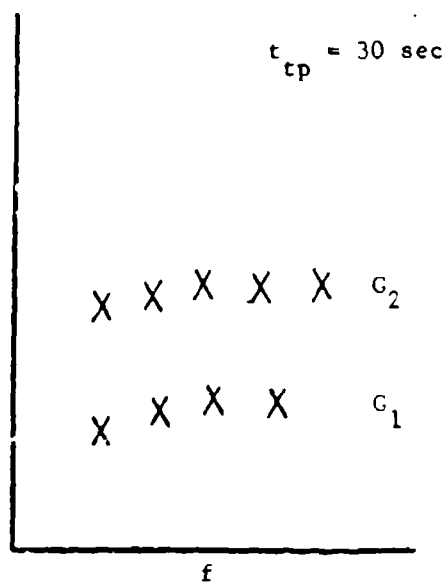


Figure 6.2.2 Example of 611 Update and/or Summary Display

## OPERATION OF THE SYSTEM

7.0 The data acquisition system will require a control console for interfacing between 1) Data Coordinator and 2) System Operator during the experiment. The System Operator is seated at the main console and is responsible for controlling and editing data sent to the DAS. This is accomplished by input from Teletype No. 2 (TTY2). The Coordinator also uses TTY2 for calibration inputs (/CAL), comments (/MSG), and judges the quality of data and results by viewing analog signals. Both the System Operator and Coordinator must communicate in order to define the various measurement periods. A layout of the control console is presented in Fig. 7.0.1. It has three major divisions, (1) control of data acquisition, (2) hardcopy 10 sec. (or an integer multiple of sec.) averages of data on teletype No. 1 and hardcopy analog signals of physiological data, and (3) CRT graphic displays for data inspection. The layout of the Control Indicator light panel in the control console is shown in Fig. 7.0.2.

### 7.1 Operational Procedure

A. The System Operator turns on the Control indicator light panel by pressing the 'ON' panel button. He also enters through TTY2 the information for the identification record described in section 5.1.1.

B. The Coordinator inspects the incoming analog data. When these are acceptable, he announces readiness to begin the experiment.

C. The System Operator then enters (ON TTY2) the appropriate frequency (/FRQ) and G-level, "Begin Control Period" (/CON), which initiates data acquisition for transfer to digital magnetic tape and TTY1 output. This action also initiates a timer to time the control period. (See Table 7.1.1 for TTY commands).

D. After consultation with the Coordinator, the control period is terminated by entering "End Period" (/END) and "Begin Test Period" (/TST) code on the TTY2. This resets the timer to zero, cues the shake table operator to begin vibration, and stops transfer of data to the digital magnetic tape. After steady state values



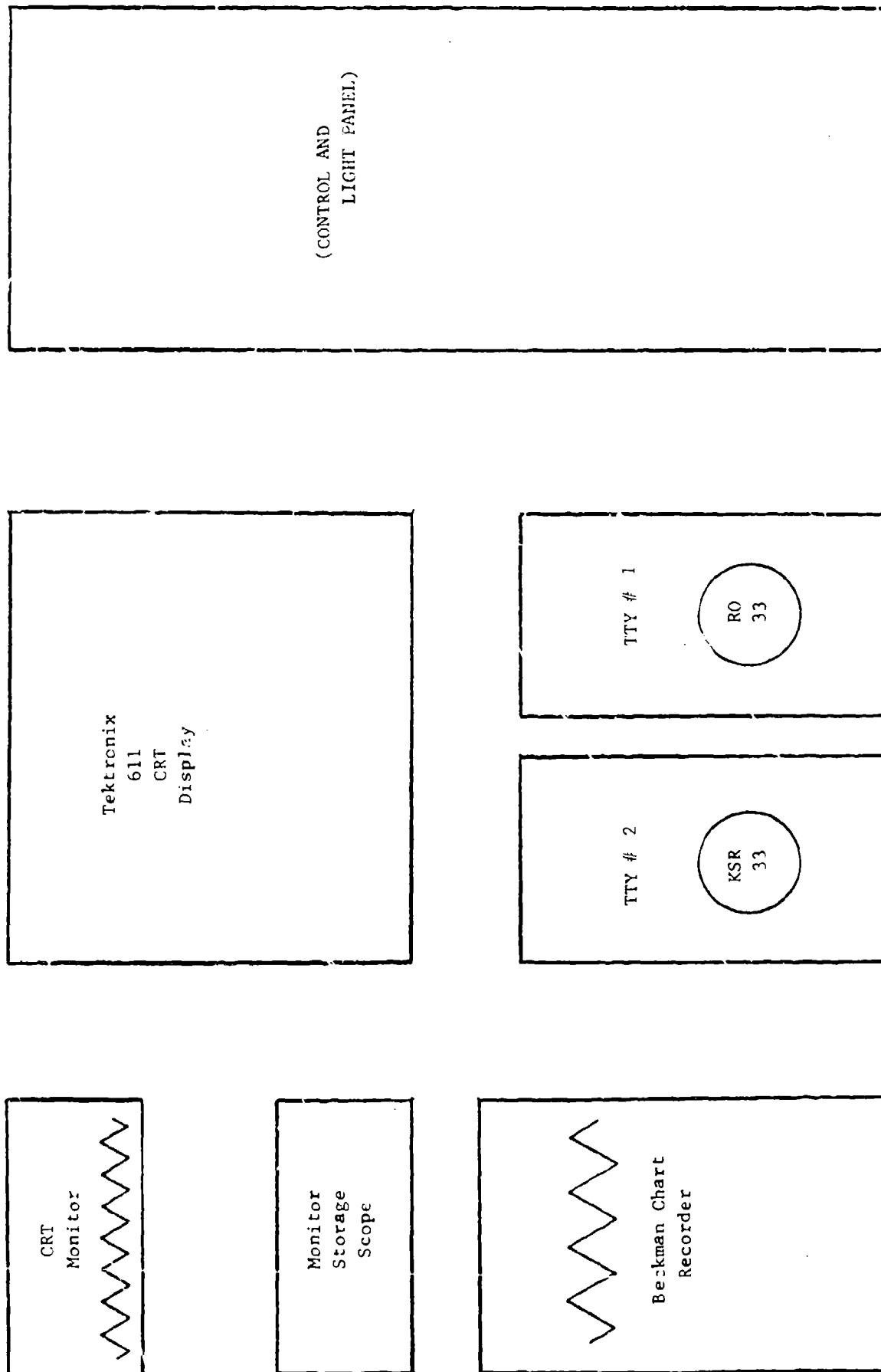


Figure 7.0.1 Control Console

ON/OFF		EASTERN STANDARD TIME		TIMER	
		HH	MM	HH	MM
		SS		SS	

SYSTEM STATUS	DATA WORD QUALITY	SYSTEM OPERATION	DAS CONFIDENCE	SYSTEM STATUS
SUBJECT READY	EXCELLENT DATA	CALIBRATION	TABLE ACTIVE	
DAS LOCAL READY	CALIBRATION TRANSFER	CONTROL	TCG ACTIVE	
CHECKOUT	FINE ERROR	TEST	EXT ACQUISITION	
HALT	COARSE ERROR	RECOVERY	EXT SYNC. LOST	
SPARE	UNCHECKED DATA	REST	PROGRAM NO-GO	
	INITIAL TRANSFER	ACTIVE	SPARE	
	AVERAGE DATA ONLY	PASSIVE	SPARE	
	UNUSABLE DATA	SPARE		

GRAPHIC DISPLAY	
P L O T	
y	x
	f
	t
	$\phi$
ENTER	

Figure 7.C.2 Control Indicator Light Panel of Control Console

TABLE 7.1.1

TELETYPE COMMANDS

/CXL	Cancel Present Data Period
/CAL	Calibrate Analog Channels
/CON	Begin Control Period
/END	End Period
/RCV	Begin Recovery Period
/RST	Begin Test Period
/EOT	Write End of File on Tape
/BYE	Terminate Experimental Procedure
/MSG	Next Line Entered Should go to Comments Part of MAG Tape Record
/FRQ	Enter Vibration Frequency
/GLV	Enter G-Level

\* Rubout key cancels command just entered

\* Carriage Return and Line Feed Initiates Command.

of vibration have been reached, the Shake Table Operator presses his Table Ready button. This turns on the Table Ready light on the Control Console and again resets the timer to zero and data transfer to the digital magnetic tape is resumed.

E. The Vibration Test period is terminated by typing (/END) and "Begin Recovery Period" (/RCV) by the System Operator. The (/RCV) signal 1) cues the Shake Table Operator to stop vibration; 2) resets the timer; and 3) automatically initiates the recovery sequence. Sequence (3) consists of a DAS search for zero output from the oscillator driving table. When the output reaches zero, the DAS resets the panel timer and activates the "Recovery" panel light.

F. Recovery period can be terminated by typing (/END). This stops transfer of data to digital magnetic tape (TTY 1 output continues). CRT 611 is now accessible for update. Any other option is available after this button is activated. For example, (/BYE) inactivates all digital data acquisition, with CRT 611 remaining accessible for update. Or, enter f (/FRQ), G (/CLV), and (/CON) to repeat above sequence.

G. Typing (/CAL) indicates to the DAS a calibration operation is to be performed. The operation will be carried out by interaction with TTY2.

H. A "Cancel Present Data Record Period" (/CXL) will also be available. This label indicates the data from the preceding period is invalid and is not to be used in the standard data reduction routine. For any other corrections, the TTY2 comments will be used. The (/CXL) command also enables restart of the previous period.

I. The Coordinator may enter comments via TTY2 at any time during the experimental period.

## 7.2 Displays

The System Operator may choose the desired plots of data defined in Section 6.2. The 611 display is initiated by (1) pressing "PLOT", (2) pressing up to four variables for Y and one for X, and (3) depressing "ENTER".



**an ASME  
publication**

The Society shall not be responsible for statements or opinions advanced in papers or in discussion at meetings of the Society or of its Divisions or Sections, or printed in its publications. Discussion is printed only if the paper is published in an ASME journal or Proceedings.

Released for general publication upon presentation.

Full credit should be given to ASME, the Professional Division, and the author (s).

## **A Model to Predict the Mechanical Impedance of the Sitting Primate During Sinusoidal Vibration**

**R. G. EDWARDS**

Assoc. Mem. ASME

**J. F. LAFFERTY**

Yenner-Gren Research Laboratory,  
University of Kentucky,  
Lexington, Ky.

This paper describes a novel approach to quantifying the coefficients of a bio-vibrational model. Unanesthetized Rhesus monkeys were exposed to vertical sinusoidal vibrations at discrete frequencies from 2 to 30 Hz at 0.5 and 1.0 g acceleration amplitudes. With the subjects in a sitting position whole body mechanical velocity impedance was obtained from measurements of vibration exciter velocity, transmitted force and the phase relationship between velocity and force. The data obtained were applied to a two-mass, single-degree-of-freedom model to determine the coefficients of elasticity and damping as a function of frequency and body mass. The coefficients were obtained for each test at each frequency by requiring the impedance of the model to match that of the primate. A part of the model is an empirical equation defining, as a function of vibration frequency and intensity, the ratio of nonreactive to reactive animal mass. After normalizing for body mass and averaging, functions for the elastic and damping coefficients were developed such that the impedance response of the model closely matched the experimental results throughout the 2 to 30 Hz range at 0.5 g and also at 1.0 g.

Contributed by the Vibration and Sound Committee of the Design Engineering Division of The American Society of Mechanical Engineers for presentation at the Design Engineering Technical Conference, Cincinnati, Ohio, September 9-12, 1973. Manuscript received at ASME headquarters June 6, 1973.

Copies will be available until July 1, 1974.

# A Model to Predict the Mechanical Impedance of the Sitting Primate During Sinusoidal Vibration

R. G. EDWARDS

J. F. LAFFERTY

High-speed vehicles frequently transmit dynamic forces to their occupants. Depending upon the intensity and duration of such disturbances, serious impairment of operator or passenger functioning may occur. This problem has led to extensive research directed toward defining and understanding the dynamic response of the human body. Laboratory testing of man at low acceleration amplitudes has demonstrated that whole body vibration in the 2- to 30-Hz frequency region produces the most pronounced mechanical effects for any given acceleration amplitude. Ziegenruecker and Magid (1)<sup>1</sup> reported the intensity tolerance of sitting man to vertical vibration to be lowest in the 4- to 8-Hz frequency range. Coermann (2) recorded the force transmitted to both sitting and standing man and found a whole body primary resonant frequency of 4 to 6 Hz. He also demonstrated a remarkably good approximation to this experimental data by use of a simple linear spring-mass-damper model of the human body. Other investigators (3-8) have confirmed these results and contributed additional information to help define man's vibration response. Although high acceleration intensities are at times encountered in vehicles and machinery, man cannot, for safety reasons, serve as a laboratory subject in high intensity vibration tests. In such cases, animals have typically been used as human surrogates (9-12).

Analytical models to predict the dynamic response of man and animals have proven useful in many instances (2 and 7). This paper describes such a model to accurately predict the impedance response for the sitting Rhesus monkey when vibrated vertically (i.e.,  $\pm g_z$ ).

## ANALYSIS

For the system shown in Fig. 1, whole body mechanical velocity impedance (hereafter termed

simply "impedance") is defined as the complex ratio of the interface (transmitted) force to the velocity at the point of force transmission (the vibration exciter velocity in the case of whole body impedance).

$$\bar{Z} = \frac{F}{V} \angle \phi$$

where

- $\bar{Z}$  = complex impedance
- $F$  = amplitude of the transmitted force
- $V$  = vibration exciter velocity amplitude
- $\phi$  = phase angle relationship of the transmitted force relative to the vibration exciter velocity.

Coermann (2) has shown that for a system consisting of one mass ( $m$ ) atop a linear spring (of spring constant, or coefficient of elasticity,  $k$ ) and linear damper (of damping constant, or coefficient of damping,  $c$ ) in parallel, the following equations define the impedance:

$$Z = m\omega \left[ \frac{k^2 + c^2\omega^2}{k^2 + m^2\omega^4 + c^2\omega^2 - 2km\omega^2} \right]^{1/2} \quad (1)$$

$$\phi = \tan^{-1} \left[ \frac{k^2 + c^2\omega^2 - km\omega^2}{cm\omega^3} \right] \quad (2)$$

where  $\omega = 2\pi f$  and  $f$  is the vibration frequency. He illustrated that the impedance of sitting and standing subjects could be approximated by that of the model defined by (1) and (2) with appropriate values of whole body damping and elastic coefficients. It should be noted that this model assumes linearity of coefficients, and thus the impedance is independent of vibration exciter displacement (and therefore acceleration amplitude).

The model as shown in Fig. 2 evolved from the Broderick-Von Gierke (9) model (Fig. 1) and from experimental observations of a number of

<sup>1</sup> Underlined numbers in parentheses designate References at end of paper.

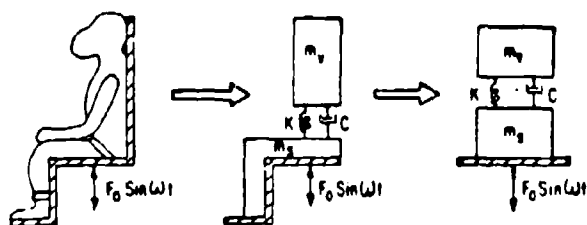


Fig. 1 Development of a single-degree-of-freedom model for impedance response of the restrained primate. From Broderson and Von Dierke (2)

vibration tests with Rhesus monkeys. The impedance modulus and phase angle equations for this model can be shown to be (12):

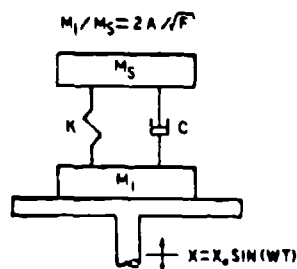
$$Z = \frac{[(1+r)^2(k^2 + c^2\omega^4) + r\omega^2(2km_1(1+r) - m_1^2\omega^2)]^{1/2}}{k^2 + \omega^2(m_1^2\omega^2 + c^2 - 2km_1)} \quad (3)$$

$$\phi = \tan^{-1} \left[ \frac{(1+r)(c^2\omega^2 + k^2) + m_1\omega^2(m_1\omega^2 - k(1+r))}{cm_1\omega^3} \right] \quad (4)$$

where  $r = m_1/m_2$ , the ratio of "inert" to "sprung" mass.

The development of equations (3) and (4) require that  $k$  and  $c$  be independent of amplitude, but permit a nonlinear frequency dependence. A nonlinear variation of  $k$  and  $c$  with frequency would imply that system strain is sensitive to the rate of loading. While such a response is not uncommon for biological materials, a frequency dependence of  $k$  and  $c$  may depend, in part, on the nature of the model itself.

The function,  $r$ , is expected to vary with both frequency and acceleration amplitude. Body subsystems may well be amplitude restricted relative to whole-body motion, i.e., the displacement of some subsystems are limited by the presence of other body components. Subsystems which reach their relative displacement limits will tend to increase the inert mass response of the total system as acceleration amplitude is further increased; however, amplitudes in excess of 1.0 g may well result in a more complicated amplitude dependence of  $r$ . At constant acceleration amplitude, whole-body response is typically characterized (2-8) as having a relatively large inert mass component at low frequencies, while an increased damping response at higher frequencies indicates a relative decrease in the inert mass component. The ratio,  $r$ , might then be expected to increase with increased acceleration ampli-



$$\begin{aligned} k/\omega &= 0.134 + 0.543F : 2 \leq F \leq 5 : C/\omega = -0.045 + 0.024F \\ &2.54 + 0.062F : 5 \leq F \leq 10 : 0.16 - 0.004F \\ &-1.15 + 0.431F : 10 \leq F \leq 30 : 0.0433 + 0.00125F \end{aligned}$$

Fig. 2 A two-mass, single-degree-of-freedom model for impedance response of the sitting, restrained primate

tude and decreasing frequency.

By requiring that  $k$  and  $c$  be independent of amplitude, the amplitude dependence of  $r$  can be determined from impedance data obtained for various amplitudes at constant frequency. Successive iterations at each frequency resulted in an expression for  $r$  in the form

$$r = \frac{2A}{\sqrt{f}} \quad (5)$$

where  $A$  is the acceleration amplitude expressed in units of  $g$ .

Equations (3), (4), and (5) define the vibration response of the two-mass model. The experiments and results discussed in the following sections (a) establish the experimental impedance response of the Rhesus monkey vibrated from 2 to 30 Hz at 0.5 and 1.0 g acceleration amplitudes, (b) establish, based upon the model just presented, whole-body elastic and damping coefficients as a function of frequency, and (c) compare the response of the model to that experimentally measured.

## METHODS

The Wenner-Gren Research Laboratory's vertical electrohydraulic vibration exciter (13, 14) was utilized in this study. A force cell arrangement (12, 14) allowed direct recording of the force transmitted between vibration exciter and subject. Vibration exciter displacement and velocity were recorded from the output of rectilinear potentiometers attached to the exciter. By supplying vibration exciter velocity and net transmitted force to a phase angle meter, an analog signal was produced which was proportional to



Fig. 3 Primate positioned atop vertical vibration exciter

Table 1 Summary of Animals Tested and Vibration Parameters

ANIMAL (WEIGHT)	ACCELERATION AMPLITUDE	NUMBER OF EXPOSURES (Random Order) to: 2, 3, 4, 5, 6, 7, 8, 9, 10, 11, 12, 14, 16, 20, 30 Hz
A (25 lb.)	0.5 g	5
B (26 lb.)	0.5 g	5
C (10.5 lb.)	0.5 g	5
D (11.5 lb.)	0.5 g	5
C (10.5 lb.)	1.0 g	5
D (11.5 lb.)	1.0 g	5

the phase difference of the two input signals. Mechanical velocity impedance was thus obtained by continuously recording (a) net transmitted force, (b) vibration exciter velocity, and (c) the phase relationship between equations (1) and (2). Fig. 3 is a photograph of the experimental setup.

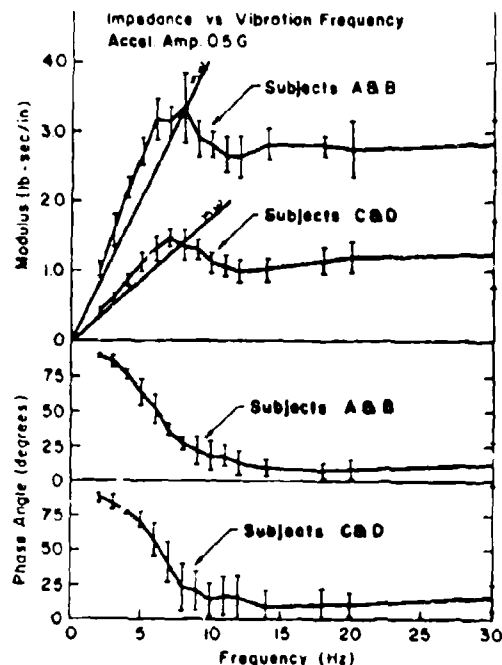


Fig. 4 Complex impedance versus frequency for 0.5-g vibration of primates A, B, C, and D

The primates were exposed to a series of frequencies (see Table 1), each at the same acceleration amplitude. Four animals were so tested five times each at an acceleration amplitude of 0.5 g. The two smaller animals (C and D) were then each tested five times at an acceleration amplitude of 1.0 g. An exposure duration of 30 sec at each condition was specified on the basis of previous tests which established 30 sec to be sufficient to obtain reliable results. Extended exposures also introduce temporal effects. Tests on any given animal were separated by at least one day.

The monkeys required no sedation or other medication for these experiments since they were well adapted to the experimental environment. In addition to daily handling, the subjects were previously submitted to repeated exposures of extended duration at all frequencies including 6-hr exposures at resonance. When placed in the impedance chair the animals were securely restrained by a lap belt and by belts around each ankle. The subject was restrained from bending by a rigid, metal neck piece which physically contacted the animal only if he attempted to bend out of the upright position.



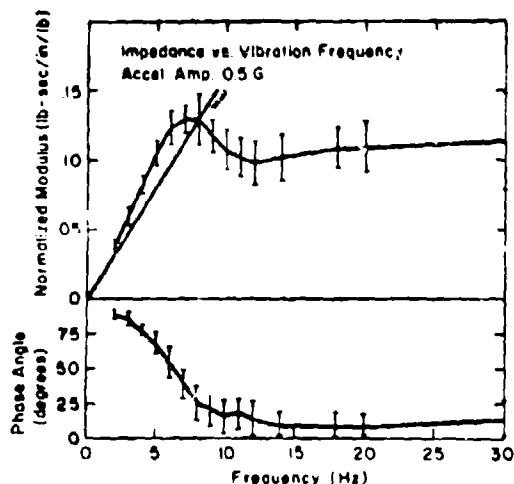


Fig. 5 Impedance phase angle and normalized modulus versus frequency for 0.5-g vibration of primates A, B, C, and D

## RESULTS

The complex impedance for the 0.5 g experiments is presented in Fig. 4 as a function of vibration frequency. The data from Subjects A (25 lb), and B (26 lb), are grouped together, as are those from Subjects C (10.5 lb), and D (11.5 lb), since the animals in each group differed in weight by only 1 lb; thus, two curves are shown for both impedance modulus and phase angle. Since each animal was tested five times at 0.5 g, each curve in this figure represents the mean of 10 tests. The limits shown correspond to the mean value plus or minus one standard deviation. The two straight lines designated as "mw" in the modulus graph correspond to the impedance magnitude of an "inert" mass of weight equal to that of the average for the subjects. A peak impedance occurs at 7 to 8 Hz for each group. At lesser frequencies the impedance moduli follow closely those of an inert mass of like weight. At frequencies immediately greater than those of the moduli peaks the impedance magnitudes decrease. From 12 to 30 Hz the moduli remain about constant. The phase angle curves are approximately 90 deg (the impedance phase angle of an inert mass) at 2 Hz, and then decrease rapidly in the "impedance moduli peak" region. Beyond about 10 Hz the curves are in the 10- to 20-deg range. This could indicate a predominant damping response since the impedance phase angle of a mass-less damper is 0 deg.

The moduli data shown in Fig. 4 were normalized by body weight and plotted in Fig. 5, versus vibration frequency. Since the phase

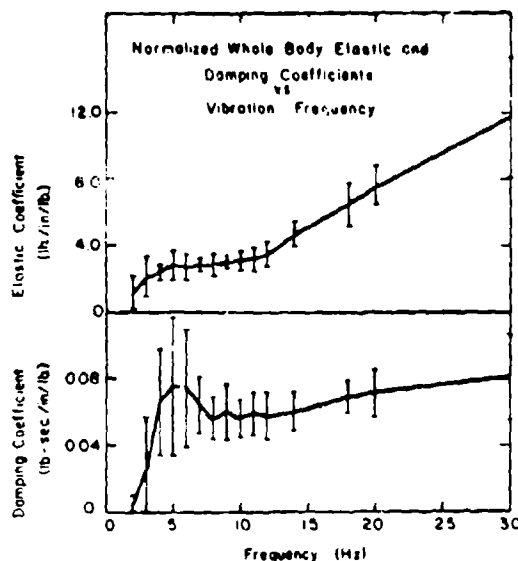


Fig. 6 Normalized whole body coefficients of elasticity and damping versus frequency for the sitting, restrained primate

angle curves as shown in Fig. 4 did not appreciably differ between the different size animals, these data, for each frequency, were combined without normalization. This figure thus represents the complex impedance response of any size Rhesus monkey, in the sitting position, when vibrated vertically at 0.5 g from 2 to 30 Hz.

The curves of Fig. 5 represent mean values as determined at each test frequency by twenty data points. For each frequency 20 complex impedance values were used in equations (3), (4), and (5) to solve for  $k$  and  $c$ . Therefore, for each of the 15 different test frequencies, 20 sets of  $k$  and  $c$  were determined. Each set represents the magnitude of elastic and damping coefficients which, when applied to the model of Fig. 2, resulted in a complex impedance response which matched that experimentally measured at that frequency. The average values of  $k$  and  $c$  thus determined at each test frequency are presented in Fig. 6. The mean elastic coefficient varies approximately directly with vibration frequency. On the other hand, the mean damping coefficients exhibit a curve which looks similar in shape to the impedance modulus plot of Fig. 5; however, the peak of the damping coefficient curve is at 5 Hz rather than at 7 to 8 Hz.

The curves of Fig. 6, along with equation (5), completely quantify the model presented in Fig. 2. For computational purposes, values of  $k$  and  $c$  from Fig. 6 were approximated by three linear segments, as defined in Fig. 2, for the 2-

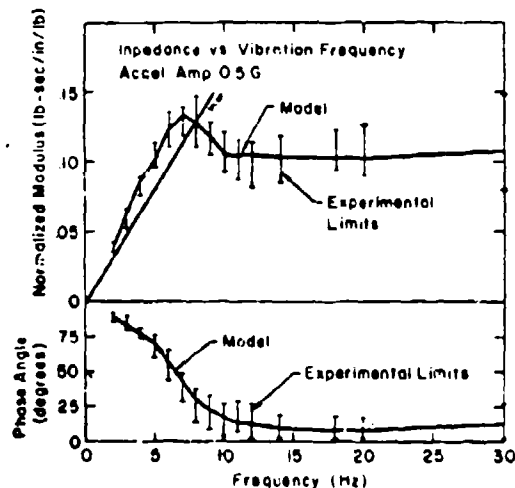


Fig. 7 Impedance phase angle and normalized modulus versus frequency for 0.5-g vibration of primates A, B, C, and D compared to that predicted by the model of Fig. 2

to 5-Hz, 5- to 10-Hz, and 10- to 30-Hz regions.

Complex impedance obtained from the model is compared in Fig. 7 with experimental results for an acceleration amplitude of 0.5 g. Inasmuch as these experimental data were used to obtain the frequency dependence of  $k$  and  $c$ , the excellent fit to the data verifies the validity of the computational procedures.

The generality of the model is demonstrated in Fig. 8, where the calculated impedance for 1.0 g acceleration amplitude is compared to the experimental results from Subjects C and D. The variation of the modulus as predicted by the model provides a very good approximation to the experimental results in both magnitude and shape. The impedance phase angle from the model generally falls within the experimentally measured limits for frequencies up to 14 Hz. For 14 to 30 Hz the phase angle predicted by the model is generally about 10 deg higher than the upper limit of the experimentally determined values.

## DISCUSSION

The object of this investigation was to establish experimentally the impedance response of the sitting Rhesus monkey during 0.5 and 1.0 g vibration at 2 to 30 Hz, and to develop a model which would predict an impedance closely matching that experimentally measured. The impedance response of the model (based upon the experimentally derived coefficients presented in Fig. 6) very closely matches that experimentally measured during 0.5 and 1.0 g vertical vibration (Figs.

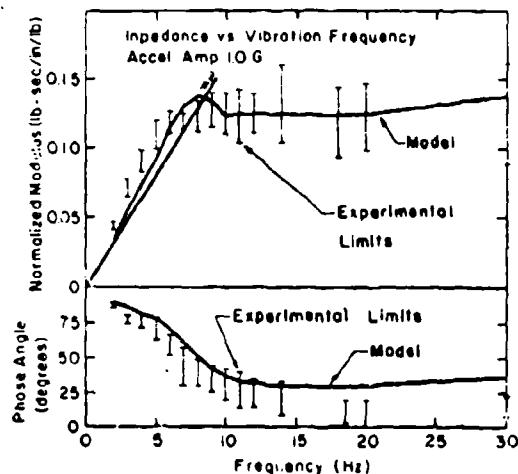


Fig. 8 Impedance phase angle and normalized modulus versus frequency for 1.0-g vibration of primates C and D compared to that predicted by the model of Fig. 2

7 and 8).

The model of Fig. 2 and its manner of derivation are somewhat novel. Although the model is composed of linear elements, the elastic and damping coefficients are defined to be functions of vibration frequency. In addition, the ratio of nonreactive (inert) to reactive mass in the model is defined to vary directly with input acceleration amplitude, and inversely with the square root of vibration frequency. Thus for any given acceleration intensity, most of the total mass is inert at the lower frequencies, and becomes more reactive, or "sprung," as frequency increases. This is consistent with previous experimental measurements which show the subject to exhibit a "mass-like" response at lower frequencies and a predominant damping response at higher frequencies. For any given frequency, increasing the acceleration amplitude increases the amount of inert, relative to total, mass. It is postulated that increasing the input intensity could cause "bottoming" of certain suspended internal organs (or "parts") and that such a system would thus respond in a more nonreactive manner at the higher intensities.

How well the model responds to input acceleration greater than 1.0 g remains to be established. It is interesting to compare the results of Broderson and Von Gierke (2) to those of the present investigation. A whole body elastic coefficient of 51.7 lb/in. and a whole body damping coefficient of 0.86 lb-sec/in. were reported for a 14.5 lb Rhesus monkey vibrated at 1.0 g. These figures were extracted by matching the equation

for impedance modulus from the model of Fig. 1 to that experimentally established during 8- and 12-Hz vibration. The model of the present study, as shown in Fig. 2, yields (for a 14.5 lb Rhesus) a damping coefficient of 0.812 lb-sec/in. and an elastic coefficient of 45.8 lb/in. (using a 10-Hz frequency). A favorable comparison, therefore, exists between these two models; however, that of the present investigation, being derived from both impedance modulus and phase angle data at each frequency during 0.5 g vibration, yields an exact match to the experimental data at 0.5 g, but more importantly, responds to changes in acceleration in a manner similar to those experimentally recorded.

Future experiments are now planned in which Rhesus monkeys will be vibrated at higher acceleration amplitudes for short periods of time at discrete frequencies from 2- to 30-Hz. Temporal effects due to extended vibration at given frequencies will also be determined, and hopefully incorporated into the model.

#### ACKNOWLEDGMENTS

This work was supported in part by the United States Air Force, 6570 Aerospace Medical Research Laboratories, Aerospace Medical Division, United States Air Force, Wright-Patterson Air Force Base, under Contract No. F33615-72-C-1112, and by the United States Air Force Office of Scientific Research under Contract No. F33615-72-C-1112, and by the United States Air Force Office of Scientific Research under Contract No. P44620-62-C-0127.

#### REFERENCES

- 1 Ziegenrucker, O. H., and Magid, E. B., "Short Time Human Tolerance to Sinusoidal Vibration," AMRL-TR-59-391, Wright-Patterson Air Force Base, Ohio, 1959.
- 2 Coermann, R. R., "The Mechanical Impedance of the Human Body in Sitting and Standing Position at Low Frequencies," Human Factors, Vol. 4, 1962, pp. 227-253.
- 3 Edwards, R. O., and Lange, K. O., "A Mechanical Impedance Investigation of Human Response to Vibration," AMRL-TR-64-91, Wright-Patterson Air Force Base, Ohio, 1964.
- 4 Lange, K. O., and Edwards, R. O., "Force Input and Thoraco-Abdominal Strain Resulting From Sinusoidal Motion Imposed on the Human Body," Journal of Aerospace Med., Vol. 41, No. 5, 1970, pp. 538-543.
- 5 Wittwer, A. L., "The Measurement of Mechanical Impedance of the Body of Man," Master's Thesis, University of Kentucky, Lexington, 1958.
- 6 Krause, H. E., and Lange, K. O., "Non-linear Behavior of Bio-Mechanical Systems," ASME Paper No. 63-WA-278, 1963.
- 7 Von Gierke, H. E., ed., "Symposium on Biodynamic Models and their Applications," AMRL-TR-71-29, Wright-Patterson Air Force Base, Ohio, 1971.
- 8 Weis, E. B., Jr., Clarke, N. P., and Von Gierke, H. E., "Mechanical Impedance as a Tool in Biomechanics," ASME Paper No. 63-WA-280, 1963.
- 9 Broderick, A. B., and Von Gierke, H. E., "Mechanical Impedance and Its Variation in the Restrained Primate During Prolonged Vibration," ASME Paper No. 71-WA/BHF-8, 1971.
- 10 Edwards, R. O., and Knapp, C. F., "Changes in Whole Body Force Transmission of Dogs Exposed Repeatedly to Vibration," ASME Paper No. 72-WA/BHF-11, 1972.
- 11 Edwards, R. O., McCutcheon, E. P., and Knapp, C. F., "Cardiovascular Changes Produced by Brief Whole Body Vibration of Animals," Journal of Applied Physiology, Vol. 32, No. 3, 1972, pp. 386-390.
- 12 Lafferty, J. F., et al., "A Standard Psychophysiological Preparation for Evaluating the Effects of Environmental Vibration Stress. Phase I: Development," AMRL-TR-72-112, Wright-Patterson Air Force Base, Ohio, 1972.
- 13 Vaught, E. W., "An Electro Hydraulic Vibration Exciting System," Master's Thesis, University of Kentucky, Lexington, 1963.
- 14 Sharp, T. D., "A Live Load Force Table," Proceedings of the Institute of Environmental Sciences, 1963, pp. 139-144.

ANALOG COMPUTER SIMULATION OF THE RESPONSE OF THE  
CIRCULATORY SYSTEM TO WHOLE-BODY ACCELERATIONS

By

Roger Lee Starnes

---

(Director of Thesis)

---

(Director of Graduate Study)

---

(Date)

## ABSTRACT OF THESIS

### ANALOG COMPUTER SIMULATION OF THE RESPONSE OF THE CIRCULATORY SYSTEM TO WHOLE-BODY ACCELERATIONS

The closed-loop response of the human circulatory system to whole-body acceleration patterns of both constant and time-varying periodic forms was simulated in this study. Tilt responses of the developed model were first determined. In a head-up tilt cardiac output decreased, and in a head-down tilt it increased. Then, various types of time-varying acceleration patterns with zero average value were applied to the model in a nonsynchronous manner (acceleration cycle was independent of the heart cycle). For sinusoidal acceleration patterns the model's aortic pressure and flow responses exhibited resonance in the 2 - 6 Hz frequency range, as has been observed experimentally; with 3 G peak acceleration in this frequency range, peak left ventricular ejection flow rate increased 75%, aortic pulse pressure increased 330%, and stroke volume, on a per-cycle basis, increased over 40%. However, cardiac output was not changed under any applied acceleration pattern with zero average value, although it was changed with asymmetrical time-varying patterns (time-varying patterns of zero average value combined with a tilt). Time-varying acceleration patterns were also applied in a synchronous manner. It was found that model responses effected by nonsynchronous accelerations producing long beat patterns could be reproduced synchronously.

---

Roger Lee Starnes

---

Date

## ACKNOWLEDGEMENTS

The author expresses deepest appreciation for the help and guidance provided by Drs. Jerry C. Collins of the Department of Electrical Engineering and Charles F. Knapp of the University of Kentucky Wenner-Gren Research Laboratory and Department of Mechanical Engineering. Their patience was unlimited. The encouragement of Mr. Philip Camill, Jr. in the undertaking of this project is appreciated. Special thanks are given to Dr. Ernest P. McCutcheon of the Department of Physiology and Biophysics, Dr. Richard G. Edwards of the Wenner- Gren Laboratory, and Dr. Don J. Wood of the Department of Civil Engineering for their helpful comments. The aid of Mr. Jack W. McKnight, Electrical Engineering undergraduate, and Mr. P. C. Magoun, Electrical Engineering Laboratory Supervisor, is appreciated. Thanks are given to Miss Charlotte A. Combs for her patience in typing this thesis. The financial aid provided by the United States Air Force under Contract No. F44620-69-C-0127 and presented through the University of Kentucky as a Research Assistantship is gratefully acknowledged.

## TABLE OF CONTENTS

	Page
Acknowledgements	
List of Illustrations	
List of Tables	
Chapter I. Introduction	1
Chapter II. Development of the Model	
Heart and Pulmonary Section	4
Arterial Section	4
Venous Sections	5
Chapter III. Results of Simulating Circulatory Responses to Accelerations	
Constant Accelerations	17
Nonsynchronous Time-varying Accelerations	25
Synchronous Time-varying Accelerations	34
Chapter IV. Discussion and Conclusions	
Constant Accelerations	40
Time-varying Accelerations	45
Variation of Model Parameters	50
Conclusions	51
Recommendations for Improvement of Model	53

	Page
Appendix A	55
Appendix B	57
Bibliography	61



## LIST OF ILLUSTRATIONS

	Page
1A. Area vs. Pressure for a Segment of Vein <sup>14</sup> .	7
1B. Volume vs. Pressure for Upper Venous System Model.	7
2. Analog Diagram of Piecewise-linear Venous Flow Equation with Nonlinear Flow Resistance.	7
3. Nonlinear Venous Flow Resistance.	7
4. Composite Electrical Equivalent Diagram.	10
5. Analog Diagram of Arterial and Venous Sections of the Model.	13
6. Analog Diagram of Heart-lung Section of Model.	14
7. Response of Model to Zero Acceleration: Typical Simulated Pressures, Flows, and Volume.	18
8. Typical Waveforms Associated with the Heart <sup>6</sup> .	21
9. Response of Model to Simulated Head-up Tilt.	22
10. Response of Model to Simulated Head-down Tilt.	23
11A. Typical Response of Model to Simulated Nonsynchronous 2 G, 1.25 Hz Sinusoidal Acceleration.	26
11B. Selected Portion within Beat Pattern of Fig. 11A.	27
12A. Typical Response of Model to Simulated Nonsynchronous 3 G, 3 Hz Sinusoidal Acceleration.	29
12B. Examples of Recordings of Arterial Pressure and Aortic Flow from a Dog, at rest and under 3 G Vibration at 3 Hz <sup>9</sup> .	30

	Page
13A. Simulated $\Delta P_{MAX}$ vs. Normalized Acceleration Frequency with Acceleration Amplitude as a Parameter.	31
13B. Simulated $Q_{MAX}$ and $Q_{MIN}$ vs. Normalized Acceleration Frequency with Acceleration Amplitude as a Parameter.	32
13C. Simulated $SV_{MAX}$ and $SV_{MIN}$ vs. Normalized Acceleration Frequency with Acceleration Amplitude as a Parameter.	33
14. Response of Model to Simulated Nonsynchronous Asymmetric Acceleration.	35
15. Response of Model to Synchronous 2 G, 1.25 Hz Sinusoidal Acceleration with $t_D = 0$ Milliseconds.	36
16. Simulated Stroke Volume (Normalized) for 1 and 2 G Synchronous Sinusoidal Accelerations of 1.25 Hz Applied at Various Values of $t_D$ .	38
17. Response of Model to a Simulated Synchronous Asymmetric Acceleration Pattern with $t_D = 760$ Milliseconds.	39
18. Simulations of Ventricular Contractions in the Model.	52
19A. Axial Acceleration of a Rigid Tube Containing a Newtonian Fluid with Direction of Acceleration the Same as that of the Original Fluid Acceleration.	58
19B. Axial Acceleration of a Rigid Tube Containing a Newtonian Fluid with Direction of Acceleration Opposite that of the Original Fluid Acceleration.	58

## LIST OF TABLES

Table		Page
1	Parameters of the Model	11
2	Analog Potentiometer Settings and Their Corresponding Parameters	15
3	Volume Distribution of the Model	20

## CHAPTER I

### INTRODUCTION

It has become evident that acceleratory stresses imposed on man in many of his modern environments can have substantial effects on cardiovascular function. Investigators have been exploring these effects for some time. The first studies in cardiovascular response to whole-body accelerations dealt primarily with arterial responses to constant acceleration patterns, such as those produced by centrifuges. Later, arterial and venous responses were examined for prolonged constant acceleration patterns, as well as for constant patterns of shorter duration. Thus, the importance of certain time parameters of whole-body acceleration, such as rate of onset of acceleration, duration of acceleration, etc., became apparent, and time-varying accelerations of various forms were imposed upon the cardiovascular system<sup>10</sup>. More recently, the effects on the cardiovascular system of time-varying accelerations of periodic nature have been investigated<sup>9,13</sup>. These studies have shown that certain patterns of whole-body acceleration can produce profound changes in the circulation. For example, some patterns present stresses to the cardiovascular system which can drastically reduce stroke volume, whereas other patterns may be used to assist a

failing heart by increasing cardiac output. Primary emphasis in these studies has been given to arterial responses. However, the earlier constant-acceleration studies suggest that venous responses are also an important part of the total cardiovascular response to whole-body accelerations.

The purpose of this study was to analyze human cardiovascular response to whole-body 2-axis accelerations by means of a closed-loop analog computer simulation. The responses to both constant and time-varying periodic acceleration patterns were studied.

## CHAPTER II

### DEVELOPMENT OF THE MODEL

The systemic circulation involves the movement of blood through the left heart and high-pressure arterial system to the microcirculation and the return of the blood from the microcirculation into the right heart through the low-pressure venous system. The pulmonary circulation returns the blood from the right heart to the left heart. The arterial system has been studied extensively, and many arterial models, some modified to account for whole-body accelerations, have been developed<sup>6,15,19</sup>. Although some venous studies have been made<sup>17</sup>, understanding of the role of the venous system in cardiovascular response to whole-body accelerations is not nearly as advanced.

The divisions into which the circulatory system has been separated in this study and their abbreviations, also used as subscripts, are listed below (see Fig. 4):

#### A. Heart and Pulmonary Section

1. Right Ventricle (RV)
2. Lungs (LG)
3. Left Ventricle (LV)

#### B. Arterial Sections

1. Aortic Arch (AA)
2. Upper Arterial System (UAS)

3. Lower Arterial System (LAS)

4. Upper Capillary Bed (UCB)

5. Lower Capillary Bed (LCB)

C. Venous Sections

1. Upper Venous System (UVS)

2. Lower Venous System (LVS)

3. Right Atrium-Venae Cavae  
Junction (RA')

Heart and Pulmonary Section

The equations describing flow through the heart and lung sections are similar to those used in an earlier open-loop model<sup>6</sup>. Contractions of the ventricular sections were achieved by means of time-varying inverse compliances consisting of biased rectified sinusoids operating at 1.25 Hz (75 beats/minute). The pulmonary section was modeled as a linearly compliant element; its resistance was included with the ventricular valve resistances.

Arterial Sections

The equations describing flow through the upper and lower arterial sections are similar to those used in an earlier model<sup>6</sup>. The equations for flow through the aortic arch section have the same form as RLC L-section equations with the compliance parameter divided between the ends of the section.

The equivalent heights<sup>[1]</sup> determined by Camill<sup>6</sup> for the upper and lower arterial systems of standing man were modified by the inclusion of the ascending aortic arch section. This section's equivalent height of 7.6 cm reduced the equivalent height of the upper arterial system to 29.7 cm and increased the equivalent height of the lower arterial section to 50.3 cm.

The capillary beds were represented as resistive elements in the model.

#### Venous Sections

There are several venous system characteristics and external mechanisms which affect venous system function. One outstanding feature is the nonlinear pressure-volume characteristic, which enables the venous system to contain a large volume of blood at a relatively low pressure without being excessively compliant. These large volumes become especially important when whole-body accelerations are imposed since accelerations tend to produce volume shifts in the circulation<sup>10</sup>.

An empirical pressure-area relationship for a segment of vein is shown in Fig. 1A<sup>14</sup>. Assuming volume is proportional to area, the

---

[1] By "height" is meant the difference in elevation of the two ends of a length of artery in an applied gravitational field. The "equivalent height" of a composite section representing branching flow raised to different heights has been shown to be the average height of the branches weighted as their flow rates<sup>6,10</sup>.



slope of this curve represents the compliance of a venous segment. In the model an approximation to this compliance curve was used to represent the composite compliance of the venules and small veins in the upper venous system as shown in Fig. 1B and described by the following equation:

$$P_{UVS} = \frac{V_{UVS} - V_{0UVS}}{C_{UVS}} \quad (II-1)$$

where  $V_0$  represents the total unstressed volume of the system, or the volume at which the compliance changes value (see Appendix A). The composite compliance of the lower venous system was represented likewise.

A second very important characteristic of the venous system is venous valves. When accelerations which tend to reverse flow are applied, the valves close and substantially impede backflow, thus partially preventing venous pooling in the extremities. Physically, these valves are located in some but not all of the venules, small veins, and large veins. These valves were modeled by incorporating ideal valve models (ideal diodes) in the sections representing equivalent venous flow (flow from the venules and small veins through the large veins to the region of the right atrium)<sup>8</sup>. The ideal valve models modify the flow equations, producing unidirectional flow towards the right heart:

$$\begin{aligned} Q_{UVS} &= \frac{1}{L_{UVS}} \int [P_{UVS} - P_{RA'} - Q_{UVS}R_{UVS}]dt, & Q'_{UVS} > 0 \\ Q_{UVS} &= 0 & , Q'_{UVS} \leq 0 \end{aligned} \quad (II-2)$$

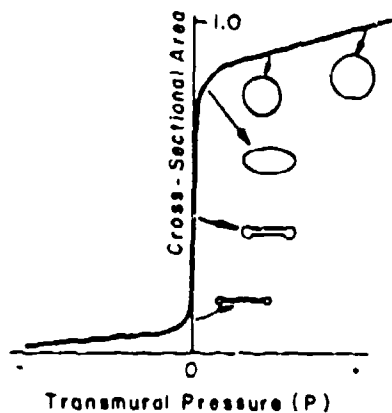


Figure 1A. Area vs. Pressure for a Segment of Vein<sup>14</sup>

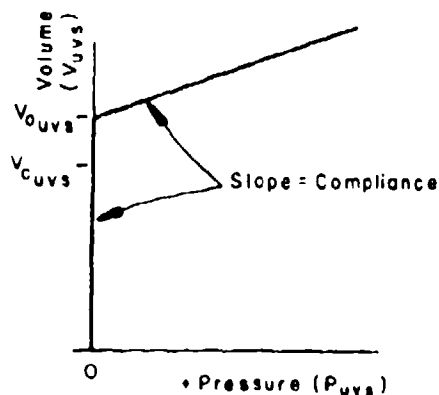


Figure 1B. Volume vs. Pressure for Upper Venous System Model

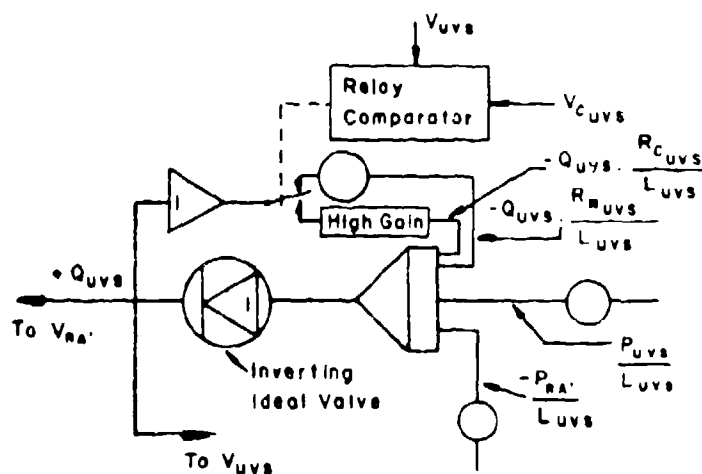


Figure 2. Analog Diagram of Piecewise-Linear Venous Flow Equation with Nonlinear Flow Resistance

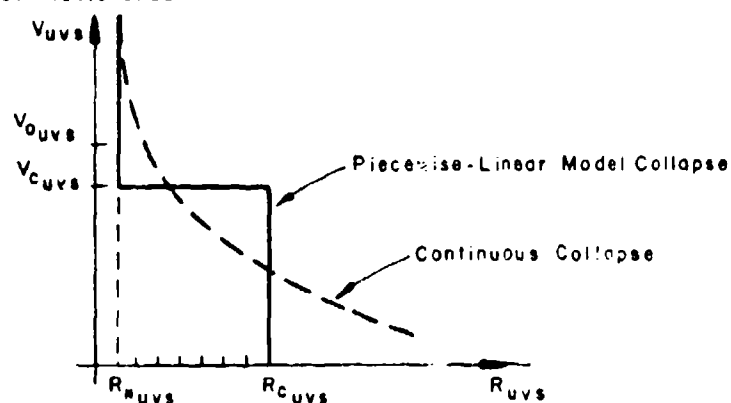


Figure 3. Nonlinear Venous Flow Resistance

where  $Q'_{UVS}$  represents bidirectional flow, which could occur during accelerations if no valves were present, and  $Q_{UVS}$  represents modified or physiological flow. The analog computer representation of this piecewise-linear equation is shown in Fig. 2. The position of the ideal valve in the circuit is at the end of the equivalent venous flow section distal to the heart. This positioning corresponds to the observation that no anatomical valves exist in the venae cavae near the heart.

The third mechanism which affects venous function is the ability of some of the large veins to collapse under low transmural pressures. Physiologically, this collapse phenomenon manifests itself as a partial collapse<sup>3,4</sup> occurring locally rather than throughout an entire vessel. Examples of this phenomenon include jugular collapse and partial superior vena cava collapse upon standing and collapse of abdominal and leg veins in the head-down position<sup>12</sup>. Therefore, this mechanism tends to prevent or delay large volume shifts due to acceleration of the blood in the large veins. In the model, changing the resistance of a venous flow section without changing its inertance, since both vary with volume or cross-sectional area, is analogous to local partial collapse. The resulting flow equation is of the same form as Eq. (II-2) with  $R_{UVS}$  nonlinear as shown in Figs. 2 and 3; this step increase in resistance is a piecewise approximation to the continuous collapse depicted in earlier models<sup>14,17</sup>. Flow in the lower venous system was modified similarly. (In Fig. 3  $R_N$  is the resistance for the case of no collapse,

or "normal" flow resistance, and  $R_C$  is the resistance during local partial collapse, which is produced by volume shifts due to acceleration. The volume at which local partial collapse is assumed to occur is  $V_C$  and is also shown in Fig. 1B.)

Although the external mechanism of muscle contractions and the presence of negative intrathoracic pressure and its variations produced by breathing affect venous function, these were not included in the model for the sake of simplicity.<sup>[1]</sup> However, they can be added if desired.

Since the heart, lungs, and capillary beds were assumed to have an equivalent height of zero, the equivalent heights determined by an earlier investigator<sup>6</sup> for the arterial system were used as the equivalent heights of the venous system; therefore,  $h_{UVS} = 37.3$  cm and  $h_{LVS} = 42.7$  cm, where  $h$  indicates equivalent height. Acceleratory stresses modified flow equations in those sections of the model which had non-zero equivalent height (see Appendix B).

The electrical equivalent circuit of the composite model is shown in Fig. 4, and the corresponding parameter values are given in Table 1. The polarities of the constant voltage sources in Fig. 4 represent a head-upward tilt; for a head-downward tilt the polarities are reversed. Time-varying accelerations with zero average value are

---

<sup>[1]</sup> These omissions imply that the extravascular pressure of the circulatory system is zero.

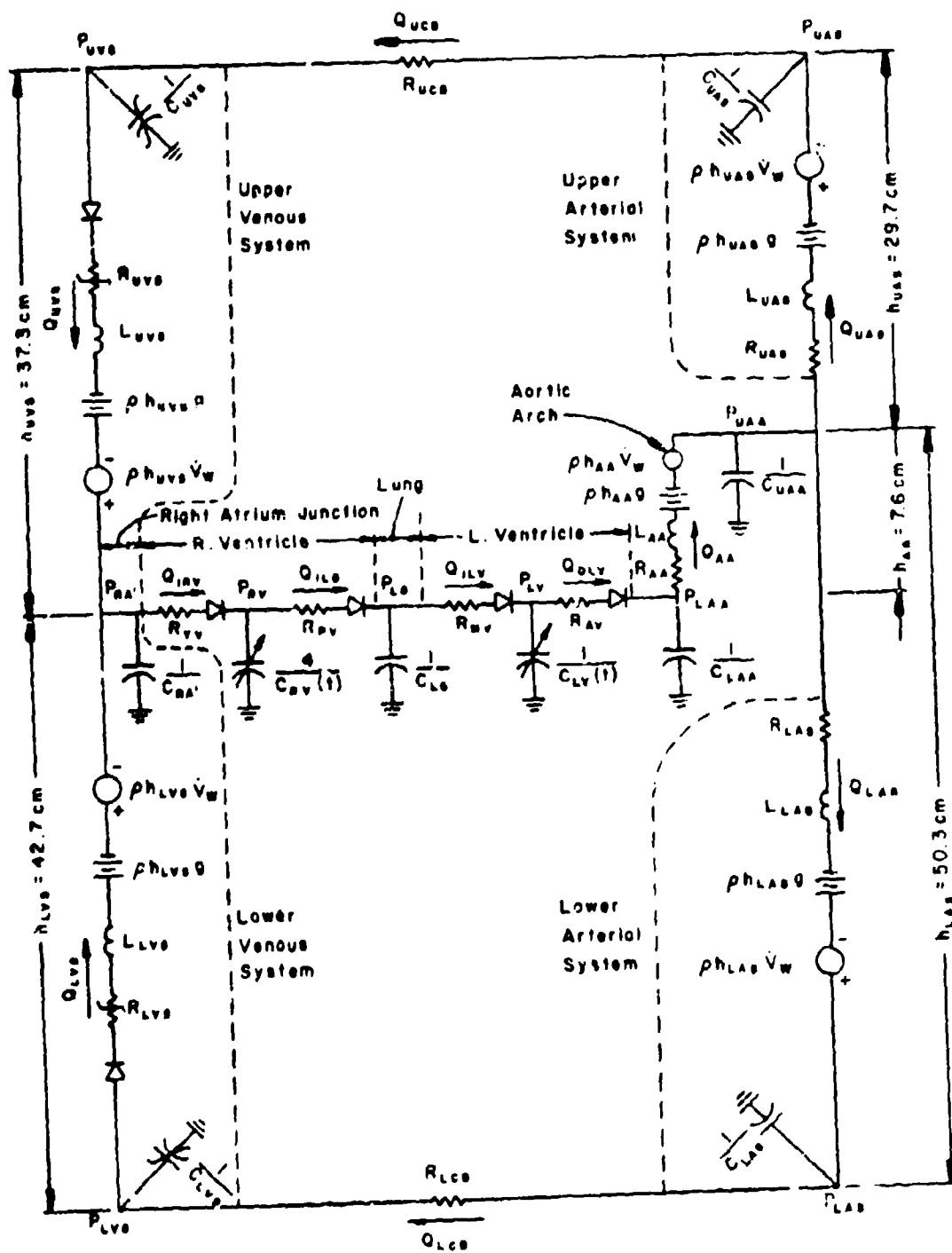


Figure 4. Composite Electrical Equivalent Diagram.

TABLE 1: Parameters of the Model

SECTION	RESISTANCE $\frac{\text{dyne-sec}}{\text{cm}^5}$	INERTANCE $\frac{\text{dyne-sec}^2}{\text{cm}^5}$	COMPLIANCE $\frac{\text{cm}^5}{\text{dyne}} \times 10^{-6}$	OTHER PARAMETERS
RV	$R_{TV} = 20;$ $R_{PV} = 10$			
LG			$C_{LG} = 60,000$	
LV	$R_{MV} = 10;$ $R_{AV} = 20$			
AA	$R_{AA} = 48.2$	$L_{AA} = 2$	$C_{LAA} = 600;$ $C_{UAA} = 600$	
UAS	$R_{UAS} = 241$	$L_{UAS} = 33$	$C_{UAS} = 316$	
LAS	$R_{LAS} = 52.5$	$L_{LAS} = 5.33$	$C_{UAS} = 552$	
UCB	$R_{UCB} = 4,000$			
LCB	$R_{LCB} = 1,400$			
UVS	$R_{N_{UVS}} = 510$ $R_{C_{UVS}} = 4,100$	$L_{UVS} = 13$	$C_{UVS} = 3,560^{[1]}$	$V_{O_{UVS}} = 474 \text{ cc}$ $V_{C_{UVS}} = 382 \text{ cc}$
LVS	$R_{N_{LVS}} = 710$ $R_{C_{LVS}} = 35,000$	$L_{LVS} = 35$	$C_{LVS} = 15,000^{[1]}$	$V_{O_{LVS}} = 2,060 \text{ cc}$ $V_{C_{LVS}} = 2,000 \text{ cc}$
RA'			$C_{RA'} = 9,360$	

[1] Value of finite compliance

represented by the sources  $ph\dot{V}_W$  (see Appendix B). The analog computer diagram of the composite model is shown in Figs. 5 and 6; the digital voltmeter readings of the coefficient potentiometers and the parameters represented by the corresponding potentiometer setting-amplifier gain products are given in Table 2. All pressures were scaled in mm Hg; all other variables were scaled in cgs units. The heart valves and their abbreviations are tricuspid valve (TV), mitral valve (MV), pulmonary valve (PV), and aortic valve (AV).







**Figure 6. Analog Diagram of Heart - Lung Section of Model.**

TABLE 2. Analog Potentiometer Settings and  
Their Corresponding Parameters.

<u>Pot No.</u>	<u>Pot Setting</u>	<u>Parameter Represented</u>
00	.666	$1/R_{PV}$
01	.532	$1/C_{RA} R_{TV}$
03	.500	$1/R_{TV}$
04	.157	$1/CLG$
05	.500	S.F.
06	.083	$1/C_{UAA} L_{AA}$
07	.505	$1/C_{UAA} L_{UAS}$
08	.314	$1/C_{UAA} L_{IAS}$
09	.141	Acceleration <sup>[1]</sup>
10	.820	$1/C_{RA} L_{UVS}$
11	.312	$1/C_{RA} L_{LVS}$
13	.919	Acceleration
14	.463	Acceleration
15	.063	$1/CLG$
16	.200	S.F.
17	.133	$1/R_{MV}$
18	.666	$1/R_{AV}$
19	.598	Acceleration
20	.083	$1/C_{LAA} R_{AV}$
21	.083	$1/CLAA L_{AA}$
22	.241	$R_{AA}/L_{AA}$
23	.186	Acceleration

<sup>[1]</sup> All acceleration potentiometer settings shown are for 1 G constant or peak acceleration.

TABLE 2 Continued

<u>Pot No.</u>	<u>Pot Setting</u>	<u>Parameter Represented</u>
24	.015	Blood Infusion <sup>[1]</sup>
31	.731	$R_{UAS}/L_{UAS}$
32	.950	$1/C_{UAS}$
33	.101	$1/L_{UAS}$
35	.084	$1/R_{UCB}$
36	.843	$1/C_{UVS}$ <sup>[2]</sup>
37	.256	$1/L_{UVS}$
38	.392	$R_{N_{UVS}}/L_{UVS}$
39	.199	$V_{O_{UVS}}$
40	.190	$V_{O_{LVS}}$
41	.100	$V_{C_{LVS}}$
42	.315	$R_{C_{UVS}}/L_{UVS}$
44	.191	$V_{C_{UVS}}$
46	.985	$R_{LAS}/L_{LAC}$
47	.544	$1/C_{LAS}$
48	.625	$1/L_{LAS}$
50	.238	$1/R_{LCB}$ <sup>[2]</sup>
51	.184	$1/C_{LVS}$
52	.951	$1/L_{LVS}$
53	.203	$R_{N_{LVS}}/L_{LVS}$
54	.028	I.C.

[1] Potentiometer 24 was used to produce a constant signal which was presented to a volume integrator for a sufficient period of time to build up blood volume in the system. Potentiometer 54 was used to set volume integrator initial conditions so that overloads would not occur before the system reached a steady state. Together, these potentiometers established a total system volume of 4,800 cc.

[2] This potentiometer represents the finite compliance of the corresponding venous system.

## CHAPTER III

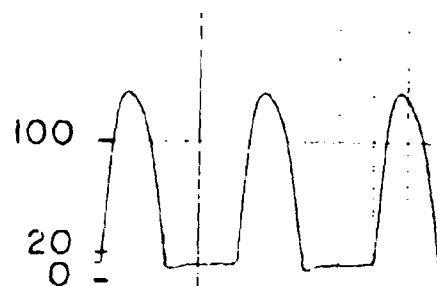
### RESULTS OF SIMULATING CIRCULATORY RESPONSES TO ACCELERATIONS

#### Constant Accelerations

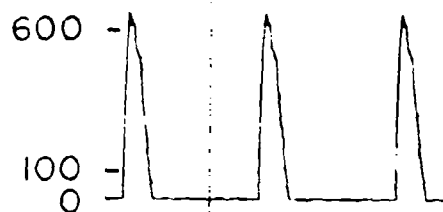
The model's response to zero acceleration, simulating man in the prone or supine position (all the blood vessels are assumed to lie in the horizontal plane), is shown in Fig. 7. Only those variables of the model which have a physiological counterpart are shown. On the arterial side these are left ventricular pressure ( $P_{LV}$ ), ejection flow out of the left ventricle ( $Q_{OLV}$ ), pressure in the lower aortic arch ( $P_{LAA}$ ), volume of the left ventricle ( $V_{LV}$ )<sup>[1]</sup>, flow through the aortic arch ( $Q_{AA}$ ), and pressure in the upper aortic arch ( $P_{UAA}$ ). The simulated pressure  $P_{LAA}$  corresponds to aortic pressure just outside the left ventricle;  $P_{UAA}$  corresponds to aortic pressure at the junction of the aorta and the carotid and subclavian arteries. On the venous side the variables shown are pressure outside the right ventricle or composite pressure of the right atrium and large veins ( $P_{RA}$ ), flow into the right ventricle ( $Q_{RV}$ ), and pressure in the right ventricle ( $P_{RV}$ ).

[1] In the model  $V_{LV} = \int (Q_{ILV} - Q_{OLV})dt = \int Q_{ILV}dt - \int Q_{OLV}dt$ , where  $Q_{ILV}$  is flow into the left ventricle and the last integral represents stroke volume (SV); since  $Q_{ILV}$  and  $Q_{OLV}$  always occurred in different portions of the heart cycle, the value of SV is the absolute difference between end-diastolic  $V_{LV}$  and end-systolic  $V_{LV}$ .

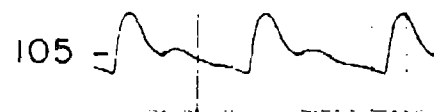
Left Ventricular  
Pressure (mm Hg)



Left Ventricular  
Ejection Flow (cc/sec)



Lower Aortic Arch  
Pressure (mm Hg)



Left Ventricular  
Volume (cc)

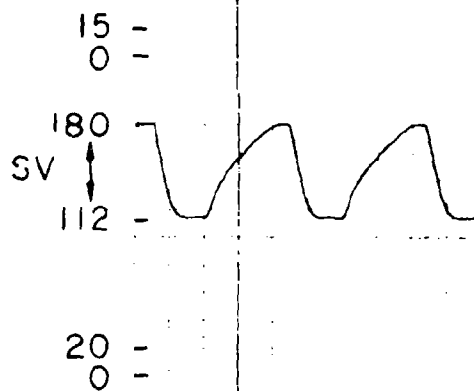


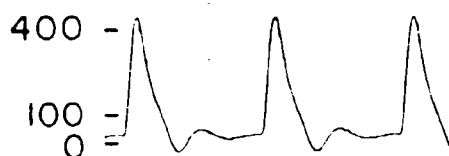
Figure 7. Response of Model to Zero Acceleration:  
Typical Simulated Pressures, Flows, and  
Volume.

Upper Aortic Arch  
Pressure (mm Hg)



15 -  
0 -

Aortic Arch  
Flow (cc/sec)

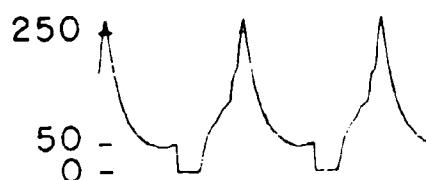


Right Atrial  
Pressure (mm Hg)



3 -  
0 -

Right Ventricular  
Inflow (cc/sec)



Right Ventricular  
Pressure (mm Hg)

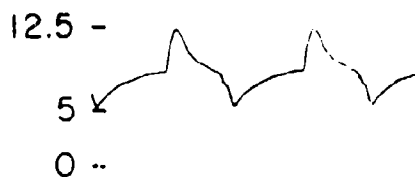


Figure 7. Continued

Some of the physiological counterparts of these variables are shown in Fig. 8.

Model responses to zero acceleration which are not shown are pressures and flows in the upper and lower arterial and venous systems and in the lung section. The upper and lower arterial systems' pressures and flows were similar in detail to those generated by an earlier, open-loop model<sup>6</sup>.

The volume distribution throughout the model with zero acceleration is shown in the following table:

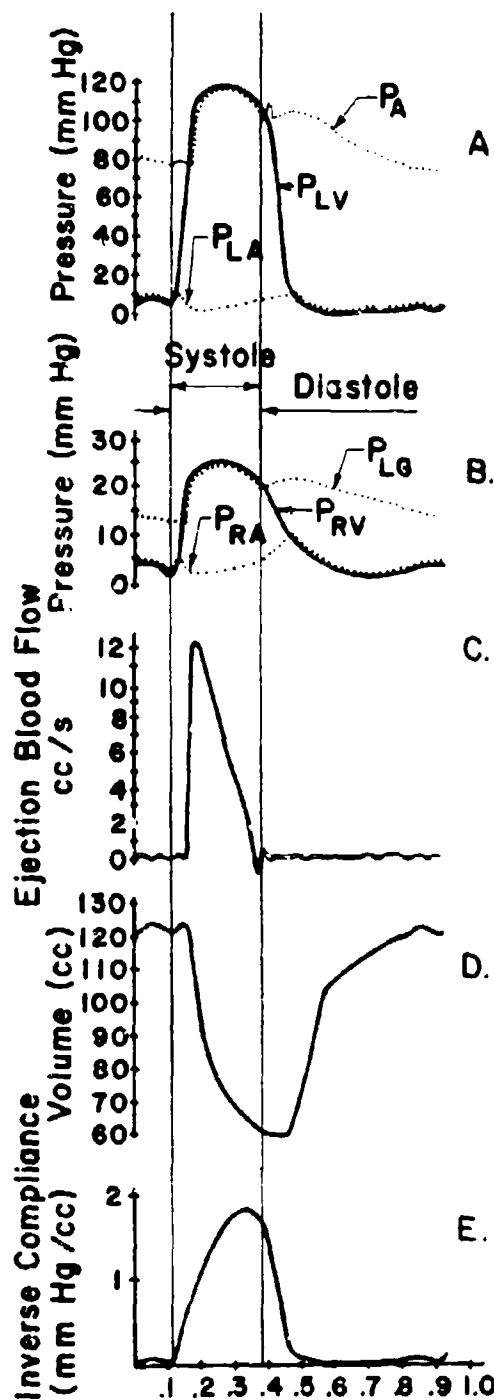
TABLE 3. Volume Distribution of the Model

<u>Venous Sections</u>		<u>Thoracic Sections</u>		<u>Arterial Sections</u>	
UVS	580 cc	RV	50 cc	LAA	81 cc
RA'	120 cc	LC	620 cc	UAA	81 cc
LVS	3,000 cc	LV	144 cc	UAS	40 cc
				LAS	71 cc

The total system volume was approximately 4,800 cc.

The model's response to positive 1 G acceleration, simulating a head-up tilt, is shown in Fig. 9. Response of the model to negative 1 G acceleration, simulating a head-down tilt, is shown in Fig. 10.

For a simulated head-up tilt, lung, ventricular, and upper venous system volumes decreased, and lower venous system volume increased. The volume changes were quantitatively similar to those observed experimentally in man<sup>11</sup>. These effects were reversed in a simulated head-down



A. Pressures in Left Heart  
(Berne and Levy "Cardiovascular Physiology"  
Mosby Co. 1967)

B. Pressures in Right Heart

C. Ejection Flow From the  
Left Ventricle (Berne and  
Levy "Cardiovascular  
Physiology" Mosby Co.  
1967)

D. Heart Volume (Berne and  
Levy "Cardiovascular  
Physiology" Mosby Co.  
1967)

E. Inverse Compliance of the  
Heart

Figure 8. Typical Waveforms Associated with the  
Heart<sup>6</sup>.



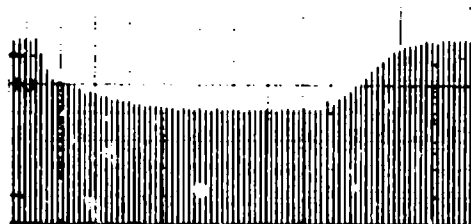
Left Ventricular  
Pressure (mm Hg)

100  
20  
0



Left Ventricular  
Ejection Flow  
(cc/sec)

600  
100  
0



Lower Aortic Arch  
Pressure (mm Hg)

90  
30  
0



Left Ventricular  
Volume (cc)

180  
112



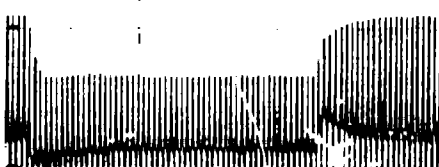
Right Atrial  
Pressure (mm Hg)

20  
0  
9  
3  
0



Right Ventricular  
Inflow (cc/sec)

250  
50  
0



Acceleration (G's)

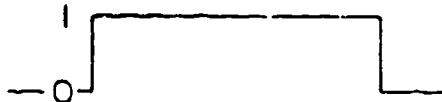


Figure 9 Response of Model to Simulated Head-Up Tilt.

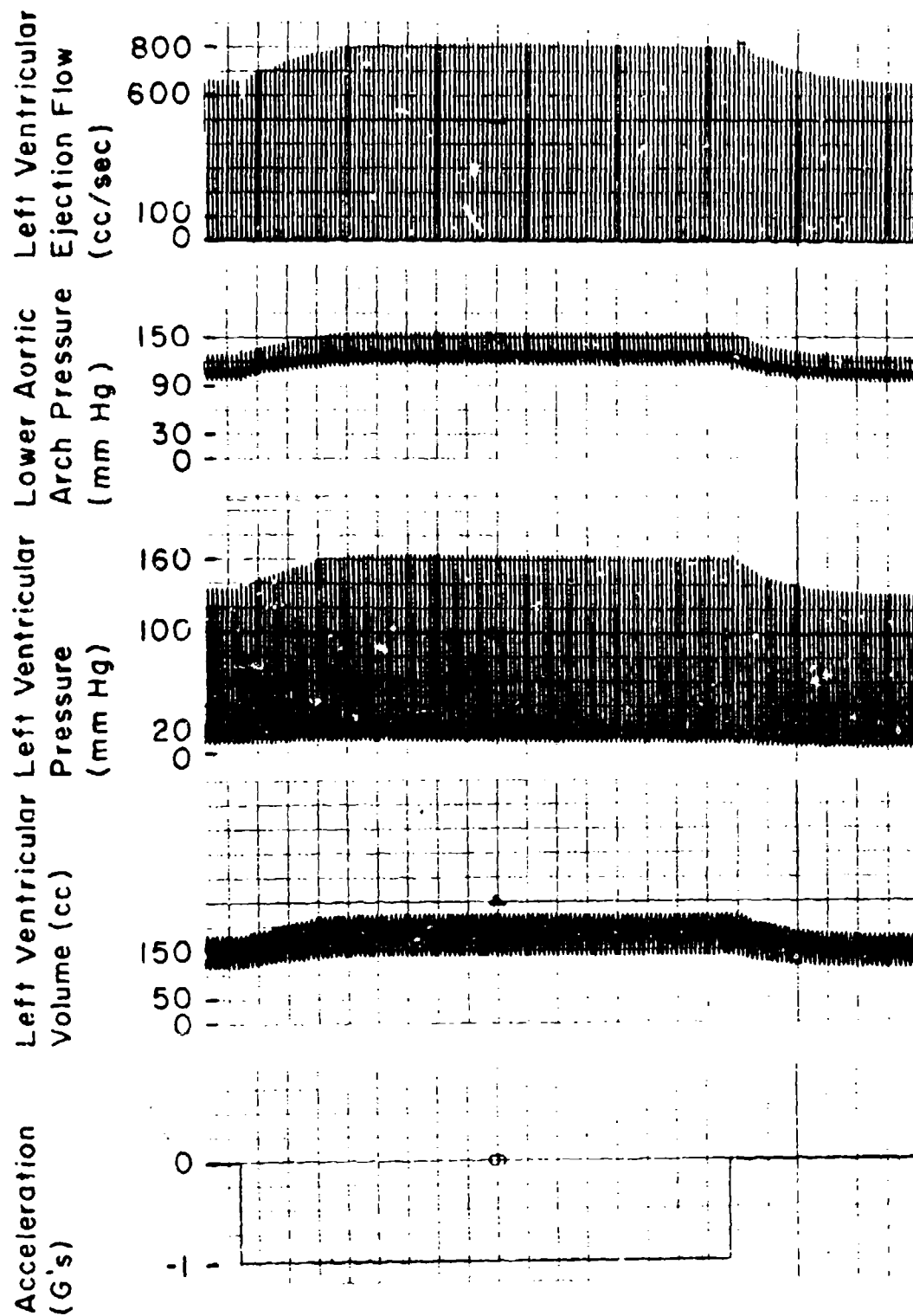
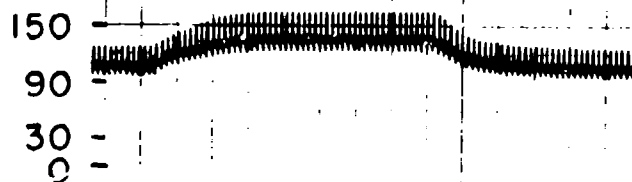


Figure 10. Response of Model to Simulated Head-Down Tilt.

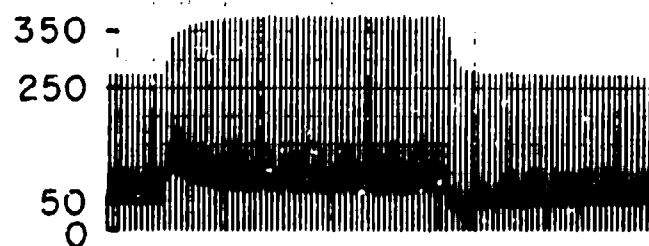
Lower Aortic Arch  
Pressure (mm Hg)



Right Atrial  
Pressure (mm Hg)



Right Ventricular  
Inflow (cc/sec)



Acceleration (G's)



Figure 10. Continued

tilt. In the head-up tilt collapse of the upper venous segment between UVS and RA' did occur and  $Q_{UVS}$  was altered accordingly; however, in the head-down tilt collapse of the lower venous segment between LVS and RA' did not occur.

#### Nonsynchronous Time-varying Accelerations

Time-varying accelerations of periodic nature were applied to the model in a nonsynchronous manner. Nonsynchronous accelerations are those which are applied in a continuous mode--the acceleration pattern is not related to the heart cycle. This situation of two independent oscillators was characterized by the production of beat patterns<sup>[1]</sup> in the flows and pressures in the model.

A typical response of the model to nonsynchronous time-varying acceleration producing long beat patterns is shown in Fig. 11A, where the acceleration pattern is sinusoidal with a peak amplitude of 2 G and a frequency of nearly 1.25 Hz. Figure 11B shows a selected portion of Fig. 11A recorded at a faster chart speed.

A typical response of the model to nonsynchronous time-varying acceleration producing short beat patterns is shown in Fig. 12A, where

---

[1] The period of a beat pattern is the length of time required for a nonsynchronous periodic acceleration pattern to "drift through" the heart cycle so that its occurrence, or timing, in a particular heart cycle is similar to that in an earlier cycle. This timing can be indicated by defining a parameter  $t_D$  as the time delay in milliseconds between the positive zero crossing of acceleration and the initial rise in the inverse compliance curve or pressure of the left ventricle.

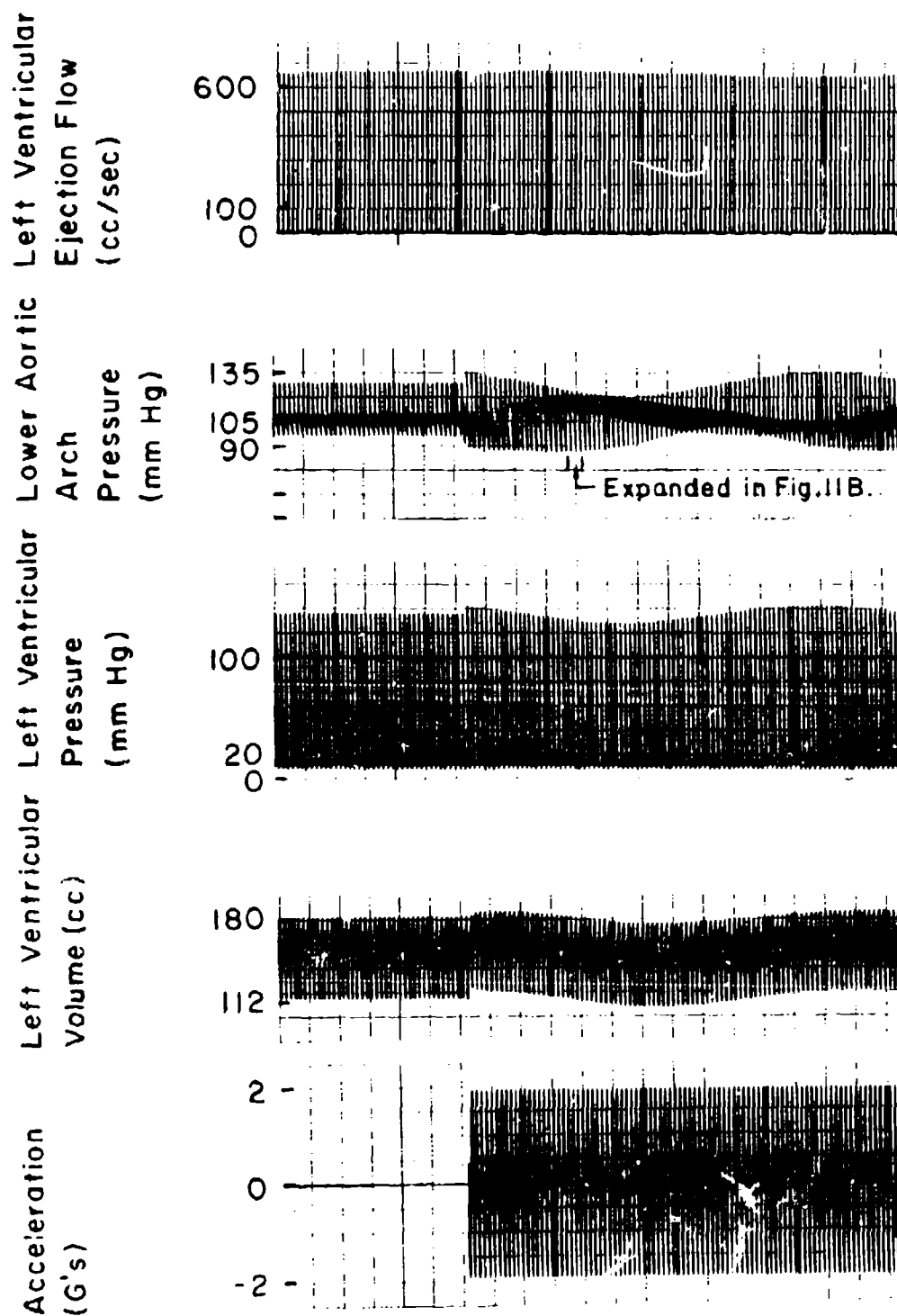


Figure IIA. Typical Response of Model to Simulated Non-synchronous 2G, 1.25Hz Sinusoidal Acceleration.

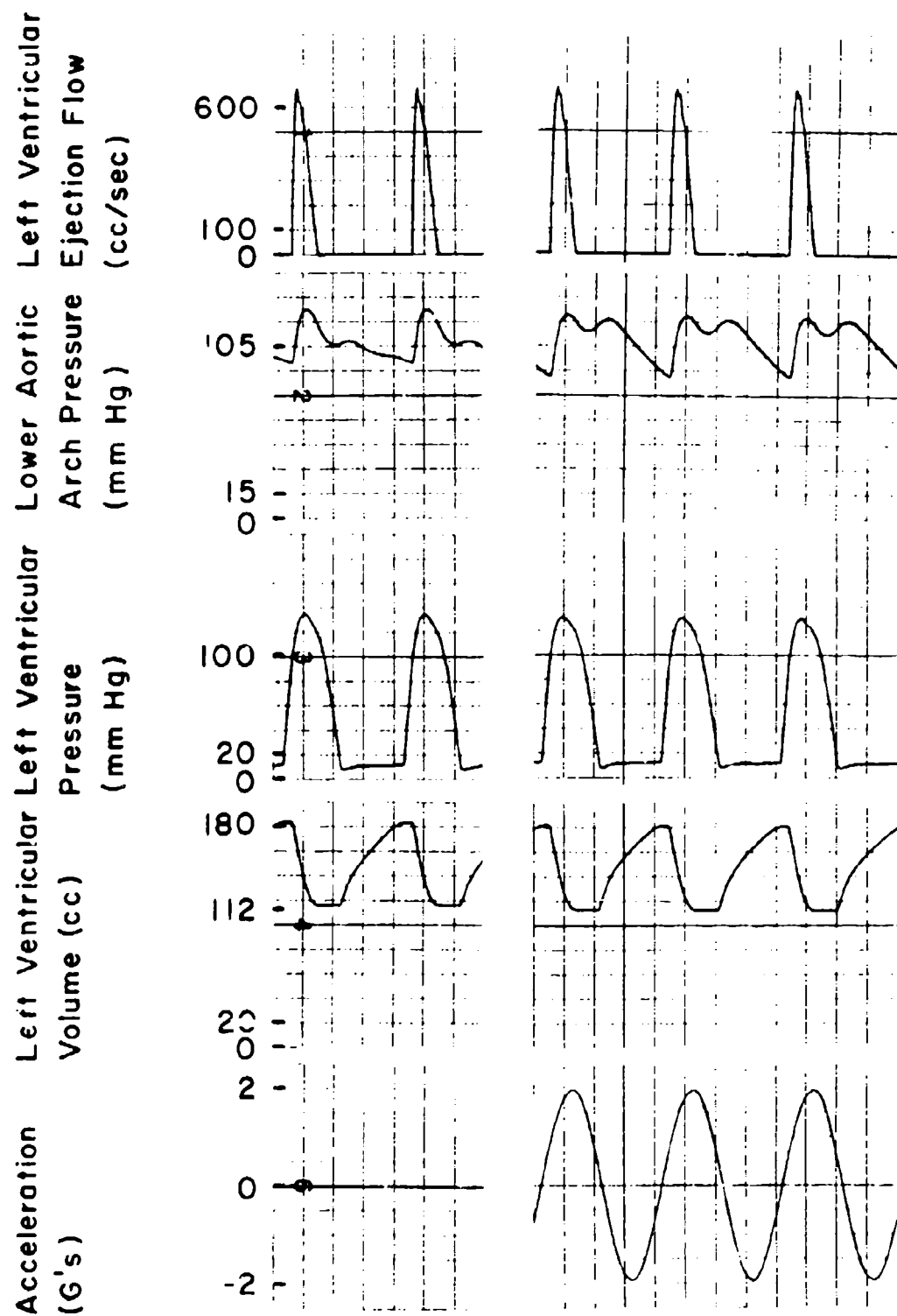


Figure II B. Selected Portion within Beat Pattern of Figure II A.

the acceleration pattern is sinusoidal with peak amplitude of 3 G and frequency of 3 Hz. An experimental response to this same acceleration pattern is presented in Fig. 12B<sup>9</sup>.

Response of the model to nonsynchronous sinusoidal accelerations of different amplitudes and frequencies is shown in Figs. 13A, 13B, and 13C. The experimental variables are defined as follows:

- (1)  $\Delta P_{MAX}$ : maximum difference of pressure in the lower aortic arch ( $P_{LAA}$ ) during any single excursion<sup>6,9</sup> (see Fig. 12B).
- (2)  $Q_{MAX}$ : maximum peak left ventricular ejection flow ( $Q_{OLV}$ ) during a single heart cycle<sup>6,9</sup> (see Fig. 12B).
- (3)  $Q_{MIN}$ : minimum peak left ventricular ejection flow ( $Q_{OLV}$ ) during a single heart cycle<sup>6,9</sup> (see Fig. 12B).
- (4)  $SV_{MAX}$ : maximum stroke volume of a single heart cycle (see Fig. 12A).
- (5)  $SV_{MIN}$ : minimum stroke volume of a single heart cycle (see Fig. 12A).

Response of the model to other nonsynchronous time-varying accelerations was also determined. For the case of square-wave acceleration patterns,  $\Delta P_{MAX}$ ,  $Q_{MAX}$ ,  $Q_{MIN}$ ,  $SV_{MAX}$ , and  $SV_{MIN}$  curves were obtained which were similar to the corresponding curves presented in Figs. 13A, 13B, and 13C but which had generally greater deviation from control than the sinusoidal responses for any given G level.

A nonsynchronous asymmetric rectangular waveform of 1 G peak magnitude and a frequency of approximately 1.25 Hz was applied to the

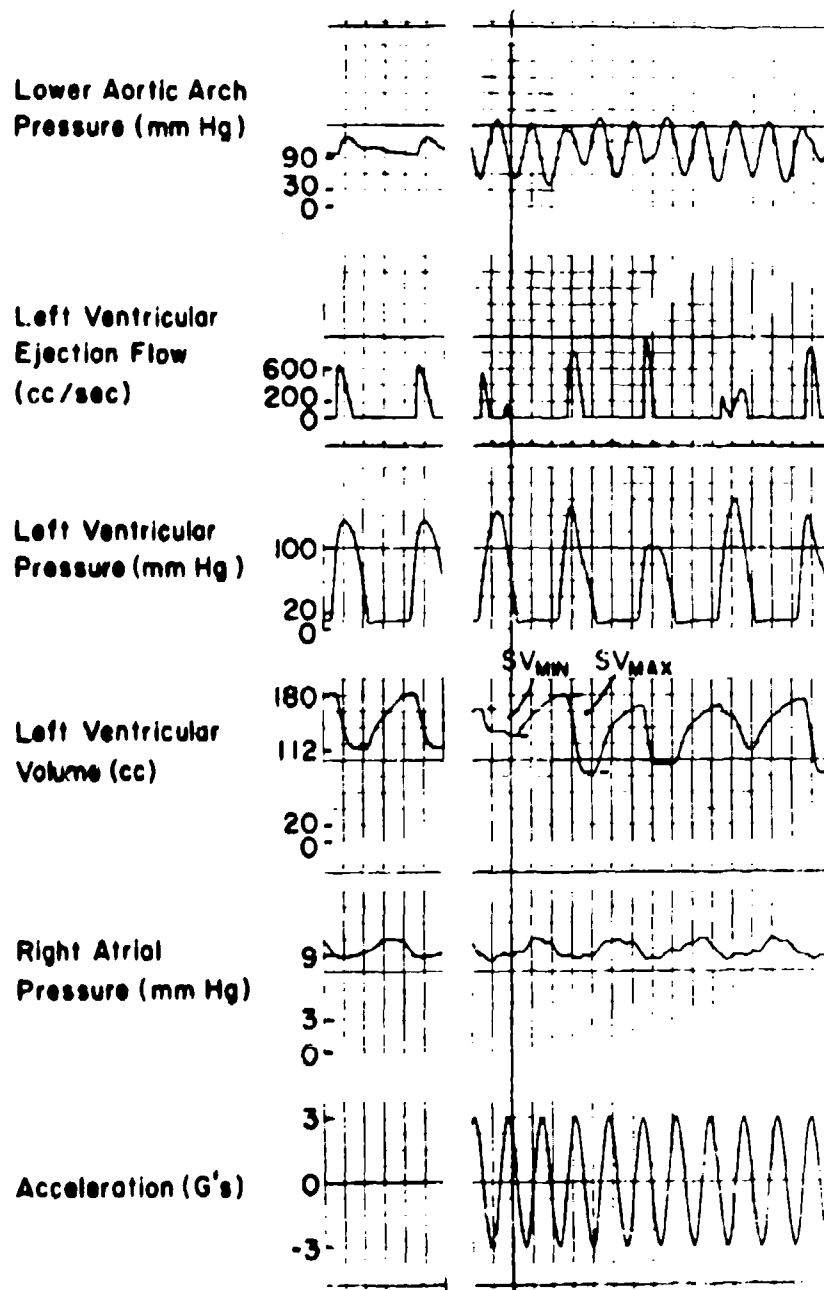


Figure 12 A. Typical Response of Model to Simulated Nonsynchronous 3G, 3 HZ Sinusoidal Acceleration.



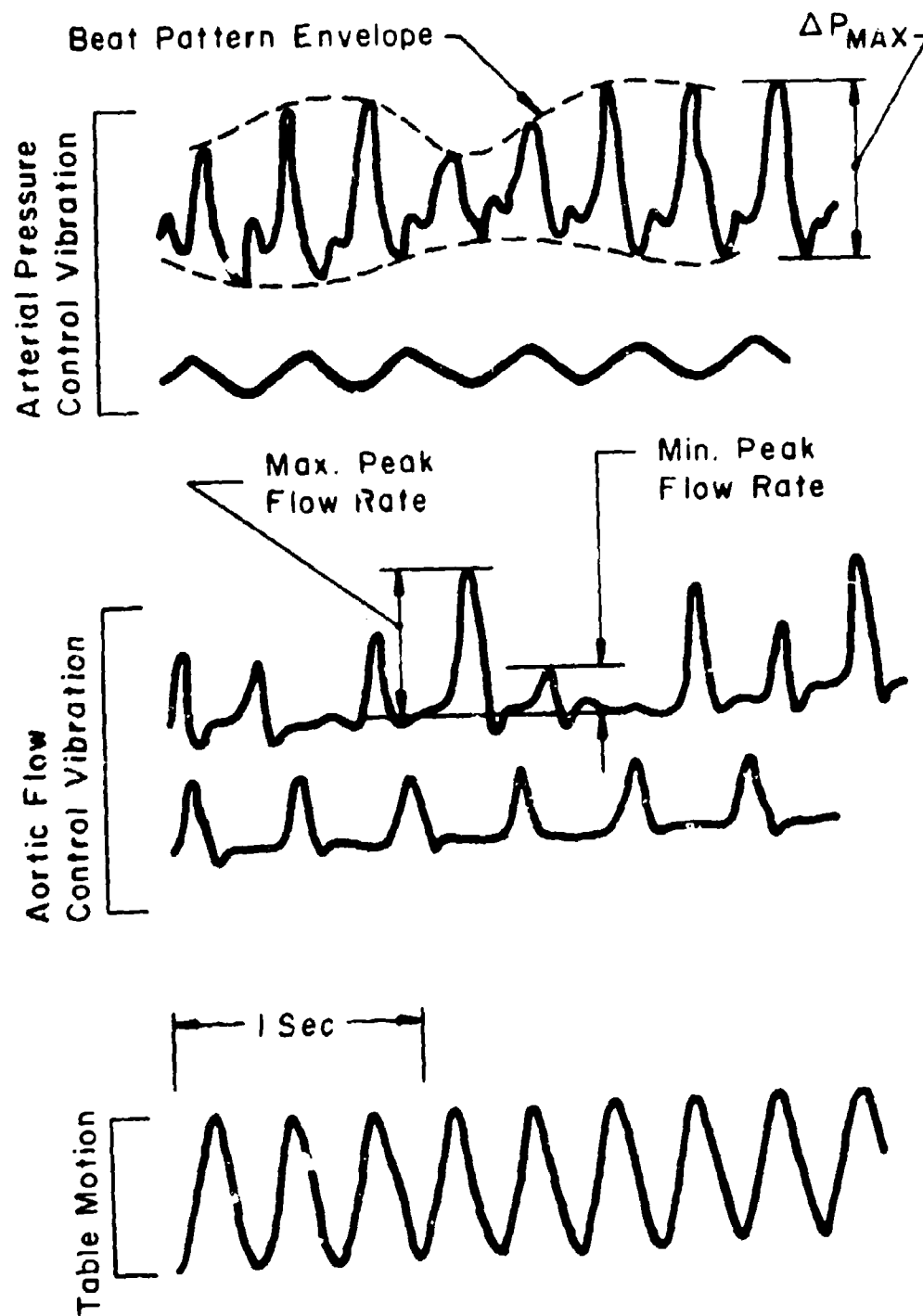


Figure 12B. Examples of Recordings of Arterial Pressure and Aortic Flow from a Dog, at Rest and under 3G Vibration of 3 Hz<sup>9</sup>.

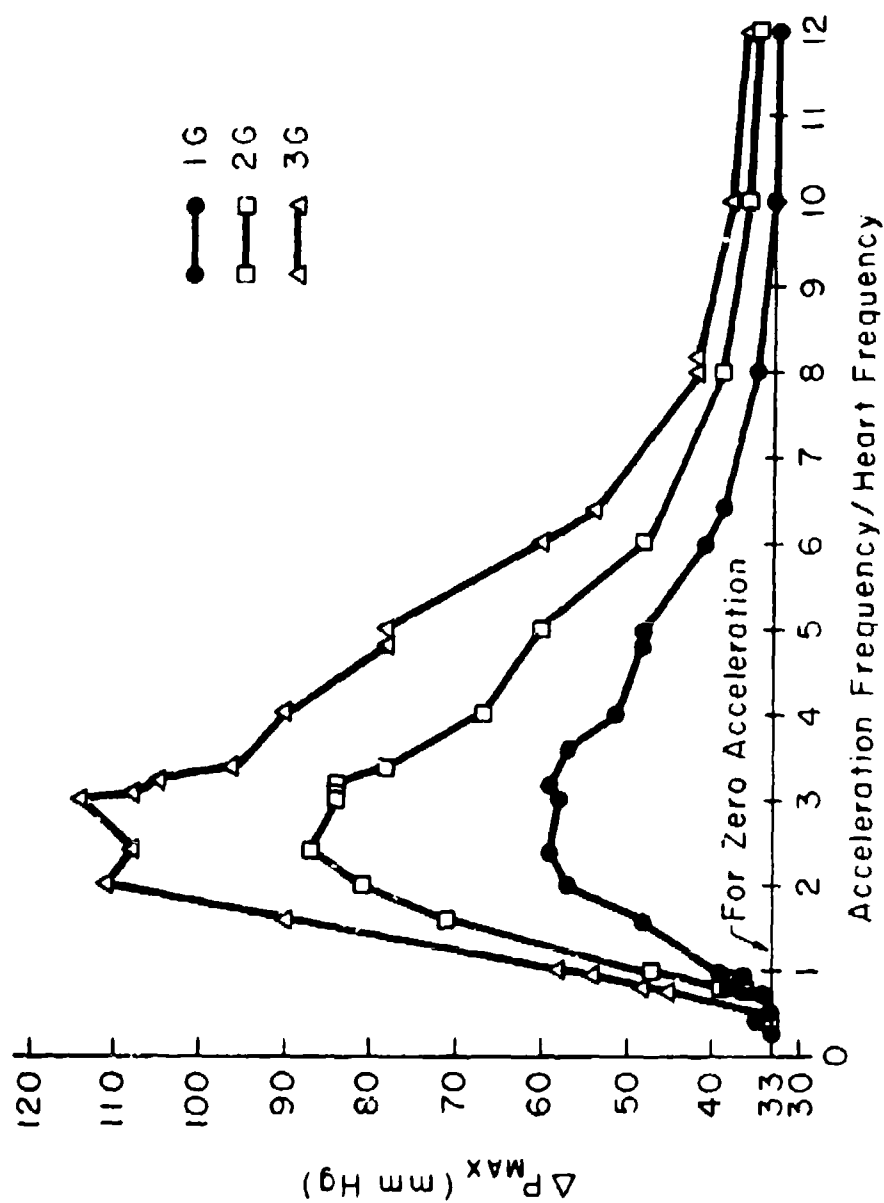


Figure 13A. Simulated  $\Delta P_{MAX}$  vs. Normalized Acceleration Frequency with Acceleration Amplitude as a Parameter.

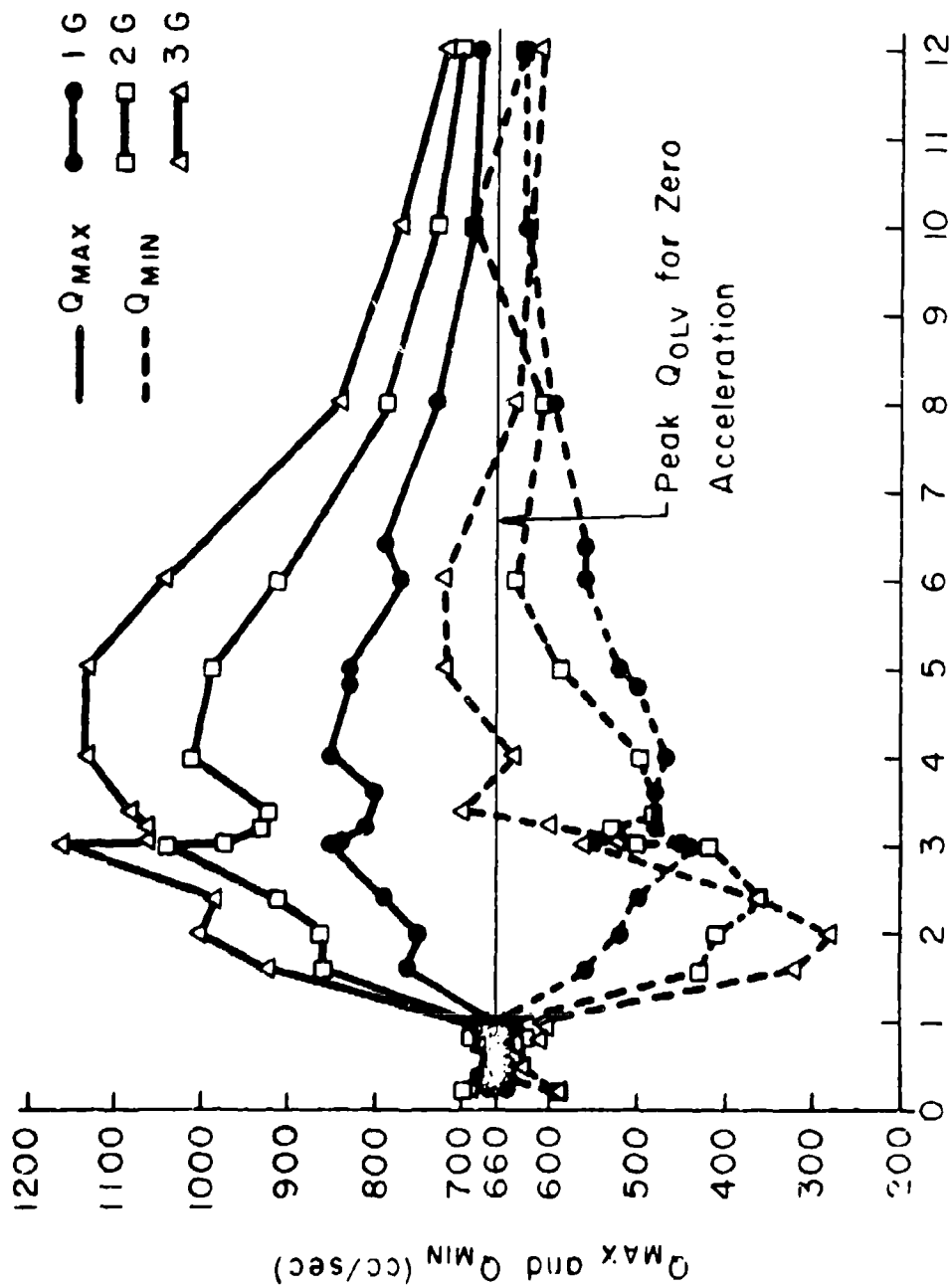


Figure 13B. Simulated  $Q_{MAX}$  and  $Q_{MIN}$  vs. Normalized Acceleration Frequency with Acceleration Amplitude as a Parameter.

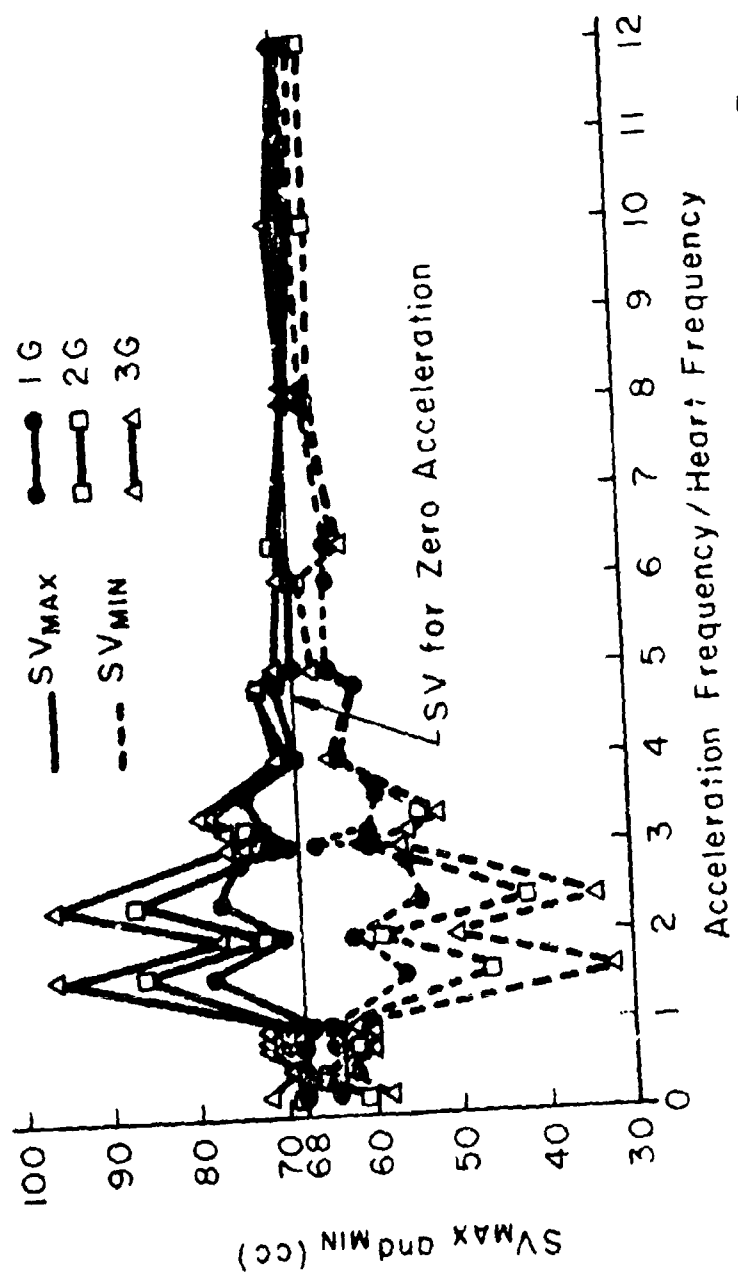


Figure 13C. Simulated SV<sub>MAX</sub> and SV<sub>MIN</sub> vs. Normalized Acceleration Frequency with Acceleration Amplitude as a Parameter.

model<sup>[1]</sup>. Shown in Fig. 14 is the model's response to this waveform. A selected portion of the slow chart speed is shown at a faster chart speed. Note that SV is above the normal value of 68 cc for all acceleration timings. For a 2 G rectangular waveform with positive and negative portions of the same durations as for the 1 G case above, the model's responses were similar to, but greater in magnitude than, the 1 G responses.

#### Synchronous Time-varying Accelerations

A time-varying acceleration pattern is considered synchronous if its frequency is a fixed integral multiple of the heart frequency. In this idealized situation no beat patterns result; i.e., each cycle of the model's response is identical to the previous cycle, once the model reaches steady-state (usually after only a few cycles).

Several patterns of synchronous time-varying acceleration were applied to the model. Shown in Fig. 15 is the response of the model to synchronous sinusoidal acceleration of 1.25 Hz, 2 G peak amplitude, and  $t_D = 0$  milliseconds.

Presented in Fig. 16 is the simulated stroke volume when synchronous sinusoidal accelerations of 1.25 Hz and 1 G and 2 G peak

---

[1] In the model an acceleration pattern with a non-zero average value is the same as a pattern with zero average value combined with a tilt. The average value of this 1 G rectangular waveform is about  $-1/3$  G, corresponding to an approximate  $19^\circ$  head-down tilt.

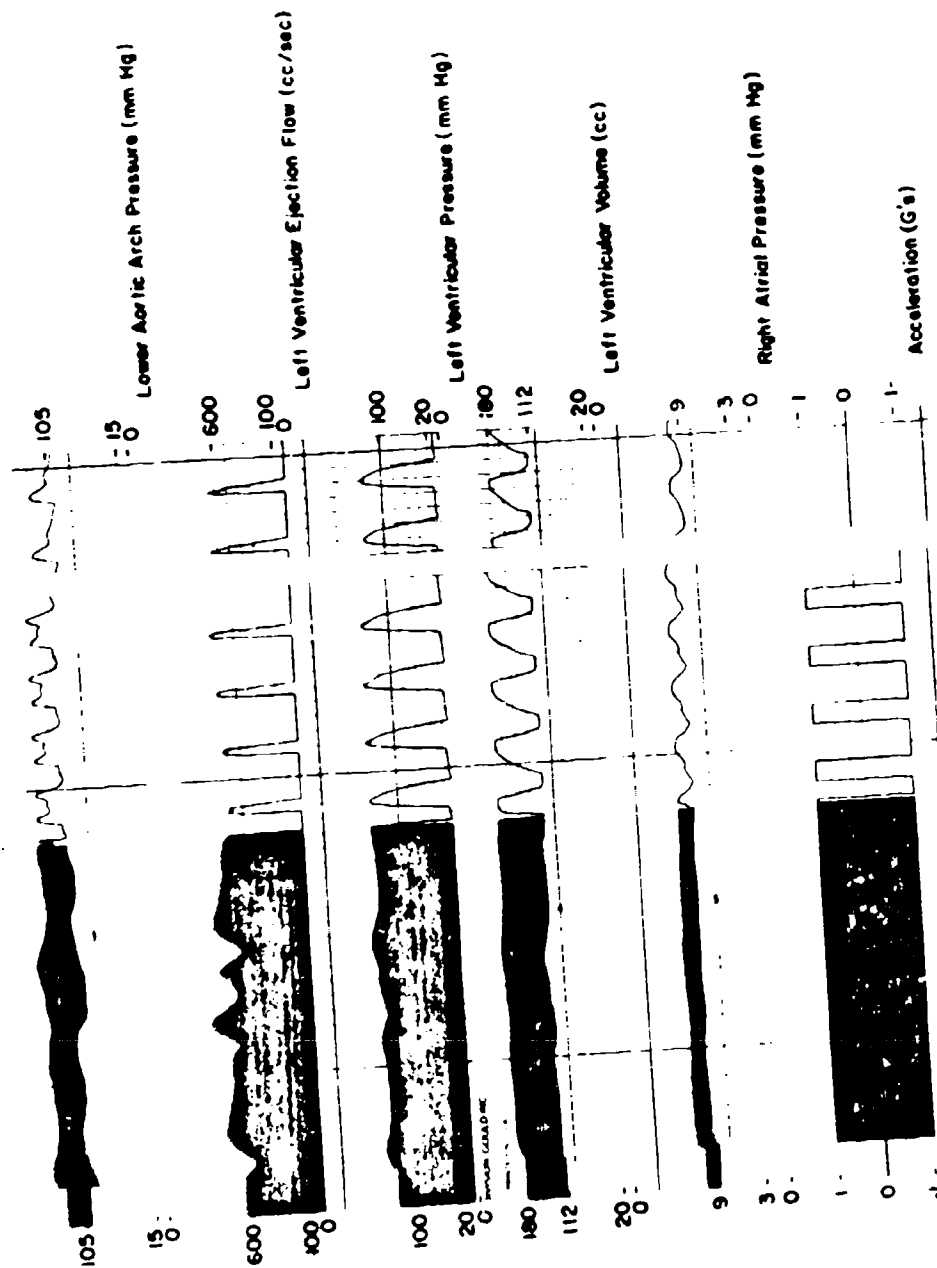


Figure 14 Response of Model to Simulated Nonsynchronous Asymmetric Acceleration.

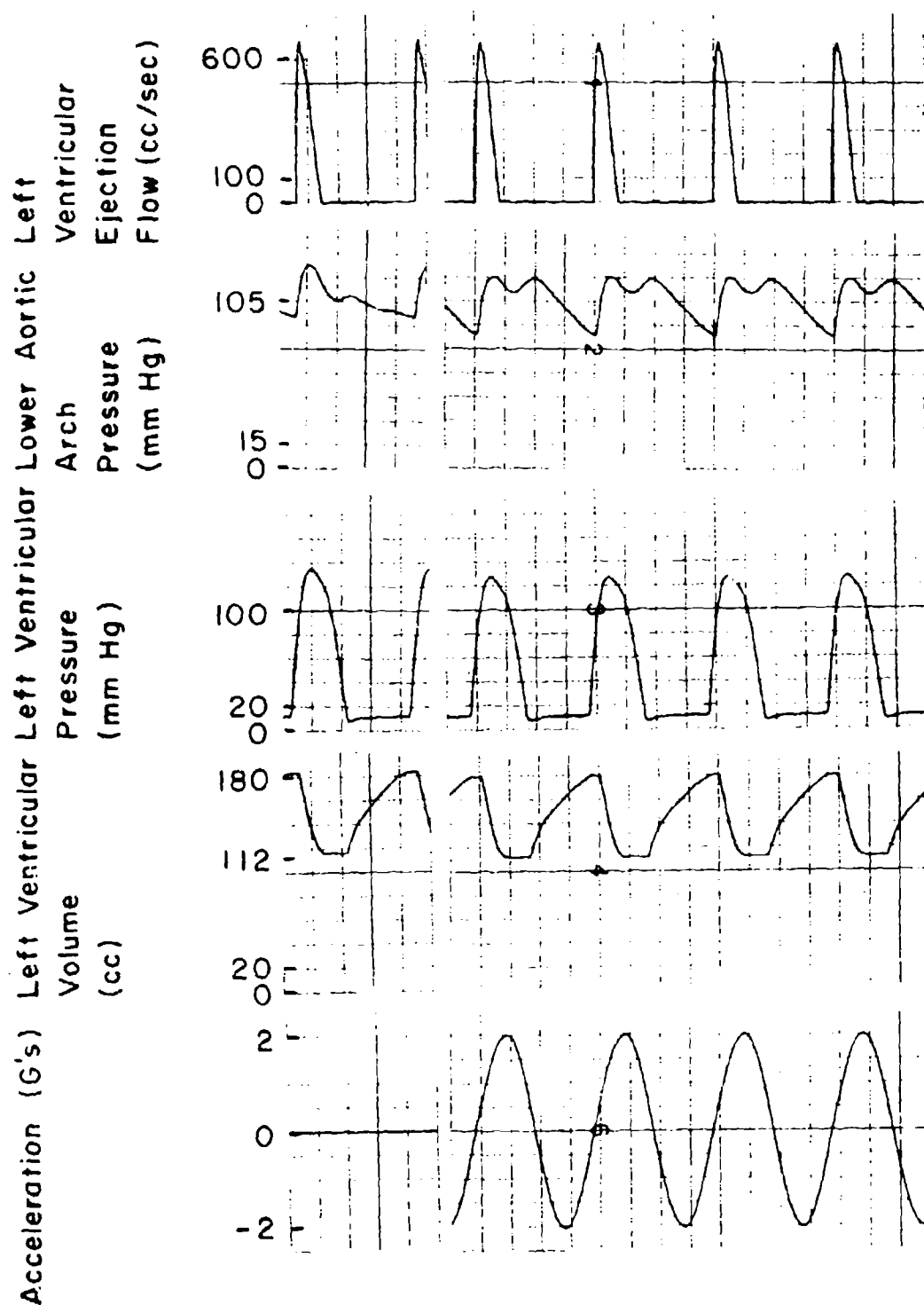


Figure 15. Response of Model to Synchronous 2G, 1.25 Hz Sinusoidal Acceleration with  $t_D = 0$  Milliseconds.

amplitude were applied to the model at various values of  $t_D$ . The simulated stroke volume obtained with square-wave accelerations of 1.25 Hz and 1 G and 2 G amplitude, in which  $t_D$  was again the parameter, was similar to that shown for sinusoidal accelerations in Fig. 16 in the sense that stroke volume was never substantially different from that of zero acceleration.

In Fig. 17 the model's response to a synchronous asymmetric rectangular acceleration pattern of 1 G peak amplitude and  $t_D = 760$  milliseconds is shown. This rectangular waveform has the same positive and negative durations as the nonsynchronous rectangular acceleration pattern described earlier (p. 28).



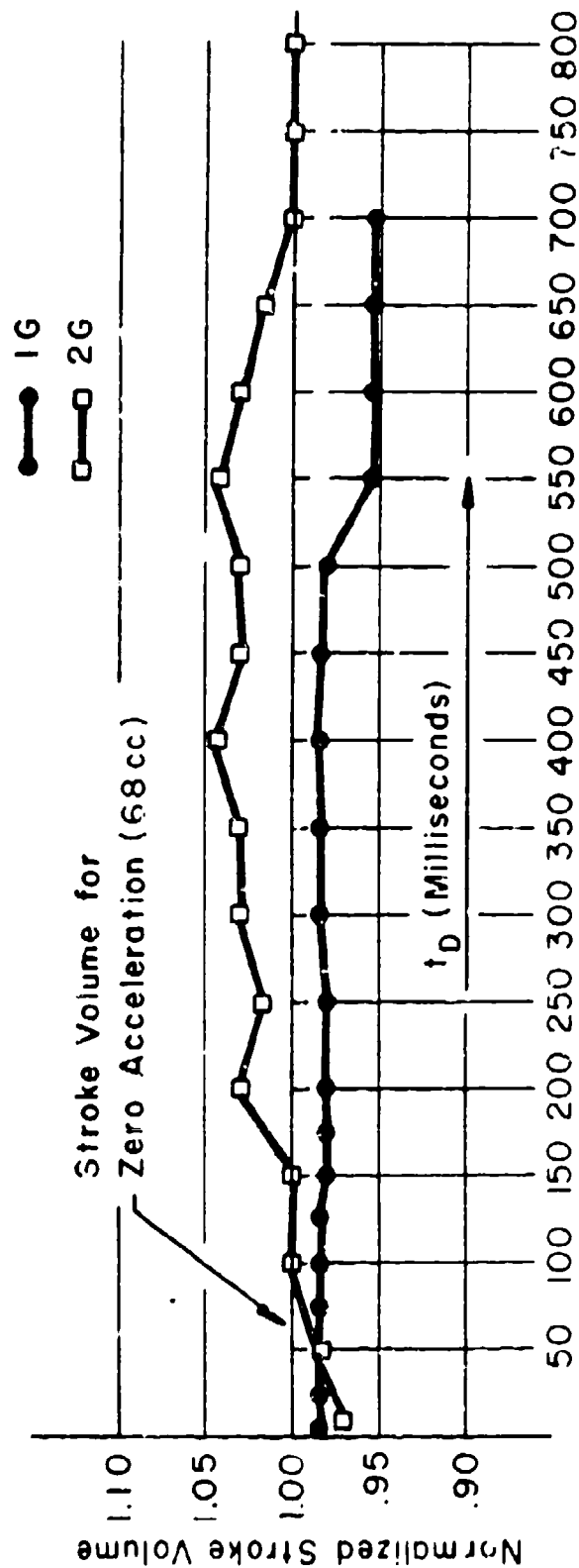


Figure 16. Simulated Stroke Volume (Normalized) for 1 and 2G Synchronous Sinusoidal Accelerations of 1.25 Hz Applied at Various Values of  $t_D$ .

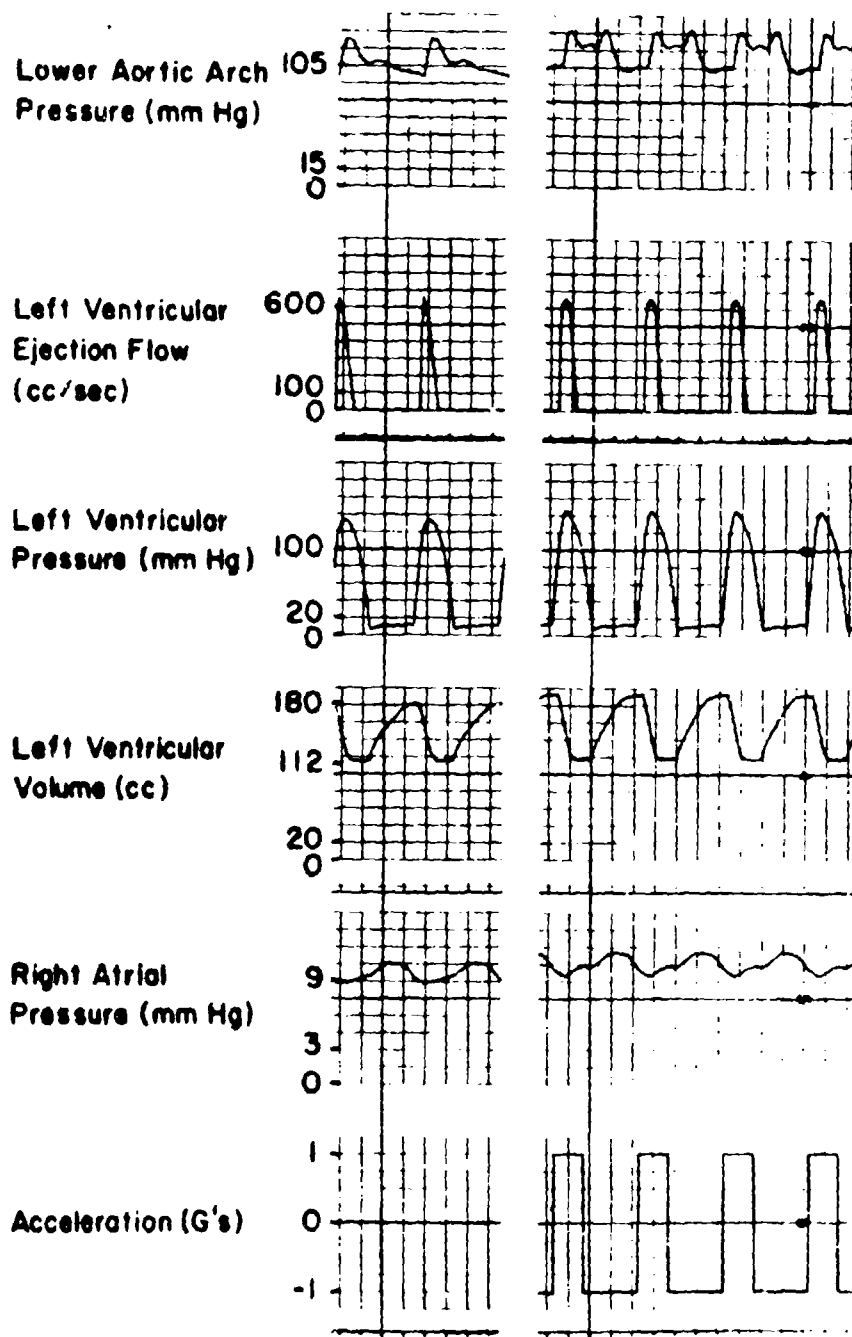


Figure 17. Response of Model to a Simulated Synchronous Asymmetric Acceleration Pattern with  $t_D = 760$  Milliseconds.

## CHAPTER IV

### DISCUSSION AND CONCLUSIONS

#### Constant Accelerations

In the prone position the arterial waveforms of the model are similar to those observed physiologically. However, the model's peak left ventricular pressure and mean left ventricular volume are higher than those observed in man, whereas stroke volume and pulse pressure are lower. Although the discrepancies could have been reduced by reducing both the frequency and magnitude of the ventricular compliance, a normal heart rate was first chosen and a magnitude of the compliance was then selected which compromised stroke volume and left ventricular pressure accuracies.

The venous waveforms of the model do not match physiological data as accurately as the arterial waveforms since such factors as negative intrathoracic pressure, breathing, and right atrial contractions were not taken into account in the model. Thus, right atrial junction pressure seems rather high, but this pressure is a composite pressure due to the extensive lumping of the model and its exact physiological identification is not possible. However, it is somewhat similar in waveform to right atrial pressure in man. The right

ventricular pressure waveform can be made more like its physiological counterpart by decreasing the resting ventricular compliance, but this change results in high initial flow into and out of the right ventricle. Therefore, more steady flows were achieved at the expense of the right ventricular pressure simulation.

Because the values of arterial compliance needed to reproduce arterial pressure waveforms accurately in the model were much smaller than physiological values, volumes were very low in the upper and lower arterial sections. With linear compliances it is impossible to achieve in a highly lumped arterial model the degree of simultaneous accuracy of pressure and volume possible in a more distributed model. If arterial volumes were to be raised by increasing arterial compliance in the lumped model, the arterial pressure waveforms would lose much of their characteristic variation. On the other hand, if volumes were to be raised by increasing mean arterial pressures, serious inaccuracies in pressure and flow waveforms throughout the model would result. Since an error in arterial volume is a small percentage of the total system volume, arterial volume accuracy was sacrificed for pressure accuracy.

The above situation was circumvented on the venous side of the model by using piecewise-linear compliances, which provide large residual volumes at zero pressures. The parallel combination of many

venous segments which have the pressure-volume characteristic depicted in Fig. 1A (p. 7) would ideally contain a rather large volume at zero pressure but would begin to resist volume increases once all the segments have been filled to the point of distention. This observation, together with the fact that large venous volumes do exist at relatively low pressures although the venous system is not excessively compliant, provided the basis for postulating an overall pressure-volume relationship such as that of Fig. 1B. In agreement with physiological observation, the upper and lower venous systems of the model contained most of the venous volume<sup>2</sup>. The thoracic volume of the model was low because of the simplicity of the lung model. However, the venous and thoracic volumes were similar to the general volume distribution obtained in a more extensive model<sup>17</sup>.

Since, in a head-up tilt, nervous regulation is involved in adjusting the compliance of the physiological system (venomotor tone), the slopes of the pressure-volume relationships for the venous sections of the model, which have no neural control simulations, were chosen to result in volume shifts of proper magnitude<sup>11</sup> and therefore to represent compliance values averaged over all conditions of venomotor tone.

When a man stands up, aortic and left ventricular pressures and stroke volume tend to decrease; however, nervous control changes

in peripheral resistance and venomotor tone occur, tending to raise these quantities<sup>7,11,16</sup>. Still, cardiac output will be down by as much as 20 percent because the decrease in stroke volume more than offsets the increase in heart rate<sup>5</sup>. In the model changes in peripheral resistances were not simulated; therefore, in a simulated head-up tilt aortic and left ventricular pressures and stroke volume decreased to about 60 to 70 percent of their original value. These responses are similar to those obtained in a more detailed model operating with only one nervous control loop (heart-rate control)<sup>18</sup>, but the percentage decreases in the detailed model were greater than those in the model used in this study.

A major difference between simulated and physiological tilt response occurred with right atrial pressure during a head-down tilt. In the model this pressure increased, whereas it has been consistently found to decrease with a head-down tilt in man<sup>10,11</sup>. This apparent limitation of the model was caused in part by the extensive lumping of the upper venous system compliance, much of which was placed at heart level ( $C_{RA}'$ ) in the model. As a result, the shift in blood volume away from heart level and the associated shift in hydrostatic indifference point<sup>11</sup> induced by a simulated head-down tilt were not as large in the model as those that would be observed experimentally. However, this limitation was an advantage in other ways. Both the

model and anesthetized animals<sup>1</sup> showed increases in stroke volume and lower venous system flow under conditions of head-down tilts. In the model, increased stroke volume can be related directly to increased  $P_{RA'}$ , which should cause in sequence increases in right ventricular, pulmonary, and left ventricular pressures and volumes. These increased pressures and volumes should bring about increased stroke volumes since the inverse compliance curve of the left ventricular model is invariant under postural changes. In the animals, neurally-controlled changes in peripheral resistance and venomotor tone, heart rate, and ventricular compliance probably occurred, more than offsetting the decrease in right atrial pressure and resulting in a net increase in stroke volume.

Excessively large volume shifts related to large acceleratory-induced pressure changes on the venous side of the model were avoided by using piecewise-linear resistances to reduce flows under those conditions. These discontinuities simulated the increase in resistance to blood flow that occurs physiologically when local partial collapse of large veins occurs as, for example, during a head-up tilt.

Elucidation of the model's responses to tilt experiments is provided by examination of the heart-lung section of the model. It appears that change in mean flow rate through the simple heart-lung section is determined by the change in mean right atrial pressure ( $P_{RA'}$ ) together with the change in mean pressure outside the left

ventricle ( $P_{LAA}$ ). For example, if  $P_{RA'}$  is held constant while  $P_{LAA}$  is decreased, flow rate through the heart-lung section will increase (as has been observed in an open-loop model<sup>6</sup> with head-up tilt); or, if  $P_{RA'}$  is held constant and  $P_{LAA}$  increased, flow should decrease. Conversely, when  $P_{LAA}$  is held constant and  $P_{RA'}$  is allowed to change, the flow should decrease if  $P_{RA'}$  is decreased and increase if  $P_{RA'}$  is increased. Now, consider postural changes in a closed-loop model where both  $P_{RA'}$  and  $P_{LAA}$  change. In the head-up tilt, where  $P_{RA'}$  decreased 36% and  $P_{LAA}$  decreased 25%, stroke volume decreased 38%. In the head-down tilt, where  $P_{RA'}$  increased 34% and  $P_{LAA}$  increased 28%, stroke volume increased 32%. In all the preceding cases it is seen that stroke volume of the model varies with right atrial pressure; in addition, if a linear dependence of stroke volume on  $P_{RA'}$  and  $P_{LAA}$  is assumed, it is found that the influence of  $P_{RA'}$  on stroke volume is about twice as great as the influence on  $P_{LAA}$ . Thus, in the model constant accelerations affect mean right atrial or filling pressure, which in turn affects stroke volume. The importance of the effect of postural changes on right atrial pressure has also been recognized in physiological studies<sup>7</sup>.

#### Time-varying Accelerations

Comparison of Figs. 12A and 12B shows similarity between pressure and flow responses obtained from the model for simulated sinusoidal



accelerations and responses obtained experimentally with whole-body sinusoidal accelerations. Also, the  $\Delta P_{MAX}$  and peak Q curves of Figs. 13A and 13B seem to match experimental data<sup>9</sup> more closely than these curves produced by an open-loop model<sup>6</sup> because the curves of Figs. 13A and 13B have a wider frequency response. Thus, there is fairly good qualitative and quantitative agreement between the model investigated in this study and experimental results. However, these agreements must be viewed in light of the fact that although the simulated accelerations were applied directly to the model, the experimental accelerations may be modified by the unknown transfer function between the shake table and the cardiovascular system.

The response of the simulated stroke volume (Fig. 13C) indicates the fact that for any particular sinusoidal acceleration pattern, stroke volume was enhanced during one portion of the beat pattern and diminished for the other portion of the beat pattern in such a way that cardiac output was about the same as for zero acceleration. In addition, at multiples of the heart frequency, stroke volume was near control throughout the length of the beat pattern.

Although the square-wave acceleration pattern effected great changes in pressures and large peak flow rates in the model, it did not increase cardiac output at either 1, 2, or 3 G peak amplitudes. As in the case for sinusoidal acceleration, simulated stroke volume was first enhanced and then decreased within a beat pattern in such a way that cardiac output did not increase.

The rectangular waveform in Fig. 14 provides an excellent example of simulated stroke volume when the acceleration pattern was asymmetrical. The figure shows that for time-varying acceleration patterns cardiac output could be changed using an asymmetrical pattern. It is also seen that this pattern resulted in increased mean right atrial and lower aortic arch pressures, which is similar to the results obtained for constant accelerations in a head-downward tilt. Thus, it may have been the tilt that produced the increased filling pressure and increased cardiac output.

Comparison of Fig. 11B to Fig. 15 and Fig. 14B to Fig. 17 illustrates a result that was consistently found in this study; that is, the simulated responses of the model occurring at a particular timing of an acceleratory pattern which was producing long beat patterns could be reproduced synchronously by using the same pattern and timing. Synchronous accelerations at heart frequency and multiples of heart frequency were used and, in all cases examined, reproduced the responses obtained with nonsynchronous acceleration of corresponding pattern and timing. These results indicate that any transient responses resulting from acceleratory timing changes were of relatively short duration.

Because of inertial effects the responses of the model to simulated time-varying accelerations were more difficult to analyze than the responses to simulated constant accelerations. However, some

observations were consistently evident. For example, when the direction of acceleration of a square wave pattern shifted to headward, the initial response in  $P_{LAA}$  (lower aortic arch pressure) was a slight rise, indicating a shift of blood toward the heart in the ascending aortic arch section. Since this section had a smaller inertance and was closer to the left ventricle than the other arterial sections, it determined the initial response of  $P_{LAA}$ . The length of this section (7.6 cm) limited the magnitude of the rise. The initial rise in  $P_{LAA}$  was followed by a considerable drop, corresponding to a shift of blood footward (away from the heart) into the lower arterial system, reducing volume and therefore pressure in the aortic arch. After a longer interval,  $P_{LAA}$  increased to near original values as the blood in the relatively high-inertance upper arterial system shifted footward (toward the heart). This aortic refilling may have been assisted by backflow from the lower arterial section<sup>[1]</sup>. These effects were reversed when the direction of acceleration shifted to footward. With sinusoidal accelerations similar effects were present but were often not as evident because this acceleratory pattern tended to smooth the inertial effects much more than a pattern with abrupt changes.

---

[1] The oscillatory frequency of the step response of the lower arterial section was about twice that of the upper section, so that, depending on the initial conditions imposed on the sections by previous acceleration, the second oscillatory half-cycle (first compliant reaction) of the lower section may have occurred during the first oscillatory half-cycle (primary inertial response) of the upper section.

From the preceding discussion it is evident that if left ventricular ejection is to be enhanced by modifying aortic pressure in the model, an acceleratory pattern must be chosen which optimizes the inertial effects of all the arterial sections. In this study some symmetrical acceleratory patterns increased peak left ventricular ejection flow rate by nearly 100% for a portion of the usually long beat pattern (Fig. 13B). However, these patterns did not produce maximum stroke volumes; rather, maximum stroke volumes occurred at acceleratory frequencies producing short beat patterns (Fig. 13C). Heart cycles with large stroke volumes were preceded or followed by cycles with low stroke volumes. As a result, over a beat period cardiac output remained about the same as for zero acceleration. Thus, with symmetrical accelerations large peak ejection flow rates could be produced synchronously, but increased cardiac output could not be sustained. With an asymmetrical acceleratory pattern increased cardiac output was sustained although peak left ventricular ejection was not maximized (Figs. 14 and 17). Therefore, optimization of the inertial effects of the arterial system may not result in increased cardiac output.

The data obtained in this study do not indicate that zero-mean accelerations caused sustained increases in right atrial pressure. This observation might partially explain why increased cardiac output

did not occur with symmetrical acceleratory patterns, since cardiac output varied with mean right atrial pressure under applied constant acceleration. Although time-varying accelerations combined with tilts did increase mean right atrial pressure and cardiac output, it is not evident that the time-varying patterns were responsible for these changes.

#### Variation of Model Parameters

In the nonlinear venous sections of the model three parameter values have not been identified physiologically; these are  $V_0$ ,  $V_C$ , and  $R_C$  (Chapter II). The value of  $V_0$  of a section was chosen in conjunction with the value of finite compliance to give approximately normal operating volumes and pressures in the prone position. The value of  $V_C$  helped to determine the amount of volume a section would lose due to sustained acceleration. The parameter  $R_C$  determined how the flow was curtailed to prevent excessive volume loss of a section. With constant accelerations the system responded in an overdamped manner with large values of  $R_C$  and in an underdamped manner with relatively small values of  $R_C$ . Thus, for a simulated tilt,  $R_C$  could be adjusted so that the steady-state equivalent flow through a venous section was almost constant, as with zero acceleration, or exhibited flutter, which is characteristic of flow through a vertical collapsible tube<sup>12</sup>.

The acceleratory patterns which invoked  $R_C$  and the infinite compliances were constant accelerations or time-varying accelerations of low frequency. For example, with sinusoidal acceleratory patterns of 1, 2, and 3 G's peak amplitude and frequencies from 0.5 to 10 Hz,  $V_{UVS} \leq V_{O_{UVS}}$  for all frequencies below 1.5 Hz and  $R_{C_{UVS}}$  was invoked only by the 1 G, 0.5 Hz pattern. For the sinusoidal patterns above and all other acceleratory patterns in this study,  $V_{LVS} > V_{O_{LVS}}$  in all cases and  $R_{C_{LVS}}$  was never invoked.

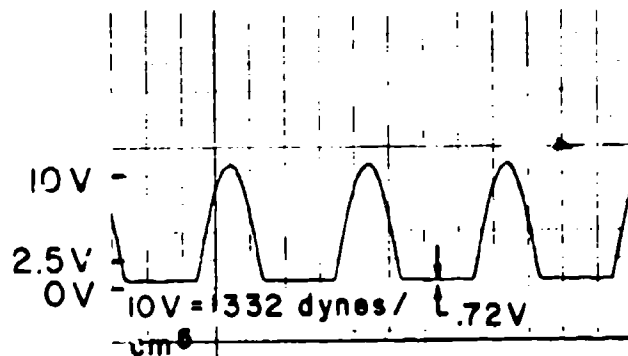
Variation of the phase between the simulated right and left ventricular contractions (p. 4) did not appear to change the model's responses to accelerations. Pressure and flow responses to simulated acceleratory patterns with ventricular contractions in phase were identical to those responses obtained with ventricular contractions 180° out of phase. The inverse compliances simulating ventricular contractions used in this study are presented in Fig. 18.

### Conclusions

Some of the major conclusions drawn from this study are:

1. Simulated tilts produced sustained responses in cardiac output: in head-up tilts cardiac output decreased, in head-down tilts it increased.
2. Simulated zero-mean time-varying accelerations did not change cardiac output, although they did change peak left ventricular ejection flow

Left Ventricular  
Inverse Compliance,  
 $1/C_{LV}(t)$  (volts)



Right Ventricular  
Inverse Compliance  
Times 4,  $4/C_{RV}(t)$   
(volts)

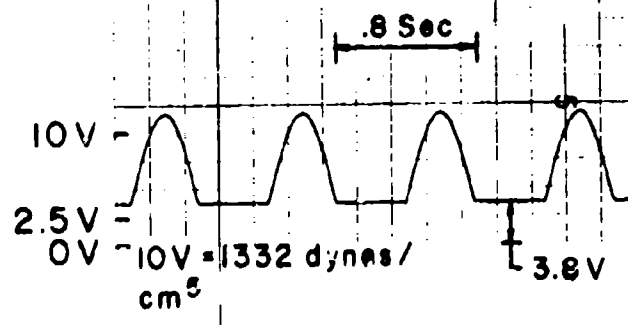


Figure 18. Simulations of Ventricular Contractions in the Model.

rate by 75% and aortic pulse pressure by 330%. On a per-cycle basis, stroke volume was also changed by 40% or more.

3. A simulated head-down tilt combined with a zero-mean time-varying acceleratory pattern did produce increased cardiac output.
4. The model's aortic pressure responses to zero-mean sinusoidal accelerations exhibited resonance in the 2 - 5 Hz frequency range, and the peak aortic flow responses were most extreme in the 2 - 6 Hz range. Resonance of these quantities in these frequency ranges has also been observed experimentally<sup>9</sup> and in an open-loop model<sup>6</sup>.
5. Model responses effected by nonsynchronous time-varying accelerations producing long beat patterns could be reproduced synchronously.

#### Recommendations for Improvement of the Model

1. Active right atrium. This study has shown that the effect of accelerations on right atrial pressure is important; therefore, the timing of accelerations with respect to venous system events may be an important factor in changing cardiac output. The sensitivity of cardiac output to right atrial pressure in the model indicates that the timing of venous acceleration with respect to right atrial contraction may modify cardiac output.
2. More detailed pulmonary model. This addition should produce better tilt responses in the model since the lung is known to have an



equivalent height<sup>10</sup> and might produce sustained changes in cardiac output with zero-mean time-varying acceleration.

3. If the inclusion of (2) results in sustained changes in stroke volume with zero-mean accelerations, the timing of left ventricular filling pressure is probably important and an active left atrium would be desirable.

## APPENDIX A

The inclusion of a piecewise-linear pressure-volume characteristic, postulated for the upper and lower venous systems of the model investigated in this study, could conceivably introduce error into the performance of the system in the following way. Consider the piecewise-linear pressure-volume relationship

$$V = PC \quad (A-1).$$

The derivative of Eq. (A-1) with respect to time is

$$\frac{dV}{dt} = C \frac{dP}{dt} + P \frac{dC}{dt} \quad (A-2)$$

where  $\frac{dV}{dt}$  represents the difference between flow in and flow out of a section. Since  $C$  may be discontinuous in time, the last term in Eq. (A-2) may be impulsive in nature if the discontinuity in  $C$  occurs at  $P \neq 0$ . If volume were computed by direct integration of Eq. (A-2), step changes could result in system volume, an undesirable condition. However, volumes were computed in this study in such a way that discontinuities did not occur, as can be argued by considering Fig. 5 (p ). If a step change in  $V_{UVS}$  or  $V_{LVS}$  is assumed, it would be integrated and produce a continuous feedback flow signal; thus, the assumed step change in volume must be a consequence of impulsive flow from the

preceding section of the model. However, flow from the preceding section cannot be impulsive even with a step change in volume in that section because a step change in volume would produce a step change in pressure and therefore, at most, a finite discontinuity in flow. Applying this reasoning to all model sections shows that the impulsive  $\frac{dV}{dt}$  required to produce a discontinuity in volume was not generated in the analog model.

## APPENDIX B

In order to determine the effect of external forces upon a composite section of flow in the model, consider the axial acceleration of a rigid tube of length  $h$  and cross-sectional area  $A$  in which a Newtonian fluid subjected to an axial component of gravitational acceleration  $g$  and an axial pressure gradient  $(P_1 - P_2)$  is undergoing laminar flow (as in Fig. 19A). A force balance for this section can be written

$$(P_1 - P_2) A - W - F = m(\dot{V} + \dot{V}_W), \quad (B-1)$$

where:  $V$  = mean velocity of blood with respect to wall,  
 $V_W$  = velocity of wall with respect to Newtonian frame,  
 $W$  = weight of fluid in section, and  
 $F$  = viscous forces.

Since  $W = \rho h A g$ , where  $\rho$  is fluid density, Eq. (B-1) becomes

$$V = \frac{1}{\rho h A} [(P_1 - P_2) A - \rho h A g - \rho h A \dot{V}_W - F] dt \quad (B-2)$$

when rearranged and integrated to solve for  $V$ . If the viscous forces,

$F$ , are assumed proportional to the velocity,  $V$ , then

$$\frac{F}{A} = \frac{KV}{A} = \frac{RQ}{A^2} = QR, \quad (B-3)$$

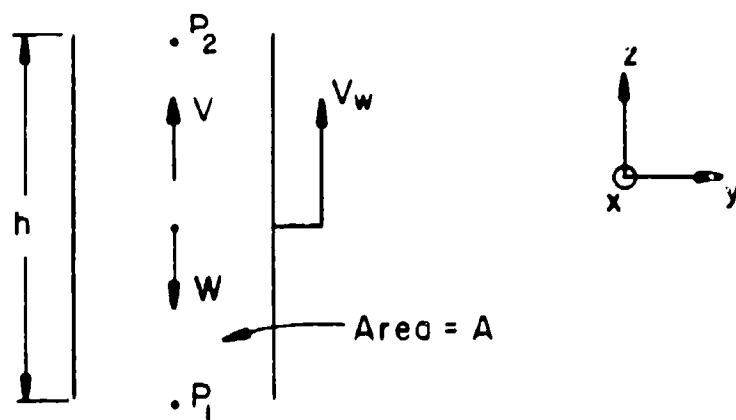


Figure 19A. Axial Acceleration of a Rigid Tube Containing a Newtonian Fluid with Direction of Acceleration the Same as That of the Original Fluid Acceleration.

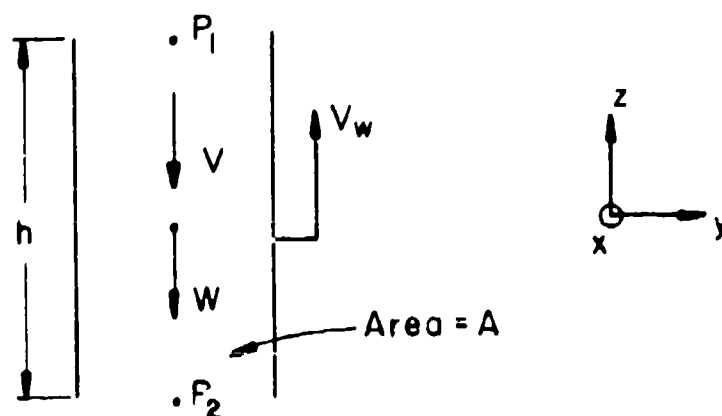


Figure 19B. Axial Acceleration of a Rigid Tube Containing a Newtonian Fluid with Direction of Acceleration Opposite That of the Original Fluid Acceleration.

where  $Q = VA$  is a volumetric flow rate and  $R = \frac{K}{A^2}$  is interpreted as the fluid resistance of the section. Making these assumptions and expressing  $L = \frac{\rho h}{A}$  as the inertance of the section produces the following modification of Eq. (B-2):

$$Q = \frac{1}{L} \int [P_1 - P_2 - \rho h(g + \dot{V}_W) - QR] dt. \quad (B-4)$$

For a section in which  $V$  is in the negative  $Z$ -direction (Fig. 19B),

$$Q = \frac{1}{L} \int [P_1 - P_2 + \rho h(g + \dot{V}_W) - QR] dt. \quad (B-5)$$

From Eqs. (B-4) and (B-5) the effect of external forces upon a composite section of flow is to modify the flow by instantaneously increasing or decreasing the pressure gradient depending upon the instantaneous directions of the external forces and the direction of the flow. Since accelerations appear as pressure modification terms in the model, they were simulated by series voltage sources in the RLC vascular sections (Fig. 4). The polarities of all sources for all acceleration patterns were determined from Eqs. (B-4) and (B-5).

The effect of the earth's gravitational force was simulated in this study by the conditions of  $\dot{V}_W = 0$  and

- (a)  $g = 0$  G (prone position)
- (b)  $g = +1$  G (head-up tilt)
- (c)  $g = -1$  G (head-down tilt)

The effect of time-varying whole-body accelerations was simulated by  $g = 0$  G and  $\dot{V}_W$  a time-varying periodic waveform with zero average value.

The combined effect of gravitational and time-varying accelerations was simulated by  $g = -\frac{1}{3} G$  (an approximate  $19^\circ$  head-down tilt) and  $\dot{V}_W$  a time-varying periodic waveform.

#### LIST OF REFERENCES

1. Abel, F. G., and Waldhausen, J. A. "Influence of Posture and Passive Tilting on Venous Return and Cardiac Output." American Journal of Physiology, Vol 215, No. 5, pp. 1058-1066, Nov. 1968.
2. Attinger, E. O. "Wall Properties of Veins." IEEE Transactions on Bio-Medical Engineering, Vol. BME-16, No. 4, pp. 253-261, Oct. 1969.
3. Berne, R. M., and Levy, M.N. Cardiovascular Physiology. Saint Louis: The C. V. Mosby Co., 1967.
4. Brecher, G. A. Venous Return. New York: Grune and Stratton, 1956.
5. Burton, A. C. Physiology and Biophysics of the Circulation. Chicago: Year Book Medical Publishers Inc., 1965.
6. Camill, P., Jr. "Computer Modeling of Whole Body Sinusoidal Accelerations on the Cardiovascular System." MS Thesis, University of Kentucky, 1971.
7. Carleton, R. A. and Graybiel, A. "The Cardiovascular System in Aerospace Medicine." In Department of the Navy, Office of the Chief of Naval Operations and the Bureau of Medicine and Surgery. U. S. Naval Flight Surgeon's Manual. Washington, D. C.: Government Printing Office, 1968.



8. Collins, J. C.; Knapp, C. F.; Starnes, R. L.; and Bhargava, V.  
"Electrical Analog Modeling of Cardiovascular Valves." Proceedings,  
Fourth Annual Southeastern Symposium on Systems Theory, University  
of Kentucky, Lexington, April 3 - 4, 1972.
9. Edwards, R. G.; McCutcheon, E. P.; and Knapp, C. F. "Cardiovascular  
Changes Produced by Brief Whole-Body Vibrations of Animals."  
Journal of Applied Physiology, Vol. 32, No. 3, pp. 386-390, March,  
1972.
10. Gauer, O. H., and Zuidema, G. D. Gravitational Stress in Aerospace  
Medicine. Boston: Little, Brown and Co., 1961.
11. Gauer, O. H., and Thron, H. L. "Postural Changes in the Circula-  
tion." In Dow, P. (Exec. Ed.) and Hamilton, W. F. (Sec. Ed.).  
Handbook of Physiology, Sec. 2, Vol. 3: Circulation. (American  
Physiology Society) Baltimore: Williams and Wilkins Co., 1965.
12. Koit, J. P. "Flow Through Collapsible Tubes and Through in Situ  
Veins." IEEE Transactions on Bio-Medical Engineering, Vol. BME-16,  
No. 4, pp. 274-283, Oct. 1969.
13. Jackson, D. H. (Ed.). "Circulatory Assist and Ballistocardiographic  
Studies." Proceedings, Fifteenth Annual Meeting of Ballistocardi-  
ographic Research Society, Atlantic City 1971; Bibliotheca  
Cardiologica 29:1-69 (Karger, Basel 1972).

14. Moreno, A. H.; Katz, A. I.; and Gold, L. D. "An Integrated Approach to the Study of the Venous System with Steps Toward a Detailed Model of the Dynamics of Venous Return to the Right Heart." IEEE Transactions on Bio-Medical Engineering, Vol. BME-16, No. 4, Oct. 1969.
15. Noordergraaf, A. "Hemodynamics." In Schwan, H. P. (Ed.). Biological Engineering. New York: McGraw-Hill Book Co., 1969.
16. Rushmer, R. F. Cardiovascular Dynamics. Philadelphia: W. B. Saunders Co., 1961.
17. Snyder, M. F. "A Study of the Human Venous System Using Hybrid Computer Modeling." Ph.D. Dissertation, University of Wisconsin, 1969.
18. Snyder, M. F. and Rideout, V. C. "Computer Simulation Studies of the Venous Circulation." IEEE Transactions on Bio-Medical Engineering, Vol. BME-16, No. 4, Oct. 1969.
19. Verdouw, P. D. "Ballistics of Ventricular Performanc." Ph.D. Dissertation, University of Wisconsin, 1970.

### BIOGRAPHICAL SKETCH

The author was born November 16, 1949 in Albany, Kentucky. He graduated Valedictorian of Clinton County High School in Albany, Kentucky May 1967 and entered the University of Kentucky in August 1967. He received the Bachelor of Science Degree in Electrical Engineering in December 1971.

E-64